

Tasmanian Geological Survey

Record 1999/06

The nature and origin of gold mineralisation at the Forster Prospect, Glovers Bluff/Weld River area



By R. S. Bottrill, J. Taberi and C. R. Calver



MINERAL RESOURCES TASMANIA

The nature and origin of gold mineralisation at the Forster Prospect, Glovers Bluff/Weld River area

by R. S. Bottrill, J. Taheri and C. R. Calver,
with an appendix by J. L. Everard

CONTENTS

| | |
|---|----|
| INTRODUCTION | 4 |
| Early prospecting and mining | 4 |
| Recent mineral exploration | 5 |
| Previous geological studies | 7 |
| GEOLOGICAL SETTING | 8 |
| Introduction | 8 |
| Proterozoic | 8 |
| Cambrian | 10 |
| Late Carboniferous-Permian | 10 |
| Jurassic dolerite | 13 |
| Felsic intrusive rock of unknown age | 13 |
| Geophysics | 13 |
| Tectonic setting and possible structural controls | 14 |
| HOST ROCK PETROLOGY | 14 |
| Proterozoic | 14 |
| Cambrian | 18 |
| Parmeener Supergroup (Permo-Carboniferous sediments) | 18 |
| Jurassic dolerite | 18 |
| Undated intrusive rocks | 18 |
| MINERALISATION AND ASSOCIATED ALTERATION | 19 |
| Overview | 19 |
| Siliceous rocks | 19 |
| Silicified ultramafic rocks with disseminated arsenides | 20 |
| Galena veinlets in massive chert | 20 |
| Opal | 20 |
| Other | 20 |
| Discussion | 20 |
| Skarns | 22 |
| Calc-silicate rocks | 22 |
| Ophicalcites | 23 |
| Diopside skarn | 23 |
| Carbonate alteration | 23 |
| Altered Cambrian rocks | 23 |

| | |
|---|----|
| Silica-clay/ 'argillic alteration' zone | 23 |
| Limonite-hosted | 25 |
| Summary | 25 |
| GEOCHEMISTRY OF MINERALISED AND HYDROTHERMALLY-ALTERED ROCKS | 26 |
| FLUID INCLUSIONS | 30 |
| Freezing and heating experiments | 30 |
| OXYGEN ISOTOPE STUDIES | 31 |
| DISCUSSION AND PETROGENESIS | 33 |
| Possible origins of gold and skarn mineralisation | 33 |
| <i>Previous studies</i> | 33 |
| <i>Gold in Tasmania</i> | 33 |
| <i>Pertinent Forster Prospect features from this study</i> | 33 |
| <i>High sulphidation-type gold mineralisation</i> | 34 |
| <i>Carlin-type gold mineralisation</i> | 35 |
| <i>Jurassic dolerite related mineralisation</i> | 36 |
| Summary | 37 |
| ACKNOWLEDGEMENTS... | 37 |
| REFERENCES | 38 |
| Appendix 1: Glossary of rocks and minerals | 41 |
| Appendix 2: Abbreviations used in rock descriptions | 43 |
| Appendix 3: Summarised sample details | 44 |
| Appendix 4: Logs of diamond-drill holes SW1 and SW2 | 51 |
| Appendix 5: A silicified karst breccia in the Mt Weld area | 52 |
| Appendix 6: Petrology of an aplite from the Weld River, southern Tasmania | 54 |
| Appendix 7: XRF analyses of rock samples | 57 |
| Appendix 8: ICP analyses | 70 |
| Appendix 9: Microprobe analyses | 72 |
| Appendix 10: XRD analyses | 81 |
| Appendix 11: Fluid inclusion data | 85 |
| Appendix 12: Correlation coefficients | 87 |

TABLES

| | |
|---|----|
| 1. Distribution of metals in gold-mineralised rocks, Forster Prospect | 26 |
| 2. Oxygen isotope data, Weld River | 32 |
| 3. Chemical analysis of Sample WRS | 55 |

FIGURES

| | |
|--|----|
| 1. Location map | 5 |
| 2. Geology map, Forster Prospect area, showing main mineral prospects and diamond drill holes | 6 |
| 3. Solid geology of Glovers Bluff inlier and ground magnetic traverses | 9 |
| 4. Cross-sections of Glovers Bluff inlier and surrounds | 11 |
| 5. Cross-sections, Forster Prospect area, based on drillhole data | 12 |
| 6. Stability relations in the system $\text{CaMg}(\text{CO}_3)_2\text{-SiO}_2\text{-H}_2\text{O}$ at 1 kbar H_2O | 15 |
| 7. Triangular diagram showing Ti-Y-Zr plots for the main igneous rocks | 19 |
| 8. Geochemical diagrams showing log-log plots in the different rock groups | 27 |
| 9. Geochemistry over the mineralised zone along Fletchers Road/Forster Road | 29 |
| 10. Histograms showing frequency distribution of T_{homog} for fluid inclusions | 31 |
| 11. Normative composition of Weld River aplite sample | 56 |

PLATES

| | |
|---|----|
| 1. Dolostone showing breccia and oolitic textures... .. | 16 |
| 2. Dolostone showing partial replacement by ophicalcite | 16 |
| 3. Magnified view of Plate 2, showing serpentine pseudomorphic after forsterite (?)... .. | 16 |
| 4. Brucite pseudomorphic after periclase (?) in calcite | 16 |
| 5. Granular to fibrous diopside in reaction rims between quartz and dolomite in siliceous dolostone ... | 16 |
| 6. Diopside reaction rims between quartz and dolomite in siliceous dolostone, showing prismatic diopside needles | 16 |
| 7. Massive, fine-grained diopside skarn, showing breccia texture and calcite porphyroblasts... .. | 16 |
| 8. Talc pseudomorphic after forsterite (?)... .. | 16 |
| 9. Quartz breccia showing chromite grains | 21 |
| 10. The probable precursor Plate 9: ultramafic-derived greywacke showing tremolitic amphibole, chromite and talc | 21 |
| 11. Quartz breccia showing net fracturing and vuggy clasts | 21 |
| 12. Quartz breccia showing a network of cherty quartz infilled with coarser, partly vuggy, quartz | 21 |
| 13. Vuggy quartz breccia infilled with fibrous xonotlite and pectolite | 21 |
| 14. Quartz breccia clast in dolerite | 21 |
| 15. Quartz breccia showing chert cut by banded and recrystallised quartz and later opal/chalcedony veins | 21 |
| 16. Quartz-opal breccia showing angular quartz in an opal matrix | 21 |
| 17. Quartz breccia showing replacement by various silicate minerals | 24 |
| 18. Quartz breccia altering to various silicate minerals | 24 |
| 19. Quartz breccia showing a vein of xonotlite, calcite and sphalerite | 24 |
| 20. Calcitic diopside breccia showing dark areas with fine grained Fe-Ni-Co arsenides | 24 |
| 21. Brecciated ophicalcite showing stockwork veins of sjogrenite, loellingite, magnetite, sphalerite, andradite and other phases | 24 |
| 22. Chert showing irregular veins of chalcedony, galena, sphalerite, pyrite, tetrahedrite, chalcopyrite and other sulphides | 24 |
| 23. Magnified view of Plate 22, showing tetrahedrite altering to chalcopyrite and cubanite, plus galena and framboidal pyrite in chalcedony | 24 |
| 24. Diopside skarn breccia showing grains of pinkish niccolite altering to loellingite and rammelsbergite... .. | 24 |

While every care has been taken in the preparation of this report, no warranty is given as to the correctness of the information and no liability is accepted for any statement or opinion or for any error or omission. No reader should act or fail to act on the basis of any material contained herein. Readers should consult professional advisers. As a result the Crown in Right of the State of Tasmania and its employees, contractors and agents expressly disclaim all and any liability (including all liability from or attributable to any negligent or wrongful act or omission) to any persons whatsoever in respect of anything done or omitted to be done by any such person in reliance whether in whole or in part upon any of the material in this report.

Abstract

The Forster gold-zinc-nickel prospect, in southeastern Tasmania, occurs in an altered assemblage of Proterozoic dolostone and Cambrian ultramafic-derived conglomerate surrounded by a large Jurassic dolerite cone sheet. Weak, disseminated, sulphide-poor gold mineralisation occurs with minor Ni-Fe-Co-arsenides and Pb-Zn-Cu sulphides in high-temperature magnesian skarns and associated siliceous zones, and silica-clay zones. The skarns include diopside skarn, ophicalcite (serpentinised forsterite marbles and brucite marbles) and brucite marbles (some replacing periclase marbles). Siliceous breccia is prominent as a common alteration type in the skarns, and may contain complex retrograde calc-silicate assemblages, gold and arsenides, but is mostly unmineralised. It is probably post-Permian and at least partly pre-Jurassic dolerite in age (being intruded by dolerite), but fluid inclusions in the quartz are of high temperature (300–400°C), low salinity and are CO₂-bearing. Higher grade gold (>1 g/t) is virtually restricted to argillaceous silica-clay zones overlying these skarns. The primary mineralisation is considered to be related to the intrusion of the Jurassic dolerite into ultrabasic-derived conglomerate and dolostone, which formed skarns, alteration and associated mineralisation and also mobilised some gold and base metals into pre-existing, silicified karst structures. Gold was concentrated during the later (Tertiary?) weathering which produced the silica-clay zones, which may occupy karst-fill structures.

Introduction

The Forster gold prospect lies in an inlier of Cambrian and Precambrian rocks exposed at Glovers Bluff, near the Weld River in southern Tasmania (fig. 1–3). Metallic mineralisation recorded from the area includes gold, nickel and zinc, although anomalous copper, lead, silver, arsenic, antimony, chromium and cobalt are also present. This mineralisation is spatially related to magnesian skarns, dolerite and some argillaceous and silicified zones.

Although the occurrence of alluvial gold in the Glovers Bluff area has been known since about 1880, the primary mineralisation has attracted little attention until recent years. As a result, the nature and genesis of the mineralisation, which is distinctly different from other known mineralisation types in Tasmania, have not been understood. This has acted as a disincentive for exploration companies to actively explore this area and other similar terrains in Tasmania for gold.

The purpose of this study is to investigate the nature and origin of the gold mineralisation through fieldwork, drill core re-logging, petrological, geochemical, fluid inclusion and stable isotope studies.

Early prospecting and mining

The history of early exploration is poorly recorded and is summarised below.

Gold was first recorded in the Weld River by Charles Glover, who prospected the Weld River with Henry Judd in from 1877 to 1881 (Abbott, 1995; *Huon Times*, 1881). Although the actual locations of his discoveries are uncertain, his mention of gold in “a white marble reef crossing the river” and of a nearby quartz ridge cut by the river (*Huon Times*, 1881) strongly suggests it must be the Glovers Bluff area. Glover also found lead, gold and pyrite further up river, at an unknown site described as “Hollow Tree Point”, near the foot of Mt Lefroy (“of similar size to Mt Weld”: this name is now unrecognised, but is perhaps Snowy South, some 12 km NNW of Glovers Bluff). He mentioned one area “where

nearly every small spade full of gravel contains one or more pieces of metal”. Henry Judd returned to the area in 1882 to prospect with Benjamin Griggs and Michael Gallagher (Abbott, 1995).

The next known prospecting in the area was in the 1890s, when George Renison Bell and other prospectors visited the district and also reported gold, but records are scanty (Lewis, 1924). In 1891 a Gold Reward Claim (289/91), somewhere near the northern end of the Arthur Range, was granted to Henry Judd and Michael Gallagher (Department of Mines records). The lease was dropped in 1900. Another gold reward lease (956/93G) was granted to Judd and Gallagher from 1897 to 1919, probably at Reward Claim Creek, about seven kilometres WNW of Mt Weld (but described as “Mount Weld, north of the Weld River”: Department of Mines records; Jennings, 1978). Adits and an old grindstone remain, although the workings have apparently not been visited for decades (R. N. Woolley, pers. comm.). Gold was also reported in the bed of the Weld River (*Cyclopaedia of Tasmania*, 1900). Two Reward Leases for silver (1688/93M, 4859/93M) were granted to George Griggs (brother of Benjamin and brother-in-law of Michael Gallagher) in 1897 and 1900, to the north and east of the above lease. Around this time, George’s brother Henry Griggs found gold in Manuka Creek, southwest of Mt Weld (*Huon Times*, 1916). No production was recorded from any of these leases.

Charles Fletcher discovered nickel and osmiridium in the Weld River area in 1916. A Reward Lease (ML7275M) for nickel and cobalt, covering an area to the north of the Weld River and immediately east of Hogsback Hill (presumably the same area), was granted to H. E. Evenden in 1917. Several shafts and a water race were dug, and a hut was built near the river (Department of Mines lease records). A report by F. W. Fletcher (brother of Charles) considered that this prospect “would be payable with facilities”, and also referred to the presence of deposits of iron and scheelite in the same area (*Huon Times*, 4 November 1921; actual

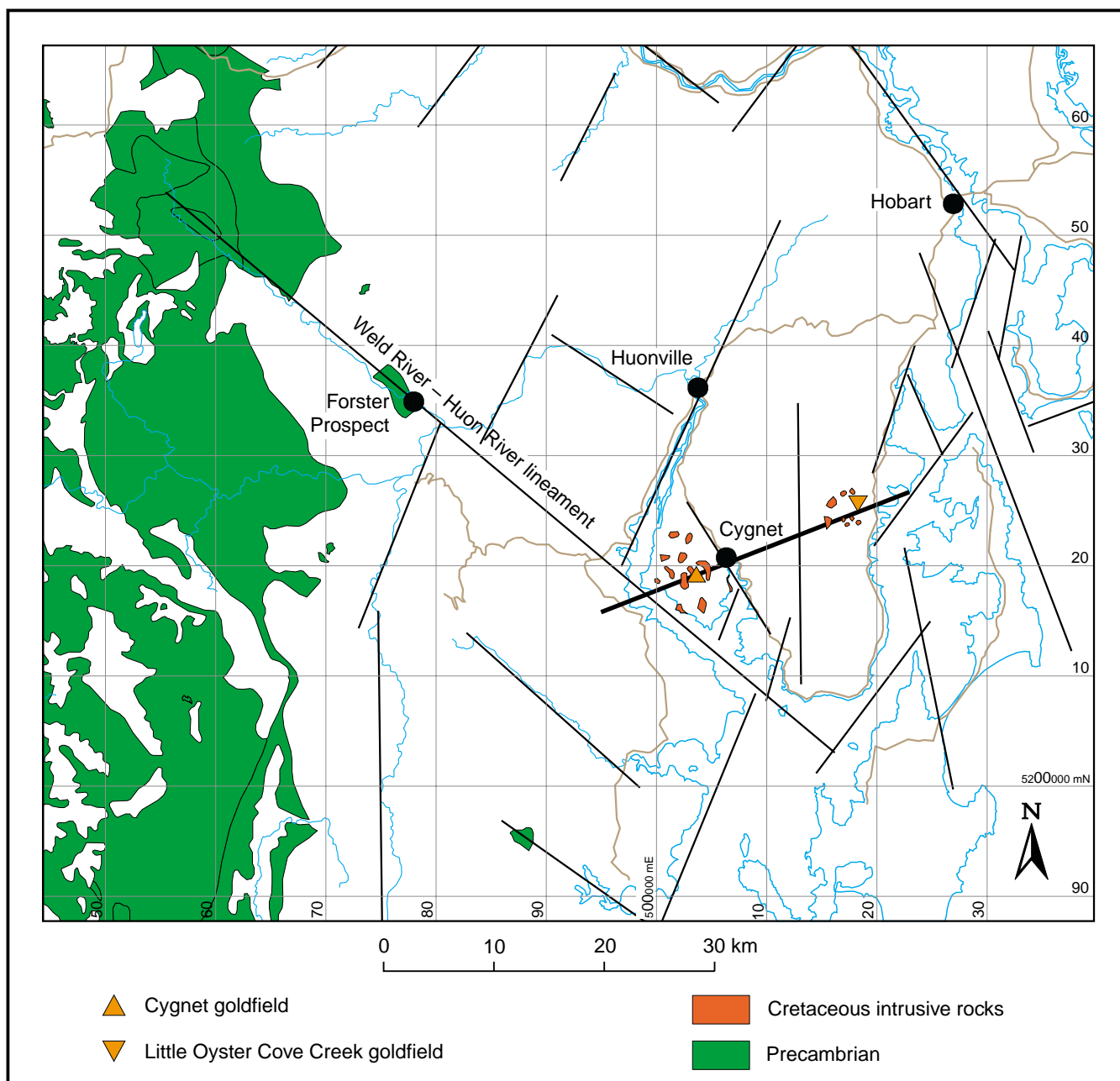


Figure 1

Location map, showing the Forster and Cygnet gold prospects, and the possible related Weld River–Huon River lineament.

locations not stated and not confirmed by later studies). The potential for flint in this prospect was also considered (Lewis, 1924). No production was recorded and the lease expired in 1928.

The Stacey brothers found “a very rich pocket of gold”, valued at about £300, in a valley in the Jubilee Range (running along the north side of the Weld River), prior to discovering the Adamsfield osmiridium field in 1924 (Gowlland and Gowlland, 1977). The exact location is unknown but it may be Gold Creek, a tributary of the Styx River, to the north.

In 1926, during the ‘osmiridium boom’, a reward lease south of the Weld River was granted to a Rev. W. G. Fitzgerald (a Victorian clergyman), C. T. Fletcher and L. Wilson for osmiridium and gold. Good osmiridium was reported in the Weld River as far down as the Huon

junction. The lease expired in 1936, with no recorded production. Workings in the area, presumably resulting from the above activities, consist of several shallow shafts and pits. An adit was also driven around this time in the south end of Hogsback Hill (on the north bank of the Weld River; fig. 2), but Summons (1985) considered this to be a prospecting adit for gold. A sluiced creek just east of the adit may also have been worked about this time.

Recent mineral exploration

Modern mineral exploration is summarised below from Summons (1985), Bacon (1989) and various departmental records and company reports.

During the ‘nickel boom’ in 1968, the late Mac Forster, a part-time prospector, applied for two Special

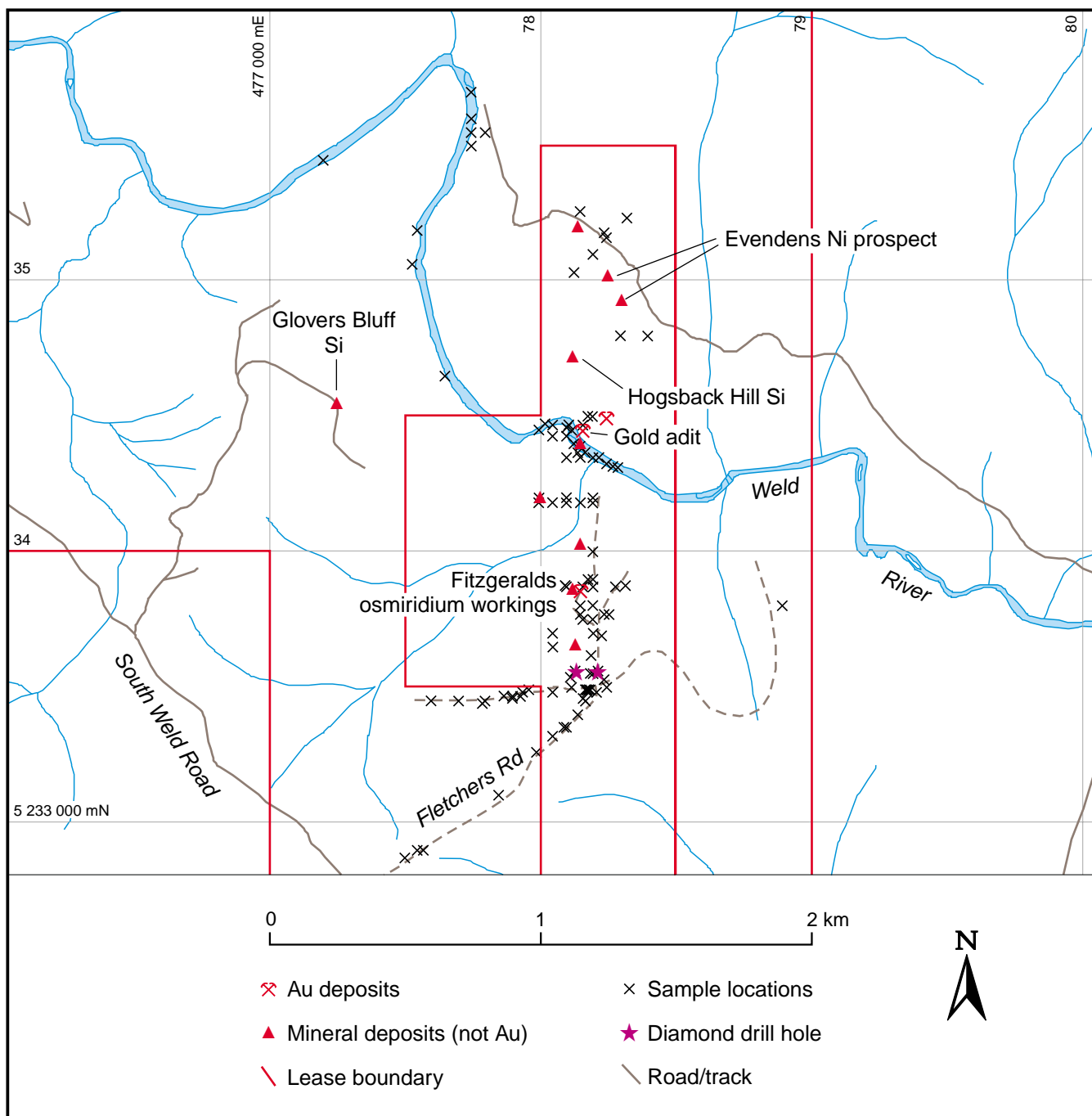


Figure 2
 Location map of the Forster Prospect area, showing main mineral prospects and diamond drill holes.

Prospecting Licences in the area. A track was bulldozed into this relatively inaccessible area, but little other work was done.

Inland Exploration NL took out an Exploration Licence (EL) covering the area in 1970. They noted the occurrence of ultrabasic rocks and prospected for chromite, gold, nickel and platinoids, but no interesting results were reported (Wood, 1971).

F. K. H. Scheppein took out two Mining Leases in the area in 1970 and 1971 to explore for marble, but apparently little work was done.

Mac Forster applied for a new Special Prospecting Licence and four Mining Leases in the area in the 1970s to explore the silica prospects on the lease. The leases were joint-ventured with Consolidated Goldfields of Australia (later Kemmerton Pty Ltd, which ran the Electrona carbide works). A moderate amount of exploration and drilling was conducted, but none of the silica resources identified proved suitable for processing.

The Broken Hill Proprietary Company, through its subsidiary Tasmanian Electro Metallurgical Company (TEMCO), entered an option agreement in 1980 and drilled six cored holes in the Glovers Bluff silica deposit. The agreement was terminated in 1982.

The Kaiser Chemical Corporation of Australia and Pioneer Concrete Services Ltd joint-ventured the Glovers Bluff Mining Lease, plus the Bernard Spur and Camels Back Mining Leases north of the Weld River, in 1982. Kaiser's options were taken over by Pechiney Australia Ltd in 1985. Pioneer and Pechiney conducted considerable drilling, analyses, and detailed feasibility studies for silicon production.

The area originally held by Forster's company (The North West Bay Co.) has been joint-ventured with various other companies, including Pioneer, Pechiney, Pegasus Gold Australia Ltd, Metals Exploration Pty Ltd, and Sedimentary Holdings NL. It is presently covered by leases RL9803 and EL33/96 and EL3/94, the last of which is still held by The North West Bay Co. but joint-ventured with Sedimentary Holdings NL; the other two leases are held by Sedimentary Holdings NL. The leases have been explored for various commodities including silica, talc, platinoids, chromite, nickel, gold, jade and marble (Summons, 1985; Carthew *et al.*, 1988). Work conducted recently has concentrated on gold exploration, and has included numerous reverse circulation drill holes and three diamond-drill holes.

Some significant gold intersections (including 11 m @ 3 g/t) have been reported during a current phase of exploration by Sedimentary Holdings NL, which has termed the area 'the Forster Prospect' in memory of Mac Forster. An inferred low-grade resource of 1.14 Mt @ 0.45 g/t Au was delineated from twenty drill holes (Sedimentary Holdings, report to the Australian Stock Exchange for the quarter ended June 1996).

The only mineral production recorded from the area is silica from Glovers Bluff, which was used for trials in the now defunct Electrona silicon works.

Previous geological studies

The earliest geological studies in the area are those of Lewis (1924). Some reconnaissance geological mapping has been carried out during mineral exploration, and is reported by Summons (1985) and Carthew *et al.* (1988).

Taheri (1990) conducted some brief petrographic, oxygen isotope, clay mineralogy and fluid inclusion studies of some samples from the gold-bearing silica-clay zone. He suggested that the siliceous rocks were altered dolomite, and found low salinity fluids with $T_{\text{homog}} \sim 250\text{--}280^\circ\text{C}$. Oxygen isotope values of quartz suggested that silica was formed from a mixture of magmatic and meteoric fluids.

Boyd (1996) studied the geochemistry, petrography and mineralogy of the alteration and mineralisation, and briefly described the skarn, silica and carbonate alteration. He also reported a Pb isotope analysis of galena in chert.

Bottrill and Woolley (1996) briefly described the nature and origin of the altered and mineralised rocks. This indicated that retrogressed skarns, calc-silicate hornfels, dolerite contacts, ultrabasic conglomerate, and variable siliceous breccias all host minor gold and base metal mineralisation. Significant findings included altered Jurassic dolerite, gold grains *in situ* in skarn, and chert clasts in Jurassic dolerite.

Dell (1997) conducted some geochemical, petrographic, clay mineralogy and sulphur isotope studies of the mineralisation and host rocks. Fluid inclusion studies were conducted on a quartz veinlet in Jurassic dolerite.

The geophysics of the area has been recently reviewed and re-interpreted, with some additional work, by Dunstan (1997).

The geology of the area was regionally mapped by Calver (1998).

Geological Setting

Introduction

The Forster Prospect lies close to the boundary between the two contrasting geological terrains that make up southwestern and southeastern Tasmania. The western terrain consists mainly of polydeformed Proterozoic sediments and metasediments, dominantly quartzite, phyllite, schist and dolomite. There are smaller areas of Cambrian ultramafic rocks, basalt, polymict conglomerate and sandstone, mudstone and chert. Part of the Cambrian assemblage, including the ultramafic rocks, is thought to represent the remnants of an oceanic island arc obducted onto the Proterozoic core of Tasmania in the middle Cambrian (Berry and Crawford, 1988; Seymour and Calver, 1995). This event, together with deformation and regional metamorphism of the older rocks, comprises the Tyennan Orogeny (Turner *et al.*, 1998). A thick Late Cambrian to Early Devonian succession of siliciclastic rocks and carbonate (the Wurawina Supergroup), unconformably overlying the older rocks, is locally preserved in the western terrain. A mid-Devonian tectonic event produced open upright regional folds in the Wurawina Supergroup.

The eastern terrain consists of a flat-lying sedimentary sequence of Late Carboniferous to Triassic age, the Parmeener Supergroup, and Jurassic dolerite. The Parmeener Supergroup rests with landscape unconformity upon the pre-Carboniferous rocks, and is up to 1.5 km thick. Jurassic dolerite forms widespread sheets and sills, typically 500 m thick, within the Parmeener Supergroup. The dolerite is erosionally resistant and forms most of the topographic highs in eastern Tasmania, such as (near Forster Prospect) Weld Ridge and the Snowy Range. Near Cygnet, 30 km southeast of Grovers Bluff, minor alkaline intrusive rocks of Cretaceous age within the Lower Parmeener Supergroup are associated with minor gold mineralisation (Taheri and Bottrill, 1999). Some workers have proposed a genetic similarity between the Forster Prospect and the gold mineralisation at Cygnet (Summons, 1999).

Scattered outliers of Parmeener Supergroup and dolerite in the western terrain show that these rocks were originally much more extensive, and have been removed by erosion from southwestern Tasmania. Potential field data (Leaman, 1990) and a few deep drillhole intersections show that the deformed Proterozoic to lower Palaeozoic rocks of the western terrain underlie the Parmeener Supergroup over most of southeastern Tasmania.

The Forster Prospect occurs in an area of Proterozoic and Cambrian rocks which forms an inlier within the eastern terrain, about 10 km east of the roughly meridional, but irregular, western erosional limit of the Parmeener Supergroup. The inlier, which is about 6 × 3 km in extent, is known as the Grovers Bluff inlier

and is surrounded and probably underlain by Jurassic dolerite (fig. 3, 4)

The local geology is known from regional 1:25 000 scale geological mapping (Calver, 1998). In the following synthesis we have also utilised larger scale mapping, ground magnetics and drilling by exploration companies in the vicinity of the Forster Prospect (Carthew *et al.*, 1988; Summons, 1997, 1998; Young, 1997). The main elements and structure of the Grovers Bluff inlier are described below. The detailed petrology and mineralogy of the altered rocks associated with the Forster Prospect are described in a later section.

Proterozoic

The oldest rock unit of the Grovers Bluff inlier is a formation of cross-bedded quartz arenite, about one kilometre thick, which dips subvertically, striking northwest and younging northeast. The quartz arenite forms the prominent strike ridge of Grovers Bluff and Bernard Spur along the western side of the inlier (fig. 3). The quartz arenite is conformably overlain by thinly interbedded siltstone and shale, exposed in the Weld River just downstream from where the river transects the strike ridge. The quartz arenite and siltstone-shale unit are correlates of the Needles Quartzite and lowermost Humboldt Formation, respectively, of the Clark Group, which crops out extensively at The Needles and Jubilee Range, 20–40 km northwest of the Grovers Bluff inlier. In common with the Proterozoic rocks of those areas, the Clark Group in the Grovers Bluff inlier is essentially unmetamorphosed (except for local contact metamorphism by Jurassic dolerite). The Clark Group is late Mesoproterozoic or early Neoproterozoic in age (Seymour and Calver, 1995).

Dolostones of the Neoproterozoic Weld River Group (Calver, 1989) lie to the east of the Clark Group in the Grovers Bluff inlier. These rocks, like the Clark Group, strike northwest and young to the northeast, but northeast dips are moderate (50–70°). The contact between Weld River Group and Clark Group is not exposed. Elsewhere, such as near Jubilee Range, the contact is conformable or nearly so; at the Grovers Bluff inlier it is probably a fault at a low angle to bedding because of the discordance of dips and because most of the Humboldt Formation is missing.

Typically, the Weld River Group consists of massive to thickly bedded, fine-grained, pale grey dolostone. In places there are beds of oolitic, intraclastic dolograstone and, at one locality, stromatolitic dolostone. Some dolograstone beds contain 10–30% fine-grained quartz as a diagenetic, late cement phase. The eastern part of the dolostone is strongly contact metamorphosed by Jurassic dolerite, typically to a massive white diopside calciphyre.

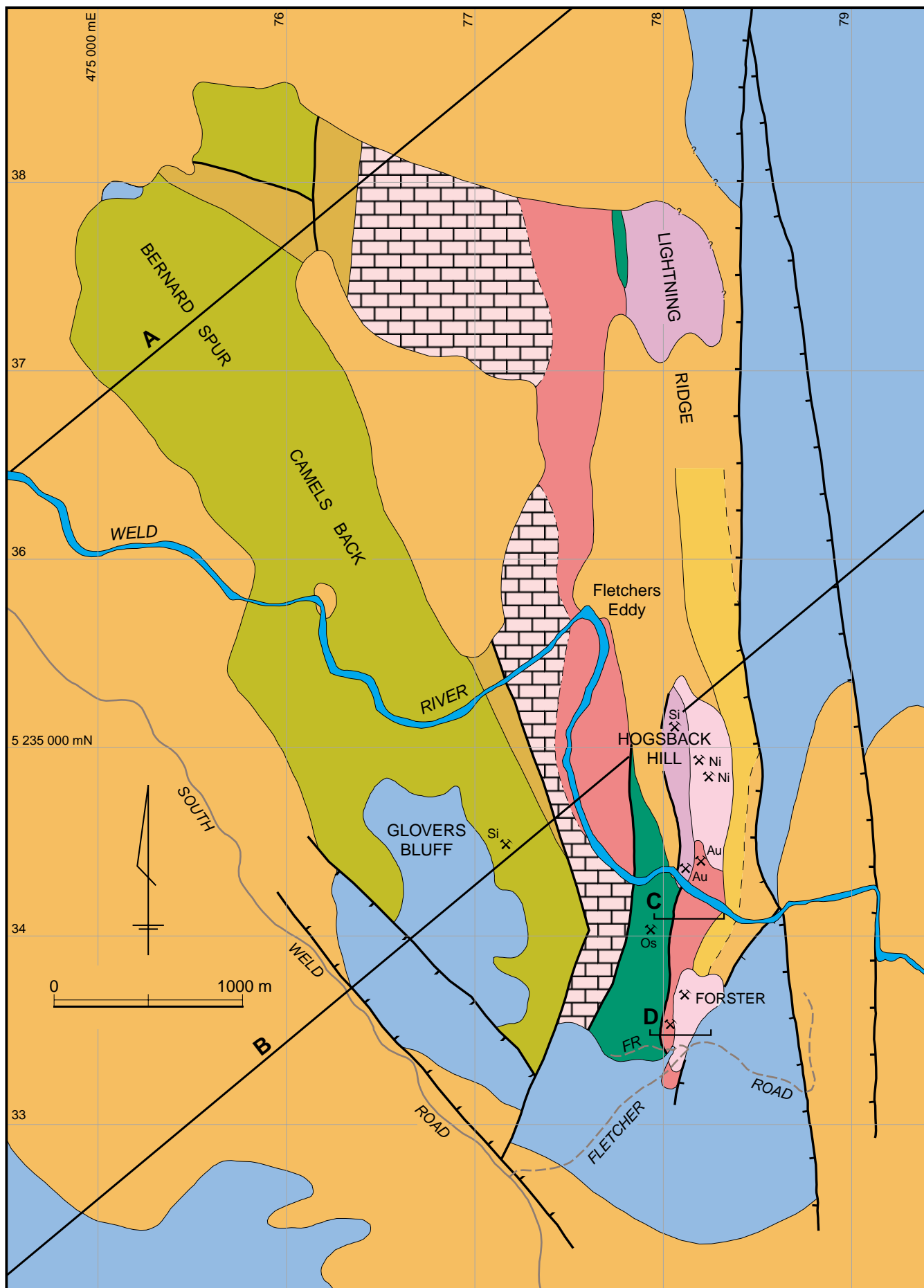


Figure 3

Solid geology of Grovers Bluff inlier, based on Calver (1998) and ground magnetic traverses. For legend see Figure 5. Locations of sections A and B (fig. 4), sections C and D (fig. 5), and mineral prospects are shown. FR = Forster Road.

At the southeastern end of the Glovers Bluff inlier, a second, smaller area of skarn, ophicalcite and marble lies east of a narrow faulted wedge of Cambrian rocks and probably also represents highly altered dolostone of the Weld River Group. This, the 'eastern marble/skarn unit', is poorly exposed and is mostly covered by a thick surficial lag of secondary silicification products, but drillholes, costeans and outcrop in the Weld River show magnesian-calcareous skarns and marble in the shallow subsurface. Drillhole data also suggest that these altered carbonate rocks are underlain by Jurassic dolerite at depths of 15–80 m over much or all of this area.

South of the Weld River, part of the eastern marble/skarn unit is overlain by a unit of fragmental silica and clay (the 'silica-clay zone') which is up to 60 m thick. This is interpreted to be mainly a weathering product of the underlying marble/skarn unit.

Minor Au, Ni and base metal mineralisation in a silica zone, and underlying the eastern marble-skarn unit, comprises the Forster Prospect. North of the Weld River, the eastern marble/skarn unit is abutted on the west by a more-or-less massive unit of fine-grained secondary quartzite which crops out as a narrow meridional strike ridge ('Hogsback Hill'). Further north, at the northeastern corner of the Glovers Bluff inlier, a similar silicified zone crops out on 'Lightning Ridge'. This latter occurrence is along strike from Hogsback Hill, but there is an intervening area of Jurassic dolerite.

Cambrian

In the southern part of the Glovers Bluff inlier, south of the Weld River, is a narrow meridional wedge of Cambrian rocks which is interpreted to be faulted against unmetamorphosed Weld River Group dolomite to the west, and against the eastern marble/skarn unit to the east. The southern end of the wedge is well exposed in road cuttings along Forster Road, with the northern end being exposed on the banks of the Weld River. The predominant rock type is an altered, polymict, foliated conglomerate of mainly mafic provenance. The conglomerate along Forster Road is deeply weathered, poorly bedded, of pebble to cobble grade, with subrounded clasts of basalt, gabbro, minor granitoid, rare feldspar porphyry, and rare pink chert. There are minor intervals of coarse-grained lithic sandstone and micaceous siltstone. Most outcrops here are strongly foliated, with many clasts altered to deformed lenticular bodies of red, green or white halloysite, talc or talcose phyllite. A poorly outcropping, weathered pyroxenite occurs at the western end of the Forster Road transect. The western part of the Cambrian package along the Weld River, and in costeans nearby to the south, consists of foliated grey-green slate.

Ground magnetic surveys show that the Cambrian rocks are variably, and in places strongly magnetic, in contrast to the essentially non-magnetic carbonate

rocks to the east and west. The easternmost part of the Cambrian fault wedge has the strongest magnetic response, with readings up to 7000 gammas above the regional background field of 62 000 gammas (Carthew *et al.*, 1988).

At Lightning Ridge, in the northeastern corner of the inlier, a small area of Cambrian rocks lies between secondary quartz and opal (formerly Weld River Group carbonate?) to the east and the western marble/skarn unit to the west. This area contains hornblende-rich basalt, some of which is mainly altered to prehnite.

Polymict conglomerate and lithic sandstone occur in the middle reaches of the Weld River, 10 km northwest of the Glovers Bluff inlier. These rocks closely resemble the talcose conglomerate in the Glovers Bluff inlier, and are probably relatively fresh and little-altered equivalents. They are distant from Jurassic dolerite intrusion, are faulted against Proterozoic rocks and are unconformably overlain by Parmeener Supergroup rocks (fig. 3–5). They include conglomerate of up to boulder grade, with well-rounded clasts of basalt, chert, granite, Proterozoic quartzite, Weld River Group-type dolostone and siliceous dolostone, and mudstone.

The Cambrian conglomeratic rocks at Glovers Bluff and in the middle reaches of the Weld River resemble the conglomerate in the Tyler Creek beds, which crop out on the south coast of Tasmania (Berry and Harley, 1983; Dell, 1997), and the Blythe Creek beds in the Beaconsfield area (Bottrill, unpublished data), both of which are polymict Cambrian conglomerates with ultramafic clasts. They may also correlate with Middle Cambrian quartzose sandstone and conglomerate, the Island Road Formation and Trial Ridge beds, of the Adamsfield district, 50 km northwest of Glovers Bluff.

Late Carboniferous–Permian

The southern part of the Glovers Bluff inlier is unconformably overlain by a flat-lying succession of diamictite and pebbly mudstone, a correlate of the Late Carboniferous to Early Permian Truro Tillite of the Lower Parmeener Supergroup. The diamictite is a massive rock with subrounded to well-rounded pebbles, cobbles and rare boulders, dominantly of quartzite, chert and schist in a matrix of silty mudstone. Rare marine fossils are present. South of Forster Road, the basal several metres of diamictite consists of sparse clasts in a matrix of white silty kaolinitic clay. This may be a result of deep weathering, or a result of argillic alteration.

An area of contact-metamorphosed fossiliferous mudstone lies three kilometres southwest of Glovers Bluff, and rests on dolerite with a gently northeast-dipping contact. Other hornfelsed mudstone occurs along Fletchers Road.

Elsewhere, the basal tillite passes up into a several hundred metres thick succession of cold-water marine

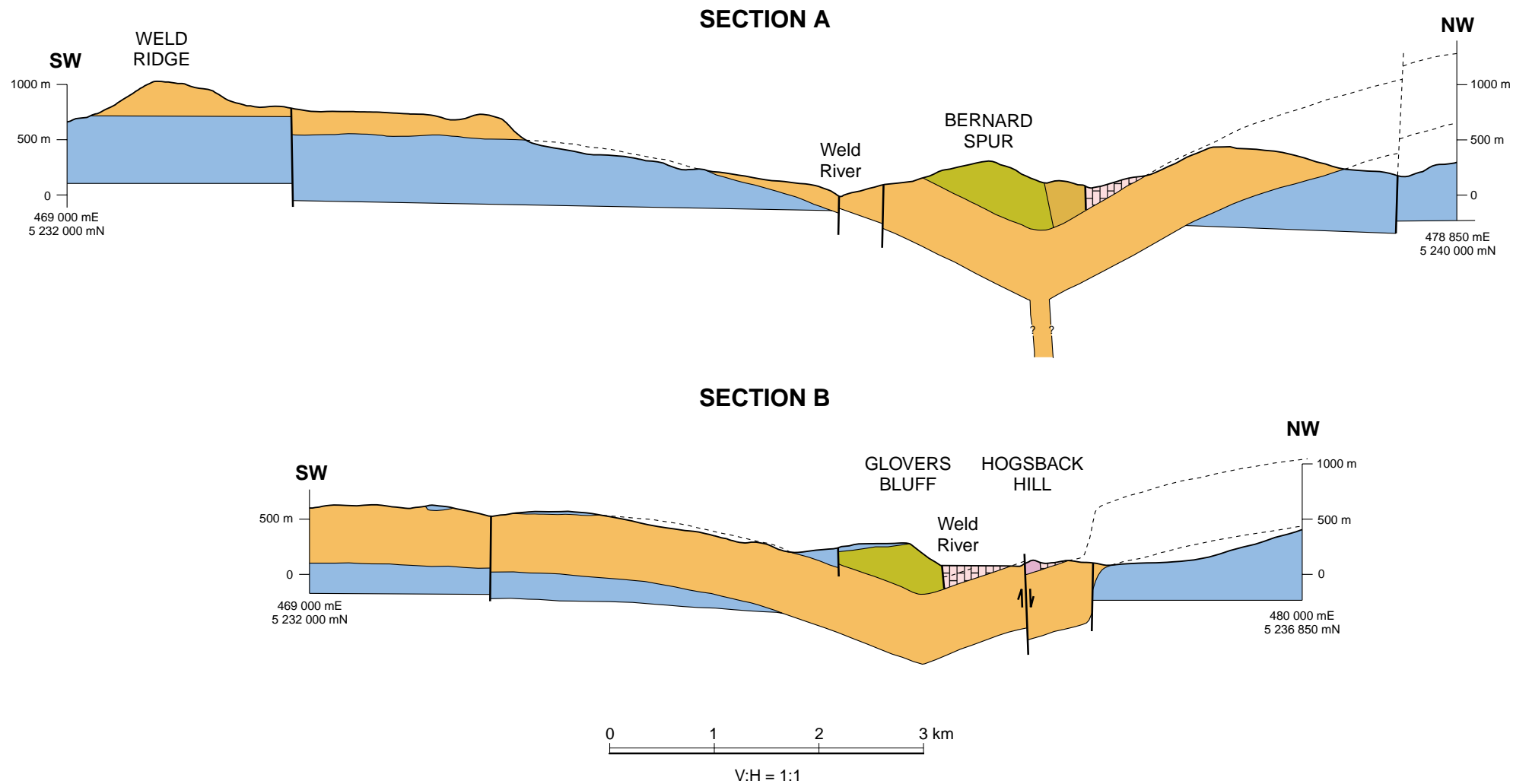


Figure 4

Cross-sections of Glovers Bluff inlier and surrounds. See Figure 3 for section locations and Figure 5 for legend.

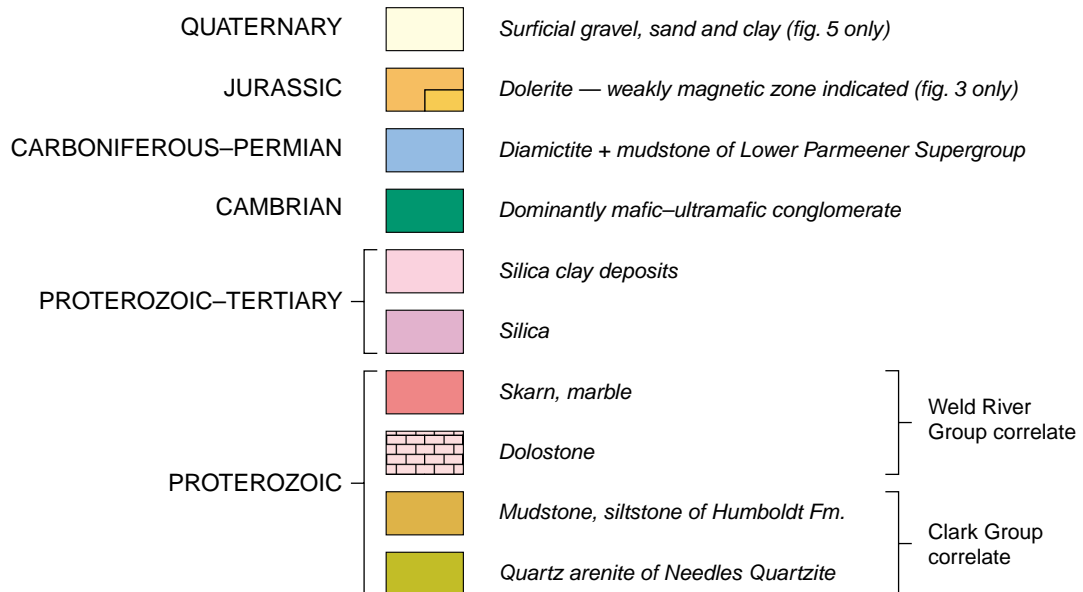
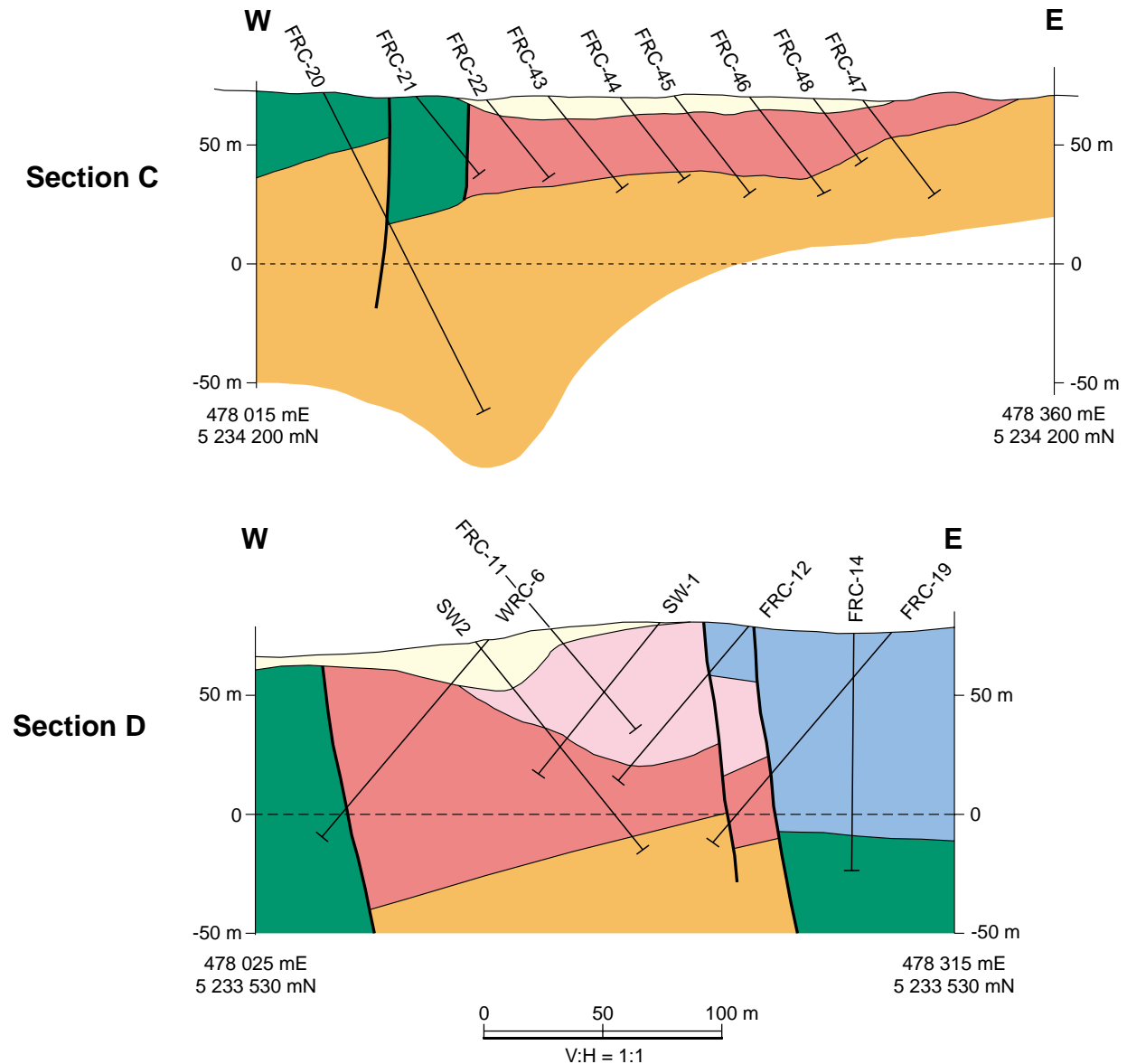


Figure 5

Cross sections, Forster Prospect area, based on drillhole data. See Figure 3 for section locations.

Logs of diamond drillholes SW1 and SW2 (section D) are given in Appendix 4.

Data of reverse-circulation holes (prefixed FRC) are from Young (1997).

mudstone and sandstone (Lower Parmeener Supergroup) succeeded by freshwater sandstone of latest Permian to Triassic age (Upper Parmeener Supergroup).

Jurassic dolerite

Dolerite surrounds the Glovers Bluff inlier. Observed contacts (e.g. at 476 300 mE, 5 234 300 mN) are intrusive and dip gently to moderately inwards, under the inlier. The lower contact of the dolerite similarly dips gently towards the inlier (fig. 4). The intrusion is thus in the form of a large irregular cone sheet, with the Glovers Bluff inlier comprising the eroded remnant of the uplifted roof rocks in the core of the cone sheet.

The area of contact-metamorphosed Permian mudstone southwest of the Glovers Bluff inlier is another roof-rock remnant. The limbs of the cone sheet flatten out while rising gently away to the north and west of the inlier, merging with the high-level horizontal sills capping the Weld Ridge and Snowy Range. The southeastern side of the cone sheet is locally narrower, more steeply intrusive and partly faulted (fig. 3, 4). A thickness of about 500 m may be inferred for most of the intrusion.

A major dolerite feeder is inferred to underlie the inlier. The form and exact location of the feeder are a matter of conjecture, but there are large sub-circular aeromagnetic anomalies at 476 700 mE, 5 236 300 mN (near the centre of the inlier) and at 474 900 mE, 5 237 200 mN on the northwestern side of the inlier that may indicate the locations of large, vertical, pipe-like feeders at depth.

A number of smaller dolerite intrusions occur within the inlier. Exposures of Clark Group and Cambrian rocks in the Weld River are intruded by dolerite dykes 100 mm to a few metres wide. Dykes, and the chilled margins of larger intrusions, are characteristically fine grained and contain small (<1 mm) phenocrysts of green orthopyroxene. A large (1 km²) irregular area of dolerite occurs north of the Weld River in the approximate centre of the inlier. The form of this body at depth is unknown – it is presumably continuous with the main cone sheet – but it is fine grained close to contacts, suggesting an intrusive rather than faulted relationship with the surrounding Proterozoic rocks.

The narrower dolerite body on the southern part of Lightning Ridge is interpreted to be the eastern side of the cone sheet and has a steep contact (probably a normal fault) on its eastern side. The limits of this body, and attitudes of contacts (mostly concealed by soil and talus), have been constrained in part by ground magnetic traverses (by C. R. Calver). This body is interpreted to dip gently west under the contact-metamorphosed Weld River Group carbonate rocks (the 'western marble/skarn unit') to the west, and is probably continuous with the fine-grained dolerite outcrop at Fletchers Eddy. The Lightning Ridge dolerite body bifurcates to the south; between the two

'arms' lie silicified and skarn-altered rocks of the Weld River Group (the 'eastern marble/skarn unit' and the Hogsback Hill quartzite). The eastern arm extends south of the Weld River, where drillhole data show that the dolerite dips gently west to underlie the eastern marble/skarn unit at depths of up to 80 m, as far south as the Fletchers Road–Forster Road junction.

The cone sheet geometry of the dolerite surrounding the Glovers Bluff inlier explains the elevation of the Proterozoic to Cambrian basement rocks to relatively high levels within the eastern terrain, without the need for major faults. This geometry is also consistent with the strong alteration and high-temperature, low-pressure metamorphism seen in the reactive siliceous dolomite and conglomerate in the eastern part of the inlier, which is predicted to be shallowly underlain by several hundred metres of dolerite (fig. 4). The inlier, surrounded and underlain by dolerite, would have been the focus of an unusually large heat flux at the time of intrusion. Dolerite magmas are typically relatively anhydrous, and so are not usually considered to be the source of large volumes of hydrothermal fluid. The dolerite at the Forster Prospect, however, typically contains a few percent of biotite and/or amphiboles, plus some minor sulphides, so may have contained more fluid than normal.

Felsic intrusive rock of unknown age

A small (3 m) isolated outcrop of aplite occurs on the northern bank of the Weld River close to the contact between Jurassic dolerite and Proterozoic quartz arenite, at the western edge of the Glovers Bluff inlier. This is composed of fine-grained, sericitised alkali feldspar, quartz and minor altered biotite. It is geochemically dissimilar to both the Cretaceous alkaline intrusive rocks near Cygnet, and to a lesser extent, mid-Palaeozoic Tasmanian granites (Everard, Appendix 6, this report). It may represent a minor intrusive body related to the extensive Devonian granite pluton interpreted to underlie the area (see below). The rock contains low quantities of base metals and As, and less than 0.05 g/t gold, and a genetic link to the Forster Prospect is considered unlikely.

Geophysics

The geophysics of the area has been recently reviewed and re-interpreted, with some new work, by Dunstan (1997). Her gravity surveys indicate the presence of a probable Devonian granite at ~3–4 km depth below the area. Forster Prospect lies over the northeast edge of an extensive subsurface granite body, interpreted from gravity data (Leaman and Richardson, 1992). A depth to granite beneath the Glovers Bluff inlier of about nine kilometres is given by Leaman and Richardson (1992). Other gravity anomalies may reflect density contrasts between the silica-rich units and dolerite and skarns.

Ground magnetic surveys (Carthew *et al.*, 1988) indicate the presence of shallow north-trending

magnetite-rich units, probably representing the polymict, mostly mafic to ultramafic-derived conglomerate.

Tectonic setting and possible structural controls

The Proterozoic to Cambrian rocks are mostly moderately deformed by the Cambrian (Tyennan) and Late Devonian (Tabberabberan) orogenies. The Lower Parmeener Supergroup is faulted and only gently folded by structures largely related to the intrusion of Jurassic dolerite sills and dykes.

As well as the controls related to the Jurassic dolerite emplacement discussed above, the Glovers Bluff Inlier may be related to major faults, expressed as topographic lineaments and in particular, the Macquarie-Huon Fault Zone (following radiometric, topographic and magnetic linears; fig. 1; Summons, 1999). The Cygnet goldfield (Taheri and Bottrill, 1999) lies on this lineament, and that area is characterised by doming and intrusion of Cretaceous alkaline porphyries. Both deposits are probably also controlled by major north-south faults.

The lineament also passes close to the Adamsfield platinum-group mineral-Ni-Au mineralisation and can be projected to be close to the Jane River goldfield,

although this is highly speculative. Summons (1999) relates an inferred underlying intrusive rock at the Forster Prospect to dextral shearing and dilational jogging along this northwest-trending structure. None of the above-mentioned structures have been verified in the field and their significance or existence is uncertain.

Dell (1997) conducted some structural mapping in the Fletchers Road area. Based on aerial photographs, he proposed several different fault directions and also interpreted that the silica and skarn alteration was located at the intersection of an east-directed thrust and a northeast-trending extensional strike-slip fault. The Cambrian conglomerate is poorly bedded but was interpreted by Dell (1997) to be intensely folded and sheared, with shear zones suggesting east-directed thrusting. He also proposed that the Jurassic dolerite contact to the east is another east-directed thrust. These structures are yet to be confirmed.

Summons (1999) interprets the major north-south structure to be a major mineralisation corridor ('the Forster corridor'), perhaps related to dextral shears along the Macquarie-Huon Fault Zone, focussing the fluids from an underlying Devonian or Cretaceous intrusive body. The interpretation of the Forster prospect lying above a Jurassic cone sheet is preferred.

Host-rock Petrology

The samples studied are listed in Appendix 3 and are summarised below, from detailed sample descriptions in Bottrill and Woolley (1996). The drillholes sampled are attached as Appendix 4. A glossary of terms is included as Appendix 1, and abbreviations are given in Appendix 2. Various analyses of samples are tabulated in Appendices 7 to 10.

Proterozoic

Dolostone

The dolostones occurring in the Glovers Bluff inlier belong to the Neoproterozoic Weld River Group (Calver, 1998). These rocks are white to dark grey, massive or oolitic, and mostly fine grained. They can be seen in the Weld River near Fletchers Eddy (477 800 mE, 5 235 550 mN).

The dolostones are variable in texture and composition and include the following varieties:

- relatively pure, fine-grained and mainly textureless dolostone;
- breccias which may contain very minor serpentine and clays (plate 1);
- oolitic dolostone (plate 1); and

- siliceous dolostone.

One sample exhibits diopside reaction rims between carbonate grains and disseminated chert patches (plates 5, 6). This sample indicates that some siliceous material was present prior to metamorphism and alteration, perhaps being authigenic, diagenetic or introduced during an early brecciation event. Calver (1989) has shown that quartz is an abundant diagenetic cement phase in many dolostones. In the Forster Prospect area, subsequent metamorphism and metasomatism formed various magnesian skarns and siliceous zones, which are described below. Most of these skarns were later retrogressed (described below under *Alteration*).

Magnesian skarns

This group of rocks is complex and variable and their inter-relationships are poorly understood. Some different subtypes, based on the dominant minerals, have been defined and are described below. They are mostly magnesian skarns, in accord with the definition of Pertsev (1991), Zharikov (1991) and Aleksandrov (1998). The term skarn is used here in the non-genetic sense for a calc-silicate-rich rock, although they could also be described as calc-silicate hornfels or skarnoid (Meinert, 1992).

Diopside skarns

These rocks are not prominent in outcrop, but can be seen near Fletchers Eddy in the Weld River (477 800 mE, 5 235 550 mN, fig. 3), in the vicinity of the infilled costean at 478 100 mE, 5 234 080 mN, and in the core of diamond drill holes SW1 and SW2 (Appendix 4). Pure dolostone and pure diopside skarn occur within a metre of each other near Fletchers Eddy, with no obvious intermediate rock types. Jurassic dolerite is usually found in close proximity.

Some of these rocks consist of only diopside-clinopyroxene (some almost pure diopside, with <0.1% FeO_{tot} and <0.1% Al₂O₃), but they usually also contain variable to major amounts of quartz, calcite and retrograde serpentine and xonotlite; some also contain minor sulphide and arsenide minerals, magnetite, andradite, wollastonite, brucite, aragonite, fluorapophyllite and tobermorite (Appendix 1).

The diopside skarns are mostly very fine grained, but usually contain some coarser patches, bands and veins. Some textures resemble ooids, breccias and other sedimentary carbonate textures in the dolostones, but similar textures may also form during hydrothermal brecciation and skarn formation.

Sample R007647 exhibits diopside reaction rims between carbonate grains and disseminated chert patches in dolostone, indicating incipient diopside skarn formation, with the reaction controlled by silica diffusion (plates 5, 6). Fine-grained diopside veins and zones grade over several millimetres into coarser patches (crackle brecciation: G402165; plate 7), suggesting replacement of the carbonates was initiated along early net fractures. Later breccias exhibit cement fill texture (G402164; plate 20).

The direct reaction of dolomite and quartz to diopside indicates very high CO₂ fugacity (~0.99) and temperatures of 495 to 545°C at ~1 kb pressure (Winkler, 1976; Dipple and Ferry, 1996; fig. 6). The rarity of talc, tremolite or other hydrous prograde metamorphic minerals in the skarns indicates very low water activity and probably little prograde metamorphic reaction in the dolostones below 500°C (Winkler, 1976; Dipple and Ferry, 1996).

The Ca-silicates occur mostly in veins and vugs, and the assemblages suggest late overprinting of quartz and diopside-rich rocks by Ca-metasomatism at temperatures from >400°C to less than ~100°C (see *Alteration* section). There is some serpentine + carbonate alteration of diopside, but this is mostly very minor.

These rocks probably formed rapidly during contact metamorphism of variably siliceous dolostone, associated with near-anhydrous Jurassic dolerite emplacement. This can be deduced from the close association with dolerite; the mineralogy (lacking primary hydrous phases and volatile elements); remnant dolostone textures; the fine grain size of the

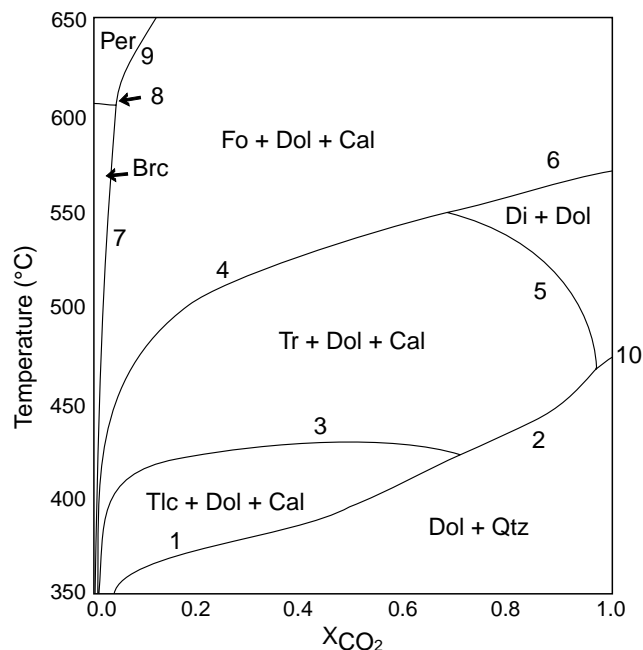


Figure 6

Stability relations in the system CaMg(CO₃)₂-SiO₂-H₂O at 1 kbar H₂O. Adapted from Dipple and Ferry, 1996.

Reactions (with increasing T):

- 1: Dol + qtz + H₂O → Talc + Cal + CO₂
- 2: Dol + qtz + H₂O → Trem + Cal + CO₂
- 3: Tlc + cal + qtz → Trem + H₂O + CO₂
- 4: Dol + Trem → Fo + Cal + qtz + CO₂ + H₂O
- 5: Trem + Cal → Di + Dol + CO₂ + H₂O
- 6: Dol + Di → Fo + Cal + qtz
- 7: Dol + H₂O → Brc + Cal + CO₂
- 8: Dol → Periclase + Cal + CO₂
- 9: Brc + Cal + CO₂ → Periclase + H₂O

skarn; and evidence of primary quartz in dolostone. The distribution of the diopside skarns may be controlled more by the original silica content of the dolostones rather than by the degree of infiltration of siliceous hydrothermal fluids.

Ophicalcite

This is probably the most common of the magnesian skarn types in this area. It is not abundant in outcrop, as it is readily weathered and eroded in the acid soils of the region, but can be found in the Weld River near Fletchers Eddy (477 800 mE, 5 235 550 mN) and in the vicinity of the infilled costean at 478 100 mE, 5 234 080 mN. Most of the studied samples came from the core of diamond-drill holes SW1 and SW2 (Appendix 4).

These highly altered rocks consist mostly of calcite and serpentine, usually with calcite dominant. Diopside may also be major, and minor amounts of brucite, andradite, talc, tremolite, magnetite, loellingite, protographite, sphalerite and galena are common.

The ophicalcites appear to have been derived, in part, from the silicification of the brucite-bearing rocks (see

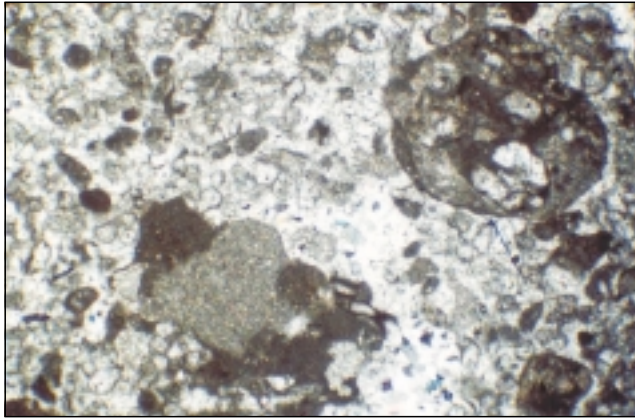


Plate 1

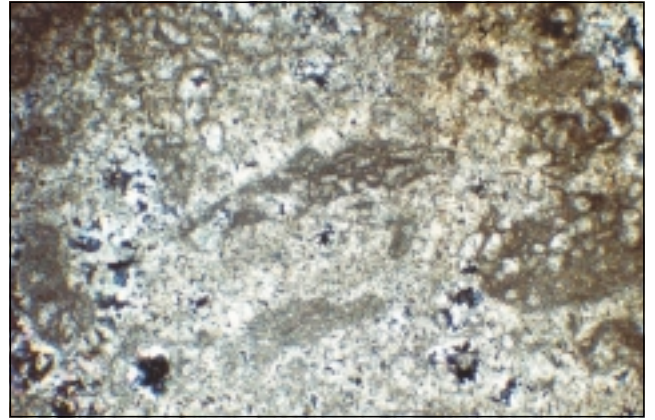


Plate 2

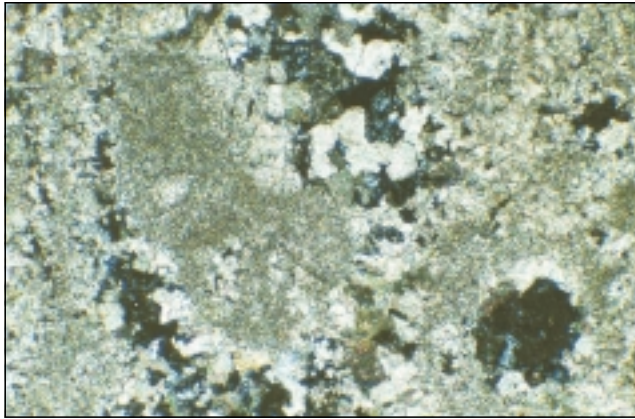


Plate 3

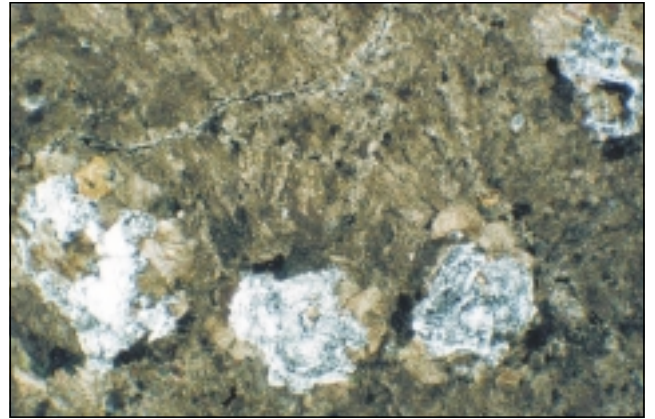


Plate 4

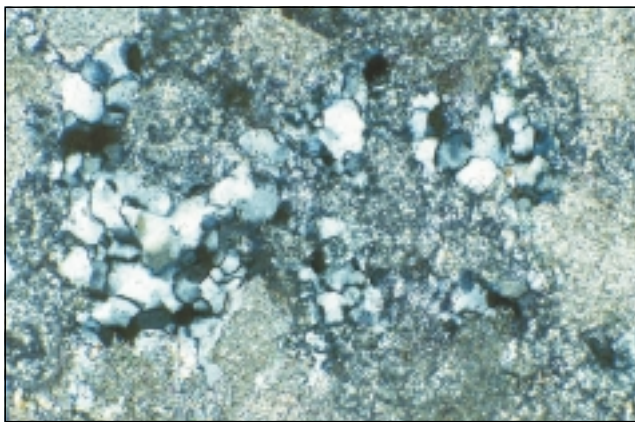


Plate 5

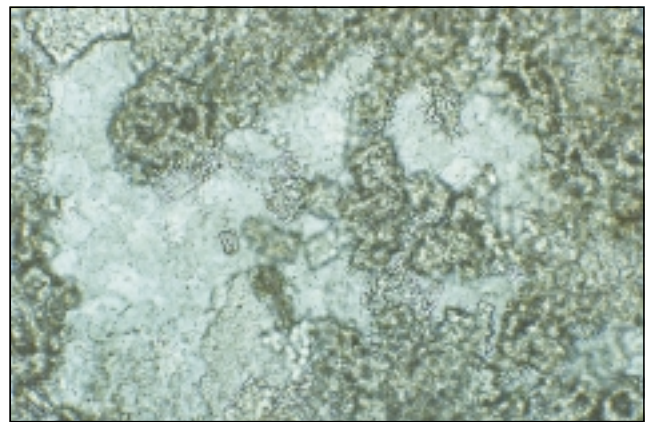


Plate 6

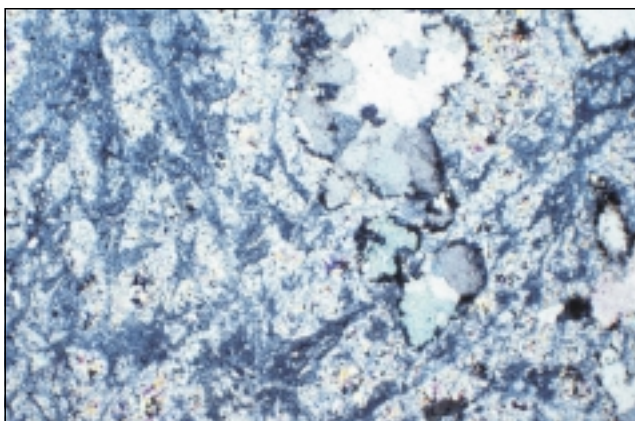


Plate 7

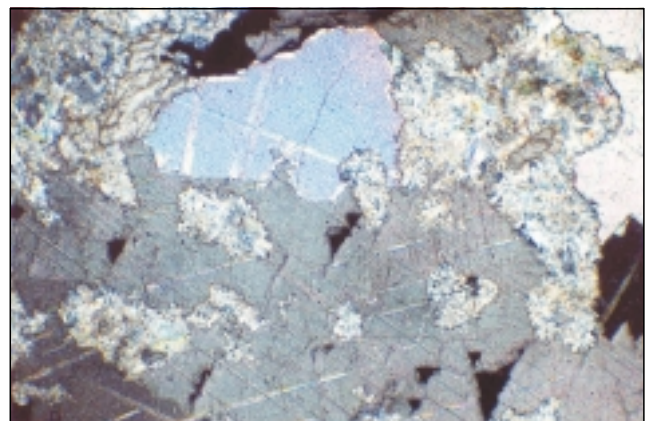


Plate 8

Captions, Plates 1–8

Plate 1. Dolostone showing breccia and oolitic textures. Sample R007645, cross polarised light. Field of view: 1.7×1.1 mm.

Plate 2. Dolostone showing partial replacement by ophicalcite (calcite-serpentine aggregates). Sample R007642, cross polarised light. Field of view: 4.4×3.0 mm.

Plate 3. Magnified view of previous photograph, showing serpentine pseudomorphic after forsterite(?). Sample R007642, cross polarised light. Field of view: 1.7×1.1 mm.

Plate 4. Brucite pseudomorphic after periclase(?) in calcite. Sample R007646, cross polarised light. Field of view: 4.4×3.0 mm.

Plate 5. Granular to fibrous diopside in reaction rims between quartz and dolomite in siliceous dolostone. Sample R007647, cross polarised light. Field of view: 0.7×0.5 mm.

Plate 6. Diopside reaction rims between quartz and dolomite in siliceous dolostone, showing prismatic diopside needles. Sample R007647, plain polarised light. Field of view: 0.7×0.5 mm.

Plate 7. Massive, fine-grained diopside skarn, showing breccia texture and calcite porphyroblasts. Sample G402165, cross polarised light. Field of view: 7×11 mm.

Plate 8. Talc pseudomorphic after forsterite(?). Sample R007641, cross polarised light. Field of view: 4.4×3.0 mm.

below), but probably also resulted in large part by retrograde or hydrothermal alteration of forsterite calciphyres (a common rock type in magnesian skarns; Aleksandrov, 1998). Forsterite was not directly observed due to pervasive alteration, but is inferred from serpentine pseudomorph textures (plates 2, 3). In the absence of tremolite, forsterite is stable above about 550°C , at very high CO_2 fugacity (~ 0.99) and ~ 1 kb pressure (Dipple and Ferry, 1996, 1976; fig. 6).

Brucite marbles

These rocks are rare in outcrop, but can be found north of Hogsback Hill ($477\ 720$ mE, $5\ 237\ 470$ mN) and in the core of diamond-drill holes SW1 and SW2 (Appendix 4). They were probably more abundant, but are obscured by alteration (serpentinisation).

Brucite marbles contain mostly calcite, with up to $\sim 35\%$ brucite and 10% serpentine, plus minor diopside, andraditic garnet, sulphides and other minerals. Talc is rare. The brucite occurs mostly as aggregates in small equant grains (<0.5 mm but usually <0.1 mm), probably pseudomorphing periclase (plate 4), but in some rocks it occurs as fine-grained primary flakes. Brucite appears to be partially replaced by serpentine in some rocks. The rocks are cut by some serpentine veins, with

minor brucite, andradite, and sulphide minerals. Andradite and sulphides are mostly restricted to these serpentine veins, and may have been introduced with siliceous serpentine-forming hydrothermal fluids, rather than originating in the dolostone. The andradite is very hydrous (Appendix 9), indicating that it was formed at relatively low temperature (probably $<350^{\circ}\text{C}$; Gustafson, 1974).

The brucite marbles were probably derived from the thermal decarbonation of dolostone, and the presence of primary brucite indicates temperatures of ~ 550 – 600°C , at low CO_2 fugacity (~ 0.1) and ~ 1 kb pressure (Winkler, 1976; Dipple and Ferry, 1996). Periclase indicates peak temperatures $>600^{\circ}\text{C}$ at low CO_2 fugacity, or $>800^{\circ}\text{C}$ at high CO_2 fugacity, at ~ 1 kb pressure (fig. 6). The formation of brucite thus indicates a change during progressive alteration from original CO_2 -dominated fluids, to H_2O -dominated retrograde metamorphism.

Talc marble

This was found in only one outcrop in the Weld River ($477\ 530$ mE, $5\ 235\ 065$ mN), some 300 m laterally from the nearest known dolerite body. The rock contains mostly calcite and talc, possibly replacing forsterite (plate 8), with only minor serpentine and trace tremolite, in a brecciated marble. These talc-calcite assemblages indicate thermal metamorphism at intermediate values of f_{CO_2} at $T \sim 350$ – 600°C (Winkler, 1976; Dipple and Ferry, 1996; fig. 6).

Discussion

Overall, the magnesian skarns indicate a range of metamorphic conditions, probably initiated at very high CO_2 fugacity and high temperature ($>600^{\circ}\text{C}$). Although the zoning is obscure, the diopside-rich rocks mostly appear to occur close to dolerite with brucite more distant, relative to ophicalcite (although primary quartz contents may affect this). These prograde assemblages fit in well with the common skarn sequence described by Aleksandrov (1998) in contact metamorphosed dolostones at moderate to high temperature, in situations where there is only minor siliceous metasomatism:

igneous intrusive \rightarrow diopside skarn \rightarrow forsterite
calciphyre \rightarrow periclase calciphyre \rightarrow dolostone

This sequence, and the general mineralogy and textures, implies a local heat source, especially for the diopside skarns, and the Jurassic dolerite is the only reasonable candidate. In contrast to Devonian granite-related skarns, these skarns are limited in distribution, their grain size is relatively fine, there is very limited metasomatic infiltration, and few typical skarn minerals are present. For example, grossular-andradite, vesuvianite, magnetite, tremolite-actinolite and talc are all comparatively rare; and no epidote, scheelite, fluorite, tourmaline, chondrodite or bismuth or molybdenum minerals were observed. The hydrous andradite that is present occurs

in serpentine veins and indicates introduction of late-stage oxidising fluids.

The thermal decarbonation induced by intrusion of the dolerite into dolostone probably resulted in crackle brecciation, due to fluid overpressure by the resulting CO₂-rich fluids. This brecciation and resultant pressure drop would have caused a subsequent influx of CO₂-poor groundwater and/or metamorphic water, progressively forming periclase, brucite and serpentine with waning temperature. Devolatilised calcium-rich fluids migrated into siliceous breccia and formed the Ca-silicate rocks.

Overall, these assemblages indicate a range of conditions, probably initiated soon after the intrusion of the Jurassic dolerite and accompanying devolatilisation-related brecciation. The resultant pressure drop resulted in an influx of dolerite-heated, siliceous, CO₂-poor groundwater and/or metamorphic water, replacing periclase and forsterite with brucite and serpentine, with waning temperatures.

Cambrian

Mafic-ultramafic conglomerate (talc-amphibole rocks)

This is a variable group of sheared, mainly ultramafic and mafic-derived clastic rocks, varying from amphibolitic greywacke to talcose, ultramafic-rich polymict conglomerate. Where highly sheared and altered the rocks are talc-rich mylonite and phyllite, which are silicified in places. They are well exposed in the Forster Road outcrops, and on the south bank of the Weld River east of the adit (477 500 mE, 5 234 430 mN to 478 100 mE, 5 234 430 mN).

During low grade metamorphism and hydrothermal alteration the ultramafic rocks were replaced by talc, magnetite and hematite, and mafic rocks by chlorite and actinolite and possibly gedritic amphiboles (plate 10, analyses in Appendices 9 and 10). Some rocks are almost pure talc, and have been investigated as a commercial source of talc (Forster, 1992). The finer grained rocks contain mixtures of all the above minerals. Some of these rocks are very fine grained and mylonitic but some very coarse-grained pyroxenite-textured rocks occur. Most of the ultramafic rocks still contain chromite (analyses in Appendix 9), and some plagioclase is rarely preserved in the mafic clasts. One sample is a calcite-hosted ultramafic breccia, with talc-rich clasts partly altered to serpentine (i.e. grading into an opicalcite).

These rocks appear to have originally been poorly sorted arenite and rudite mostly derived from mafic-ultramafic complexes, and were highly tectonised and metamorphosed to upper greenschist facies, probably during regional metamorphism in the Devonian. They may also have been metamorphosed by the intrusion of the Jurassic dolerite.

Phyllite

A quartz-bearing, chloritic, feldspathic phyllite (sample G402210) occurs in a small area on the Weld River, between the dolostone and polymict conglomerate (478 000 mE, 5 234 450 mN). This may be an altered Cambrian intermediate volcanoclastic or epiclastic rock.

Parmeener Supergroup (Permo-Carboniferous sedimentary rocks)

Truro Tillite correlate

Palaeozoic mudstone is abundant in the area, particularly to the south of Forsters Prospect, and is exposed along Fletchers and Forster roads (fig. 2). The rocks mostly consist of pebbly, glaciogene mudstone of Late Carboniferous to Permian age. Some of the fresher rocks are hornfelsed (along the southern part of Fletchers Road) and contain prehnite and clinopyroxene. Most are highly argillised (weathered or hydrothermally altered) and some appear weakly silicified. The clasts (mostly <50 mm) include quartzite, conglomerate, phyllite, slate and possibly dolostone. The dolostones are usually leached out and the cavities filled with clays, and may be lined with prehnite.

Jurassic dolerite

These rocks are abundant in the area as sills and dykes, from less than a metre to several hundred metres thick. They are medium to very fine grained, mostly hard and dense (except when altered), with no obvious inhomogeneity or foliation. Most contain abundant orthopyroxene microphenocrysts, indicating that they are relatively undifferentiated and crystallised rapidly. Some dolerite bodies exhibit chilled margins, and some of these are bleached and variably to completely altered to prehnite, serpentine, amphiboles and smectites. Sporadic veins variably containing laumontite, calcite, quartz and/or prehnite cut the dolerite. Some dykes intrude the skarns, probably partly in the breccia zones. No amphibolitised or hybrid dolerite, as found near Cygnet and Kettering (Edwards, 1947; Taheri and Bottrill, 1999), has been identified near this area.

Undated intrusive rocks

Hornblende-rich igneous rocks

A collection of boulders, possibly representing a small igneous body, occurs in the Cambrian polymict conglomerate near 478 100 mE, 5 234 200 mN, about 300 m south of the Weld River (e.g. samples 107639, 107640). These boulders are of a slightly porphyritic, amphibole-rich, fine to coarse-grained igneous rock which contained moderate amounts of brown titaniferous hornblende, plagioclase, clinopyroxene, olivine(?) and biotite prior to alteration. The rock has been variably to moderately altered to assemblages including tremolite-actinolite, chlorite, carbonates, sericite, epidote-clinozoisite and serpentine. The rock

appears to be a calc-alkaline lamprophyre in texture and composition, probably a spessartite (Rock, 1991), although the coarser texture of some parts would indicate classification as an appinite. Some electron microprobe analyses of pyroxene and amphibole minerals in sample 107640 are included in Appendix 9. Some basaltic rocks collected at Lightning Ridge (3.5 km to the north) are also Ti-amphibole-pyroxene bearing and are probably related.

Geochemistry undertaken by Boyd (1996, including REE analysis) and in this study suggests that this rock has affinities with the basalt of the Neoproterozoic Crimson Creek Formation of northwestern Tasmania (fig. 7; Brown, 1986), but more whole-rock and microprobe analyses are needed to confirm this correlation. Petrographically, the rock is similar to both

the Devonian or Cretaceous lamprophyres suites which occur in western and northeastern Tasmania (Sutherland and Corbett, 1974; McClenaghan *et al.*, 1994). Cretaceous lamprophyres are reported from the Cygnet area but these are mineralogically quite different (sanidine-rich) to the rock observed at the Forster Prospect, although they may be temporally related (Taheri and Bottrill, 1999).

Other mafic dyke-like bodies have been recognised within the Cambrian sequences in the Weld River (478 150 mE, 5 234 390 mN) and in the Forster Road roadcuts (477 950 mE, 5 233 480 mN). These are all highly weathered, but differ substantially in geochemistry to the lamprophyric rocks and the Jurassic dolerite dykes (fig. 7, Appendices 7, 8).

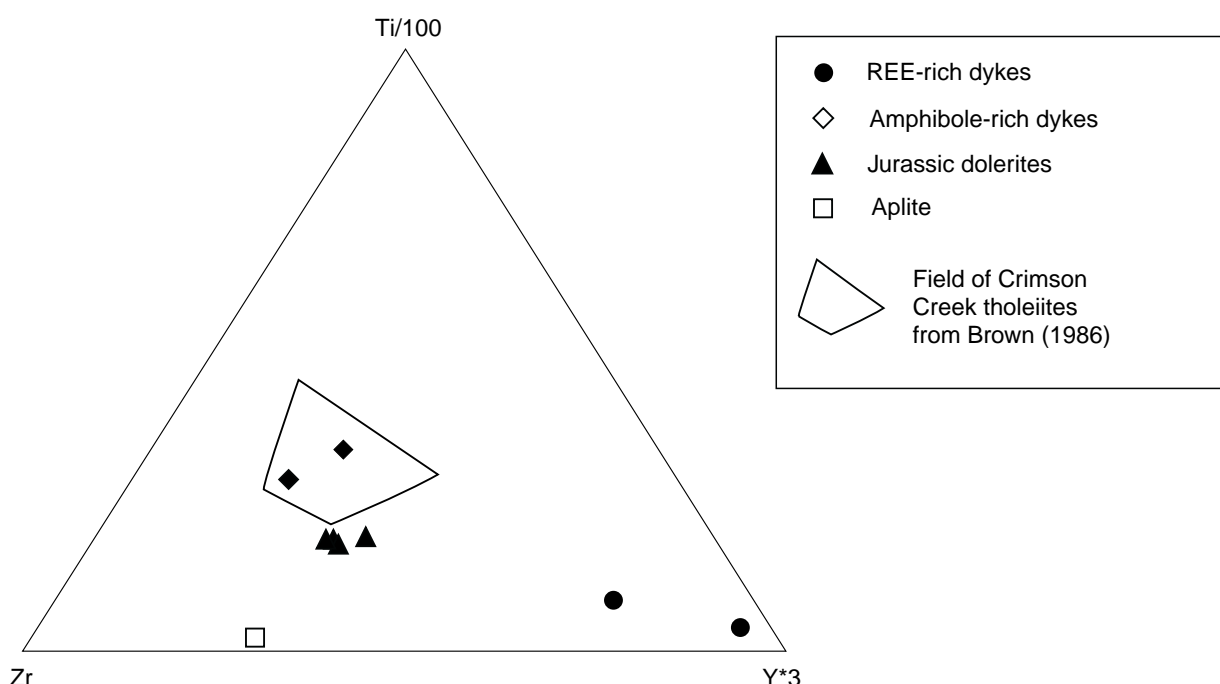


Figure 7

Triangular diagram showing Ti-Y-Zr plots for the main igneous rocks of the Forster Prospect area.

Mineralisation and Associated Alteration

Overview

Metallic mineralisation recorded from the area includes gold, nickel and zinc, although anomalous copper, lead, silver, arsenic, antimony, chromium and cobalt are also present (Appendices 7, 8). The alteration associated with the mineralisation is variable and poorly defined. It includes siliceous, serpentinous, carbonate, talc-hematite, argillic and calc-silicate styles. Sulphide mineralisation is rare and limited to traces in skarns and cherts. Gold has only been observed visually in the 'silica-clay zone' (as grains from 50–125 μm , Summons, 1997) and in some skarn (see *Mineralisation*), but it is anomalous in various rock types, as described below. Most medium to high-grade

gold mineralisation (>1 g/t) in the area is related to a silica-clay zone, but low grade Au, Zn, Pb, Ni and As mineralisation is more widespread. The mineralisation is spatially related to magnesian skarns and some argillaceous, limonitic and silicified zones, described below.

Siliceous rocks

This alteration type includes a major but variably silicified zone that runs north from the Forster Road/Fletchers Road junction over the Weld River to north of Hogsback Hill. Mineralisation in this rock type occurs in at least three parageneses; disseminated, in opal veins, and in galena veins.

The siliceous rocks are remarkably diverse, and include massive fine-grained cherts, opaline veins and highly porous coarse quartz breccias. Remnant included minerals, clasts and textures indicate various origins, including silicified mudstone (Permo-Carboniferous and/or Proterozoic?), Proterozoic dolostone and Cambrian ultramafic and mafic rocks (plate 9). Clasts of these different groups are intimately intermixed in some breccias (e.g. samples G402190, G402207). Fine-grained quartz appears to have filled intra-clast cavities prior to leaching and partial replacement of dolostone clasts, although these zones grade over several millimetres into the coarser patches and vughs (samples G402481, G402194, plates 11, 12). Some of the quartz vughs are filled and partly replaced by xonotlite, other Ca-silicates and minor sulphide minerals, indicating calc-silicate alteration post-dated most silicification (samples G402153, G402163, plate 13). Contacts between Jurassic dolerite intrusions and the siliceous, cherty rocks show dolerite injecting and enveloping the chert (sample G402154; plate 14), which indicates that the major silicification event predates the Jurassic dolerite.

The vuggy silica zones are possibly, in part, silicified collapse breccias formed in the dolostone and some basal parts of the overlying Permo-Carboniferous rocks, as at Mt Weld (Appendix 5). No evidence for tectonic breccias was found, and there is no evidence for these zones forming conduits, cutting the Permo-Carboniferous rocks, to the surface. The coarser grained quartz breccias (e.g. G402153) are probably straight-forward dolostone-replacement breccias (as from the silicified caves at Mt Weld), although some have been Ca-metasomatised (see the quartz-xonotlite skarns) or re-silicified. Late-stage chalcedony and opal veins cut these and other rocks. Minor amounts of fine organic material (pyrobitumen?), hematite, magnetite and pyrite occur in some of these rocks.

Silicified ultramafic rocks with disseminated arsenide minerals

This style of mineralisation was only observed in an outcrop on the Weld River at 478 290 mE, 5 234 310 mN. The host rock is a chert that contains chromite and talc, and appears to be a silicified ultramafic rock.

A sample from this locality (C107889) was studied petrographically, geochemically and by electron microprobe analysis and found to contain fine-grained euhedral to anhedral, disseminated Ni-Co-Fe arsenide, sulphide and sulpharsenide minerals. Primary grains of antimonian nickeline and cobaltite (both mostly <50 μ m) are rimmed and partly replaced by antimonian and cobaltian gersdorffite (<10 μ m). Very fine-grained aggregates of nickeloan marcasite and symplectite appear to be a late-stage hydrothermal or weathering product. Millerite may also be present but was not confirmed. Gold is not anomalous in this sample (<0.05 g/t; see *Geochemistry* section).

Captions, Plates 9–16

Plate 9. Quartz breccia showing chromite grains, probably derived from the Cambrian greywacke and conglomerate. Sample G400235, cross polarised light. Field of view: 4.4 \times 3.0 mm.

Plate 10. The probable precursor to Plate 9: ultramafic-derived greywacke showing tremolitic amphibole, chromite and talc. Sample G402138, cross polarised light. Field of view: 4.4 \times 3.0 mm.

Plate 11. Quartz breccia (near C107825) showing net fracturing and vuggy clasts.

Plate 12. Quartz breccia showing a network of cherty quartz infilled with coarser, partly vuggy, quartz. Sample G402481, cross polarised light. Field of view: 11 \times 7 mm.

Plate 13. Vuggy quartz breccia infilled with fibrous xonotlite and pectolite. Sample G402141, cross polarised light. Field of view: 7 \times 11 mm.

Plate 14. Quartz breccia clast in dolerite (near the contact). Sample G402154, cross polarised light. Field of view: 7 \times 11 mm.

Plate 15. Quartz breccia showing chert cut by banded and recrystallised quartz and later opal/chalcedony veins. Sample G402163, cross polarised light. Field of view: 4.4 \times 3.0 mm.

Plate 16. Quartz-opal breccia showing angular quartz in an opal matrix. Sample C107806, cross polarised light. Field of view: 7 \times 11 mm.

Galena veinlets in massive chert

This style of mineralisation was only observed in an outcrop on the Weld River at 478 150 mE, 5 234 390 mN, and in percussion drilling about 300 m to the south. The massive chert host may be a silicified dolostone.

A sample (C107884) from the former locality was studied petrographically. This rock consisted of highly irregular to stylolitic veins of quartz, galena, sphalerite, and minor chalcopyrite, tetrahedrite and cubanite (plates 22, 23). The grain size of the sulphide minerals is mostly <50 μ m.

Gold is rarely anomalous (<0.2 g/t; see *Geochemistry* section) and was not observed visually.

Opal

Opal is common throughout the siliceous zone, particularly north of the river, and in some altered ophalcite rocks exposed along the river. Opal-hosted mineralisation was observed in outcrop on the Weld River, near 478 290 mE, 5 234 315 mN (sample C107890), in the 'gold adit' at 478 160 mE, 5 234 530 mN (samples C107838, C107842), and on the track 700 m south of the river at 478 100 mE, 5 233 870 mN (sample G402205).

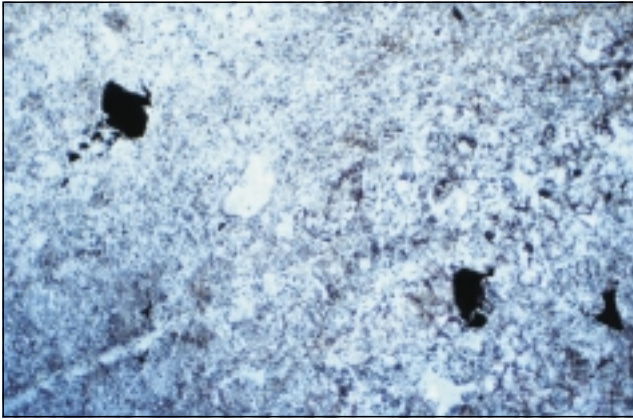


Plate 9

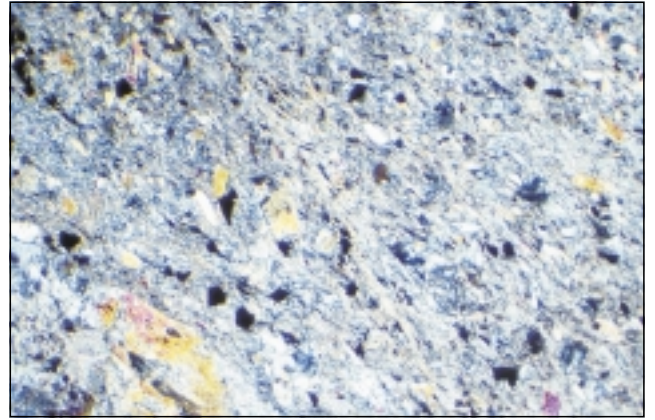


Plate 10

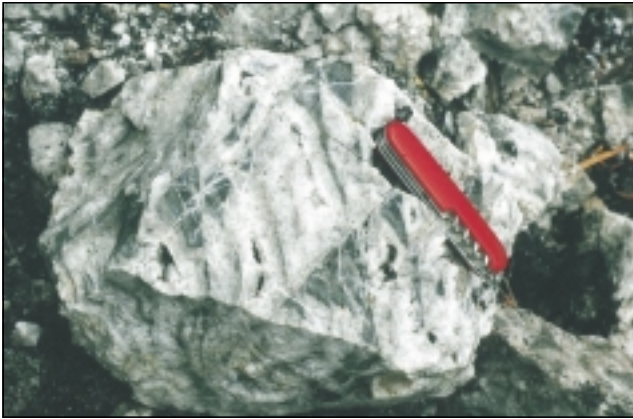


Plate 11

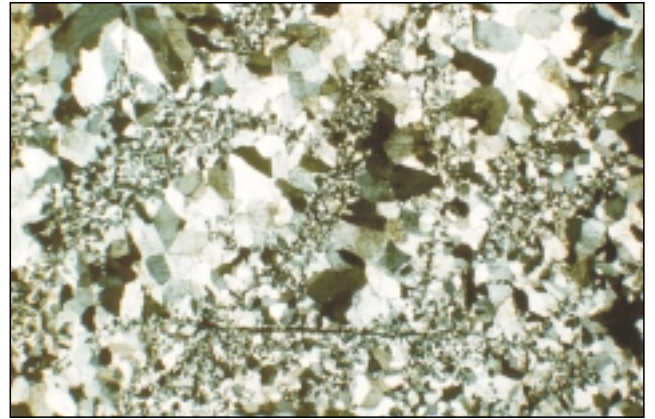


Plate 12

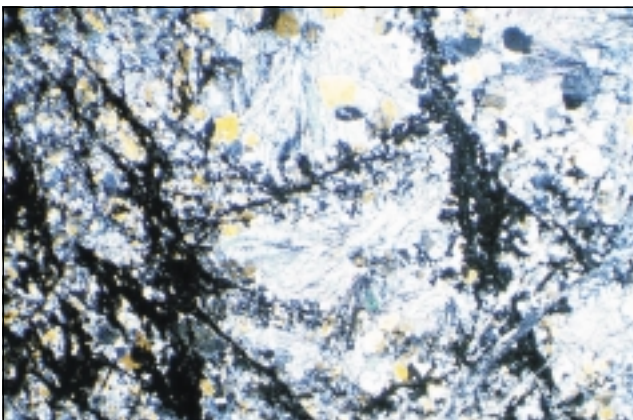


Plate 13

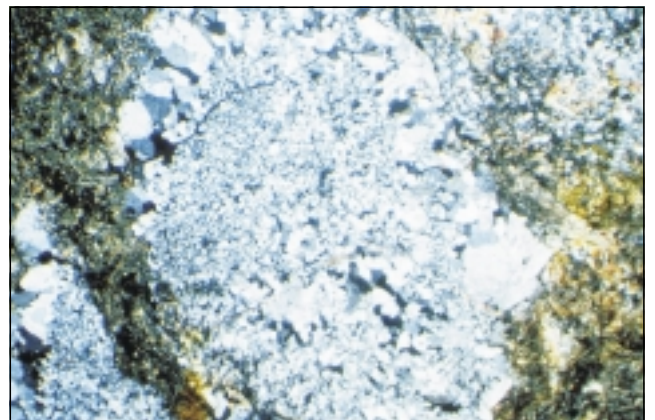


Plate 14

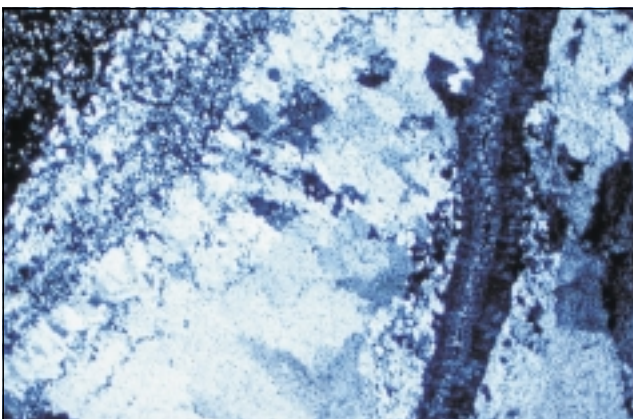


Plate 15

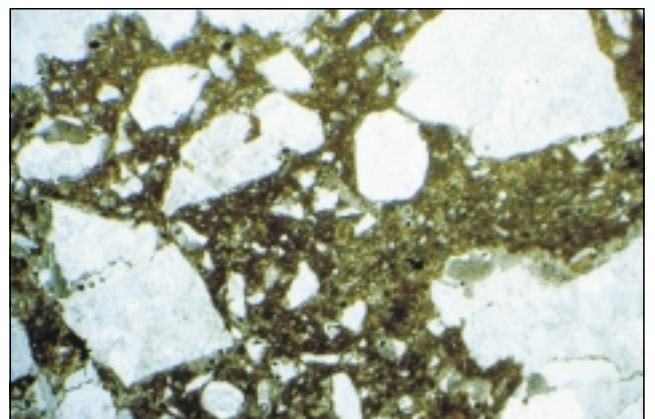


Plate 16

The opal occurs mostly in veins cutting cherts, ophicalcites and quartz breccias. It is colloform, grading into chalcedony, and is colourless to blue and black. The black opal commonly contains abundant ultrafine framboidal pyrite (<1 mm; plate 23), or is limonitic where weathered. Gold is anomalous in many opals (<0.64 g/t; see *Geochemistry* section) but was not observed visually. The opalised ophicalcites contain calcite and opal, with rare chalcedony and minor serpentine (partly altered to opal).

Other

Other siliceous rocks found in the area include hematitic chert clasts in the Cambrian conglomerate, and some possible Tertiary silcrete (not *in situ*). These are probably unrelated to mineralisation. Small quartz \pm laumontite, chlorite and prehnite veins also occur in the contact zones of Jurassic dolerite, e.g. in the southern part of the prospect (477 500 mE, 5 232 870 mN) and in DDH SW1 (samples C107864 and G402155). These appear unmineralised and are probably due to late magmatic fluids infiltrating shrinkage cracks during cooling. Similar veins have been seen in a quarry at Lower Longley, south of Hobart.

Discussion

The rocks include massive fine-grained cherts and highly porous, vuggy quartz breccias originating variously as silicified mudstone (Permo-Carboniferous and/or Proterozoic?), Proterozoic dolostone and Cambrian ultramafic and mafic rocks, in places intermixed. Silicified karst breccias in Proterozoic dolostone and Permo-Carboniferous mudstone at Mt Weld appear to be related (Appendix 5), indicating post-Permian silicification.

Some vuggy quartz zones at the Forster Prospect are filled and partly replaced by xonotlite, other Ca-silicates and minor sulphide minerals, indicating that silicification pre-dated the calc-silicate alteration. Contacts between Jurassic dolerite intrusions and cherts show dolerite injecting and enveloping the chert, which also indicates at least one silicification event pre-dating the Jurassic dolerite.

The opalised rocks may represent epithermal or groundwater-related silicification under near-surface conditions. The fresh, glassy nature of much of the opal suggests that at least some of the hydrothermal activity is relatively young (Late Mesozoic or younger).

Quartz-bearing veins in dolerite also indicate some very late-stage silicification. Similar veins have been observed in Jurassic dolerite elsewhere, such as at Longley (Bottrill, unpublished data).

Some of the silicified ultrabasic rocks and Al-Ti-Zr-rich rocks (probably Permo-Carboniferous mudstone) are very likely to be formed by the silicification of roof and wall material in collapse breccias in karst zones in dolostone, as occurs at Mt Weld (Appendix 5).

Minor amounts of fine organic material (pyrobitumen?), hematite, magnetite and pyrite occur in some of these rocks. This mineralogy, and the spatial association with gold mineralisation, suggests that there may be some potential for Carlin-style gold deposits (Kuehn and Rose, 1995), although gold is not highly anomalous in most of the highly silicified rocks. The chert textures resemble both those in the Relief Canyon gold deposit of Nevada (Wallace, 1989), which is considered to be of carbonate replacement origin, and those in the silica-rich zones of high sulphidation epithermal deposits (Thompson and Thompson, 1996).

Base metals (Pb, Zn, Cu, Ni, Co and As) are anomalous in many of the gold zones at the Forster Prospect, but these correlations are poor and are host rock dependent (see *Geochemistry* section).

Skarns

Calc-silicate rocks

These rocks are complex and their distribution is poorly understood. They occur near Fletchers Eddy in the Weld River (at 477 800 mE, 5 235 550 mN), and in the core of diamond-drill holes SW1 and SW2 (Appendix 4). All occurrences appear to overlie, and are within a few hundred metres laterally of, Jurassic dolerite. The dolerite bodies are only altered near their margins.

These rocks contain major quartz and xonotlite, with small and variable amounts of wollastonite, diopside, prehnite, pectolite, scawtite, talc, laumontite, tobermorite and several unidentified Ca-Fe, Ca-Mg and Ca silicates (see *Glossary*, Appendix 1). A 10-Angstrom silicate, originally thought to be an illite or celadonite-type mica, was later found to be an unidentified hydrous Ca-Fe-Al silicate.

Xonotlite is a hydrous calcium silicate of the pyroxenoid group, similar to wollastonite, but forming at lower temperatures (~140–400°C; Speakman, 1968; Harker, 1965). Pectolite is a similar hydrous calcium sodium silicate. Scawtite (sample G402161) is another hydrous calcium silicate, which usually forms in low temperature, CO₂-poor assemblages (~140–300°C; Harker, 1965). With the exception of wollastonite and possibly scawtite, these Ca silicate minerals do not appear to form directly from metamorphism of carbonates and quartz, or by hydration of less hydrous Ca-silicate minerals (Harker, 1965; Smith, 1954; Mason, 1957). They probably formed from the reaction of Ca-rich hydrothermal fluids (derived from the alteration of the dolostone and skarns, and heated by dolerite?) with silicified, cavernous, dolostone-derived breccias, as discussed above, under relatively low pressure.

Textures are highly variable. Some of these rocks contain the Ca-silicate and sulphide minerals as veins (plate 19), vugh-fill (plate 13) or as pervasive replacement of quartz (plates 17, 18). Fine-grained (<100 mm), disseminated sphalerite, millerite and

minor magnetite occur in the Ca-silicate clots and veins. Gold is mostly anomalous but was not observed visually (see *Geochemistry* section).

The dolerite intruding the skarns is variably altered to prehnite and smectite \pm calcic amphiboles \pm calcite \pm serpentine \pm chlorite \pm laumontite. This alteration is probably a result of the above-mentioned late-stage fluids reacting with the brecciated dolerite contact zones.

Ophicalcites

The ophicalcites, discussed above, are serpentinised magnesian skarns. They appear to have been derived, in part, from the silicification of the brucite and periclase-bearing rocks (see below), but probably were also a result, in large part, of retrograde or hydrothermal alteration of forsterite calciphyres (see above).

Alteration minerals in these rocks include calcite, serpentine, brucite, andradite, and rare talc, sjogrenite, hydromagnesite and magnetite. Ore minerals are very minor and fine grained (mostly <100 μ m) and occur mostly within serpentine-rich veins and stockworks with minor andradite, magnetite, and protographite (G402174; plate 21). The most abundant sulphide mineral is sphalerite (<0.5 vol.%), with trace gold (<0.2 g/t), galena, loellingite, pyrrhotite, millerite and chalcopyrite.

Gold is generally anomalous and one gold grain (1 \times 2 mm) was seen, associated with sphalerite, galena, loellingite, protographite and magnetite (Sample G402177).

Some ophicalcites are considered to be altered ultramafic rocks (Lavoie and Cousineau, 1995), but there is little evidence for this with these rocks (e.g. chromite is absent, and there are some possible sedimentary carbonate textures). There is, however, some distinct serpentine-carbonate alteration of both the Cambrian clastic rocks and dolomite-hosted dolerite veins.

Diopside skarn

Diopside skarns, intersected in the two diamond-drill holes and found in outcrops near the Weld River, contain minor fine-grained (<100 μ m) niccolite, rammelsbergite and loellingite in talcose breccia (plate 20). The niccolite is partly altered to ferroan rammelsbergite and nickeloan loellingite.

Gold is anomalous but was not observed visually.

Carbonate alteration

This is not a major alteration style in this area, but there is widespread carbonate veining in the skarns (with calcite, aragonite, dolomite, hydromagnesite and sjogrenite). This is probably a result of late-stage CO₂-rich fluids. No sulphide mineralisation appears to be associated with these veins. Siderite is locally

abundant and occurs in some ophicalcites. Its relation to mineralisation is not known.

Altered Cambrian rocks

The Cambrian dykes and clastic rocks are extensively altered to talc, hematite and various amphiboles (tremolite, actinolite and gedrite), but it is uncertain as to whether this is of low-grade metamorphic or hydrothermal origin, or a combination of the two. The talc and amphibole suggest minor silicification. There is no obvious relationship to the skarns or mineralisation. There is also some carbonate alteration of the Cambrian clastic rocks to form matrix calcite. Siderite is locally abundant and replaces clasts or forms patches in Cambrian clastic rocks and dolerite, but its relationship to mineralisation is not known.

Chromite is abundant throughout these rocks, and is often coarse grained and euhedral to brecciated.

Garnierite-type nickel-magnesium silicates (possibly mostly nickeloan saponite?) probably occur, representing some of the bright green clays in this sequence (which contains >0.1% Ni in places).

In summary, these rocks appear to have originated as poorly-sorted arenite and rudite, in part derived from mafic-ultramafic complexes, and were highly tectonised and weakly altered, silicified and metamorphosed to talc-amphibole-hematite rocks of greenschist facies (perhaps due to the intrusion of Jurassic dolerite?).

Silica-clay/'argillic alteration' zone

Relatively rich patches of gold (<10 g/t) have been encountered in a shallow, siliceous, argillic zone and associated ferruginous zones. The ferruginous zones resemble laterite but are poorly understood and may alternatively represent humic acid leach fronts, gossans, bog-iron deposits or mound-spring deposits. Most medium to high-grade gold mineralisation in the area is contained in this relatively shallow zone of clay and rubbly silica. This zone is best exposed at the Fletchers Road/Forster Road junction (478 200 mE, 5 233 490 mN), but the highest gold values are usually between 15–40 m from surface. Gold appears to be hosted within the clay rather than the silica (see *Geochemistry* section).

The outcrops exposed along Fletchers Road are mostly highly argillic, within the Permo–Carboniferous Truro Tillite correlate, the Cambrian ultramafic conglomerate and the silica-clay zone. Halloysite is the dominant phase, but this cannot be shown to be of hydrothermal origin, and may relate to deep Tertiary weathering of the Permo–Carboniferous sequences. Kaolinite, dickite and nacrite, the polymorphs more typical of hydrothermal deposits, appear to be absent in this zone, although kaolinite occurs in some weathered Cambrian conglomerate and dykes nearby. Green Cr–Ni-rich smectite-rich clays in the Cambrian clastic rocks may also have a weathering origin.

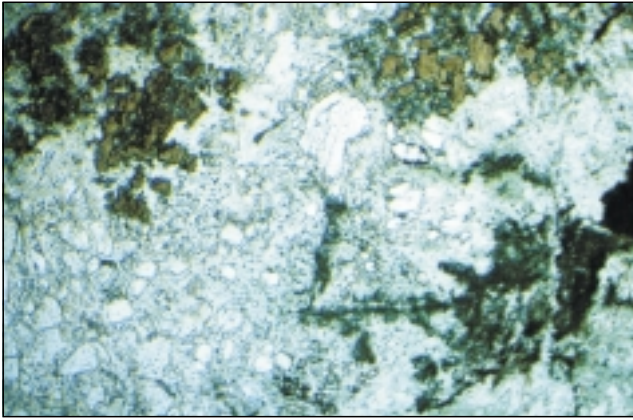


Plate 17

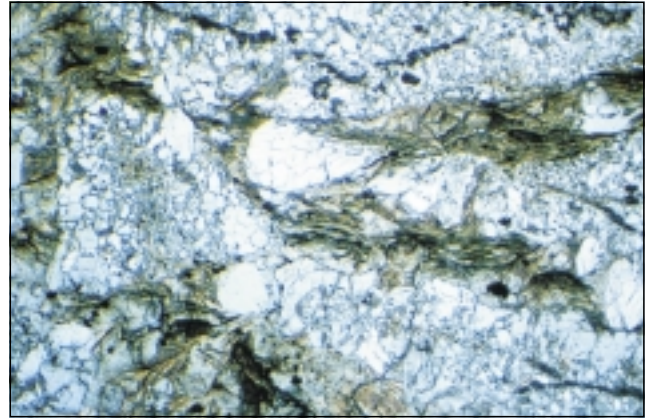


Plate 18

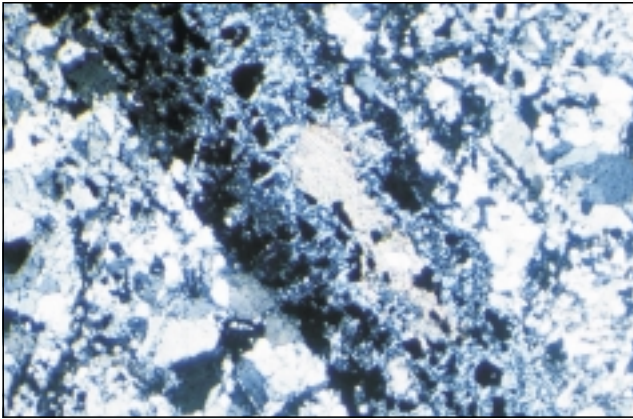


Plate 19

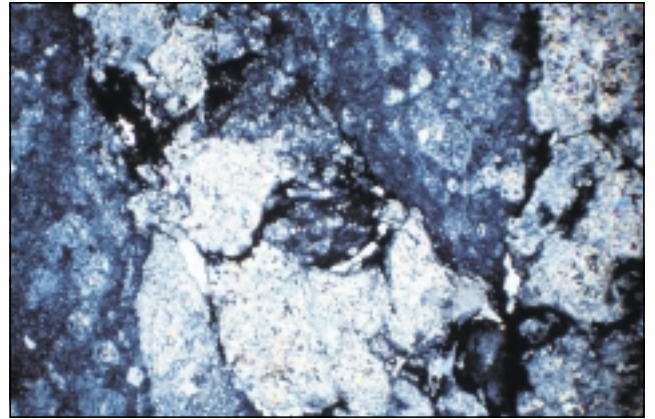


Plate 20

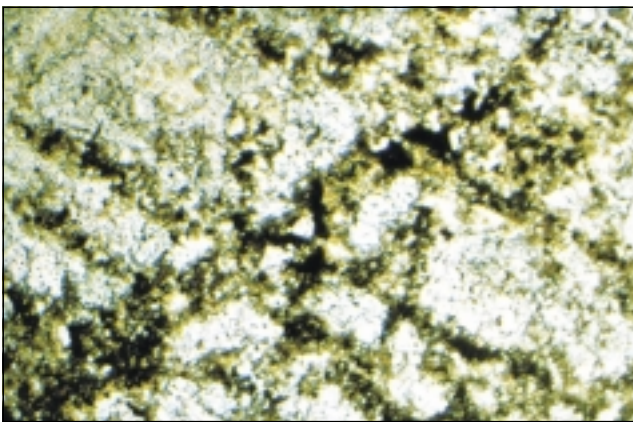


Plate 21

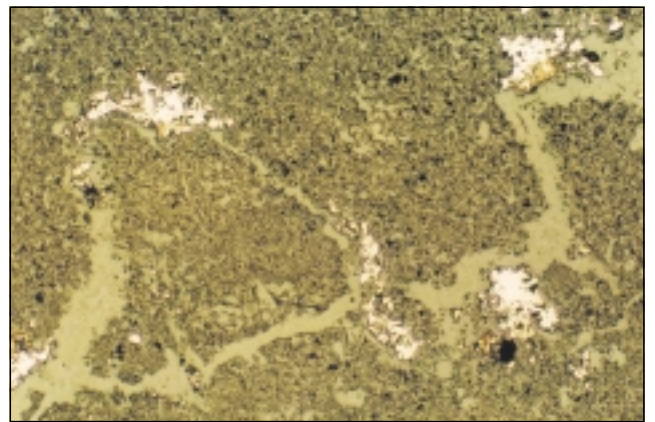


Plate 22

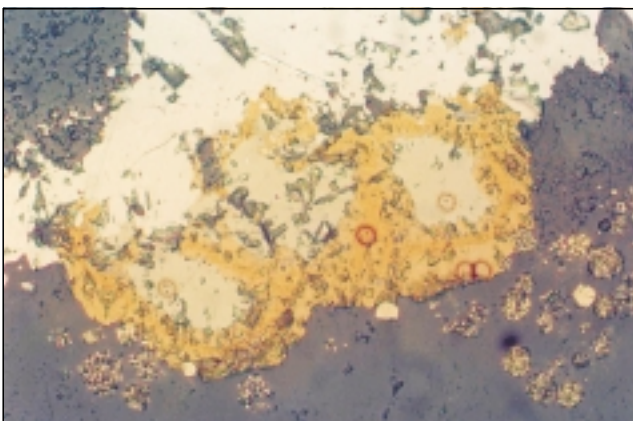


Plate 23

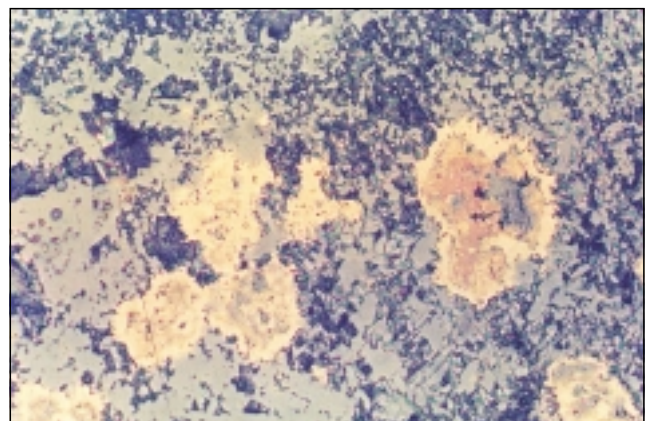


Plate 24

Captions, Plates 9–16

Plate 17. Quartz breccia showing replacement by various $\text{Ca} \pm \text{Fe} \pm \text{Al} \pm \text{Mg}$ silicates (green).

Sample G402163, cross polarised light.

Field of view: 4.4×3.0 mm.

Plate 18. Quartz breccia altering to various $\text{Ca} \pm \text{Fe} \pm \text{Al} \pm \text{Mg}$ silicates (green).

Sample G402169, cross polarised light.

Field of view: 4.4×3.0 mm.

Plate 19. Quartz breccia showing a vein of xonotlite, calcite and sphalerite (black).

Sample G402166, cross polarised light.

Field of view: 4.4×3.0 mm.

Plate 20. Calcitic diopside breccia showing dark areas with fine-grained Fe-Ni-Co arsenides.

Sample G402164, cross polarised light.

Field of view: 7×11 mm.

Plate 21. Brecciated ophicalcite showing stockwork veins of sjogrenite, loellingite, magnetite, sphalerite, andradite and other phases.

Sample G402174, cross polarised light.

Field of view: 4.4×3.0 mm.

Plate 22. Chert showing irregular veins of chalcedony, galena (white), sphalerite, pyrite, tetrahedrite, chalcopryrite and other sulphide minerals.

Sample C107884, plain polarised light.

Field of view: 2.2×1.4 mm.

Plate 23. Magnified view of Plate 22, showing tetrahedrite (pale grey) altering to chalcopryrite (brownish yellow) and cubanite (similar but paler), plus galena (white) and framboidal pyrite in chalcedony.

Sample C107884, cross polarised light.

Field of view: 0.22×0.14 mm.

Plate 24. Diopside skarn breccia (see Plate 20) showing grains of pinkish niccolite altering to loellingite and rammelsbergite (white).

Sample G402164, cross polarised light.

Field of view: 0.22×0.14 mm.

This zone contains vuggy silica identical to that in the skarns, plus more massive chert with moderate to high Ti, Zr and Cr contents (see *Geochemistry* section) which, together with the aluminous clay, strongly indicates contamination from the surrounding and overlying rocks (Permo-Carboniferous pebbly mudstone and Cambrian ultramafic and mafic-derived greywacke and conglomerate). This zone is considered to be a

weathered skarn, incorporating karst-collapse features, probably similar to the analogous gold-rich zones reported from the Browns Creek (Blayney, NSW) Cu-Au skarn (Smart and Wilkins, 1997). Texturally it resembles the siliceous sinter typical of high-sulphidation epithermal mineralisation, but it lacks veining or kaolinite, dickite, alunite, pyrite and other characteristic minerals.

Limonite-hosted

Colloform to massive and siliceous goethite occurs in surface outcrops in several areas ('gold adit'; 478 160 mE, 5 234 530 mN: Weld River; 478 100 mE, 5 233 870 mN: and on the drill track; 478 100 mE, 5 234 400 mN) and may be derived from lateritic zones in the silica-clay zone. It is mostly rich in gold and base metals (see *Geochemistry* section) but no specific ore minerals have been identified.

Summary

The traces of gold and base metals in these altered siliceous, skarn and carbonate rocks occur as variable and complex disseminated and vein-style associations:

□ Siliceous rocks

- auriferous, framboidal pyrite-bearing opal/chalcedony veins;
- galena-sphalerite veins; plus
- disseminated niccolite, cobaltite, gersdorffite, millerite and marcasite.

□ Skarns

- ophicalcites contain serpentine vein-hosted assemblages including native gold, loellingite, sphalerite, chalcopryrite and galena, associated with minor magnetite and andradite;
- quartz-calc-silicate zones contain sphalerite, millerite, magnetite and gold with xonotlite and quartz;
- diopside skarns contain niccolite, rammelsbergite and loellingite in talc-filled breccias.

□ Altered Cambrian rocks with chromite and garnierite-like nickel.

□ Silica-clay 'argillic alteration' zone: weathered skarns with intermixed residual gold, some limonite-hosted (lateritic?).

Geochemistry of Mineralised and Hydrothermally-Altered Rocks

Petrological studies failed to provide sufficient information about the occurrence and distribution of gold in altered rocks. This may be a result of either a nugget effect, or a combination of very fine-sized gold grains, plus the friable nature of many gold-rich samples (usually weathered, limonitic and clayey) and also the generally low content of gold. Therefore geochemical analysis was necessary to help resolve some unknowns such as:

- the distribution of metals, including gold;
- the relationships between the concentrations of gold and other metals; and
- the relationship between mineralisation types and gold content.

About 118 samples, including many from two diamond-drill holes, plus surface samples from mineralised and some unmineralised areas, were analysed for Au, Ag, Pb, Zn, Cu, Bi, Sn, As, Mo and many other trace elements.

Base metal analyses were conducted mostly by X-ray fluorescence, and gold and silver by AAS, in the Mineral Resources Tasmania laboratories; these are listed in Appendix 7. The Amdel laboratories conducted some ICP analyses; these are listed in Appendix 8.

The different mineralisation and alteration styles described above have different geochemical signatures; these are summarised in Table 1 and described below. Inter-element correlations are shown in Appendix 12 and Figure 8. These indicate that the mineralisation is generally low in Sn, W, Mo and Bi.

- The silica-clay zone hosts most of the medium to high-grade gold mineralisation in the area. Gold grades up to 1.1 g/t, with some variable to high arsenic (up to 740 g/t) and moderately anomalous Pb, Zn, Sb and Co. Locally high Ni, Ti, Zr and Cr contents suggest contamination from the

hanging-wall rocks (Permo-Carboniferous mudstone and polymict conglomerate).

- The cherts are mostly low in gold and base metals, but have locally high Pb, Zn, As, Cr and Ni. Gold is up to 0.2 g/t, Pb to 2400 g/t, Ni to 840 g/t, Zn and As to 500 g/t and Cr to 6500 g/t.
- Opal-bearing rocks are mostly weakly to moderately anomalous in most metals, including lead, zinc, arsenic, antimony, cobalt and gold, but excluding Cu and Cr. Gold is up to 0.6 g/t.
- Ophicalcites contain moderate to high As, and some locally moderate zinc and gold contents. Gold is up to 0.1 g/t, and As to 1400 g/t.
- Calc-silicate rocks contain moderate to high Au and Zn and moderate As, Sb, Co and Ni, with low Pb contents. Gold is up to 1.2 g/t, and Zn to 2450 g/t.
- Diopside skarns contain low to moderate Au, moderate to high arsenic, moderate Zn and Pb and some locally moderate nickel contents. Gold is up to 0.14 g/t and arsenic to 470 g/t.
- Limonitic rocks contain high Au and Pb, moderate to high As, and moderate Zn, Sb, Co, Cu and Ni. Gold is up to 6.7 g/t, Pb to 450 g/t and arsenic to 1100 g/t.
- Altered Cambrian rocks contain low Au and most base metals, except for high Cr (to 3400 g/t) and Ni (to 1250 g/t) and moderate Co.

In summary, the rocks in the Forster Prospect are highly variable in gold and base metal contents and ratios, over several different rock types. Part of this is due to a strong host-rock dependence, but the variation is also indicative of other, uncertain factors. These probably include proximity to the source of heat and fluids, and the permeability and competency of the various mineralised host rocks, which would control the fluid movement. Overall, the gold is moderately correlated with Ni, Pb, Co, Sb, Zn and Cu, but only weakly with arsenic.

Table 1
Distribution of metals in gold-mineralised rocks, Forster Prospect

| Style | Au | Cu | Pb | Zn | As | Sb | Co | Ni | Cr |
|-------------------------|-------|--------|--------|--------|--------|--------|--------|--------|----------|
| A1 silica-clay zone | l-h | l-m | m | l-h | l-h | m | l-m | l-h | l-h |
| A2 limonite | h | l-m | h | m | m-h | m | m | m | l-m |
| A3 opal | m | l | m | l-m | l-m | l-m | l-m | m | l |
| A4 chert | l-m | l | l-h | l-h | l-h | m | l-m | l-h | l-h |
| A5 quartz breccia | l | l | l-m | l | l-m | m | l | l | l |
| A6 quartz/calc-silicate | m | l | l | m-h | m | m | m | m | l |
| A7 diopside skarn | m | l | m | m | m-h | l | l | l-m | l-m |
| A8 ophicalcite | l-m | l | l | l-m | m-h | l | l | l | l |
| A9 Cambrian | l | l | l | l | l | l | m | h | m-h |
| 'moderate' range (g/t) | 0.1-1 | 30-300 | 30-300 | 50-500 | 30-300 | 10-100 | 10-100 | 50-500 | 100-1000 |

m = moderate, h = high, l = low

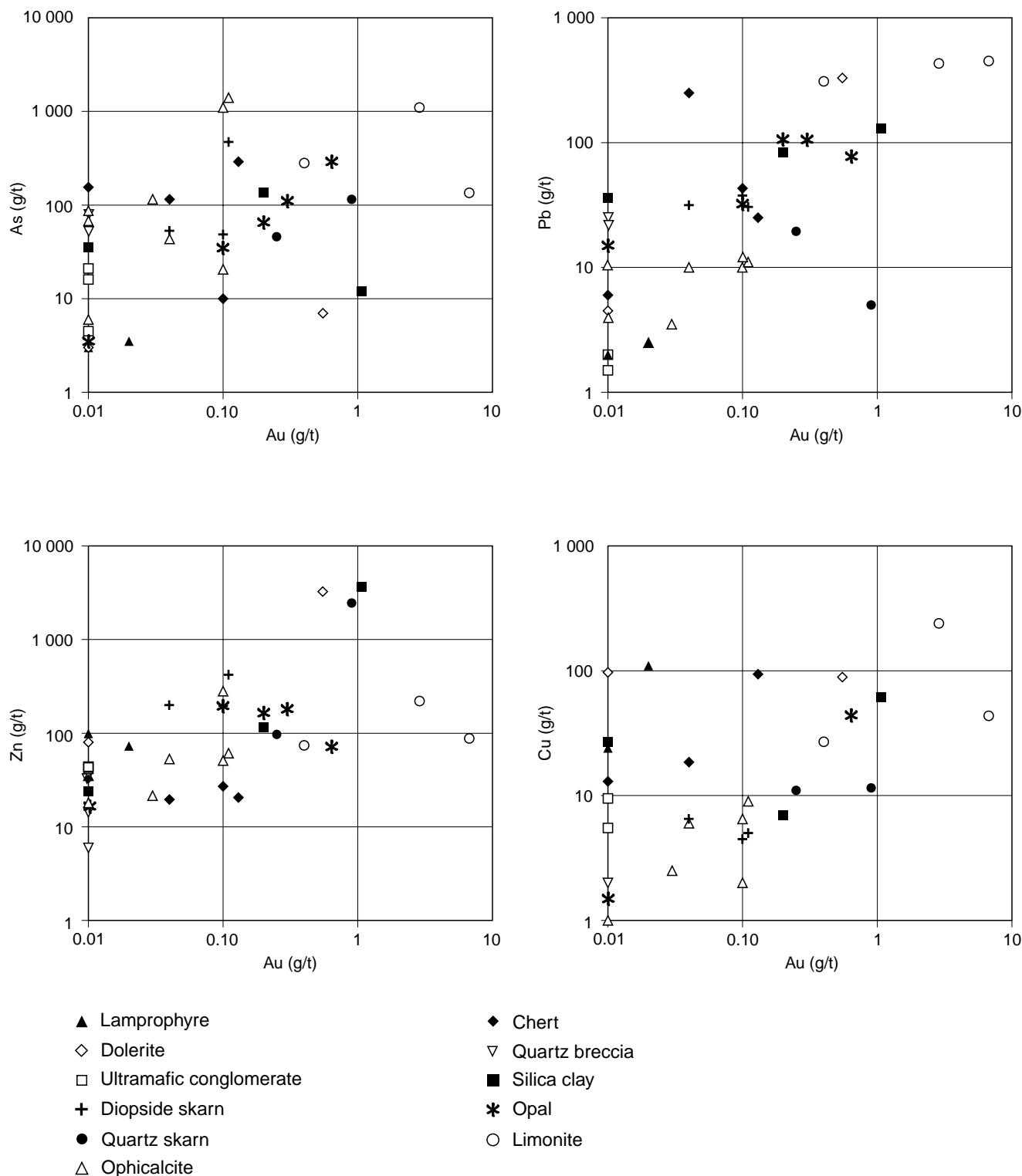


Figure 8a

Geochemical diagrams showing log-log plots of Au vs As, Au vs Zn, Au vs Pb and Au vs Cu in the different rock groups of the Forster Prospect.

The weak correlation with arsenic and negligible amounts of W, Sn, Mo, Bi and Cu suggests that there is nothing to link the skarns and mineralisation with Devonian granite. The lack of correlation with Au and As, plus weak Sb and very low Tl and Hg values, suggest that the mineralisation is not Carlin style.

A geochemical traverse along the Forster and Fletchers roads indicates a concentration of gold and arsenic in aluminous zones adjacent to the siliceous zone, rather than within the siliceous zone (fig. 9). This suggests that the quartz is present in the mineralised zone, but is not a direct gold host.

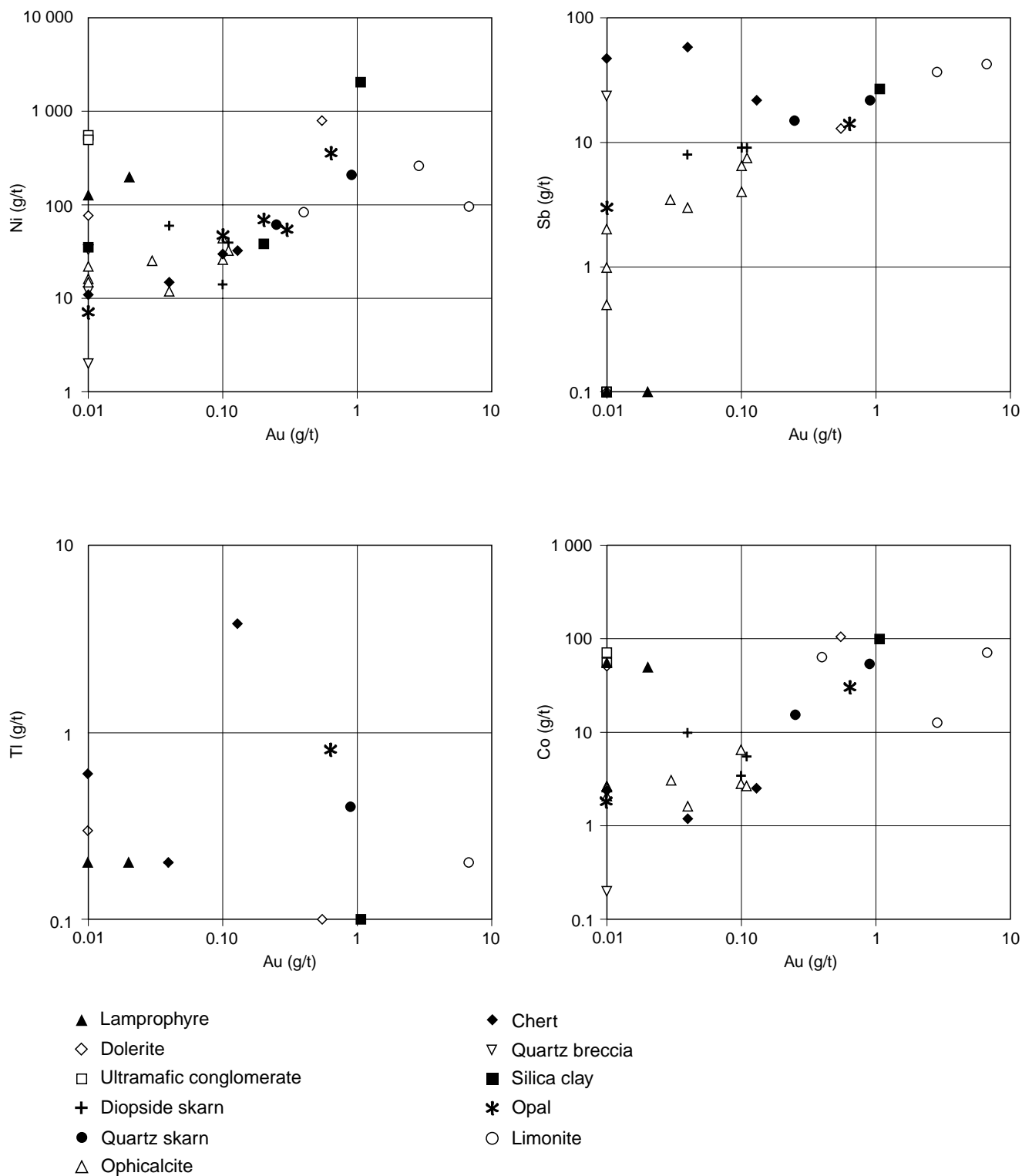


Figure 8b

Geochemical diagrams showing log-log plots of Au vs Ni, Au vs Tl, Au vs Sb and Au vs Co in the different rock groups of the Forster Prospect.

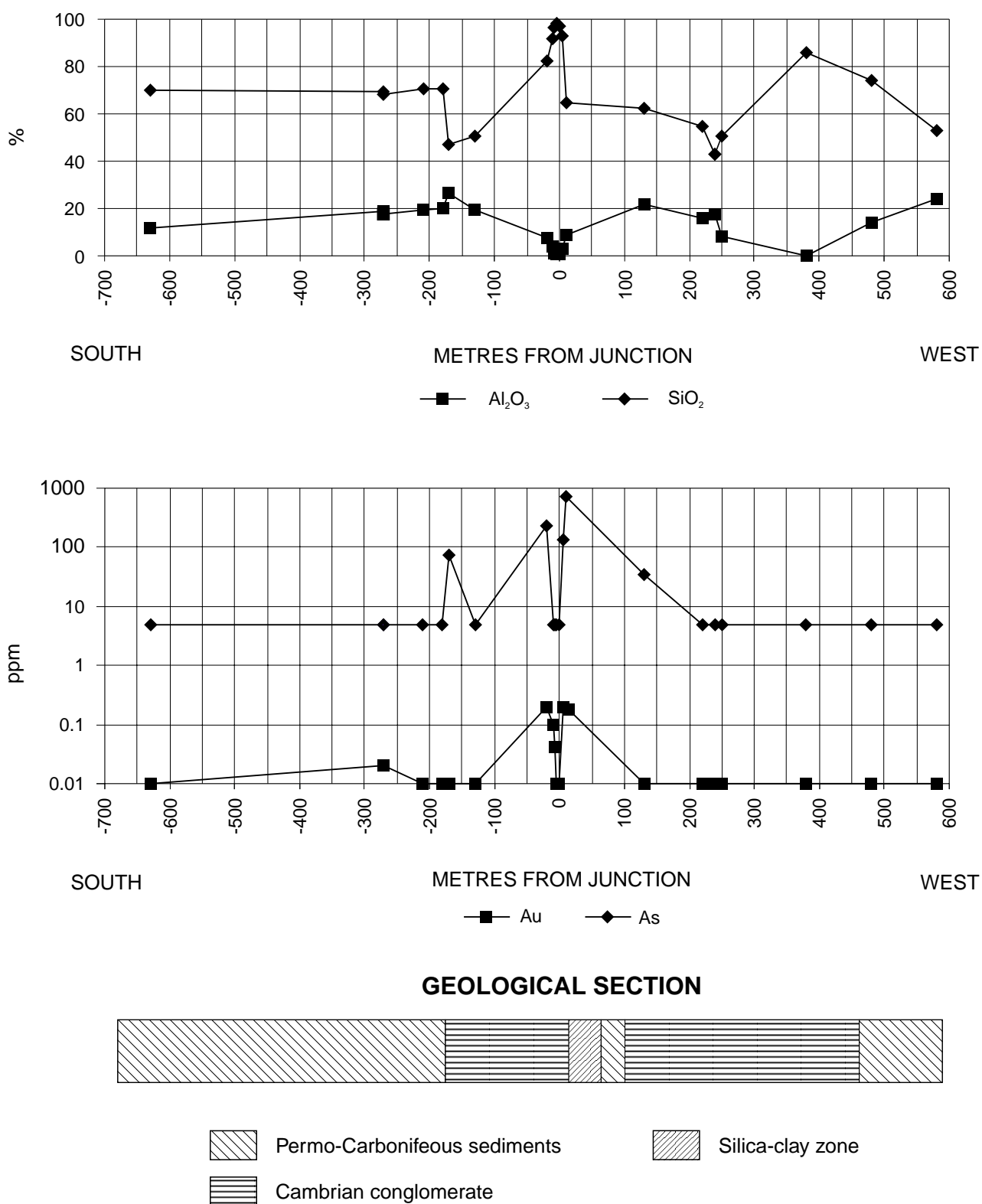


Figure 9
Geochemistry over the mineralised zone along Fletchers Road/Forster Road, showing Au, As, Al and Si trends.

Fluid Inclusions

A preliminary study of fluid inclusions from silicified rocks (mostly crystals in vughs) at the Forster Prospect was undertaken to investigate the general nature of the hydrothermal fluids responsible for the silicification and possibly the gold mineralisation within the area. A few large euhedral quartz crystals grown on the walls of a cave from the Mt Weld area were also examined for this study. The results from this study have been combined with those undertaken by Taheri (1989, 1990) and are presented in Figure 10 and Appendix 11.

There are basically two types of fluid inclusions:

- two-phase fluid inclusions, consisting of vapour and aqueous solution (type A); and
- CO₂-bearing fluid inclusions (type B).

Type A inclusions occur in isolation, as groups and also within discontinuous microfractures. These fluid inclusions appear to be of at least two distinct types; those with high vapour to liquid ratios (60 to 85% by volume, type A1) and fluid inclusions with distinctly smaller vapour bubbles (~20% by volume, type A2). There are also small ($\leq 3 \mu\text{m}$) secondary fluid inclusions with very low vapour-liquid ratios occurring along microfractures. No attempt was made to undertake any heating or freezing experiments on these secondary fluid inclusions.

Type A1 fluid inclusions range in size from less than $4 \mu\text{m}$ to about $50 \mu\text{m}$ and vary in shape from irregular, rounded forms to negative crystals. They are common in euhedral quartz crystals projecting into open veins and vughs.

Type A2 fluid inclusions appear to be independent of type A1 inclusions and occur individually and in discontinuous microfractures. The size ranges from less than $4 \mu\text{m}$ to about $10 \mu\text{m}$ and they vary in shape from rounded to negative crystals.

CO₂-bearing fluid inclusions (type B) may contain only one phase (liquid CO₂ only, B1) or two phases (liquid H₂O, vapour CO₂ + H₂O, B2). Type B1 fluid inclusions are relatively rare and appear to be associated with type B2 inclusions; this needs to be confirmed with more detailed work. Type B2 fluid inclusions are also uncommon and may be either pseudo-secondary or primary in origin.

Freezing and heating experiments

There are two main problems in estimating the compositions of these fluid inclusions:

- the existence of small ($< 4 \mu\text{m}$) inclusions with very high vapour/liquid ratios which make it difficult to determine the homogenising temperatures; and
- the similarity of CO₂ hydrate refractive indices to those of aqueous solution and also the isotropic

character of CO₂ hydrate in small CO₂-bearing fluid inclusions.

Final melting points for type A1 fluid inclusions range from -3 to -5.5°C , corresponding to 5 and 8.5 mass% equivalent NaCl.

Type A2 fluid inclusions show consistent freezing points of around -0.5°C , corresponding to salinities of around 1 mass% equivalent NaCl. A few CO₂ fluid inclusions (type B1) homogenised to liquid upon heating, with homogenisation temperatures ranging from 24.9 to 27°C . Based on two measurements, type B2 fluid inclusions showed CO₂ melting points of around -57°C and a final melting point of about 8.5°C , which corresponds to a salinity of around 2.5 mass% NaCl.

The fluid inclusions in quartz crystals from Mt Weld are irregular in shape and consist of only a liquid phase. This indicates very low formation temperatures for these fluid inclusions. The formation temperatures must have been too low to cause sufficient volume shrinkage of the liquid to form a vapour phase upon cooling.

The homogenisation temperature for fluid inclusions with high vapour-liquid ratios (type A1) range from 307 to 395°C , with the majority falling between 360 and 390°C (fig. 10). The fluid inclusions homogenised to liquid or vapour with a few showing critical phenomena. This is important, because if the composition of a fluid is known, then the critical temperature can provide an estimate for the pressure at which the inclusions were trapped in the relevant system. This was not possible to determine reliably as the compositions of the inclusions showing critical temperatures could not be measured.

If it is assumed that the fluid inclusions behaving differently upon heating are of the same generation, then they may indicate that the fluids have been trapped from a heterogeneous system (CO₂-H₂O-NaCl) in which different phases of different ratios have been trapped at the time of formation. Boiling of fluids is a special case of heterogeneous trapping, and if this is the case then type A1 fluid inclusions are on a two-phase immiscibility curve and no pressure correction is needed for the homogenisation temperatures.

Homogenisation temperatures for type A2 fluid inclusions range from 175 to 285°C , with the majority being between 250 to 280°C (Appendix 11).

The high temperature, low salinity fluid inclusions (type A1) may be due to:

- (a) entrapment of boiling ascending vapour-rich fluid (CO₂-H₂O) separated from a magmatic aqueous phase;
- (b) a boiling metamorphic fluid, or

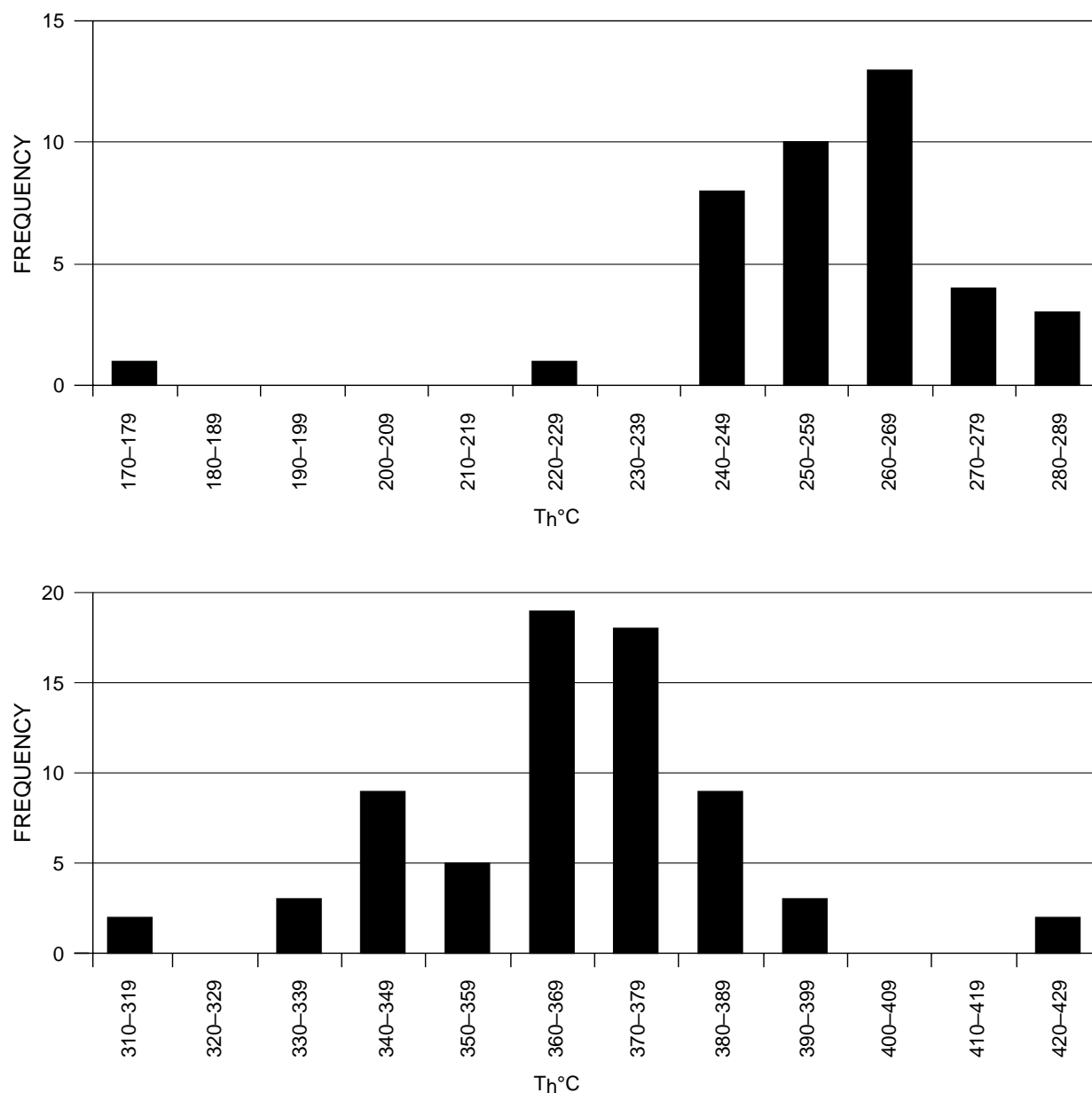


Figure 10

Histogram (in two parts) showing frequency distribution of $T_{(homog)}$ for fluid inclusions in rocks of the Forster Prospect.

- (c) hydrothermal fluids generated by heating of ambient groundwater by Jurassic dolerite intrusion.

Geological and petrological observations favour option (c). This model is elaborated in the discussion and petrogenesis section.

The fluid inclusions with lower homogenisation temperatures (type A2) were probably formed from the cooling hydrothermal fluid as it mixed with groundwater.

The nature and possible origin of hydrothermal fluids are further discussed in the last section of this report.

Oxygen isotope studies

Eight quartz samples from silicified rocks from the Forster Prospect were selected for oxygen isotope

analysis. The data, together with three oxygen isotope results reported from similar rocks by Taheri (1990), are shown in Table 2. One quartz sample from silicified dolostone karst at Mt Weld, about 10 km to the northwest of the Forster Prospect, was also analysed. The quartz types shown in Table 2 were mostly vuggy silica from the silica-clay zone, two cherts and a colloform chalcedony vein.

The oxygen isotope values vary widely from 5.9‰ to 20.8‰, although seven out of eleven samples show a narrow range of $\delta^{18}\text{O}$ of 9.8 to 13.1‰.

The two highest oxygen isotope values were obtained from the chert samples (107836, 107883). Sample 107836 is brecciated with minor chromite and carbonaceous material present in a megachert with a weak foliation. The occurrence of chromite in this rock may indicate that the original rock was possibly a Cambrian

ultramafic intrusive or, more likely, an ultramafic-derived conglomerate, similar to those observed in the area. Sample 107883 is a chert breccia cut partly by recrystallised colloform quartz veinlets and by late opal and chalcedony. Although the oxygen isotope values of these two samples are similar, the original rock types are obscure. Evaluation of the oxygen isotope data is complicated by the occurrence of multiple generations of quartz, which are impossible to physically separate. The following is an attempt to explain the oxygen isotope values.

Based on fluid inclusion homogenisation temperatures (see *Fluid Inclusion* section), a formation temperature of around 350°C may be estimated for the seven silicified rocks with $\delta^{18}\text{O}$ between 9.8 and 13.1‰. The oxygen isotope values of water in equilibrium with these samples show a relatively narrow range of 4 to 7.3‰.

The formation temperatures for chert samples with high oxygen isotope values are not known, with the exception that the occurrence of opal and chalcedony in sample 107883 may indicate a low formation temperature for at least part of the rock.

The averaged calculated oxygen isotope value of water in equilibrium with the silicified rocks (~5‰) is probably too low for magmatic water but is not low enough for a typical meteoric water, considering the high latitude of Tasmania in the Jurassic (~65°S, Veevers, 1984).

The high $\delta^{18}\text{O}$ values for quartz may be explained if a lower formation temperature of around 150°C is

assumed. In this case, $\delta^{18}\text{O}$ values of water equilibrated with the seven quartz samples would be about -6 to -3‰, perhaps consistent with isotopically equilibrated meteoric water.

If Proterozoic dolomitic rocks are assumed to have been the original major rock type and Jurassic dolerite was the main heat source within the area, then the dolomitic rocks would have gone through extensive interaction and isotopic exchanges with convective, magmatically-heated groundwater. Oxygen isotope values of Proterozoic dolomitic rocks from the lower part of the Weld River Group are generally high, ranging from 22.7 to 29.5‰ with an average of around 27.3‰ (Calver, 1995). In this scenario, the heated groundwater increasingly became higher in $\delta^{18}\text{O}$ values with decreasing temperature through continuous interaction and isotopic exchange with the surrounding dolomitic rocks. As a result, silicified rocks formed at higher temperatures (silicified, brecciated, vuggy rocks) and show lower $\delta^{18}\text{O}$ values relative to those formed at lower temperatures (chert).

Sample 107825F is petrographically similar to other silicified vuggy quartz samples, but it has an unexpectedly low $\delta^{18}\text{O}$ value of 6.4‰. The only possible explanation for this result is analytical or sampling error.

In summary, the $\delta^{18}\text{O}$ results are complex and vary widely. The data are consistent with the formation of silicified rocks from isotopically modified meteoric water.

Table 2
Oxygen isotope data, Weld River

| <i>Sample No.</i> | <i>Description</i> | $\delta^{18}\text{O}_{\text{SiO}_2}(\text{‰})$ | <i>Formation temperature, °C (inferred)</i> | $\delta^{18}\text{O}_{\text{H}_2\text{O}}$ |
|-------------------|--|--|---|--|
| C107855 | Chert | 13.1 | 350 | 7.3 |
| C107836 | Chert | 16.7 | 150? | 0.9 |
| C107825F | Silicified (vuggy) rock | 6.4 | 350 | 0.6 |
| C107818 | Silicified (vuggy) rock | 12.6 | 350 | 6.8 |
| C107825C | Silicified (vuggy) rock | 11.4 | 350 | 5.6 |
| C107883 | Banded (colloform) quartz vein | 20.8 | 150 | 5.0 |
| C103796 | Silicified (vuggy) rock | 9.8 | 350 | 4.0 |
| C108162* | Silicified rock | 10.4 | 350 | 4.6 |
| C108163* | Silicified rock | 10.5 | 350 | 4.7 |
| C108164* | Euhedral quartz in silicified (vuggy) rock | 9.9 | 350 | 4.1 |

* From Taheri, 1990.

Discussion and Petrogenesis

Possible origins of gold and skarn mineralisation

The Forster Prospect area hosts a complex style of mineralisation new to Tasmania. As a result different workers have proposed several different genetic models for the prospect.

Previous studies

Based on a brief study, Taheri (1990) suggested that the siliceous rocks were altered dolostones, and noted that fluid inclusions and oxygen isotopes indicated a mixture of magmatic and meteoric fluids. He suggested an epithermal, Relief Canyon-style gold mineralisation.

Boyd (1996) reported a Pb isotope analysis on galena in chert, which suggested a Jurassic age of mineralisation. However, he proposed a post-Jurassic mineralisation age, based on serpentine-calcite veins in dolerite. The paragenetic position of the gold mineralisation could not be easily related to the alteration assemblages, and he considered the silica-clay zone to result from weathering.

Bottrill and Woolley (1996) noted that complex, altered magnesian skarns, derived from dolostone, host minor gold and base metal sulphide-arsenide mineralisation. Other significant observations included gold grains *in situ* in skarn, the identification of the vuggy quartz as metasomatised siliceous skarns, the complex origin of the cherts, and silicification pre-dating and post-dating Jurassic dolerite intrusion. Dolerite was implicated in the metamorphism, but the mineralisation was suggested to be of Carlin-style or of gold-skarn type.

Dell (1997) conducted some geochemical, petrographic, clay mineralogy and sulphur isotope studies of the mineralisation and host rocks. He interpreted the silica alteration as Carlin-style, despite the different host rocks, alteration styles and lack of pyrite. Trace element studies failed to link gold with any other elements. Fluid inclusions in a small quartz vein in the margins of a Jurassic dolerite body south of the prospect were tentatively related to the main silicification event in the area, despite their lower temperatures of formation and lack of evidence for any spatial, timing or geochemical relationships. Sulphur isotopes were interpreted to be of sedimentary and magmatic sources.

Summons (1999), summarising the above studies, suggested a model with early Au-base metal mineralisation accompanying retrograde skarn alteration, followed by epithermal Au mineralisation associated with silicification and argillisation, Devonian or Cretaceous in age.

Gold in Tasmania

Gold deposits are widespread throughout Tasmania (Bottrill *et al.*, 1992), but the great majority occur as

sulphide-poor mesothermal quartz veins of Devonian age in slate and sandstone in the northeast of the State. They are generally arsenic-rich, with minor Pb, Zn, Cu and Sb. Some of these deposits include stockworks and some are associated with Devonian granodiorites (e.g. at Lisle and Mt Horror; Taheri and Bottrill, 1994). The latter are typically enriched in W, Sn, Sb and Bi.

Other important styles of gold deposits in Tasmania include:

- Cambrian volcanic-hosted, sulphide-rich deposits (variably Pb-Zn-Ba, Cu, Fe or As rich; e.g. Henty, Mt Lyell, Rosebery, Hellyer, etc.). These constitute the greatest endowment of gold in Tasmania;
- Cretaceous syenite-related deposits (Cygnet), with minor Pb, Zn, As and Cu;
- Zn-Fe-Bi-F rich retrogressive skarns, Sn-W-Bi-REE-F rich veins and galena-rich veins related to Devonian granites (e.g. Moina, Stormont, Round Hill);
- poorly understood disseminated deposits in Precambrian schist, iron formations and dolostone (e.g. Savage River, Corinna and Jane River).

The mineralisation in the Forster Prospect area appears to be of a different nature and origin to the above styles of gold deposit. Difficulties in evaluating the genesis of the Forster Prospect include the paucity of fresh outcrop and relatively deep diamond-drill holes.

Pertinent Forster Prospect features from this study

In order to discuss some possible origins for the Forster Prospect mineralisation, some of the main features of the mineralisation, which constrain genetic models, are mentioned below.

- The occurrence of minor gold (<0.2 g/t) in altered high-temperature skarns (>600°C), shallowly overlying the Jurassic dolerite.
- The apparent restriction of high-tenor gold zones (up to 10 g/t) to a halloysite-rich silica-clay zone, overlying the skarns with low gold tenor.
- Vuggy silica breccias in the silica-clay zone appear identical to similar zones cutting the skarns, suggesting derivation of the silica-clay from weathering of these skarns.
- Occurrence of gold in limonite and opal.
- Silicification is one the most common features associated with mineralisation. A variety of rock types, including polymict conglomerate, dolostone and skarn, have been variably affected by silicification, leading to the formation of rocks containing up to 99% silica. Textural variations (from vuggy to massive) also reflect different original rock types and/or degrees of leaching.

- Occurrence of high temperature (300–400°C) and low salinity CO₂-bearing fluid inclusions in quartz in vuggy breccias.
- Silicification post-dates Permo-Carboniferous diamictite, but only rarely post-dates Jurassic dolerite. Much of it appears to represent groundwater-related silicification of dolostone-hosted karst breccias.
- Jurassic dolerite contains only rare quartz veins and is only significantly altered at margins.
- There is a general lack of pyrite and a low tenor of a base metal suite, including Pb, Zn, Ni, Co, As and Fe. The metals are often present as arsenides, in various late stage, moderate to low temperature (<400°C), Ca-Mg-Fe silicate veins.
- There is a lack of any distinct regional hydrothermal alteration or geochemical zoning (even allowing for poor outcrop and limited drilling).
- Carbonaceous material is present but mostly rare.

Considering the main features of the mineralisation, three genetic models may be discussed.

High sulphidation-type gold mineralisation

There are some common features between typical high-sulphidation type deposits and those observed at the Forster Prospect.

The common occurrence of silicified rocks within the area may be indicative of extensive hydrothermal leaching of the original rocks. In this scenario, the initial phase of hydrothermal activity must have had a low (or very high) pH for aluminium to be soluble (although the host rocks are mostly Al-poor). It is also known that the high tenor gold at this prospect is limited to the quartz-clay zones and fluid inclusions are of low salinities and high temperatures. These are some of the common features of high sulphidation-type mineralisation where an ascending, magmatically-derived vapour phase containing volatile components, such as HCl, SO₂, CO₂, HF and H₂S, condenses into water and forms a highly acid solution. This solution is capable of leaching most components from the host rocks, leaving an amorphous silica residue.

The dense, saline and metal-bearing liquid may be driven upward if there is a change in pressure from lithostatic to hydrostatic due to tectonism or continuous crystallisation of the intrusion. This fluid may ascend into the leached zone and precipitate gold, Cu and Ag sulphosalts and sulphides. If the saline fluid does not reach the leached zone then the silicified rocks would remain almost barren with only minor gold or sulphides, as a magmatic vapour phase is capable of carrying only small amounts of metals such as Cu and Au (Vennemann *et al.* 1993; Hedenquist *et al.* 1994). The mineralisation at the Forster Prospect may be of the latter type, where the saline, mineralising fluid did not reach the leached, altered rocks. This is consistent with

the observation of low-salinity, high-temperature fluid inclusions.

The high temperature skarn mineral assemblages may also be indicative of the existence of a shallow intrusive body. Continuous reactions between the hydrothermal fluid and host rocks and increased involvement of groundwater result in the formation of gold-bearing opal and chalcedonic silica, locally pyritic and showing colloform banding. The original minor gold was probably reconcentrated by groundwater in clay and silica zones, producing zones with relatively higher (up to 10 g/t) gold content.

Hydrothermal alteration zoning, one of the main features of many high sulphidation-type deposits, has not been positively identified at the Forster Prospect. Alunite, a characteristic mineral for high sulphidation-type deposits forming in low pH environments, was also not identified. However alunite or alteration haloes would not be expected in an environment where the original rock types were mainly dolostone. The clays are mostly halloysite rather than kaolinite or dickite, which are more typical of such deposits.

Based on this model, the potential for large or economic gold deposits within the area is low, but there would be some potential for richer Cu-Au ore bodies at depth.

One of the problems with this model is the absence of evidence for a suitable heat source. The involvement of Devonian or Cretaceous intrusive rocks in the formation of the Forster Prospect is highly unlikely for the following reasons:

- There is no evidence for the occurrence of granitic bodies within the area, with the exception of a small outcrop located about 1.5 km northwest of Glovers Bluff where a fine-grained rock was identified (J. L. Everard, 1999, see Appendix 6 for details). The rock shows aplitic texture, but detailed petrographic and geochemical investigations (Appendix 6) indicate that it is unlikely to be a granitic body of Cambrian or Devonian age. The geochemistry of the rock is also different to that known from the Cygnet Cretaceous alkaline rocks located about 30 km to the southeast. The Cretaceous alkaline rocks are associated with gold mineralisation in the Cygnet area (Taheri and Bottrill, 1999). Based on field and petrological evidence, Everard (Appendix 6) indicated that the aplitic rock is from a hypabyssal intrusion, rather than being part of a pluton. The age and the origin of the aplitic rock remain uncertain.
- MRT digital gravity data (Leaman and Richardson, 1992) suggest that a major shallow granitic pluton underlies most of southwest Tasmania. A more detailed gravity survey (Dunstan, 1997) was interpreted to indicate the presence of a probable Devonian granite at ~3–4 km depth below the Weld River area. The nearest confirmed Devonian granite crops out some 60 km to the southwest at Cox Bight.

- Tin, tungsten, boron, and fluorine-bearing minerals, such as tourmaline, fluorite, topaz, cassiterite, wolframite and scheelite, are commonly associated with granite-related mineralisation. However, there are no characteristic mineralogical or geochemical Devonian hydrothermal signatures within the Forster Prospect area. On this basis it is difficult to relate the gold mineralisation or skarns to the intrusion of granitic bodies in the area.
- Cretaceous intrusive rocks have not been identified within the area and there is no evidence to relate the mineralisation in the Forster Prospect area to any unexposed Cretaceous intrusive rocks. For example, potassic alteration is absent in Permo–Carboniferous mudstone in the Forster Prospect area but is a characteristic of hydrothermal alteration in the same rocks in the Cygnet area, where the porphyries are directly associated with the gold mineralisation (Taheri and Bottrill, 1999).

A deep-seated fluid of metamorphic origin is also an unlikely option. This is mainly because the area lacks any major veining to provide evidence for the occurrence of major conduits. There is also no evidence to consider that the characteristically near-surface clay zones are the products of hydrothermal alteration. Their distribution, mineralogical features and especially lack of quartz veining favour a weathering origin.

Carlin-type gold mineralisation

Sedimentary-hosted Carlin-type gold deposits commonly occur throughout much of the north-central and northeastern Basin and Range province of Nevada, western North America, and are the most important type of gold deposits in the United States. The mineralisation has been described reasonably well, but the genesis of the deposits is still uncertain and genetic models varying from magmatic to amagmatic (metamorphic?) have been proposed (e.g. Ilchik and Barton, 1997; Wallace, 1989; Seedorff, 1990; Sillitoe and Bonham, 1990). Basically, the deposits are hosted by a variety of sedimentary rocks, in particular thinly-bedded, silty calcareous, pyritic, carbonaceous siltstone cut by high angle faults. The deposits commonly contain felsic intrusive rocks and minor skarns, but these probably pre-date the main mineralisation event (Ilchik and Barton, 1997). The mineralisation is deficient in base metals and is characterised by very fine (to sub-micron) grained gold associated with As, Hg, Tl, Ba, Sb, F, and less commonly Sn, W and Mo. Common alteration types include calcification, silicification, sericitisation and argillisation.

Some features of the Forster Prospect that favour a Carlin-type deposit include:

- the occurrence of some original calcareous rocks which have been replaced by silica;

- the occurrence of some fine organic material (pyrobitumen?);
- the occurrence of arsenic and minor antimony anomalies;
- the possible occurrence of collapsed breccias, interpreted from some reverse circulation (RC) drilling; and
- the mineralisation could be of deep-seated origin and the high temperature, low salinity, CO₂-bearing fluid inclusions may be of metamorphic origin. Minor arsenic, observed in some altered zones, might also have been derived from the same source(s).

The mineralisation may be argued to be of different style in that:

- the mineralisation appears to have been formed, or at least hydrothermal activity started, at higher temperatures than would be expected for a Carlin-type deposit (i.e. 300–400°C compared to 150–200°C, fluid inclusion data). This is also supported by the occurrence of high temperature skarn assemblages (>600°C) within the area;
- there is no recognisable alteration zoning about major fluid conduits (feeder structures);
- there is much more intense silicification (leaching) of the Forster Prospect host rocks (i.e. possible different fluid chemistry);
- the high-grade gold occurs mainly in non-carbonaceous, non-pyritic silica-clay rocks, in contrast to Carlin-type deposits where the host rocks are mainly thinly-bedded, silty, calcareous, pyritic, carbonaceous siltstone and solution breccias; and
- there are no known felsic intrusive rocks associated with the deposit.

In summary, there is insufficient evidence to consider that the mineralisation in the Forster Prospect area is of Carlin type. However, it must be re-emphasised that there is no deep drilling within the area and, with the exception of the skarns, very few hydrothermally-altered rocks which cannot be interpreted as products of weathering have been demonstrated to exist within the area. The nature and occurrence of gold and base metals at the Forster Prospect are poorly understood, as most of the high tenor gold is dispersed in a silica-clay saprolite zone. The reverse circulation (RC) drilling hardly penetrated this weathering zone and the geology and geochemistry below the weathering zone is poorly known. The time and spatial relationships between the skarns, gold and arsenic (if any) are not known. Again these can only be verified by deeper diamond drilling in order to investigate the nature of the mineralisation below the weathering zone. The present distribution of gold may reflect secondary processes of leaching and gold reprecipitation at or near surface.

It is concluded that there is insufficient evidence to substantiate a Carlin-style model for the Forster Prospect.

Jurassic dolerite related mineralisation

The direct association of the gold mineralisation with the intrusion of the Jurassic dolerite is our preferred model as there is more evidence to support this.

Although there is no known mineralisation associated with Jurassic dolerite in Tasmania, gold deposits (with grades up to 50 g/t) are known in the equivalent Jurassic dolerite sequences in the Cradock district of South Africa. The gold there is associated with prehnite and quartz in vughs and as fissure infilling in sedimentary rocks of Permo-Triassic age which have been intruded by Jurassic dolerite dykes (Cairncross and Anhaeusser, 1992).

Jurassic dolerite is associated with skarnoids and calc-silicate hornfels in other parts of Tasmania, including: Bruny Island with wollastonite, garnet (grossular and andradite), vesuvianite, feldspars (plagioclase and orthoclase), prehnite and clinopyroxenes: Bottrill, 1995); Lake Sydney (with wollastonite: Correy, 1983); and Blackmans Bay and Proctors Road (with andradite, vesuvianite, grossular, wollastonite, laumontite and clinopyroxene: Hughes, 1957; Bottrill, unpublished data). Pyroxene-plagioclase hornfels in Permo-Carboniferous mudstone appears to extend more than 50 m above a major Jurassic dolerite sill near Margate (Bottrill, unpublished data), and such extensive alteration and contact metamorphic haloes may be more common than realised.

This is, however, probably the first time that a possible role for Jurassic dolerite in the formation and/or remobilisation of a Tasmanian mineral deposit is discussed, despite the fact that dolerite crops out over about one-third of Tasmania.

Jurassic dolerite commonly occurs as dykes and sills within the area and is the only known intrusive rock closely associated with the mineralised area and skarn. Minor basic intrusive rocks of variable composition and unknown affinity also occur in the Cambrian sequences, but these are not directly associated with mineralisation. The close association of skarns and the Jurassic dolerite can be seen in Figures 2 to 5 and in diamond-drill holes SW1 and SW2 (Appendix 4). Although the drill holes are shallow, they provide sufficient evidence to show that the Jurassic dolerite bodies have acted as local heat sources responsible for the skarn assemblages.

The deeper drill hole (SW2) clearly illustrates the occurrence of metamorphic assemblages immediately above the contact with the underlying Jurassic dolerite. The skarn mineral assemblages change into mainly quartz-chert-clay with remnants of skarns at shallow depths. The siliceous units close to the surface appear to have resulted from weathering, extensive leaching and probably silica remobilisation by groundwater, rather

than being related to hydrothermal alteration. A similar trend can also be seen in drill hole SW1.

In general, it can be argued that the rocks have been extensively leached and weathered to a depth of at least 50 metres. Totally leached, barren, vuggy quartz is commonly observed at or near surface but at deeper levels similar quartz is often infilled with hydrous calc-silicate minerals and other retrograde and minor sulphide minerals. In this model, the high temperature fluid inclusions in quartz may be indicative of metamorphic temperatures and may not necessarily represent the formation temperatures of any mineralisation.

In this model the dolerite cone sheet (fig. 3) is considered to have acted as a local heat source, forming high-temperature skarn mineral assemblages, and also to have caused convective circulation of the surrounding groundwater. The heated groundwater interacted with the surrounding sedimentary rocks and the margins of Jurassic dolerite bodies, scavenging minor gold and base metals, and subsequently deposited, with late-stage hydrous calcium and magnesium silicates and opal, as the fluid cooled.

Based on the limited outcrops, two diamond-drill holes and some RC drilling, it has been established that the hydrothermal system at the Forster Prospect is relatively low in metals and sulphur. This is probably to be expected if the metals, including gold, have been derived through leaching of country rocks by low salinity fluids, mobilised as a result of the Jurassic dolerite intrusions. Ni, Co, Cr and PGE are highly likely to have been derived locally, with the Cambrian mafic and ultramafic clasts in the polymict conglomerate being the main potential source (see *Geochemistry* section for details). No detailed exploration programs have been carried out to assess the resource potential for economic Cr or PGE deposits in the area.

Within primary assemblages, the sulphides, arsenides, magnetite and gold occur mostly in hydrothermally-altered, xonotlite-rich zones in quartz breccias in skarn, in talcose breccias in diopside skarn, and in serpentine ± andradite veins in ophicalcites. The gold, iron and base metals appear to have been introduced with the hydrothermal fluids, rather than being primary constituents of the skarns or dolostone. This is in accord with the model of Korobeinikov (1991), which inferred the early introduction of very fine grained, disseminated gold into pyroxenes, spinel and magnetite at the magmatic stage of magnesian skarn formation, with post-magmatic redistribution and reconcentration of gold with later hydrous phases (serpentine, brucite and amphiboles), magnetite and sulphides.

The Co-Ni-Fe-As mineralisation has some mineralogical similarities to the Co-Ni-Fe-arsenide mineralisation at Bou Azzer, Morocco, which occurs in veins at serpentinite contacts (Garcia, 1987; Maacha *et al.*, 1998). The Ag-Co-Ni-Fe-As mineralisation in

Ontario (Canada) and Saxony (Germany) also have some features in common but are richer in Ag, U and Bi, and occur in distinct veins (Lefebure, 1996). Gold is absent or minor in both deposit types.

Despite the great textural similarities of the siliceous rocks in the silica-clay zones and skarns, there is no conclusive evidence to prove that the high-grade gold mineralisation in the silica-clay zones is of the same origin as the low-grade gold mineralisation disseminated in the skarns. The skarns may only be reaction skarns of local importance, directly related to dolerite dykes and sills. Most data obtained to date from the area is either from weathered surface material or from shallow RC drilling. These results could be misleading, as very little is known about the fresh rocks beneath the leached, deeply weathered zone in the area. It is also probably true to say that there is very little evidence to relate the major gold mineralisation to

other particular types of mineralisation or paragenetic stages, mainly because many rocks showing different origins and alteration/weathering styles can be anomalous in gold (see *Geochemistry* section for details).

Most of the gold appears to occur within 20–40 m of the surface, mainly associated with the silica-clay zone. Detailed mineralogical and XRD work failed to find any alunite or clays of definite hydrothermal origin, such as dickite in the silica-clay zone (containing mostly quartz and halloysite). The question is whether the halloysite clay is of hydrothermal origin. Although this is a possibility, field evidence and mineralogical studies favour a weathering origin for the formation of clays within the area, a conclusion supported by the paucity of quartz veining within the silica-clay zone and by the very Al-poor compositions of the skarns and siliceous breccia.

Summary

The gold mineralisation in the Forster Prospect area occurs in magnesian skarns and weathered skarns derived from Proterozoic dolostone, overlying a Jurassic dolerite cone sheet. Siliceous breccias occur in the skarns, and are post-Permian and pre- or syn-Jurassic in age. Minor gold (<0.2 g/t), arsenic, sulphur and base metals occur in the altered skarns and siliceous zones. The heat source must be very close and must be the dolerite. Devonian granite-related skarns are mineralogically and chemically quite different.

Because of the lack of sufficient data, mineralisation at the Forster Prospect may be genetically modelled for several different mineralisation styles depending on the number and type of assumptions made for each model. However there is more evidence to relate the mineralisation within the area to the intrusion of Jurassic dolerite. The gold occurs in altered high temperature (>600°C) magnesian skarns, directly overlying Jurassic dolerite, the only feasible heat source. The skarns indicate a range of metamorphic conditions, probably initiated soon after the intrusion of Jurassic dolerite and accompanying devolatilisation-related brecciation at high temperature (>600°C), and later altered by cooler, CO₂-poor, siliceous Ca-Mg rich fluids carrying minor gold. The skarns consequently have a complex mineralogy and include original diopside skarn, forsterite calciphyre, brucite calciphyre and periclase calciphyre, now mainly altered to ophicalcite. The high-grade gold zones (up to 10 g/t) occur in a halloysite-rich silica-clay zone, overlying the skarns with low-grade gold. Vuggy silica breccias in the silica-clay zone and skarns are closely related, suggesting derivation of silica-clay from weathering of skarns, but with a component derived from the capping Permo-Carboniferous pebbly mudstone. Gold also occurs in limonite and opal.

Silicification is one the most common features associated with mineralisation. A variety of rock types, including ultrabasic conglomerate, dolerite, dolostone and skarns, have been affected by silicification, resulting in the formation of rocks containing 90–99% silica. Textural variations (from vuggy to massive) also reflect different original rock types and/or degrees of leaching. Fluid inclusions in quartz are of high temperature (300–400°C) and low salinity, and are CO₂ bearing. Some of the quartz has been strongly affected by Ca metasomatism. The silicification post-dates the Permo-Carboniferous diamictite, but appears to post-date Jurassic dolerite only as rare, small quartz-prehnite veinlets in its altered margins.

There is a general lack of pyrite and a low tenor but wide variety of base metals, including Pb, Zn, Ni, Co, As and Fe, which are mostly present as arsenides in various late-stage, low-temperature, hydrous Ca-Mg-Fe silicate veins. The mineralisation and alteration lacks any distinctive regional hydrothermal zoning.

There is no evidence to relate the occurrence of the near-surface gold to any hydrothermal activity. No intrusive rocks apart from Jurassic dolerite are known to be directly associated with the mineralisation. The nearest granite outcrop occurs about 65 km to the southwest at Cox Bight (439 000 mE, 5 185 000 mN), and is estimated to be at three kilometres depth in the Forster Prospect area.

It may be misleading to evaluate the resource potential of the area using the limited available data and previous models.

Further work, particularly deep diamond drilling, is essential for a better understanding of the nature and extent of the mineralisation.

Acknowledgements

Richie Woolley is thanked for assistance with the historical research plus XRF and XRD analyses. Les Hay and David Shaw assisted with chemical analyses, Anthony Hollick with drafting and Geoff Green for critical reviews. The paper is published with the permission of Sedimentary Holdings.

References

- ABBOTT, B. 1995. Journeys to the upper Huon (Diaries of Henry Judd). *Tasmanian Tramp* 30.
- ALEKSANDROV, S. M. 1998. *Geochemistry of skarn and ore formation in dolomites*. Utrecht : The Netherlands.
- BACON, C. A. 1989. Silica. *Mineral Resources of Tasmania* 12.
- BERRY, R. F.; CRAWFORD, A. J. 1988. The tectonic significance of the Cambrian allochthonous mafic-ultramafic complexes in Tasmania. *Australian Journal of Earth Sciences* 35:523–533.
- BERRY, R. F.; HARLEY, S. 1983. Pre-Devonian stratigraphy and structure of the Prion Beach–Rocky Boat Inlet–Osmiridium Beach coastal section, southern Tasmania. *Papers Proceedings Royal Society Tasmania* 117:59–75.
- BOTTRILL, R. S.; HUSTON, D. L.; TAHERI, J.; KHIN ZAW. 1992. Gold in Tasmania. *Bulletin Geological Survey Tasmania* 70:24–46.
- BOTTRILL, R. S. 1995. Petrographic examination of rocks from the Shittim 1 DDH, Variety Bay, Bruny Island. *Record Geological Survey Tasmania* 1995/13.
- BOTTRILL, R. S.; WOOLLEY, R. N. 1996. Mineralogy and Petrography of some rocks from the Glovers Bluff/Weld River area. *Record Geological Survey Tasmania* 1996/15.
- BOYD, D. 1996. *The origins of silica and skarn alteration in the Weld River, southern Tasmania*. B.Sc. (Hons) Thesis, University of Tasmania.
- BOYLE, R. W. 1979. The geochemistry of gold and its deposits. *Bulletin Geological Survey Canada* 280.
- BROWN, A. V. 1986. Geology of the Dundas–Mt Lindsay–Mt Youngbuck region. *Bulletin Geological Survey Tasmania* 62.
- CAIRNCROSS, B.; ANHAEUSSER, C. R. 1992. Gold in South Africa. *Mineralogical Record* 23(3):209–230.
- CALVER, C. R. 1989 The Weld River Group: a Major Upper Precambrian dolomite sequence in southern Tasmania. *Papers Proceedings Royal Society Tasmania* 123:43–53.
- CALVER, C. R. 1995. *Ediacarian isotope stratigraphy of Australia*. Ph.D. thesis, Macquarie University.
- CALVER, C. R. 1998. Geological Atlas 1:25 000 Digital Series. Sheet 4623. Weld. *Tasmanian Geological Survey*.
- CALVER, C. R.; EVERARD, J. L.; FORSYTH, S. M. *In prep.* Explanatory report for Maydena, Skeleton, Nevada, Weld and Picton 1:25 000 scale digital geological maps. Mineral Resources Tasmania.
- CARTHEW, S.; POLTOCK, R.; BELLAIRS, P. 1988. *Weld River south west Tasmania EL 11/84. Annual report for the period ending 27 September, 1988*. Metals Exploration Limited Report No. 212008. [TCR 88-2855]
- CORREY, J. J. 1983. *The geology of the rocks of the Gordon and Eldon Group correlates and the Parmeener Supergroup in the Mt Bobs–The Boomerang area, southeastern Tasmania*. B.Sc. (Hons) Thesis, University of Tasmania.
- DELL, C. 1997. *Mineralogy and trace element geochemistry of skarn, skarnoid and silica alteration at the Forster gold prospect, Weld River, southern Tasmania*. B.Sc. (Hons) Thesis, University of Tasmania.
- DIPPLE, G. M.; FERRY, J. M. 1996. The effect of thermal history on the development of mineral assemblages during infiltration-driven contact metamorphism. *Contributions to Mineralogy and Petrology* 124:334–345.
- DUNSTAN, K. 1997. *Gravity and magnetic modelling of the Weld River Prospect, southern Tasmania*. B.Sc. (Hons) Thesis, University of Tasmania.
- EDWARDS, A. B. 1947. Alkali hybrid rocks of Port Cygnet, Tasmania. *Papers Proceedings Royal Society Victoria* 58:81–115.
- FOLK, R. L.; MCBRIDE, E. F. 1976. Possible pedogenic origin of Ligurian ophicalcite: a Mesozoic calichified serpentinite. *Geology* 4:327–332.
- FORD, R. J. 1989. Cretaceous igneous rocks, in: BURRETT, C. F.; MARTIN, E. L. (ed.). *Geology and Mineral Resources of Tasmania. Special Publication Geological Society Australia* 15:381–383.
- FORSTER, M. C. 1992. *EL11/84 Borril Creek–Weld River. Annual Report – Year 7 28/9/1990 to 27/9/91*. (Unpublished) [TCR 92-3339].
- FORSTER, M. C. 1993. *EL11/84 Borril Creek–Weld River. Annual Report – Year 8 28/9/1991 to 27/9/92*. (Unpublished) [TCR 92-3412].
- GARCIA, D. 1987. Altérations hydrothermales et gîtes arsénisés de cobalt du district de Bou-Azzer (Anti-Atlas). *Notes du Service Géologique du Maroc* 321:327–337.
- GOWLLAND, R.; GOWLLAND, K. 1977. *Trampled Wilderness: The history of south-west Tasmania (2nd ed.)*. C. L. Richmond and Sons : Devonport.
- GUSTAFSON, W. I. 1974. The stability of andradite, hedenbergite and related minerals in the system Ca-Fe-Si-O-H. *Journal of Petrology* 15:455–496.
- HARKER, R. I. 1964. Dehydration series in the system $\text{CaSiO}_3\text{--SiO}_2\text{--H}_2\text{O}$. *Journal American Ceramic Society* 47:521–529.
- HARKER, R. I. 1965. Scawtite and its synthesis. *Mineralogical Magazine* 34:232–236.
- HEDENQUIST, J. W.; AOKI, M.; SHINOHARA, H. 1994. Flux of volatiles and ore-forming metals from the magmatic-hydrothermal system of Satsuma Iwojima volcano. *Geology* 22:585–588.
- HOLLAND, T.; BLUNDY, J. 1994. Non-ideal interactions in calcic amphiboles and their bearing on amphibole-plagioclase thermometry. *Contributions to Mineralogy and Petrology* 116:433–447.
- HUGHES, T. D. 1957. Limestones in Tasmania. *Bulletin Geological Survey Tasmania* 10.
- ILCHIK, R. P.; BARTON, M. D. 1997. An amagmatic origin of Carlin-type deposits. *Economic Geology* 92:269–288.

- JAKOBSSON, S. P.; MOORE, J. G. 1986. Hydrothermal minerals and alteration rates at Surtsey volcano, Iceland. *Bulletin Geological Society America* 97:648–659.
- JENNINGS, D. J. 1978. Mineral deposits, in: GEE, H.; FENTON, J. (ed.) *The South West Book. A Tasmanian Wilderness*. 226–229. Australian Conservation Foundation.
- KOROBENIKOV, A. F. 1991. Gold conduct in the contact-metasomatic processes of intrusions, in: BARTO-KYRIAKIDIS, A. (ed.). *Skarns – their genesis and metallogeny*. 203–226. Theophrastus Publications: Athens.
- KRAUSE, F. M. 1885. (Note on a rock specimen from Weld River). *Papers Proceedings Royal Society Tasmania* 1884:1xxv–1xxvi.
- KUEHN, C. A.; ROSE, A. W. 1995. Carlin gold deposits, Nevada: origin in a deep zone of mixing between normally pressured and overpressured fluids. *Economic Geology* 90:17–36.
- LAVOIE, D.; COUSINEAU, P. A. 1995. Ordovician ophiolites of southern Quebec Appalachians: a proposed early seafloor tectonosedimentary and hydrothermal origin. *Journal of Sedimentary Research* A65:337–347.
- LEAKE, B. E.; TANNER, P. W. G.; SENIOR, A. 1975. The composition of the Connemara dolomitic marbles and ophiolites, Ireland. *Journal of Petrology* 16:237–277.
- LEAMAN, D. E. 1990. Inferences concerning the distribution and composition of pre-Carboniferous rocks in southeastern Tasmania. *Papers Proceedings Royal Society Tasmania* 124:1–12.
- LEAMAN, D. E.; RICHARDSON, R. G. 1992. A geophysical model of the major Tasmanian granitoids. *Report Department of Mines Tasmania* 1992/11.
- LEFEBURE, D. V. 1996. Five-element veins Ag-Ni-Co-As ± (Bi,U), in selected British Columbia mineral deposit profiles, in: LEFEBURE, D. V.; HÖY, T. (ed.). *Metallic deposits (Volume 2). Open File Report British Columbia Ministry of Employment and Investment* 1996/13:89–92.
- LEWIS, A. N. 1924. Notes on a geological reconnaissance of Mt Anne and the Weld River valley, southwestern Tasmania. *Papers Proceedings, Royal Society Tasmania* 1923:9–42.
- MAACHA, L.; AZIZI, R.; BOUCHTA, R. 1998. Gisements cobaltifères du district de Bou Azzer (Anti-Atlas): structure, minéralogie et conditions de genèse. *Chronique de la Recherche Minière* 531–532:65–75.
- MASON, B. 1957. Larnite, scawtite and hydrogrossular from Tokatoka, New Zealand. *American Mineralogist* 42:379–392.
- MCCLLENAGHAN, M. P.; SEYMOUR, D. B.; VILLA, I. M. 1994. Lamprophyre dyke suites from western Tasmania, their radiometric dating and the age of thrust faulting in the Point Hibbs area. *Australian Journal of Earth Sciences* 41:47–54.
- MEINERT, L. D. 1992. Skarns and skarn deposits. *Geoscience Canada* 19:145–162.
- PERTSEV, N. N. 1991. Magnesian skarns, in: BARTO-KYRIAKIDIS, A. (ed.). *Skarns – their genesis and metallogeny*. 229–324. Theophrastus Publications: Athens.
- PISTORIUS, C. W. F. T. 1963. Thermal decomposition of portlandite and xonotlite to high pressures and temperatures. *American Journal of Science* 261:79–87.
- RADTKE, A. S.; RYE, R. O.; DICKSON, F. W. 1980. Geology and stable isotope study of the Carlin gold deposit, Nevada. *Economic Geology* 75:641–672.
- ROCK, N. M. S. 1984. The nature and origin of calc-alkaline lamprophyres: minettes, vogesites, kersantites and spessartites. *Transactions Royal Society of Edinburgh: Earth Sciences* 74:193–227.
- ROCK, N. M. S. 1991. *Lamprophyres*. Blackie: London.
- SEEDORFF, E. 1990. Magmatism, extension and ore deposits of Eocene to Holocene age in the Great Basin – mutual effects and preliminary proposed genetic relationships, in: RAINES, G. L.; WILKINSON, W. H. (ed.). *Geology and ore deposits of the Great Basin. Symposium proceedings*. Geological Society of Nevada 90-1(1):133–178.
- SEYMOUR, D. B.; CALVER, C. R. 1995. Explanatory notes for the Time-Space Diagram and Stratotectonic Elements Map of Tasmania. *Record Geological Survey Tasmania* 1995/01.
- SHOJI, T. 1975. Role of temperature and CO₂ pressure in the formation of skarn and its bearing on mineralization. *Economic Geology* 70:739–749.
- SILLITOE, R. H.; BONHAM, H. F. 1990. Sediment-hosted gold deposits: Distal products of magmatic-hydrothermal systems. *Geology* 18:157–161.
- SMART, G.; WILKINS, C. 1997. The geology of the Browns Creek gold-copper skarn deposit, Blayney, NSW, in: DENWER, K. et al. (ed.). *Proceedings Third International Mining Geology Conference. Australasian Institute of Mining and Metallurgy Publication Series* 6/97:59–64.
- SMITH, C. H. 1954. On the occurrence and origin of xonotlite. *American Mineralogist* 39:531–532.
- SPEAKMAN, K. 1968. The stability of tobermorite in the system CaO-SiO₂-H₂O at elevated temperatures and pressures. *Mineralogical Magazine* 36:1090–1103.
- SUMMONS, T. G. 1985. *Exploration Licence 11/84, Mac Campbell Forster, Weld River, Southern Tasmania. Annual report of activities for the year ended 27.9.85*. Summons Geoservices Pty Ltd [TCR 85-2480].
- SUMMONS, T. G. 1997. *Annual Report – exploration Licences 11/84 and 3/94. Forster Project. Combined annual report for the period ended September 1996*. Sedimentary Holdings NL [TCR 97-3993].
- SUMMONS, T. G. 1998. *Annual Report for the Forster Project, southern Tasmania. EL's 11/84, 3/94 and 33/96 for the period ended September 1998*. Sedimentary Holdings NL [TCR 99-4312].
- SUMMONS, T. G. 1999. Forster – a new metallogenic district in Tasmania. *Papers Tasmanian Mineral Exploration and Investment '99 Conference, Hobart, May 1999*. Australian Journal of Mining.
- SUTHERLAND, F. L.; CORBETT, E. B. 1974. The extent of Upper Mesozoic igneous activity in relation to lamprophyric intrusions in Tasmania. *Papers Proceedings Royal Society Tasmania* 107:175–190.
- TAHERI, J. 1989. Preliminary fluid inclusion and petrographic study on samples SW1-1 and SW1-2, Weld River area, south-west Tasmania. *Consultancy Report Department of Mines Tasmania*.

- TAHERI, J. 1990 Petrographic, oxygen isotope and fluid inclusion studies, and the clay mineralogy of some core samples from DDH BC15 and sample BCF8, Weld River area. *Consultancy Report Division of Mines and Mineral Resources Tasmania*.
- TAHERI, J.; BOTTRILL, R. S. 1994. A study of the nature and origin of the gold mineralisation, Mangana-Forester area, northeast Tasmania. *Report Department Mines Tasmania* 1994/05.
- TAHERI, J.; BOTTRILL, R. S. 1999. Porphyry and sedimentary-hosted gold deposits near Cygnet. New styles of gold mineralisation in Tasmania. *Record Geological Survey Tasmania* 1999/01.
- THOMPSON, A. J. B.; THOMPSON, J. F. H. (ed.). 1996. Atlas of alteration — A field and petrographic guide to hydrothermal alteration minerals. *Special Publication Geological Association of Canada (Mineral Deposits Division)* 6.
- TURNER, N. J.; BLACK, L. P.; KAMPERMAN, M. 1998. Dating of Neoproterozoic and Cambrian orogenies in Tasmania. *Australian Journal Earth Sciences* 45:789–806.
- VEEVERS, J. J. (Ed.). 1984. *Phanerozoic Earth history of Australia*. Clarendon Press : Oxford.
- VENNEMANN, T. W.; MUNTEAN, J. L.; KESLER, S. E.; O'NEIL, J. R.; VALLEY, J. W.; RUSSELL, N. 1993. Stable isotope evidence for magmatic fluids in the Pueblo Viejo epithermal acid sulfate Au-Ag deposit, Dominican Republic. *Economic Geology* 88:55–71.
- WALLACE, A. R. 1989. The Relief Canyon gold deposits, Nevada: a mineralised solution breccia. *Economic Geology* 84:272–290.
- WINKLER, H. G. 1976. *Petrogenesis of metamorphic rocks*. (4th edition). Springer-Verlag : Berlin.
- WOOD, B. L. 1971. *Inland Exploration NL. Exploration Licence 3/70, Weld River area, Tasmania*. Hall, Relph and Associates Pty Ltd [TCR71-741].
- YOUNG, S. 1997. 1996–97 *Annual Report for the Forster Project, southern Tasmania*. EL's 11/84, 3/94 and 33/96. Sedimentary Holdings NL [TCR 97-4081].
- ZHARIKOV, V. A. 1991. Skarn types, formation and ore mineralization conditions, in: BARTO-KYRIAKIDIS, A. (ed.). *Skarns — their genesis and metallogeny*. 455–466. Theophrastus Publications : Athens.

[30 November 2000]

APPENDIX 1

Glossary of rocks and minerals

Rock types

Appinite

A medium to coarse-grained hornblende-phyric intrusive igneous rock with a feldspar-rich matrix, related to the lamprophyres.

Calciophyre

A crystalline limestone containing silicate minerals.

Ophicalcite

A rock essentially composed of calcite and serpentine, usually derived from a forsterite marble.

Spessartite

A dioritic lamprophyre composed mostly of hornblende and plagioclase.

Minerals from the Forster Prospect

Native Elements

| | |
|------------------------|-------------|
| Gold | Au |
| Iridium ('Osmiridium') | (Ir, Os) |
| Osmium ('Osmiridium') | (Os, Ir) |
| Protographite | amorphous C |

Sulphide minerals

| | |
|-----------------------|---|
| Chalcopyrite | CuFeS ₂ |
| Cobaltite | CoAsS |
| Cubanite | CuFe ₂ S ₃ |
| Galena | PbS |
| Gersdorffite | NiAsS |
| Loellingite | FeAs ₂ |
| Marcasite | FeS ₂ |
| Millerite | NiS |
| Niccolite (nickeline) | NiAs |
| Proustite | Ag ₃ AsS ₃ |
| Pyrite | FeS ₂ |
| Pyrrhotite(?) | Fe _{1-x} S |
| Rammelsbergite | NiAs ₂ |
| Sphalerite | ZnS |
| Tetrahedrite | (Cu,Fe,Zg) ₁₂ (Sb,As) ₄ S ₁₃ |

Oxide minerals

| | |
|------------------|--|
| Anatase | TiO ₂ |
| Brucite | Mg(OH) ₂ |
| Chromite | (Fe, Mg)Cr ₂ O ₄ |
| Goethite | FeO(OH) |
| Hematite | Fe ₃ O ₄ |
| Ilmenite | FeTiO ₃ |
| Magnesiochromite | (Mg, Fe)Cr ₂ O ₄ |

| | |
|-------------|--------------------------------|
| Magnetite | Fe ₃ O ₄ |
| (Periclase) | MgO |
| Rutile | TiO ₂ |

Carbonate minerals

| | |
|----------------|---|
| Aragonite | CaCO ₃ |
| Calcite | CaCO ₃ |
| Dolomite | CaMg(CO ₃) ₂ |
| Siderite | FeCO ₃ |
| Hydromagnesite | Mg ₅ (CO ₃) ₄ (OH) ₂ .4H ₂ O |
| Sjogrenite | Mg ₆ Fe ₂ (CO ₃)(OH) ₁₆ .4H ₂ O |

Phosphate and arsenate minerals

| | |
|--------------|---|
| Fluorapatite | Ca ₅ (PO ₄) ₃ F |
| Symplectite | Fe ₃ (AsO ₄) ₂ .8H ₂ O |

Silicate minerals

| | |
|--|--|
| Andradite | Ca ₃ Fe ₂ (SiO ₄) ₃ |
| Actinolite | Ca ₂ (Mg,Fe) ₅ Si ₈ O ₂₂ (OH) ₂ |
| Andesine | (Na,Ca)Si ₄ O ₈ |
| Augite | (Ca,Na)(Mg,Fe)Si ₂ O ₆ |
| Biotite | K(Mg,Fe) ₃ AlSi ₃ O ₁₀ (OH) ₂ |
| Chrysotile | Mg ₃ Si ₂ O ₅ (OH) ₄ |
| Clinocllore | (Mg,Fe,Al) ₆ Si ₄ O ₁₀ (OH) ₈ |
| Clinozoisite | Ca ₂ Al ₃ Si ₂ O ₇ (SiO ₄)(OH) ₂ |
| Diopside | CaMgSi ₂ O ₆ |
| Edenite | Na(Ca,Na) ₂ (Mg,Fe,Al) ₅ (Si,Al) ₈ O ₂₂ (OH) ₂ |
| Enstatite | MgSiO ₃ |
| Epidote | Ca ₂ (Al,Fe) ₃ Si ₂ O ₇ (SiO ₄)(OH) ₂ |
| Ferroactinolite | Ca ₂ (Fe,Mg) ₅ Si ₈ O ₂₂ (OH) ₂ |
| Fluorapophyllite | KCa ₄ Si ₈ O ₂₀ (F,OH).8H ₂ O |
| (Forsterite) | Mg ₂ SiO ₄ |
| Garnierite | a variable group of nickel-rich hydrous Mg-silicates |
| Gedrite | (Mg,Fe)Al ₄ Si ₆ O ₂₂ (OH) ₂ |
| Grossular | Ca ₃ Al ₂ (SiO ₄) ₃ |
| Gyrolite | NaCa ₁₆ AlSi ₂₄ O ₆₀ (OH) ₈ . 14H ₂ O |
| Halloysite | Al ₂ Si ₂ O ₅ (OH) ₄ |
| Hedenbergite | CaFeSi ₂ O ₆ |
| Heulandite | (Na,K,Ca) ₅ Al ₉ Si ₂₇ O ₇₂ .26H ₂ O |
| Hydro-andradite (hydrous andradite) | Ca ₃ Fe ₂ (SiO ₄ ,H ₂ O) ₃ |
| Hydrogrossular (garnets in the grossular-hibschite-katoite series) | Ca ₃ Al ₂ (SiO ₄ ,H ₂ O) ₃ |
| Illite | (K,H ₃ O)Al ₃ Si ₃ O ₁₀ (OH) ₂ |
| Kaolinite | Al ₂ Si ₂ O ₅ (OH) ₄ |
| Laumontite | CaAl ₂ Si ₄ O ₁₂ .4H ₂ O |
| Lizardite (Serpentine) | Mg ₃ Si ₂ O ₅ (OH) ₄ |
| Magnesio-Hornblende | (Ca,Na) ₂ (Mg,Fe,Al) ₅ (Si,Al) ₈ O ₂₂ (OH) ₂ |
| Montmorillonite | (Na,Ca) _{0.3} (Al,Mg) ₂ Si ₄ O ₁₀ (OH) ₂ |
| Muscovite | KAl ₃ Si ₃ O ₁₀ (OH) ₂ |

| | | | |
|------------|--|--------------|---|
| Okenite | $\text{Ca}_{10}\text{Si}_{18}\text{O}_{46} \cdot 18\text{H}_2\text{O}$ | Serpentine | A group of hydrous Mg silicates: see lizardite and chrysotile |
| Opal | $\text{SiO}_2 \cdot n\text{H}_2\text{O}$ | Smectite | A group of clay minerals, including montmorillonite and saponite |
| Orthoclase | KAlSi_3O_8 | Sphene | CaTiSiO_5 |
| Pargasite | $\text{NaCa}_2(\text{Mg,Fe})_4\text{Al}(\text{Si,Al})_8\text{O}_{22}(\text{OH})_2$ | Talc | $\text{Mg}_3\text{Si}_4\text{O}_{10}(\text{OH})_2$ |
| Pectolite | $\text{NaCa}_2\text{Si}_3\text{O}_8(\text{OH})$ | Tobermorite | $\text{Ca}_5\text{Si}_6\text{O}_{16}(\text{OH})_2 \cdot x\text{H}_2\text{O}$ |
| Pigeonite | $(\text{Mg,Ca,Na,Fe})_2\text{Si}_2\text{O}_6$ | Tremolite | $\text{Ca}_2\text{Mg}_5\text{Si}_8\text{O}_{22}(\text{OH})_2$ |
| Prehnite | $\text{Ca}_2\text{AlSi}_4\text{O}_{10}(\text{OH})_2$ | Truscottite | $\text{Ca}_{14}\text{Si}_{24}\text{O}_{58}(\text{OH})_8 \cdot 2\text{H}_2\text{O}$ |
| Quartz | SiO_2 | Vesuvianite | $\text{Ca}_{19}\text{Fe}(\text{Mg,Al})_8\text{Al}_8(\text{SiO}_4)_{10}(\text{OH})_{10}$ |
| Saponite | $(\text{Na,Ca})_{0.3}(\text{Mg,Al})_2\text{Si}_4\text{O}_{10}(\text{OH})_2$ | Wollastonite | CaSiO_3 |
| Scawtite | $\text{Ca}_7(\text{Si}_3\text{O}_9)_2(\text{CO}_3) \cdot 2\text{H}_2\text{O}$ | Xonotlite | $\text{Ca}_6\text{Si}_6\text{O}_{17}(\text{OH})_2$ |
| Sepiolite | $\text{Mg}_4\text{Si}_6\text{O}_{15}(\text{OH})_2 \cdot 6\text{H}_2\text{O}$ | Zircon | ZrSiO_4 |
| Sericite | a fine-grained white mica | | |

Appendix 2

Abbreviations used in rock descriptions

| <i>abbreviation</i> | <i>name</i> | | |
|---------------------|-------------------|-------|----------------------------|
| abrc | autobrecciated | lim | limonite |
| adr | andradite | loll | loellingite |
| altd | altered | mgd | medium grained |
| am | amphibole | m-lay | mixed-layer clays |
| amyg | amygdaloidal | mt | magnetite |
| apo | apophyllite | MuSt | mudstone |
| arag | aragonite | nic | nickeline |
| blac | black | opl | opal |
| blea | bleached | opx | orthopyroxene |
| brc | brucite | pebb | pebbly |
| brec | brecciated | pl | plagioclase |
| brow | brown | po | pyrrhotite |
| brx | breccia | porph | porphyry/tic |
| bt | biotite | prn | prehnite |
| ca | chemical analysis | PT | polished thin section |
| carb | carbonaceous | purp | purple |
| cgd | coarse grained | py | pyrite |
| chd | chalcedonic | qtz | quartz |
| chert | cherty | ram | rammelsbergite |
| chl | chlorite | sand | sandy |
| chr | chromite | ser | sericitic |
| CO ₃ | carbonate | shear | sheared |
| cong | conglomerate | Si | siliceous/silica-saturated |
| cpx | clinopyroxene | sid | siderite |
| cpy | chalcopyrite | sifd | silicified |
| di | diopside | silt | silty |
| dol | dolomite | sjo | sjogrenite |
| ep | epidote | sl | sphalerite |
| eqgr | equigranular | sme | smectite |
| fgd, fgnd | fine grained | srp | serpentine |
| FI | fluid inclusion | sx | sulphide |
| foss | fossiliferous | tlc | talc |
| fsp | feldspar | tob | tobermorite |
| glass | glassy | trem | tremolite |
| gn | galena | TS | thin section |
| grt | garnet | umfc | ultramafic |
| gt | goethite | vein | veined |
| hall | halloysite | ves | vesuvianite |
| hbd | hornblende | vugg | vuggy |
| hem | hematite | whit | white |
| hfld | hornfelsed | woll | wollastonite |
| hyn | hauyne | WR | whole rock analysis |
| is | isotopic analysis | wthd | weathered |
| jar | jarosite | xenl | xenolithic |
| kaol | kaolinite | xon | xonotlite |
| kf | k-feldspar | XR | xrd |
| lami | laminated | yell | yellow |
| laum | laumontite | ze | zeolite |
| <i>abbreviation</i> | <i>name</i> | zeol | zeolitic |

APPENDIX 3

Summarised details of samples, Weld River

| Reg. No. | Name | Minerals | Mod | Age | Unit Code | mE | mN | Accuracy (m) | Locality | Coll. | Year | Treatment | Refs | Comments | Au (g/t) |
|----------|----------------|--------------|-----|-----|-----------|--------|---------|--------------|-------------|-------|-------|----------------|-----------|---------------------|----------|
| C102098 | mylonite | tlc | | Pzc | Cal | 478150 | 5234180 | 50 | Forsters Pr | pr | 1986? | PT | UR1996/15 | 10900N | |
| C103796 | quartz | | | | | 478200 | 5233750 | 50 | Forsters Pr | jt | 1986? | IS, FI | | | |
| G400234 | opal | | | | | 478200 | 5233800 | 100 | Forsters Pr | rsb | 1982 | | UR1996/15 | | |
| G400235 | chert | chr,dol | | | | 478200 | 5235100 | 100 | Forsters Pr | rsb | 1982 | TS, WR | UR1996/15 | Hogsback Hill | |
| G400236 | silica flour | | | | | 478300 | 5234800 | 100 | Forsters Pr | rsb | 1982 | | UR1996/15 | pit | |
| G400237 | dolerite | py,hbd,opx | | Mj | Jdl | 478110 | 5234470 | 50 | Forsters Pr | rsb | 1982 | TS, PT | UR1996/15 | north bank | |
| G400238 | dolomite | | | PR | Pw | 477750 | 5235500 | 50 | Forsters Pr | rsb | 1982 | XR, WR, PT | UR1996/15 | river bed | |
| G400239 | ophicalcite | di | | | | 477800 | 5235550 | 50 | Forsters Pr | rsb | 1982 | XR, WR, TS | UR1996/15 | pit | |
| G400240 | dolomite | srp | | PR | Pw | 477750 | 5235500 | 50 | Forsters Pr | rsb | 1982 | XR, WR, TS | UR1996/15 | pit | |
| G400241 | hornfels | di | | | | 477750 | 5235500 | 50 | Forsters Pr | rsb | 1982 | | UR1996/15 | | |
| G400242 | dolerite | opx | | Mj | Jdl | 477750 | 5235700 | 50 | Forsters Pr | rsb | 1982 | TS | UR1996/15 | big eddy | |
| G400243 | chert | | | | | 478400 | 5234800 | 100 | Forsters Pr | rsb | 1982 | WR | UR1996/15 | | |
| G400263 | hornfels | qtz, di, xon | | | | 477750 | 5235500 | 50 | Forsters Pr | McF | 1905 | TS | UR1996/15 | | |
| G400279 | chalcedony | | | | | 478200 | 5233700 | 200 | Forsters Pr | McF | 1905 | | UR1996/15 | | |
| G400299 | dolomite | | | PR | Pw | 477750 | 5235500 | 50 | Forsters Pr | McF | 1905 | | UR1996/15 | | |
| G400336 | phyllite | tlc,mag,chr | | Pzc | Cal | 478150 | 5234180 | 200 | Forsters Pr | DJ | 1984 | TS | UR1996/15 | line 10900N costean | |
| G400337 | lamprophyre | chl,hbd | | | | 478000 | 5234200 | 200 | Forsters Pr | DJ | 1984 | TS | UR1996/15 | line 10900N costean | |
| G400338 | dolerite | opx | | Mj | Jdl | 478000 | 5234200 | 200 | Forsters Pr | DJ | 1984 | TS | UR1996/15 | line 10900N costean | |
| G400904 | ophicalcite | opa, srp | | | | 478000 | 5234200 | 200 | Forsters Pr | DJ | 1984 | TS, XR | UR1996/15 | line 10900N costean | |
| G402036 | mudstone/chert | mica | | | | 478100 | 5234200 | 200 | Forsters Pr | McF | 1990 | XR, TS | UR1996/15 | line 10900N costean | |
| G402037 | hornfels | di, srp, cal | | | | 478100 | 5234200 | 200 | Forsters Pr | McF | 1990 | XR, TS | UR1996/15 | jade | |
| G402038 | conglomerate | tlc,hem,chl | | Pzc | Cal | 478150 | 5234180 | 200 | Forsters Pr | McF | 1990 | XR, TS | UR1996/15 | line 10900N costean | |
| G402039 | lamprophyre | chl,mica,hbd | | | | 478000 | 5234200 | 200 | Forsters Pr | McF | 1990 | XR, TS | UR1996/15 | line 10900N costean | |
| G402040 | lamprophyre | chl,px,hbd | | | | 478000 | 5234200 | 200 | Forsters Pr | McF | 1990 | XR, TS, WR, CA | UR1996/15 | line 10900N costean | 0.02 |
| G402136 | chert | opl,lim | | | | 478200 | 5234350 | 200 | Forsters Pr | McF | 1988 | XR, TS | UR1996/15 | riverbank? | |
| G402137 | phyllite | tlc,hem,kao | | Pzc | Cal | 478150 | 5234180 | 200 | Forsters Pr | McF | 1988 | XR, PT | UR1996/15 | line 10900N costean | |
| G402138 | greywacke | am,tlc,sme | | Pzc | Cal | 478150 | 5234180 | 200 | Forsters Pr | McF | 1988 | XR, TS | UR1996/15 | line 10900N costean | |
| G402139 | greywacke | am,chr,tlc | | Pzc | Cal | 478150 | 5234180 | 200 | Forsters Pr | McF | 1988 | XR, PT, PA | UR1996/15 | line 10900N costean | |
| G402140 | pyroxenite | tlc,mem,mt | | Pzc | Cal | 478050 | 5233700 | 200 | Forsters Pr | McF | 1988 | XR, TS, WR, CA | UR1996/15 | near old shafts | 0.01 |
| G402141 | skarn | qtz,wo,gro | | | | 478214 | 5233560 | 200 | Forsters Pr | McF | 1988 | XR, PT | UR1996/15 | Weld DDH1 | |
| G402142 | ophicalcite | brc,opl | | | | 478200 | 5234180 | 200 | Forsters Pr | McF | 1988 | XR, TS | UR1996/15 | line 10900N costean | |
| G402148 | phyllite | mag,tlc | | | | 478150 | 5234180 | 200 | Forsters Pr | McF | 1988 | XR, TS | UR1996/15 | line 10900N costean | |
| G402149 | ophicalcite | | | | | 478214 | 5233560 | 100 | Forsters Pr | McF | 1988 | XR, TS | UR1996/15 | Weld DDH1 | |
| G402150 | ophicalcite | brc | | | | 478214 | 5233560 | 100 | Forsters Pr | McF | 1988 | XR, TS | UR1996/15 | Weld DDH1 | |
| G402151 | chert | | | | | 478214 | 5233560 | 5 | Forsters Pr | rsb | 1988 | TS | UR1996/15 | Weld DDH1, 49.2 | |

| Reg. No. | Name | Minerals | Mod | Age | Unit Code | mE | mN | Accuracy (m) | Locality | Coll. | Year | Treatment | Refs | Comments | Au (g/t) |
|----------|------------------|----------------|------|-----|-----------|--------|---------|--------------|-------------|-------|------|--------------------|-----------|---|--------------------------|
| G402152 | chert | opl,cal | | | | 478214 | 5233560 | 5 | Forsters Pr | rsb | 1988 | TS | UR1996/15 | Weld DDH1, 54.8 | |
| G402153 | skarn | qtz,opl | | | | 478214 | 5233560 | 5 | Forsters Pr | rsb | 1988 | TS, XR | UR1996/15 | Weld DDH1, 55.7 | |
| G402154 | dolerite | prh,qtz,px,brx | | Mj | Jdl | 478214 | 5233560 | 5 | Forsters Pr | rsb | 1988 | PT, XR, WR, CA | UR1996/15 | dolerite? | 0.55 |
| G402155 | dolerite | opx,laum | | Mj | Jdl | 478214 | 5233560 | 5 | Forsters Pr | rsb | 1988 | TS, XR | UR1996/15 | laumontite | |
| G402156 | chert | opa,sme,clay | | | | 478214 | 5233560 | 5 | Forsters Pr | rsb | 1988 | XR | UR1996/15 | Weld DDH1, 63.7 | |
| G402157 | ophicalcite | brc | | | | 478214 | 5233560 | 5 | Forsters Pr | rsb | 1988 | XR, TS | UR1996/15 | Weld DDH1, 66.9 | |
| G402158 | ophicalcite | brc,sl | | | | 478214 | 5233560 | 5 | Forsters Pr | rsb | 1988 | XR, TS | UR1996/15 | Weld DDH1, 67.6 | |
| G402159 | ophicalcite | brc,and | | | | 478214 | 5233560 | 5 | Forsters Pr | rsb | 1988 | XR, TS, WR, CA | UR1996/15 | Weld DDH1, 68 | 0.03 |
| G402160 | ophicalcite | | | | | 478214 | 5233560 | 5 | Forsters Pr | rsb | 1988 | TS | UR1996/15 | Weld DDH1, 68.3 | |
| G402161 | dolerite contact | srp,qtz,and,Cu | | | | 478214 | 5233560 | 5 | Forsters Pr | rsb | 1988 | XR, PT, PA | UR1996/15 | sphalerite, galena, dolerite, ophicalcite | Weld DDH1, 69.2, contact |
| G402162 | ophicalcite | brc | | | | 478214 | 5233560 | 5 | Forsters Pr | rsb | 1988 | TS, XR | UR1996/15 | Weld DDH1, 73.3 | |
| G402163 | skarn | qtz,xon,di,Zn | | | | 478214 | 5233560 | 5 | Forsters Pr | rsb | 1988 | XR, PT, PA, WR, CA | UR1996/15 | green?, white?, millerite, mt | 0.25 |
| G402164 | hornfels | cal,di,tlc | | | | 478214 | 5233560 | 5 | Forsters Pr | rsb | 1988 | PT, PA | UR1996/15 | nicc, ramm, loellingite | Weld DDH1, 78.7 |
| G402165 | skarn | cal,di | | | | 478214 | 5233560 | 5 | Forsters Pr | rsb | 1988 | XR, TS | UR1996/15 | apophyllite, tobermorite | 0.07 |
| G402166 | skarn | qtz,xon,di,Ni | | | | 478214 | 5233560 | 5 | Forsters Pr | rsb | 1988 | XR, TS, PA, WR, CA | UR1996/15 | cal, sl, mill | Weld DDH1, 81.9 |
| G402167 | hornfels | di | | | | 478133 | 5233563 | 5 | Forsters Pr | rsb | 1988 | XR | UR1996/15 | South Weld DDH 2, 34.0 | |
| G402168 | opal | sme,qtz,clay | | | | 478133 | 5233563 | 5 | Forsters Pr | rsb | 1988 | XR, WR, CA, PT | UR1996/15 | smectite, tridymite | 1.07 |
| G402169 | skarn | qtz,xon,prn | | | | 478133 | 5233563 | 5 | Forsters Pr | rsb | 1988 | TS, XR, PA, WR, CA | UR1996/15 | green??., tlc, laum, sl, mill, arag. | 0.9 |
| G402170 | ophicalcite | brc,di | | | | 478133 | 5233563 | 5 | Forsters Pr | rsb | 1988 | TS, XR, WR, CA | UR1996/15 | South Weld DDH 2, 50.2 | |
| G402171 | ophicalcite | brc | | | | 478133 | 5233563 | 5 | Forsters Pr | rsb | 1988 | TS, XR | UR1996/15 | South Weld DDH 2, 52.5 | |
| G402172 | ophicalcite | brc | | | | 478133 | 5233563 | 5 | Forsters Pr | rsb | 1988 | TS | UR1996/15 | South Weld DDH 2, 53.2 | |
| G402173 | ophicalcite | di,grt | | | | 478133 | 5233563 | 5 | Forsters Pr | rsb | 1988 | TS, XR | UR1996/15 | gn, loll, cpy, sl | |
| G402174 | ophicalcite | brc,mt | | | | 478133 | 5233563 | 5 | Forsters Pr | rsb | 1988 | TS, XR, WR, CA | UR1996/15 | sjog, hydromag | 0.1 |
| G402175 | ophicalcite | brc,di | | | | 478133 | 5233563 | 5 | Forsters Pr | rsb | 1988 | TS, XR, WR, CA | UR1996/15 | garnet | 0.01 |
| G402176 | calcite | | | | | 478133 | 5233563 | 5 | Forsters Pr | rsb | 1988 | | UR1996/15 | South Weld DDH 2, 69.9 | |
| G402177 | ophicalcite | brc,grt,sl | | | | 478133 | 5233563 | 5 | Forsters Pr | rsb | 1988 | TS, XR, PA, WR, CA | UR1996/15 | gn, loll, cpy, gold | 0.1 |
| G402178 | skarn | di,srp,cal | | | | 478133 | 5233563 | 5 | Forsters Pr | rsb | 1988 | TS, XR, WR, CA | UR1996/15 | sl | 0.14 |
| G402179 | ophicalcite | brc,mt,mica | | | | 478133 | 5233563 | 5 | Forsters Pr | rsb | 1988 | TS, XR, WR, CA | UR1996/15 | sjogrenite | South Weld DDH 2, 89.9 |
| G402180 | dolerite contact | srp,prn,di | | Mj | Jdl | 478133 | 5233563 | 5 | Forsters Pr | rsb | 1988 | TS, XR, PA | UR1996/15 | ophicalcite | South Weld DDH 2, 103.8 |
| G402181 | dolerite | opx | | Mj | Jdl | 478133 | 5233563 | 5 | Forsters Pr | rsb | 1988 | TS, WR, CA | UR1996/15 | laumontite | 0.01 |
| G402182 | chert | qtz,tlc,hem | | | | 478100 | 5234180 | 100 | Forsters Pr | rsb | 1988 | XR, TS | UR1996/15 | chr | 10900N costean |
| G402183 | skarn | sme,di,srp | | | | 478133 | 5233563 | 5 | Forsters Pr | rsb | 1988 | XR | UR1996/15 | South Weld DDH 2, 48.0 | |
| G402184 | dolerite | | mgd | Mj | Jdl | 478133 | 5233563 | 5 | Forsters Pr | rsb | 1988 | TS | UR1996/15 | laumontite | South Weld DDH 2, 109.1 |
| G402185 | dolerite | | | Mj | Jdl | 478133 | 5233563 | 5 | Forsters Pr | rsb | 1988 | TS | UR1996/15 | South Weld DDH 2, 110.4 | |
| G402186 | chert | | | | | 478120 | 5233500 | 50 | Forsters Pr | rsb | 1988 | TS, WR, CA | UR1996/15 | | |
| G402187 | chert | hem | | | | 478120 | 5233500 | 50 | Forsters Pr | rsb | 1988 | TS | UR1996/15 | | |
| G402188 | breccia | hem,qtz | | | | 478120 | 5233500 | 50 | Forsters Pr | rsb | 1988 | | UR1996/15 | | |
| G402189 | chert | hem | clay | | | 478120 | 5233500 | 50 | Forsters Pr | rsb | 1988 | TS | UR1996/15 | chr | |

| Reg. No. | Name | Minerals | Mod | Age | Unit Code | mE | mN | Accuracy (m) | Locality | Coll. | Year | Treatment | Refs | Comments | Au (g/t) |
|----------|--------------|--------------|-------|-----|-----------|--------|---------|--------------|-------------|-------|------|--------------------|-----------|------------------|----------------|
| G402190 | chert | hem | | | | 478120 | 5233500 | 50 | Forsters Pr | rsb | 1988 | TS, WR, CA | UR1996/15 | | 0.13 |
| G402191 | chert | | | | | 478120 | 5233500 | 50 | Forsters Pr | rsb | 1988 | | UR1996/15 | | |
| G402192 | talc | | | Pzc | Cal | 478050 | 5233650 | 50 | Forsters Pr | rsb | 1988 | | UR1996/15 | | |
| G402194 | breccia | qtz | carb | | | 478160 | 5233750 | 50 | Forsters Pr | rsb | 1988 | TS, WR, CA | UR1996/15 | | |
| G402196 | chert | hem,py | | | | 478100 | 5233870 | 50 | Forsters Pr | rsb | 1988 | TS | UR1996/15 | | |
| G402197 | breccia | qtz | | | | 478100 | 5233870 | 50 | Forsters Pr | rsb | 1988 | | UR1996/15 | | |
| G402198 | limonite | | | | | 478100 | 5233870 | 50 | Forsters Pr | rsb | 1988 | WR, CA | UR1996/15 | opal zone, track | 2.87 |
| G402199 | opal | | | | | 478100 | 5233870 | 50 | Forsters Pr | rsb | 1988 | | UR1996/15 | | |
| G402200 | opal | | | | | 478100 | 5233870 | 50 | Forsters Pr | rsb | 1988 | | UR1996/15 | | |
| G402205 | chalcedony | lim | chert | | | 478100 | 5233870 | 50 | Forsters Pr | rsb | 1988 | PT, WR, CA | UR1996/15 | | 0.64 |
| G402206 | opal | cal,sid,srp | | | | 478220 | 5234350 | 50 | Forsters Pr | rsb | 1988 | PT, PA, XR, WR, CA | UR1996/15 | dol | 0.04 |
| G402207 | chert | opl,di,cal | | | | 478140 | 5234370 | 50 | Forsters Pr | rsb | 1988 | TS, XR | UR1996/15 | | |
| G402208 | breccia | di,sid | | | | 478000 | 5234450 | 50 | Forsters Pr | rsb | 1988 | TS | UR1996/15 | | |
| G402209 | chert | hem | | | | 478150 | 5234390 | 50 | Forsters Pr | rsb | 1988 | TS, WR, CA | UR1996/15 | Gn pt | 0.04 |
| G402210 | phyllite | chl,qtz,fsp | | Pzc | Cal | 478000 | 5234450 | 50 | Forsters Pr | rsb | 1988 | TS | UR1996/15 | | |
| G402211 | dolerite | opx | | Mj | Jdl | 478050 | 5234470 | 50 | Forsters Pr | rsb | 1988 | TS | UR1996/15 | | |
| G402214 | conglomerate | tlc,trlm,chr | | Pzc | Cal | 478150 | 5234180 | 50 | Forsters Pr | McF | 1988 | TS | UR1996/15 | mt | 10900N costean |
| G402335 | hornfels | di,srp,cal | | | | 478100 | 5234180 | 50 | Forsters Pr | McF | 1988 | XR | UR1996/15 | | 10900N costean |
| G402336 | ophicalcite | | | | | 478100 | 5234180 | 50 | Forsters Pr | McF | 1988 | XR | UR1996/15 | | 10900N costean |
| G402437 | phyllite | hem,tlc | | Pzc | Cal | 478000 | 5234180 | 50 | Forsters Pr | McF | 1989 | XR | UR1996/15 | | 10900N costean |
| G402438 | phyllite | chl,tlc | | Pzc | Cal | 478000 | 5234180 | 50 | Forsters Pr | McF | 1989 | XR | UR1996/15 | | 10900N costean |
| G402439 | conglomerate | kln,hem,tlc | | Pzc | Cal | 478000 | 5234180 | 50 | Forsters Pr | McF | 1989 | XR | UR1996/15 | | 10900N costean |
| G402440 | hornfels | cal,di,qtz | | | | 478100 | 5234180 | 50 | Forsters Pr | McF | 1989 | XR | UR1996/15 | srp | 10900N costean |
| G402441 | conglomerate | tlc,am,pl | | Pzc | Cal | 478000 | 5234180 | 50 | Forsters Pr | McF | 1989 | XR | UR1996/15 | | 10900N costean |
| G402442 | hornfels | di,srp,cal | | | | 478100 | 5234180 | 50 | Forsters Pr | McF | 1989 | TS, XR | UR1996/15 | | 10900N costean |
| G402443 | ophicalcite | spl | | | | 478100 | 5234180 | 50 | Forsters Pr | McF | 1989 | TS | UR1996/15 | | 10900N costean |
| G402444 | hornfels | di,qtz,prn | | | | 478100 | 5234180 | 50 | Forsters Pr | McF | 1989 | TS, XR | UR1996/15 | am, chl | 10900N costean |
| G402445 | opal | | | | | 478200 | 5234200 | 200 | Forsters Pr | McF | 1989 | | UR1996/15 | | 10900N costean |
| G402446 | mudstone | | | PzP | | 478000 | 5234200 | 200 | Forsters Pr | McF | 1989 | TS | UR1996/15 | | 10900N costean |
| G402447 | dolerite | | | Mj | Jdl | 478000 | 5234200 | 200 | Forsters Pr | McF | 1989 | XR | UR1996/15 | | 10900N costean |
| G402448 | pyroxenite | tlc,sme,kln | | Pzc | Cal | 478000 | 5234200 | 200 | Forsters Pr | McF | 1989 | XR | UR1996/15 | | 10900N costean |
| G402449 | dolerite? | | | Mj | Jdl | 478000 | 5234200 | 200 | Forsters Pr | McF | 1989 | | UR1996/15 | | 10900N costean |
| G402450 | opal | | | | | 478100 | 5233870 | 50 | Forsters Pr | rsb | 1989 | WR, CA | UR1996/15 | | |
| G402479 | dolerite | opx,mgd | | Mj | Jdl | 477200 | 5235450 | 50 | Forsters Pr | kcm | 1991 | TS | UR1996/15 | | |
| G402480 | hornfels | di,qtz,wol | | | | 477750 | 5235550 | 50 | Forsters Pr | kcm | 1991 | TS, XR | UR1996/15 | Xon, calcite | |
| G402481 | breccia | qtz,lim,whit | | | | 478150 | 5233800 | 50 | Forsters Pr | kcm | 1991 | TS, XR | UR1996/15 | | |
| C107635 | quartz | | | | | 478200 | 5233750 | 50 | Forsters Pr | rsb | 1990 | | UR1996/15 | | |
| C107636 | quartz | | blac | | | 478200 | 5233750 | 50 | Forsters Pr | rsb | 1990 | | UR1996/15 | | |
| C107637 | quartz | | grey | | | 478200 | 5233750 | 50 | Forsters Pr | rsb | 1990 | | UR1996/15 | | |

| Reg. No. | Name | Minerals | Mod | Age | Unit Code | mE | mN | Accuracy (m) | Locality | Coll. | Year | Treatment | Refs | Comments | Au (g/t) |
|----------|--------------|-------------|------|-----|-----------|--------|---------|--------------|-------------|-------|------|------------|-----------|------------------------------------|----------|
| C107638 | opal | | blac | | | 478150 | 5234180 | 50 | Forsters Pr | rsb | 1990 | | UR1996/15 | 10900N costean | |
| C107639 | lamprophyre | hbd | | | | 478100 | 5234180 | 50 | Forsters Pr | rsb | 1990 | PT, WR, CA | UR1996/15 | 10900N costean | |
| C107640 | appinite | hbd | | | | 478100 | 5234180 | 50 | Forsters Pr | rsb | 1990 | | UR1996/15 | 10900N costean | |
| C107641 | breccia | tlc | | Pzc | Cal | 478050 | 5234180 | 50 | Forsters Pr | rsb | 1990 | | UR1996/15 | 10900N costean | |
| C107642 | conglomerate | qtz | | | | 478170 | 5234370 | 50 | Forsters Pr | rsb | 1990 | PT | UR1996/15 | south bank | |
| C107643 | limonite | | | | | 478130 | 5234400 | 50 | Forsters Pr | rsb | 1990 | WR, CA | UR1996/15 | south bank | 6.72 |
| C107644 | dolomite | tlc | | PR | Pw | 478050 | 5234430 | 50 | Forsters Pr | rsb | 1990 | PT, XR | UR1996/15 | | |
| C107693 | mudstone | | | | | 469000 | 5240000 | 500 | Mt Weld | rsb | 1992 | PT, XR | UR1996/15 | | |
| C107694 | chert | | | | | 469000 | 5240000 | 500 | Mt Weld | rsb | 1992 | Pt | UR1996/15 | | |
| C107695 | mixtite | | | PzP | Perm | 469000 | 5240000 | 500 | Mt Weld | rsb | 1992 | PT, XR | UR1996/15 | | |
| C107696 | quartz | | | | | 469000 | 5240000 | 500 | Mt Weld | rsb | 1992 | | UR1996/15 | | |
| C107697 | quartz | | | | | 469000 | 5240000 | 500 | Mt Weld | rsb | 1992 | | UR1996/15 | | |
| C107698 | quartz | | | | | 469000 | 5240000 | 500 | Mt Weld | rsb | 1992 | | UR1996/15 | | |
| C107699 | quartz | | | | | 469000 | 5240000 | 500 | Mt Weld | rsb | 1992 | | UR1996/15 | | |
| C107805 | breccia | qtz | | | | 478190 | 5233550 | 50 | Forsters Pr | rsb | 1992 | CA | UR1996/15 | Forster Road | |
| C107806 | breccia | opa | | | | 478200 | 5233900 | 50 | Forsters Pr | rsb | 1992 | PT, XR, CA | UR1996/15 | Forster Road | |
| C107807 | lamprophyre | hbd | | | | 478100 | 5234180 | 50 | Forsters Pr | rsb | 1992 | PT, PA | UR1996/15 | 10900N | |
| C107808 | diamictite | hall | | PzP | | 478250 | 5233500 | 50 | Forsters Pr | rsb | 1992 | XR | UR1996/15 | Fletchers Road | |
| C107809 | diamictite | hall | | PzP | | 478100 | 5233350 | 50 | Forsters Pr | rsb | 1992 | XR | UR1996/15 | Fletchers Road | |
| C107810 | diamictite | prn,cpx,qtz | | PzP | | 477850 | 5233100 | 50 | Forsters Pr | rsb | 1992 | XR, PT | UR1996/15 | Fletchers Road | |
| C107811 | chert | lim | | | | 478200 | 5233550 | 50 | Forsters Pr | rsb | 1993 | XR, CA | UR1996/15 | road junction pit | 0.2 |
| C107812 | chert | | | | | 478200 | 5233550 | 50 | Forsters Pr | rsb | 1993 | CA | UR1996/15 | road junction pit, composite | 0.2 |
| C107813 | chert | | | | | 478230 | 5233690 | 50 | Forsters Pr | rsb | 1993 | CA | UR1996/15 | FRC15 | 0.1 |
| C107814 | opal | | | | | 478240 | 5233770 | 50 | Forsters Pr | rsb | 1993 | CA | UR1996/15 | track | |
| C107815 | chert | | | | | 478240 | 5233770 | 50 | Forsters Pr | rsb | 1993 | CA, FI | UR1996/15 | BC2 | |
| C107816 | chert | | | | | 478260 | 5233770 | 50 | Forsters Pr | rsb | 1993 | CA, FI | UR1996/15 | BC2 | |
| C107817 | chert | | | | | 478280 | 5233870 | 50 | Forsters Pr | rsb | 1993 | CA, FI | UR1996/15 | BC4 | |
| C107818 | breccia | qtz | | | | 478150 | 5233770 | 50 | Forsters Pr | rsb | 1993 | FI | UR1996/15 | WR76 | |
| C107819 | breccia | qtz | | | | 478100 | 5233870 | 50 | Forsters Pr | rsb | 1993 | CA, FI, PT | UR1996/15 | BC8 | |
| C107820 | chert | | | | | 478160 | 5233870 | 50 | Forsters Pr | rsb | 1993 | CA, XR | UR1996/15 | near BC7 | |
| C107821 | chert | | | | | 478160 | 5233870 | 50 | Forsters Pr | rsb | 1993 | PT, CA | UR1996/15 | near BC7 | |
| C107822 | mudstone | | | PzP | | 478160 | 5233870 | 50 | Forsters Pr | rsb | 1993 | | UR1996/15 | near BC7 | |
| C107823 | breccia | qtz,ser | | | | 478160 | 5233870 | 50 | Forsters Pr | rsb | 1993 | CA, PT, XR | UR1996/15 | near BC7 | |
| C107824 | breccia | qtz | | | | 478160 | 5233870 | 50 | Forsters Pr | rsb | 1993 | PT, CA | UR1996/15 | near BC7, misc | |
| C107825 | breccia | qtz | | | | 478200 | 5233870 | 50 | Forsters Pr | rsb | 1993 | FI | UR1996/15 | near BC7 | |
| C107826 | opal | | | | | 478220 | 5234350 | 50 | Forsters Pr | rsb | 1993 | CA | UR1996/15 | south bank, baseline | |
| C107827 | chert | | | | | 478100 | 5234430 | 50 | Forsters Pr | rsb | 1993 | PT, CA | UR1996/15 | south bank, ni pt | |
| C107828 | dolerite | | | Mj | Jdl | 478100 | 5234430 | 50 | Forsters Pr | rsb | 1993 | CA, PT, XR | UR1996/15 | south bank, dyke | |
| C107829 | chert | chr,qtz,ser | | | | 478100 | 5234430 | 50 | Forsters Pr | rsb | 1993 | CA, PT, XR | UR1996/15 | conglomerate? south bank, ni pt | |

| Reg. No. | Name | Minerals | Mod | Age | Unit Code | mE | mN | Accuracy (m) | Locality | Coll. | Year | Treatment | Refs | Comments | Au (g/t) |
|----------|-----------------|-------------|-----|-----|-----------|--------|---------|--------------|-------------|-------|------|----------------|-----------|-----------------------|-----------|
| C107830 | clast? | sid,sme,qtz | | | | 478100 | 5234430 | 50 | Forsters Pr | rsb | 1993 | CA, PT, XR | UR1996/15 | South bank, ni pt | |
| C107831 | dolerite clast? | chl | | | | 478100 | 5234430 | 50 | Forsters Pr | rsb | 1993 | CA, PT, XR | UR1996/15 | South bank, ni pt | |
| C107832 | chert | opl | | | | 478150 | 5234350 | 50 | Forsters Pr | rsb | 1993 | CA, PT, XR | UR1996/15 | South bank, galena pt | |
| C107833 | breccia | lim, qtz | | | | 478170 | 5233450 | 50 | Forsters Pr | rsb | 1993 | CA | UR1996/15 | Fletchers Road | |
| C107834 | breccia | | | | | 478250 | 5235160 | 20 | Forsters Pr | rsb | 1992 | PT, CA | UR1996/15 | Hogsback Hill, track | |
| C107835 | breccia | | | | | 478240 | 5235180 | 20 | Forsters Pr | rsb | 1992 | PT, CA | UR1996/15 | Hogsback Hill, track | |
| C107836 | chert | Chr | | | | 478150 | 5235260 | 20 | Forsters Pr | rsb | 1992 | PT, CA | UR1996/15 | Hogsback Hill, track | |
| C107837 | chert | | | | | 478130 | 5235030 | 20 | Forsters Pr | rsb | 1992 | PT, CA | UR1996/15 | Hogsback Hill | |
| C107838 | opal | qtz? | | | | 478160 | 5234470 | 20 | Forsters Pr | rsb | 1992 | CA | UR1996/15 | Au Adit | 0.3 |
| C107839 | chert | | | | | 478160 | 5234470 | 20 | Forsters Pr | rsb | 1992 | PT, CA, XR | UR1996/15 | Au Adit | |
| C107840 | chert breccia | | | | | 478160 | 5234470 | 20 | Forsters Pr | rsb | 1992 | CA | UR1996/15 | Au Adit | 0.05 |
| C107841 | quartz | | | | | 478160 | 5234470 | 20 | Forsters Pr | rsb | 1992 | CA | UR1996/15 | Au Adit | |
| C107842 | limonite | | | | | 478160 | 5234470 | 20 | Forsters Pr | rsb | 1992 | CA | UR1996/15 | Au Adit, clast | 0.4 |
| C107843 | sinter | opl | | | | 478160 | 5234470 | 20 | Forsters Pr | rsb | 1992 | CA | UR1996/15 | Au Adit | |
| C107844 | breccia | qtz | | | | 478200 | 5234000 | 20 | Forsters Pr | rsb | 1993 | | UR1996/15 | | |
| C107845 | conglomerate | | | | | 478200 | 5234000 | 20 | Forsters Pr | rsb | 1993 | PT | UR1996/15 | baseline | |
| C107846 | chert | | | | | 478180 | 5234500 | 20 | Forsters Pr | rsb | 1993 | | UR1996/15 | Au Adit | |
| C107847 | breccia | qtz | | | | 478180 | 5234500 | 20 | Forsters Pr | rsb | 1993 | PT, XR | UR1996/15 | Au Adit | |
| C107848 | opal | | | | | 478180 | 5234500 | 20 | Forsters Pr | rsb | 1993 | CA | UR1996/15 | Au Adit | 0.2 |
| C107849 | chert | opl,sid | | | | 478120 | 5234450 | 20 | Forsters Pr | rsb | 1993 | PT, XR | UR1996/15 | North bank | |
| C107850 | dolerite | | | Mj | Jdl | 478100 | 5234460 | 20 | Forsters Pr | rsb | 1993 | PT | UR1996/15 | North bank | |
| C107851 | breccia | opa,sid | | | | 478220 | 5234350 | 20 | Forsters Pr | rsb | 1993 | PT, CA, XR | UR1996/15 | South bank | |
| C107852 | quartzite? | | | | | 478200 | 5234000 | 20 | Forsters Pr | rsb | 1993 | PT, CA | UR1996/15 | South bank | |
| C107854 | conglomerate | | | ? | | 478180 | 5233900 | 50 | Forsters Pr | rsb | 1993 | | UR1996/15 | | |
| C107855 | chert | | | | | 478100 | 5234350 | 50 | Forsters Pr | rsb | 1993 | PT | UR1996/15 | South bank | |
| C107856 | conglomerate | tlc,hem | | pzc | | 477900 | 5233460 | 20 | Forsters Pr | rsb | 1993 | | UR1996/15 | roadcut | |
| C107857 | jasper | | | | | 477870 | 5233470 | 20 | Forsters Pr | rsb | 1993 | PT | UR1996/15 | roadcut | |
| C107858 | clay | tlc,sme | | | | 477790 | 5233440 | 20 | Forsters Pr | rsb | 1993 | XR | UR1996/15 | roadcut | |
| C107859 | pyroxenite? | | | pzc | | 477790 | 5233440 | 20 | Forsters Pr | rsb | 1993 | | UR1996/15 | roadcut | |
| C107860 | pyroxenite? | tlc | | pzc | | 477900 | 5233470 | 20 | Forsters Pr | rsb | 1993 | XR | UR1996/15 | roadcut | |
| C107861 | dolerite? | tlc,hall | | pzc | | 477940 | 5233480 | 20 | Forsters Pr | rsb | 1993 | XR, CA | UR1996/15 | roadcut | |
| C107862 | dolerite? | qtz,hall | | pzc | | 477960 | 5233490 | 20 | Forsters Pr | rsb | 1993 | XR, CA | UR1996/15 | roadcut | |
| C107863 | vein | pl,cpx,qtz | | | | 478900 | 5233800 | 100 | Forsters Pr | rsb | 1993 | XR | UR1996/15 | in dolerite | |
| C107864 | vein | prn,qtz,ze | | | ?? | 477500 | 5232870 | ?? | Forsters Pr | rsb | 1993 | XR, PT, FI, CA | UR1996/15 | in dolerite | |
| C107865 | diamictite | | | PzP | | 477550 | 5232900 | ?? | Forsters Pr | rsb | 1993 | XR | UR1996/15 | Gate | |
| C107880 | chert | opal | | | | 478150 | 5234390 | 20 | Forsters Pr | rsb | 1993 | PT, CA, FI | UR1996/15 | galena pt | 0.07 |
| C107881 | chert | py | | | | 478150 | 5234390 | 20 | Forsters Pr | rsb | 1993 | CA | UR1996/15 | galena pt | 0.07 |
| C107882 | chalcedony | | | | | 478150 | 5234390 | 20 | Forsters Pr | rsb | 1993 | PT, CA | UR1996/15 | galena pt | |
| C107883 | quartz | opl | | brx | | 478150 | 5234390 | 20 | Forsters Pr | rsb | 1993 | CA, FI | UR1996/15 | epithermal? | galena pt |

| Reg. No. | Name | Minerals | Mod | Age | Unit Code | mE | mN | Accuracy (m) | Locality | Coll. | Year | Treatment | Refs | Comments | Au (g/t) |
|----------|------------------|--------------|-------|-----|-----------|--------|---------|--------------|----------------|-------|------|------------|-----------|-------------------------|----------|
| C107884 | chert | gn | | | | 478150 | 5234390 | 20 | Forsters Pr | rsb | 1993 | PT, CA | UR1996/15 | galena pt | |
| C107885 | quartz | opal | | | | 478150 | 5234390 | 20 | Forsters Pr | rsb | 1993 | PT, FI | UR1996/15 | galena pt | |
| C107886 | chert | py,chr | green | | | 478100 | 5234430 | 20 | Forsters Pr | rsb | 1993 | PT, CA | UR1996/15 | Ni pt | |
| C107887 | chert | py | | | | 478100 | 5234430 | 20 | Forsters Pr | rsb | 1993 | PT, CA | UR1996/15 | Ni pt | 0.2 |
| C107888 | dolerite | | fgd | ? | | 478100 | 5234430 | 20 | Forsters Pr | rsb | 1993 | PT, CA | UR1996/15 | Ni pt | |
| C107889 | chert | py,chr | green | | | 478290 | 5234310 | 20 | Forsters Pr | rsb | 1993 | PT, CA, PA | UR1996/15 | apy pt | |
| C107890 | opal | py | | | | 478270 | 5234315 | 20 | Forsters Pr | rsb | 1993 | PT, CA | UR1996/15 | 20 m up | 0.1 |
| C107891 | siderite rock | | | | | 478250 | 5234325 | 20 | Forsters Pr | rsb | 1993 | PT, CA | UR1996/15 | 20 m up | |
| C108028 | mudstone | | brown | PzP | Perm | 477250 | 5229100 | 50 | Quarry, Tahune | | 1993 | CA, XR | UR1996/15 | | |
| C108029 | mudstone | hall | grey | PzP | Perm | 477990 | 5233260 | 50 | Fletcher Rd | rsb | 1993 | CA, XR | UR1996/15 | 300 m south of junction | |
| C108030 | mudstone | hall | purp | PzP | Perm | 477990 | 5233260 | 50 | Fletcher Rd | rsb | 1993 | CA, XR | UR1996/15 | 200 m | |
| C108031 | mudstone | hall | whit | PzP | Perm | 478050 | 5233320 | 50 | Fletcher Rd | rsb | 1993 | CA, XR | UR1996/15 | | |
| C108032 | mudstone | lim,hall | | PzP | Perm | 478100 | 5233360 | 50 | Fletcher Rd | rsb | 1993 | CA, XR | UR1996/15 | 150 m | |
| C108033 | mudstone | hall | whit | PzP | Perm | 478090 | 5233350 | 50 | Fletcher Rd | rsb | 1993 | CA, XR | UR1996/15 | 130 m | |
| C108034 | chert | chr,hall,tlc | whit | Pzc | Cal | 478140 | 5233400 | 50 | Fletcher Rd | rsb | 1993 | CA, XR | UR1996/15 | just below unconf. | |
| C108035 | mudstone | hall | brown | PzP | Perm | 478210 | 5233480 | 50 | Fletcher Rd | rsb | 1993 | CA, XR | UR1996/15 | cut west of junction | |
| C108036 | mudstone | hall | grey | PzP | Perm | 478240 | 5233530 | 50 | Fletcher Rd | rsb | 1993 | CA, XR | UR1996/15 | dam | |
| C108037 | quartz | hall | | | | 478180 | 5233480 | 50 | Fletcher Rd | rsb | 1993 | | UR1996/15 | beta! | |
| C108038 | quartz | hall | | | | 478180 | 5233480 | 50 | Fletcher Rd | rsb | 1993 | | UR1996/15 | silicified zone | |
| C108039 | jasperoid clast | | red | | | 478160 | 5233460 | 50 | Fletcher Rd | rsb | 1993 | CA, XR | UR1996/15 | clasts | |
| C108040 | chert | tlc,qtz | whit | Pzc | Cal | 477800 | 5233450 | 50 | Fletcher Rd | rsb | 1993 | CA, XR | UR1996/15 | silicified zone | |
| C108041 | mudstone | hall | whit | PzP | Perm | 477700 | 5233450 | 50 | Fletcher Rd | rsb | 1993 | CA, XR | UR1996/15 | 500 m W | |
| C108042 | mudstone | hall | brown | PzP | Perm | 477600 | 5233450 | 50 | Fletcher Rd | rsb | 1993 | CA, XR | UR1996/15 | 600 m W | |
| C108043 | mudstone | | grey | PzP | Perm | 477570 | 5232900 | 50 | Fletcher Rd | rsb | 1993 | CA, XR | UR1996/15 | near gate | |
| C108044 | mudstone | | hf | PzP | Perm | 520000 | 5242000 | 500 | Leslie Vale | rsb | 1993 | XR | UR1996/15 | HBMI Q | |
| C108107 | conglomerate | tlc | | Pzc | Cal | 477930 | 5233470 | 20 | Fletcher Rd | rsb | 1993 | CA | UR1996/15 | 280 m W baseline | |
| C108108 | silica-clay zone | | | Pzc | Cal | 478050 | 5233480 | 20 | Fletcher Rd | rsb | 1993 | CA | UR1996/15 | 150 m W baseline | |
| C108109 | silica-clay zone | | | Pzc | Cal | 478175 | 5233490 | 20 | Fletcher Rd | rsb | 1993 | CA | UR1996/15 | baseline | |
| C108110 | breccia | qtz | white | | | 478185 | 5233490 | 20 | Fletcher Rd | rsb | 1993 | CA | UR1996/15 | baseline | |
| C108111 | breccia | qtz | | | | 478180 | 5233490 | 20 | Fletcher Rd | rsb | 1993 | CA | UR1996/15 | baseline | |
| C108112 | clay | qtz,lim | | | | 478170 | 5233490 | 20 | Fletcher Rd | rsb | 1993 | CA | UR1996/15 | H/W | |
| C108113 | clay | qtz | | Pzc | Cal | 478190 | 5233490 | 20 | Fletcher Rd | rsb | 1993 | CA | UR1996/15 | F/W | |
| G108142 | breccia | qtz | | | | 478185 | 5233490 | 20 | Fletcher Rd | rsb | 1994 | | UR1996/15 | road junction pit | |
| G108143 | breccia | qtz | | | | 478185 | 5233490 | 20 | Fletcher Rd | rsb | 1994 | | UR1996/15 | road junction pit | |
| G108144 | breccia | hall | | | | 478185 | 5233490 | 20 | Fletcher Rd | rsb | 1994 | | UR1996/15 | road junction pit | |
| R007639 | hornfels | di,qtz,tlc | | | | 477550 | 5237950 | 50 | Forsters Pr | CRC | 1991 | TS | UR1996/15 | | |
| R007640 | ophicalcite | opl | | | | 478200 | 5234350 | 50 | Forsters Pr | CRC | 1992 | TS | UR1996/15 | | |
| R007641 | marble | tlc | | | | 477530 | 5235065 | 50 | Forsters Pr | CRC | 1992 | TS | UR1996/15 | | |
| R007642 | ophicalcite | tlc,sid | | | | 477550 | 5235190 | 50 | Forsters Pr | CRC | 1992 | TS | UR1996/15 | | |

| <i>Reg. No.</i> | <i>Name</i> | <i>Minerals</i> | <i>Mod</i> | <i>Age</i> | <i>Unit Code</i> | <i>mE</i> | <i>mN</i> | <i>Accuracy (m)</i> | <i>Locality</i> | <i>Coll.</i> | <i>Year</i> | <i>Treatment</i> | <i>Refs</i> | <i>Comments</i> | <i>Au (g/t)</i> |
|---------------------|--------------|-----------------|------------|------------|----------------------|-----------|-----------|-------------------------|-----------------|--------------|-------------|------------------|-------------|-----------------|---------------------|
| R007643 | conglomerate | tlc,cal,srp | | Pzc | Cal | 478020 | 5234475 | 50 | Forsters Pr | CRC | 1992 | TS | UR1996/15 | | |
| R007644 | basalt? | prn | | Pzc | | 477850 | 5237500 | 50 | Forsters Pr | CRC | 1992 | TS | UR1996/15 | | |
| R007645 | lamprophyre | hbd | | ? | | 478000 | 5234200 | 50 | Forsters Pr | CRC | 1992 | TS | UR1996/15 | | |
| R007646 | marble | brc | | Pr | | 477720 | 5237470 | 50 | Forsters Pr | CRC | 1992 | TS | UR1996/15 | | |
| R007647 | hornfels | qtz,di,cal | | | | 477750 | 5235600 | 50 | Forsters Pr | CRC | 1992 | TS | UR1996/15 | | |
| R007648 | dolomite | | | PR | Pw | 477650 | 5234650 | 50 | Forsters Pr | CRC | 1992 | TS | UR1996/15 | | |
| C108162 | breccia | qtz | | | | 478320 | 5233874 | 5 | Forsters Pr | JT | 1990 | IS, FI | | BC3 | |
| C108163 | breccia | qtz | | | | 478096 | 5233876 | 5 | Forsters Pr | JT | 1990 | IS, FI | | BC8 | |
| C108164 | breccia | qtz | | | | 478115 | 5233540 | 5 | Forsters Pr | JT | 1990 | IS, FI | | BC5 | |
| C108165 | breccia | qtz | | | | 478133 | 5233563 | 5 | Forsters Pr | JT | 1990 | IS, FI | | SW1 | |

For explanations and list of abbreviations, see UR 1988/13 or TASROK database

APPENDIX 4

Logs of diamond-drill holes SW1 and SW2

| | | |
|--|------------------------------|---|
| Diamond drill hole SW1 (BC15), South Weld/Glovers Bluff | | |
| Drilled for: | The North West Bay Co. | Company Report Reference: Forster, 1993 |
| Relogged by: | R. S. Bottrill, 16 July 1992 | Bearing: 270° Mag |
| Dip: | 50° S | Total Length: 82 m |
| Location (AMG): | 478 214 mE, 5 233 560 mN | |

| Depth (m) | Description | Samples |
|-----------|--|--|
| 0–34 | No core (percussion drilling) | |
| 34–58.8 | Vuggy, medium to fine-grained quartz and chert Pink and grey zones. Minor skarn and opal near base | 49.2 m: G402151 (grey chert) 54.8 m: G402152 (pink chert) 55.7 m: G402153 (skarn/chert) |
| 58.8–59.1 | Jurassic dolerite, fine grained | 59.1 m: G402154 (dolerite) |
| 59.1–62.0 | Vuggy quartz and chert, as above | |
| 62.0–63.0 | Jurassic dolerite, fine grained | 62.8 m: G402155 (dolerite) |
| 63.0–66.5 | Vuggy quartz and chert, finer and more massive between 63.7–64.7 | 63.7 m: G402156 (chert) |
| 66.5–79.8 | 'Dolomite marble': fine-grained dolomite, largely replaced by 'ophicalcite' (calcite-serpentine rock). Some opal veining. Towards the base it is increasingly brecciated and grades into a diopside hornfels. Some small, altered, dolerite dykes occur. | 66.9 m: G402157 (ophicalcite) 67.6 m: G402158 (ophicalcite) 68.0 m: G402159 (ophicalcite) 68.3 m: G402160 (ophicalcite) 69.2 m: G402161 (dolerite/ophicalcite) 73.3 m: G402162 (brucite marble) 76.1 m: G402163 (quartz-xonotlite skarn) 78.7 m: G402164 (diopside skarn) 79.7 m: G402165 (diopside skarn) |
| 79.8–82.0 | Skarn (quartz-diopside-xonotlite) | 81.9 m: G402166 (quartz-xonotlite skarn) |
| 82.0 | EOH | |

| | | |
|---|------------------------------|---|
| Diamond drill hole SW2 (BC5), South Weld/Glovers Bluff | | |
| Drilled for: | The North West Bay Co. | Company Report Reference: Forster, 1993 |
| Relogged by: | R. S. Bottrill, 23 July 1992 | Bearing: 090° Mag |
| Dip: | 50° S | Total Length: 110 m |
| Location (AMG): | 478 133 mE, 5 233 563 mN | |

| Depth (m) | Description | Samples |
|-------------|--|--|
| 0–21 | Pink and yellow clay, with weathered siliceous pebbles | |
| 21–24 | White clay | |
| 24–27 | Red clay with manganese oxides(?) | |
| 27–41 | White clay, with some relict diopside skarn | 34 m: G402167 (diopside skarn) |
| 41–42 | Opal-montmorillonite zone | 41 m: G402168 (opal and clay) |
| 42–45 | Vuggy quartz and chert | |
| 45–48.4 | 'Dolomite marble': fine grained, largely replaced by 'ophicalcite' (calcite-serpentine rock). Variably weathered | 46.6 m: G402169 (quartz skarn) 48.0 m: G402183 (diopside skarn) |
| 48.4–69.0 | 'Dolomite marble': fine grained, partly replaced by 'ophicalcite' (calcite-serpentine rock) | 50.2 m: G402170 (ophicalcite) 52.5 m: G402171 (ophicalcite, blue and white zones) 53.2 m: G402172 (ophicalcite, veined) 56.1 m: G402173 (ophicalcite/diopside hornfels, with clots) 58.2 m: G402174 (ophicalcite, with veins) 67.0 m: G402175 (ophicalcite/skarn, green & grey) |
| 69.0–69.9 | Brecciated zone in 'dolomite marble', with large calcite crystals | 69.9 m: G402176 (calcite) |
| 69.9–73.5 | Grey 'dolomite marble': fine-grained, partly replaced by skarn and 'ophicalcite' (calcite-serpentine rock) | 72.0 m: G402177 (ophicalcite/skarn) |
| 73.5–103.7 | White 'dolomite marble'/ophicalcite/skarn | 74.7 m: G402178 (ophicalcite/skarn) 89.9 m: G402179 (ophicalcite) |
| 103.7–110.0 | Jurassic dolerite. Fine grained, serpentinised top contact. Calcite-zeolite veining. | 103.7m: G402180 (contact) 107.5 m: G402181 (dolerite) 109.1 m: G402184 (dolerite) 110.4 m: G402185 (dolerite) |
| 110.0 | EOH | |

APPENDIX 5

A silicified karst breccia in the Mt Weld area

R.S. Bottrill, J. Taheri and C.R. Calver

Introduction

A brief reconnaissance visit was made to the Mt Weld area to compare the silicified dolomite caves, reported from that location, with the Forster Prospect. The authors were accompanied by Chris Sharples of Forestry Tasmania. Samples collected were studied by thin section, fluid inclusion and X-ray diffraction.

Geology

The regional geology is summarised by Bottrill *et al.* (this report). The area is largely covered by dolerite scree from the summit of Mt Weld, but Proterozoic dolostone can be seen in places, overlain unconformably by Permo-Carboniferous mudstone and diamictite. The unconformity is highly irregular, suggesting palaeo-karst topography.

The caves are quite large (several metres wide in places) and very irregular. Most of the walls and large loose blocks of wallrock are covered in quartz crystals.

The rock types found are described below.

Rock descriptions

W1: Quartz crystals.

These are mostly clear crystals to several centimetres in size. They are well terminated but lack prism faces, and completely coat the wall rocks.

W2, W6: Proterozoic laminated sediment

This is a wall rock to the quartz crystals. In hand specimen this rock is fine grained and strongly laminated, with dark grey-brown and buff mottled layers and some small quartz veinlets (<3 mm thick).

In thin section the rock is a fine-grained dolomitic chert. XRD indicates ~2% dolomite and ~2% mica, the remainder quartz. The layers are alternating fine and coarse-grained zones, the dark coloured layers containing finely dispersed, intergranular, dark brown-black, bituminous material. The buff laminae are coarser grained, with an arenaceous or fragmental texture (clasts <0.5 mm). The veins are comb-textured and vuggy in part. It was presumably originally a dolostone that has been dolomitised and silicified.

W3: Precambrian dolostone

This is a wall rock to the quartz crystals. In hand specimen this rock is dark brown-grey, fine grained and mottled, with weak lamination.

In thin section, the rock appears to be an almost pure carbonate, although XRD indicates ~5% quartz and 95% dolomite. The rock is finely granular, with a grainsize ranging from about 10–100 µm, with a mottled texture and cloudy zones. The grainsize variation probably reflects an original arenaceous or clastic texture, with recrystallisation and minor veinlets <0.2 mm in size. Quartz is present as sparse silt in some layers, and veinlets <20 µm thick.

W4: Precambrian dolostone

This is a wall rock to the quartz crystals. In hand specimen this rock is pale grey-brown, fine grained and unlaminated, with fine quartz boxworks of veinlets <3 mm in thickness.

In thin section the rock is a brecciated carbonate (dolomite confirmed by XRD), with clasts of very fine to medium-grained dolomite and fragments of quartz veinlets, in a granular quartz-dolomite matrix. It appears to be a fault breccia or similar rock type.

W7: Permo-Carboniferous diamictite

This is a rock from the Parmeener sequences higher up from the caves. In hand specimen this rock is a pale brown, pebbly mudstone with quartz and phyllite pebbles.

In thin section the rock is a slightly weathered, poorly sorted, pebbly mudstone with clasts of quartz, quartzite, chert and schist, in a sandy, silty micaceous matrix. No veining or foliations were evident.

XRD indicates about 35% mica, 10% chlorite, and 5% plagioclase, the remainder being quartz.

W8: Permo-Carboniferous diamictite

In hand specimen this rock is a pale brown, pebbly mudstone with quartz and quartzite pebbles, and minor quartz veinlets. It is well indurated.

In thin section the rock is a poorly sorted pebbly mudstone with clasts of quartz, quartzite, chert and schist, in a very cherty, sandy, silty micaceous matrix. Chert occurs as irregular veins and patches, and some clasts (clay and chlorite rich?) are partly silicified. There is minor quartz veining but no foliations were evident. It is slightly weathered and is very similar to the above sample, although more silicified.

XRD indicates about 10% mica and 2% chlorite, with the remainder being quartz.

W9: Silicified Precambrian dolostone and quartz crystals

This is a hanging-wall rock to the cave systems. In hand specimen this rock exhibits a coarse quartz vein (clear quartz crystals to >40 mm, well-terminated but lacking prism faces), on a porous, buff to white-coloured matrix, fine grained and unlaminated, but with fine quartz boxworks of veinlets <3 mm in thickness.

In thin section the rock is a dolomitic chert (~5% dolomite), mottled with vuggy quartz patches as well as quartz veinlets, and containing dolomite-rich layers. The border of the larger vein is disrupted at the junction with the fine veinlets, suggesting that they may be synchronous. The quartz crystals contain some early, strained, fibrous, chalcedonic zones, which suggest low temperature formation.

XRD indicates this material is largely amorphous.

Fluid inclusion and isotope studies

A preliminary fluid inclusion study on a few quartz samples from Mt Weld indicated that only one phase (liquid) was observed. The quartz samples were taken from a cave containing very large crystals. The fluid inclusions indicate that the quartz in this locality has been formed from very low temperature (<100°C) groundwater. A meteoric origin is also indicated by a

very light $\delta^{18}\text{O}$ value (5.9‰, see *Oxygen Isotope* section for details).

Conclusions

The rocks examined represent Precambrian dolostone (W3), dolomite-quartz breccia (W4) and silicified dolostone (W2 and W6), partly silicified Permo-Carboniferous mixtite (W7 and W8), and largely amorphous cave sediment, possibly Tertiary in age (W9). There is no evidence for the presence of Precambrian siliciclastic rocks.

This group of rocks indicates progressive silicification, veining and brecciation of the dolostone and mixtite in post-Permian, probably pre-Tertiary times. The origin of the silica is unknown, but it may derive from the overlying siliciclastic sediments. Acidic groundwaters percolating down through the Parmeener sequences probably reacted with alkaline, silica-bearing formation waters in dolostone, precipitating silica on contact, as the solubility decreased with decreasing pH.

The fluid inclusion and an oxygen isotope result indicate that the quartz in this locality has been formed from very low temperature meteoric water.

This is a highly unusual geological site and should be examined and sampled only with care.

APPENDIX 6

Petrology of an aplite from the Weld River, southern Tasmania

J. L. Everard

Abstract

An isolated outcrop of aplite on the lower Weld River (475 950 mE, 5 235 880 mN) has probably intruded Proterozoic orthoquartzite. The rock consists of mainly sericitised alkali feldspar and quartz with minor altered probable biotite. Although its composition plots close to the haplogranite minimum at pressures of 400–500 MPa, trace element geochemistry suggests that it is not a fractionated melt but probably formed as a minimum melt at lower to mid-crustal levels (15–20 km). Its age is unknown, and it is geochemically dissimilar to both Cretaceous alkaline rocks at Port Cygnet and, to a lesser extent, mid-Palaeozoic Tasmanian granites. Nearby gold mineralisation at Glovers Bluff is probably unrelated.

Introduction

Some geological observations were made in early 1997 by C. R. Calver and J. L. Everard during a private rafting traverse along the Weld River from approximately 470 400 mE, 5 240 300 mN to 478 000 mE, 5 234 400 mN. This information was subsequently incorporated into the Weld 1:25 000 scale geological map (Calver, 1998).

Of particular interest was an outcrop of aplite noted at 475 950 mE, 5 235 880 mN, as similar rock types had not been previously recorded from the area. A connection was thought possible with low-grade gold and base metal mineralisation then being explored around Glovers Bluff (Forster prospect; Sedimentary Holdings, 1997, pp. 6–10).

Field occurrence

The aplite occurs as a single, small, low water-polished outcrop, a few metres across, on the north bank of the Weld River, about 1.5 km northwest of Glovers Bluff. No contacts are exposed and the outcrop is surrounded with river alluvium, which is covered in low dense riverine scrub. The immediate country rock is probably Proterozoic orthoquartzite, which crops out on a bend on the right bank about 250 m downstream. Regional mapping (Calver, 1998) has shown that the orthoquartzite is part of a 5 km long, NNW-trending, steeply-dipping and ENE-facing inlier which forms the prominent strike ridges of Bernard Spur and Camels Back, and also Glovers Bluff, where it is unconformably overlain by flat-lying Late Carboniferous sedimentary rocks. The eastern part of the inlier is composed of Neoproterozoic dolostone, which is partly contact metamorphosed to ophealcite marble. This is the result of intrusions of Jurassic dolerite, which surround and locally intrude within the inlier; contacts are mostly steep and intrusive, although locally faulted. Dolerite,

probably close to the concealed contact with the orthoquartzite, crops out in the river about 100 m upstream of the aplite outcrop.

The hand specimen is a tough, fine-grained massive rock with a subconchoidal fracture. Freshly broken surfaces are cream coloured to pale greenish yellow (Geological Society of America rock colour chart 10YR8/2 to 10Y8/2), with a few scattered oblong to irregularly polygonal outlines of pale yellow feldspar phenocrysts visible in a barely phaneritic groundmass. Thin brown to orange-brown (10YR5/4 to 10YR6/6) weathering rinds are developed on external surfaces and along a few closely-spaced but inconspicuous fractures.

Petrography

In two thin sections the rock contains scattered irregularly polygonal to oblong outlines of euhedral turbid feldspar phenocrysts, commonly up to 750 μm across but occasionally elongate to 4 mm. They occur both as isolated grains and as interlocking glomerocrystic aggregates. Simple twinning is visible, and a few show suggestions of zoning and/or perthitic exsolution textures. The few interference figures obtainable are biaxial negative, and the mineral is alkali feldspar. There is a pervasive partial alteration to fine-grained sericite.

There are also a few phenocrysts of euhedral to slightly embayed clear quartz, up to 1 mm across.

Some diffuse globular (<100 μm) to elongate blade-like aggregates of fine-grained dark orange-brown material are present. Relict pleochroic and strongly birefringent patches suggest that this material is altered, oxidised biotite. Some biotite aggregates have narrow alteration rims of paler, less birefringent probable chlorite.

The alkali feldspar and quartz phenocrysts grade down in size to a groundmass (100–200 μm) of these minerals, together with clear colourless micrographic intergrowths of quartz and alkali feldspar. There are some finer-grained (15–30 μm) patches within the groundmass which are commonly less strongly sericitised.

There are a few anhedral (<170 μm) of nearly opaque to deep red, probably secondary hematite, and a tenuous dissemination of very fine-grained, scaly to dust-like opaque grains pervades the slides.

Geochemistry and petrogenesis

Weathering rinds were trimmed off a portion of the sample before chemical analysis, mainly by x-ray

fluorescence. The major element analysis is that of a felsic alkali-feldspar granite. The most abundant oxide other than SiO₂, Al₂O₃, Na₂O and K₂O is iron (total iron as FeO = 1.72%). TiO₂, CaO, MgO and P₂O₅ are very low (<0.30%). The alumina saturation index (ASI; molar Al₂O₃/(Na₂O + K₂O + CaO)) of 1.134 and the presence of 1.90% normative corundum indicates that the rock is mildly peraluminous, and may be derived from a sedimentary protolith (i.e. is an S-type). However as Chappell and White (1992) suggest an ASI of 1.10 as the boundary between I and S-type granites, this designation is somewhat ambiguous.

The CIPW norm indicates an albite-rich composition (Ab_{46.9}-Or_{26.0}-Q_{27.1}) which plots closest to the water-saturated haplogranite eutectic (fig. 11) at a pressure of about 400–500Mpa (4–5kb) (Steiner *et al.*, 1975; Luth *et al.*, 1964; compilation of Rollinson, 1993). This suggests a depth of last equilibration with quartz and feldspar of 15–20 km. If other components were present in sufficient amounts, the inferred pressure would be substantially altered; for example 1–1.5% fluorine would allow equilibrium near this composition at 100 MPa (Manning, 1981). The rock is very depleted in Li, B and F (Table 3) and there is no petrographic evidence for substantial amounts of other components.

Similar felsic haplogranite melts can be produced in two main ways: by a minimal degree of partial melting of a quartzofeldspathic protolith, thereby melting or entraining negligible amounts of mafic minerals; or by fractionation of a less felsic melt, removing CaO, FeO, MgO and TiO₂ in precipitated mafic minerals. In either case the composition of the melt will approach that of the haplogranite minimum (which above about 350 MPa intersects the two feldspar solvus, thereby becoming a eutectic) at the appropriate pressure.

For this rock the low level of Rb (<250 ppm) and high levels of Sr (>50 ppm) and Ba (>200 ppm) indicates (criteria of Chappell and White, 1992; Chappell *et al.*, 1991) that the rock is relatively unfractionated. This is also consistent with the low Li and F. Therefore it is more likely to have been produced as a minimum melt, probably at depths of 15–20 km. On ascent, decreasing pressure shifts the position of the ternary minimum away from albite in the system Ab-Or-Q and enlarges the liquidus field of albite, thus favouring crystallisation of alkali feldspar phenocrysts in preference to quartz.

Discussion

The grain size, massive character and limited extent of the aplite suggests that it represents a minor hypabyssal intrusion, rather than part of a large pluton or a volcanic body.

Its age is unclear. By analogy with known Tasmanian geology, the most obvious possibilities are that it is a minor phase related to the Devonian (-Lower

Table 3

*Chemical analysis of sample WRS
(aplite, Weld River, DN75953588)*

| Major elements (mass %) | | Trace elements (g/t) | |
|--------------------------------|-------|----------------------|----------|
| SiO ₂ | 71.33 | Li | 6 |
| TiO ₂ | 0.09 | B | <25 |
| Al ₂ O ₃ | 15.10 | F | <100 |
| Fe ₂ O ₃ | 1.37 | Sc | <9 |
| FeO | 0.49 | V | 6 |
| MnO | 0.04 | Cr | 47 |
| MgO | 0.28 | Co | <8 |
| CaO | 0.26 | Ni | 6 |
| Na ₂ O | 5.13 | Cu | 6 |
| K ₂ O | 4.07 | Zn | 40 |
| P ₂ O ₅ | 0.03 | Ga | 20 |
| H ₂ O ⁺ | 0.74 | As | <20 |
| CO ₂ | 0.00 | Rb | 120 |
| SO ₃ | 0.07 | Sr | 51 |
| Total | 99.00 | Y | 28 |
| | | Zr | 195 |
| ASI | 1.134 | Nb | 51 |
| K/Rb | 282 | Mo | 5 |
| | | Sn | <9 |
| <i>CIPW norm</i> | | Ba | 420 |
| Q | 25.49 | La | 36 |
| C | 1.90 | Ce | 59 |
| or | 24.52 | Nd | 25 |
| ab | 44.16 | W | <10 |
| an | 1.09 | Pb | 15 |
| hy | 0.72 | Bi | <5 |
| mt | 1.48 | Th | 19 |
| il | 0.17 | U | <10 |
| hm | 0.37 | | |
| ap | 0.06 | Ag | approx 1 |
| Total | 99.96 | Au | <0.05 |

Analysis No. 970009. Li determined by atomic absorption spectroscopy, B by colorimetry, F by specific ion electrode, Ag and Au by aqua regia digestion and AAS, FeO by KMnO₄ titration, CO₂ by gravimetry, other elements by XRF and H₂O⁺ by difference.

Analyst: L. M. Hay

Carboniferous granites), or that it is related to the Cretaceous alkaline rocks of the Cygnet-Kettering area.

Although a large negative residual gravity anomaly (MRT digital data) suggests that shallow Devonian granite underlies much of southwest Tasmania as a major batholith, it does not extend as far northwest as this locality. The nearest exposure of granite is more than 60 km to the southwest at Cox Bight. Compared with Tasmanian granites (MRT Rockchem database) with similar (71–72%) SiO₂, the Weld River rock is markedly lower in TiO₂, CaO, MgO and Sr, and slightly lower in P₂O₅ and Rb. The lower levels of these elements are consistent with the Weld River rock being a minimum melt without any entrained restite. The Weld River rock is markedly higher in Nb (51 ppm

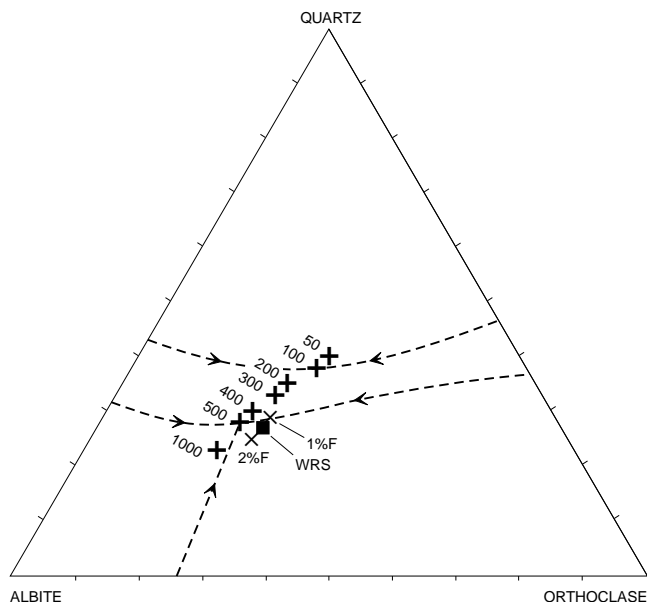


Figure 11

Normative composition of Weld River aplite sample (WRS) projected on to the haplogranite system Q-Ab-Or (wt%). Position of the water-saturated ternary minima at 500–300 MPa (Tuttle and Bowen, 1958), ternary eutectics at 400–1000 MPa (Steiner et al., 1975; Luth et al., 1964) and ternary minima with 1% and 2% fluorine at 100 MPa (Manning, 1981) are also shown. Liquidus phase field boundaries shown at 100 and 500 MPa only.

versus typically 10–20 ppm), the reason for which is unclear. Data for fluorine and lithium in Tasmanian granites are less comprehensive, but are generally much higher (e.g. fluorine 600–2600 ppm in the Poimena pluton, 3300–9900 ppm at Ben Lomond, mostly >1000 to 14 000 ppm in the Lottah pluton; lithium 46–300 ppm at Poimena, mostly >40–1150 ppm at Lottah). Other elements (e.g. total FeO, Ga, Zn, Y, Zr, Ba, Ce, Th) are within the range displayed by Devonian granites.

Cretaceous alkaline rocks occur near Cygnet, 25–30 km to the southeast. All analysed samples (Ford, 1983) are much less felsic (e.g. $\text{SiO}_2 = 54$ to 68%) with correspondingly higher total FeO and CaO. A few fine-grained felsic varieties at the higher end of this SiO_2 range have been termed aplite, but these have non-haplogranitic compositions, in particular with high CaO and $\text{K}_2\text{O}/\text{Na}_2\text{O}$. All the Cygnet rocks have high Sr contents (900–1700 ppm even in the most felsic aplite), more than an order of magnitude higher than the Weld River rock (51 ppm). CaO and Ba are also higher and Nb (typically <15 ppm) lower. None of the Cygnet rocks resemble the Weld River aplite.

Although there are few known occurrences of Cambrian felsic rocks east of the Mt Read Volcanic belt, a comparison has also been made with the Cambrian Rocky River, Darwin and Murchison Granites. These are typically more felsic ($\text{SiO}_2 > 74\%$) (except for the Murchison Granite, which is highly variable), and have generally lower Al_2O_3 and higher TiO_2 . They also have

very variable Na_2O and K_2O because of the effects of alteration. Perhaps more importantly, all are relatively depleted in the relatively immobile element Nb (<20 ppm and commonly <15 ppm), a signature characteristic of subduction-related arc or crustally contaminated rocks (e.g. Wilson, 1989, p. 21).

Sn-W mineralisation in the Lachlan Fold Belt is invariably associated with chemically reduced, highly fractionated felsic granites (both I and S type), whilst Cu-Mo-Au mineralisation is commonly associated with more mafic, oxidised I types (Blevin and Chappell, 1995). Although the original oxidation state of the Weld River aplite is not clear, it does not fit into either group.

The aplite does not contain detectable gold (<0.05 ppm). Investigations of low-grade gold mineralisation at Glovers Bluff do not indicate a genetic link with granite (J. Taheri, pers. comm.).

References

- SEDIMENTARY HOLDINGS, 1997. *Annual Report 1997*. Sedimentary Holdings NL.
- BLEVIN, P. L.; CHAPPELL, B. W. 1995. Chemistry, origin and evolution of mineralized granites in the Lachlan Fold Belt, Australia: the metallogeny of I- and S-types. *Economic Geology* 90:1604–1619.
- CALVER, C. R. 1998. Geological Atlas 1:25 000 Digital Series. Sheet 4623. Weld. *Tasmanian Geological Survey*.
- CHAPPELL, B. W.; ENGLISH, P. M.; KING, P. L.; WHITE, A. J. R.; WYBORN, D. 1991. Granites and related rocks of the Lachlan Fold Belt (1:2 500 000 scale map). *Bureau of Mineral Resources, Geology and Geophysics Australia*.
- CHAPPELL, B. W.; WHITE, A. J. R. 1992. I- and S-type granites in the Lachlan Fold Belt. *Transactions Royal Society of Edinburgh (Earth Sciences)* 83:1–26.
- FORD, R. J. 1983. *The alkaline rocks of Port Cygnet, Tasmania*. Ph.D. thesis, University of Tasmania.
- LUTH, W. C.; JAHNS, R. H.; TUTTLE, O. F. 1964. The granite system at pressures of 4 to 10 kilobars. *Journal of Geophysical Research* 69:759–773.
- MANNING, D. A. C. 1981. The effect of fluorine on liquidus phase relationships in the system Qz-Ab-Or with excess water at 1 kb. *Contributions to Mineralogy and Petrology* 76:206–215.
- ROLLINSON, H. R. 1993. *Using geochemical data: Evaluation, presentation, interpretation*. Longman.
- STEINER, J. C.; JAHNS, R. H.; LUTH, W. C. 1975. Crystallisation of alkali feldspar and quartz in the haplogranite system $\text{NaAlSi}_3\text{O}_8\text{-KAlSi}_3\text{O}_8\text{-SiO}_2\text{-H}_2\text{O}$ at 4 kb. *Bulletin Geological Society America* 86:83–93.
- TUTTLE, O. F.; BOWEN, N. F. 1958. The origin of granite in the light of experimental studies in the system $\text{NaAlSi}_3\text{O}_8\text{-KAlSi}_3\text{O}_8\text{-SiO}_2\text{-H}_2\text{O}$. *Memoir Geological Society America* 74.
- WILSON, M. 1989. *Igneous petrogenesis*. Chapman and Hall, London.

APPENDIX 7

XRF analyses of rock samples

Cambrian conglomerate

| Reg. No. Field No. | 107831 <i>Clast?</i> <i>S bank</i> | 108034 <i>Congl</i> <i>Fletcher Rd</i> | 108107 <i>Tc-cong</i> <i>Forster roadcut</i> | 402140A <i>U/B</i> <i>near SW1</i> | 402140B <i>U/B</i> <i>near SW2</i> |
|--------------------------------|--|--|--|--|--|
| SiO ₂ | 43.96 | 50.86 | 50.87 | 54.32 | 53.22 |
| TiO ₂ | 1.19 | 1.00 | 0.85 | 0.04 | 0.05 |
| Al ₂ O ₃ | 14.26 | 19.30 | 7.96 | 1.71 | 2.06 |
| Fe ₂ O ₃ | 3.13 | 0.78 | 9.13 | 6.17 | 4.65 |
| FeO | 6.21 | 1.16 | 1.09 | 3.55 | 4.46 |
| MnO | 0.09 | 0.02 | 0.45 | 0.10 | 0.15 |
| MgO | 17.37 | 14.30 | 20.42 | 23.32 | 20.97 |
| CaO | 1.89 | 0.00 | 0.03 | 5.24 | 9.71 |
| Na ₂ O | 0.18 | 0.04 | 0.11 | 0.14 | 0.12 |
| K ₂ O | 3.10 | 0.02 | 0.01 | 0.05 | 0.05 |
| P ₂ O ₅ | 0.35 | 0.03 | 0.11 | 0.04 | 0.08 |
| SO ₃ | 0.13 | 0.03 | 0.07 | 0.07 | 0.08 |
| CO ₂ | 0.22 | 1.20 | 0.15 | 0.10 | 0.28 |
| H ₂ O ⁺ | 7.13 | 9.95 | 7.02 | 3.95 | 3.47 |
| Total | 99.21 | 98.63 | 98.26 | 98.81 | 99.33 |
| LOI | 6.66 | 11.02 | 7.05 | 3.66 | 3.25 |
| Ag | 2 | ~1 | 1 | 0.2 | 0.2 |
| Au | <0.05 | 0.01 | <0.03 | 0.005 | 0.01 |
| Co | 56 | 52 | 430 | 60 | 67 |
| As | -20 | <20 | <20 | 20 | <20 |
| Bi | -5 | <5 | <5 | <5 | <5 |
| Ga | 13 | 21 | 10 | 8 | 9 |
| Zn | 53 | 54 | 69 | 53 | 55 |
| W | -10 | 26 | <10 | <10 | <10 |
| Cu | 340 | <5 | 8 | <5 | <5 |
| Ni | 310 | 920 | 1250 | 640 | 630 |
| Sn | -9 | <9 | <9 | <9 | <9 |
| Pb | 24 | 12 | 24 | <10 | <10 |
| Nd | 21 | <20 | 160 | <20 | <20 |
| Ce | 64 | <28 | 570 | <28 | <28 |
| La | -20 | <20 | 170 | <20 | <20 |
| Ba | 1800 | 57 | 94 | 80 | 89 |
| Th | 10 | 20 | 22 | <10 | <10 |
| Sr | 43 | <5 | 7 | <5 | 8 |
| U | -10 | <10 | <10 | <10 | <10 |
| Rb | 130 | <5 | <5 | <5 | <5 |
| Y | 22 | 6 | 64 | <5 | <5 |
| Zr | 130 | 185 | 110 | <5 | <5 |
| Nb | 21 | 12 | 14 | <3 | <3 |
| Mo | -5 | <5 | <5 | <5 | <5 |
| Cr | 440 | 3300 | 1500 | 3200 | 3400 |
| V | 260 | 200 | 100 | 88 | 125 |
| Sc | 34 | 18 | 28 | 39 | 61 |

Igneous rocks

| Reg. No. | 970088 | 970107 | 970193 | 970376 | 970390 | Ave Jdl | 970179 | 970180 | 970373 | 970399 |
|--------------------------------|--------------|--------|--------|---------|---------|----------------|------------|------------|-------------|-------------|
| Field No. | 107828 | 107850 | 107888 | 402154 | 402181 | Hergt | 107861 | 107862 | 402040 | 107639 |
| | Jdl | Jdl | Jdl | Jdl | Jdl | Chilled margin | Camb dykes | Camb dykes | Lamprophyre | Lamprophyre |
| | S bank, dyke | N bank | ni pt | DDH SW1 | DDH SW2 | | roadcut | roadcut | 10900N | 10900N |
| SiO ₂ | 52.62 | 53.49 | 54.91 | 56.81 | 52.14 | 54.12 | 43.16 | 54.57 | 48.00 | 47.05 |
| TiO ₂ | 0.84 | 0.62 | 0.69 | 0.64 | 0.61 | 0.64 | 1.88 | 0.97 | 1.26 | 1.33 |
| Al ₂ O ₃ | 20.84 | 14.94 | 15.76 | 11.15 | 14.62 | 14.59 | 17.80 | 15.83 | 14.01 | 14.00 |
| Fe ₂ O ₃ | 2.03 | 1.47 | 1.78 | 5.48 | 1.99 | 1.25 | 13.43 | 11.61 | 1.95 | 2.07 |
| FeO | 5.70 | 7.23 | 6.59 | 3.16 | 6.90 | 7.66 | 0.70 | 0.70 | 6.65 | 8.85 |
| MnO | 0.11 | 0.15 | 0.14 | 0.06 | 0.16 | 0.18 | 0.26 | 0.20 | 0.16 | 0.21 |
| MgO | 4.08 | 6.72 | 6.17 | 3.51 | 6.86 | 6.59 | 10.66 | 5.76 | 10.72 | 10.43 |
| CaO | 1.94 | 8.88 | 8.64 | 13.70 | 9.46 | 10.57 | 0.01 | 0.04 | 8.88 | 6.07 |
| Na ₂ O | 1.47 | 2.48 | 1.99 | 0.08 | 1.83 | 1.95 | 0.01 | 0.31 | 2.26 | 3.15 |
| K ₂ O | 2.32 | 1.68 | 1.17 | 0.07 | 0.94 | 0.88 | 0.03 | 1.59 | 2.04 | 1.40 |
| P ₂ O ₅ | 0.15 | 0.17 | 0.12 | 0.18 | 0.15 | 0.10 | 0.21 | 0.17 | 0.33 | 0.34 |
| SO ₃ | 0.18 | 0.11 | 0.08 | 0.08 | 0.15 | 0.05 | 0.04 | 0.09 | 0.10 | 0.15 |
| CO ₂ | 0.57 | 0.17 | 0.09 | 0.25 | 0.46 | | 0.50 | 0.27 | 0.00 | 0.64 |
| H ₂ O ⁺ | 6.77 | 2.07 | 2.33 | 4.34 | 2.88 | | 10.15 | 7.37 | 3.18 | 3.73 |
| Total | 99.63 | 100.18 | 100.46 | 99.51 | 99.14 | | 98.84 | 99.49 | 99.53 | 99.43 |
| LOI | 6.71 | 1.43 | 1.69 | 4.24 | 2.58 | | 10.58 | 7.56 | 2.44 | 3.38 |
| Ag | ~1 | 1 | 1 | 3.5 | 0.1 | | 1 | 1 | 0.1 | 0.1 |
| Au | <0.05 | <0.05 | <0.05 | 0.55 | 0.01 | | <0.05 | <0.05 | 0.02 | 0.005 |
| Co | 67 | 41 | 47 | | 38 | | 300 | 230 | 39 | 43 |
| As | 59 | -20 | -20 | | <20 | | -20 | -20 | <20 | <20 |
| Bi | -5 | -5 | -5 | | <5 | | -5 | 5 | <5 | <5 |
| Ga | 22 | 16 | 16 | | 17 | | 25 | 16 | 18 | 18 |
| Zn | 105 | 87 | 87 | | 85 | 79 | 125 | 200 | 75 | 94 |
| W | -10 | -10 | -10 | | <10 | | -10 | 15 | <10 | <10 |
| Cu | 93 | 66 | 75 | | 72 | 73 | 27 | 200 | 84 | 15 |
| Ni | 270 | 84 | 120 | | 81 | 78 | 580 | 270 | 230 | 140 |
| Sn | -9 | -9 | -9 | | <9 | | -9 | -9 | <9 | <9 |
| Pb | 52 | 17 | 41 | | 11 | 6 | 16 | 19 | 10 | <10 |
| Nd | 29 | -20 | -20 | | <20 | 13.1 | 590 | 560 | 21 | 23 |
| Ce | 62 | 30 | 44 | | 28 | 24 | 450 | 210 | 47 | 42 |
| La | 29 | -20 | -20 | | <20 | 11 | 770 | 640 | <20 | <20 |
| Ba | 1400 | 370 | 580 | | 450 | 334 | 53 | 330 | 420 | 210 |
| Th | 12 | -10 | 10 | | 14 | 4 | 21 | 10 | 15 | 13 |
| Sr | 135 | 240 | 160 | | 145 | 136 | <5 | 32 | 390 | 125 |
| U | -10 | -10 | <10 | | <10 | 1 | <10 | <10 | <10 | <10 |
| Rb | 98 | 62 | 51 | | 41 | 33 | 8 | 120 | 57 | 41 |
| Y | 28 | 23 | 25 | | 20 | 20 | 330 | 490 | 18 | 20 |
| Zr | 135 | 89 | 115 | | 100 | 95 | 250 | 67 | 135 | 98 |
| Nb | 4 | 5 | 7 | | 6 | 4.5 | 34 | 18 | 20 | 17 |
| Mo | -5 | -5 | <5 | | <5 | | <5 | <5 | <5 | <5 |
| Cr | 175 | 120 | 125 | | 115 | 108 | 650 | 1050 | 620 | 320 |
| V | 310 | 240 | 260 | | 240 | 225 | 220 | 360 | 280 | 270 |
| Sc | 54 | 39 | 44 | | 43 | 41 | 42 | 69 | 38 | 39 |

Chert

| Reg. No. | 970066 | 970068 | 970070 | 970071 | 970072 | 970081 | 970087 | 970092 | 970093 | 970098 |
|--------------------------------|------------------------|----------------|--------------|--------------|--------------|-----------------|-----------------|-----------------|-----------------|------------------------|
| Field No. | 107812b | 107813 | 107815 | 107816 | 107817 | 107821 | 107827 | 107832A | 107832B | 107837A |
| | Chert road junction | Chert FRC15 | Chert BC2 | Chert BC2 | Chert BC4 | Chert nr BC7 | Chert S bank | Chert S bank | Chert S bank | Chert Hogsback Hill |
| SiO ₂ | 97.49 | 98.19 | 97.49 | 97.95 | 97.59 | 97.99 | 97.80 | 97.35 | 90.44 | 98.07 |
| TiO ₂ | 0.01 | 0.01 | 0.04 | 0.01 | 0.05 | 0.01 | 0.01 | 0.01 | 0.00 | 0.01 |
| Al ₂ O ₃ | 0.28 | 0.56 | 0.57 | 0.30 | 0.53 | 0.32 | 0.26 | 0.22 | 0.13 | 0.27 |
| Fe ₂ O ₃ | 0.19 | 0.00 | 0.00 | 0.00 | 0.08 | 0.02 | 0.07 | 0.02 | 0.05 | 0.02 |
| FeO | 0.58 | 0.34 | 0.26 | 0.22 | 0.22 | 0.26 | 0.45 | 0.58 | 4.29 | 0.33 |
| MnO | 0.00 | 0.00 | 0.00 | 0.00 | 0.00 | 0.00 | 0.01 | 0.02 | 0.17 | 0.00 |
| MgO | 0.08 | 0.08 | 0.09 | 0.07 | 0.09 | 0.08 | 0.28 | 0.19 | 0.15 | 0.08 |
| CaO | 0.07 | 0.06 | 0.01 | 0.02 | 0.04 | 0.08 | 0.29 | 0.09 | 0.22 | 0.00 |
| Na ₂ O | 0.03 | 0.04 | 0.04 | 0.03 | 0.04 | 0.06 | 0.04 | 0.03 | 0.03 | 0.03 |
| K ₂ O | 0.00 | 0.02 | 0.00 | 0.00 | 0.01 | 0.02 | 0.00 | 0.02 | 0.00 | 0.00 |
| P ₂ O ₅ | 0.02 | 0.02 | 0.02 | 0.03 | 0.03 | 0.02 | 0.04 | 0.03 | 0.03 | 0.03 |
| SO ₃ | 0.03 | 0.03 | 0.03 | 0.03 | 0.02 | 0.03 | 0.03 | 0.06 | 0.09 | 0.05 |
| CO ₂ | 0.14 | 0.00 | 0.08 | 0.08 | 0.04 | 0.12 | 0.28 | 0.33 | 2.61 | 0.10 |
| H ₂ O ⁺ | 0.17 | 0.21 | 0.17 | 0.50 | 0.13 | 0.09 | 0.11 | 0.21 | 1.23 | 0.13 |
| Total | 99.09 | 99.56 | 98.80 | 99.24 | 98.86 | 99.10 | 99.66 | 99.16 | 99.44 | 99.12 |
| L.O.I. | 0.25 | 0.17 | 0.22 | 0.56 | 0.14 | 0.18 | 0.34 | 0.48 | 3.36 | 0.19 |
| Ag | <1 | <1 | <1 | <1 | <1 | <1 | <1 | <1 | <1 | <1 |
| Au | <0.05 | 0.1 | <0.05 | <0.05 | <0.05 | <0.05 | <0.05 | <0.05 | <0.05 | <0.05 |
| Co | -8 | -8 | -8 | -8 | -8 | -8 | -8 | -8 | -8 | -8 |
| As | 34 | -20 | -20 | -20 | -20 | -20 | -20 | -20 | -20 | -20 |
| Bi | -5 | -5 | -5 | -5 | -5 | -5 | -5 | -5 | -5 | -5 |
| Ga | -5 | -5 | -5 | -5 | -5 | -5 | -5 | -5 | -5 | -5 |
| Zn | 9 | 27 | 9 | 12 | 11 | 10 | 73 | 19 | 44 | 10 |
| W | -10 | -10 | -10 | -10 | -10 | -10 | -10 | -10 | -10 | -10 |
| Cu | -5 | -5 | -5 | -5 | -5 | -5 | -5 | 5 | -5 | -5 |
| Ni | -5 | 30 | 5 | 6 | -5 | -5 | 69 | 7 | 7 | -5 |
| Sn | -9 | -9 | -9 | -9 | -9 | -9 | -9 | -9 | -9 | -9 |
| Pb | 17 | 43 | 18 | 17 | 19 | 33 | 26 | 28 | 40 | 38 |
| Nd | -20 | -20 | -20 | -20 | -20 | -20 | -20 | -20 | -20 | -20 |
| Ce | -28 | -28 | -28 | -28 | -28 | -28 | -28 | -28 | -28 | -28 |
| La | -20 | -20 | -20 | -20 | -20 | -20 | -20 | -20 | -20 | -20 |
| Ba | 23 | 92 | 29 | -23 | 30 | 270 | -23 | 33 | -23 | 25 |
| Th | -10 | -10 | -10 | -10 | -10 | -10 | -10 | -10 | -10 | -10 |
| Sr | 10 | 10 | 8 | 7 | 7 | 12 | 12 | 8 | 9 | 8 |
| U | -10 | -10 | -10 | -10 | -10 | -10 | -10 | -10 | -10 | -10 |
| Rb | -5 | -5 | -5 | -5 | -5 | -5 | -5 | -5 | -5 | -5 |
| Y | -5 | -5 | -5 | -5 | -5 | -5 | -5 | -5 | 5 | -5 |
| Zr | 21 | 17 | 21 | 17 | 24 | 17 | 17 | 17 | 16 | 16 |
| Nb | -3 | -3 | -3 | -3 | -3 | -3 | -3 | -3 | -3 | -3 |
| Mo | -5 | 8 | 8 | 9 | 9 | 7 | 7 | 9 | 5 | 7 |
| Cr | 17 | 14 | 5 | -5 | 6 | 10 | -5 | 5 | 7 | 13 |
| V | 5 | -5 | -5 | -5 | -5 | -5 | -5 | -5 | -5 | -5 |
| Sc | -9 | -9 | -9 | -9 | -9 | -9 | -9 | -9 | -9 | -9 |

Chert

| Reg. No. | 970101 | 970102 | 970184 | 970185 | 970186 | 970187 | 970188 | 970189 | 970192W | 970391 |
|--------------------------------|--------------------------|-------------------|----------------|----------------|----------------|----------------|----------------|----------------|----------------|------------------|
| Field No. | 107840 | 107841 | 107880 | 107881 | 107882 | 107882B | 107883 | 107884 | 107887 | 402186 |
| | Chert breccia Au Adit | Quartz Au Adit | Chert gn pt | Chert gn pt | Chert gn pt | Chert gn pt | Chert gn pt | Chert gn pt | Chert ni pt | Chert DDH SW2 |
| SiO ₂ | 93.72 | 98.15 | 98.31 | 90.44 | 96.05 | 97.46 | 97.97 | 98.62 | 96.53 | 96.06 |
| TiO ₂ | 0.00 | 0.00 | 0.01 | 0.04 | 0.01 | 0.00 | 0.01 | 0.00 | 0.01 | 0.03 |
| Al ₂ O ₃ | 0.09 | 0.30 | 0.29 | 0.50 | 0.09 | 0.22 | 0.10 | 0.28 | 0.26 | 0.98 |
| Fe ₂ O ₃ | 0.17 | 0.10 | 0.15 | 2.32 | 0.01 | 0.12 | 0.01 | 0.05 | 0.35 | 0.65 |
| FeO | 2.88 | 0.51 | 0.48 | 1.98 | 0.45 | 0.58 | 0.51 | 0.38 | 0.96 | 0.32 |
| MnO | 0.09 | 0.00 | 0.00 | 0.01 | 0.01 | 0.00 | 0.00 | 0.00 | 0.03 | 0.01 |
| MgO | 0.19 | 0.16 | 0.05 | 0.14 | 0.07 | 0.14 | 0.04 | 0.05 | 0.16 | 0.15 |
| CaO | 0.17 | 0.11 | 0.12 | 0.16 | 0.11 | 0.16 | 0.05 | 0.07 | 0.16 | 0.20 |
| Na ₂ O | 0.03 | 0.03 | 0.00 | 0.00 | 0.01 | 0.00 | 0.00 | 0.00 | 0.00 | 0.04 |
| K ₂ O | 0.01 | 0.00 | 0.02 | 0.05 | 0.01 | 0.00 | 0.01 | 0.01 | 0.01 | 0.09 |
| P ₂ O ₅ | 0.03 | 0.02 | 0.00 | 0.01 | 0.00 | 0.00 | 0.00 | 0.01 | 0.00 | 0.00 |
| SO ₃ | 0.10 | 0.06 | 0.02 | 0.06 | 0.03 | 0.02 | 0.03 | 0.02 | 0.03 | 0.09 |
| CO ₂ | 1.62 | 0.20 | 0.10 | 1.08 | 0.19 | 0.13 | 0.08 | 0.15 | 0.32 | 0.26 |
| H ₂ O ⁺ | 0.52 | -0.02 | 0.24 | 3.07 | 1.89 | 0.27 | 0.58 | 0.13 | 0.96 | 0.27 |
| Total | 99.61 | 99.62 | 99.79 | 99.87 | 98.92 | 99.10 | 99.39 | 99.76 | 99.77 | 99.13 |
| LOI | 1.82 | 0.12 | 0.28 | 3.93 | 2.03 | 0.34 | 0.60 | 0.24 | 1.17 | 0.49 |
| Ag | <1 | <1 | <1 | 1 | <1 | <1 | <1 | <1 | <1 | 1 |
| Au | 0.05 | <0.05 | 0.07 | 0.07 | <0.05 | <0.05 | <0.05 | <0.05 | 0.2 | 0.005 |
| Co | -8 | -8 | -8 | 11 | -8 | -8 | -8 | -8 | | <8 |
| As | 26 | 500 | 21 | 130 | -20 | -20 | -20 | -20 | 34 | 120 |
| Bi | -5 | -5 | -5 | -5 | -5 | -5 | -5 | -5 | -5 | <5 |
| Ga | -5 | -5 | -5 | 7 | -5 | -5 | -5 | 23 | -5 | 7 |
| Zn | 140 | 15 | 63 | 74 | 450 | 47 | 13 | 510 | 62 | 14 |
| W | -10 | -10 | -10 | -10 | -10 | -10 | -10 | -10 | | <10 |
| Cu | 7 | -5 | 5 | 25 | -5 | -5 | -5 | 13 | -5 | 8 |
| Ni | 28 | 5 | 10 | 20 | 5 | 5 | -5 | -5 | 19 | 14 |
| Sn | -9 | -9 | -9 | -9 | -9 | -9 | -9 | -9 | -9 | <9 |
| Pb | 44 | 145 | 210 | 570 | 170 | 195 | 30 | 2400 | 34 | <10 |
| Nd | -20 | -20 | -20 | -20 | -20 | -20 | -20 | -20 | -20 | <20 |
| Ce | -28 | -28 | -28 | -28 | -28 | -28 | -28 | -28 | -28 | <28 |
| La | -20 | -20 | -20 | -20 | -20 | -20 | -20 | -20 | -20 | <20 |
| Ba | -23 | 25 | 25 | 230 | 28 | 35 | 42 | -23 | 32 | 115 |
| Th | -10 | -10 | | <10 | <10 | <10 | <10 | <10 | | <10 |
| Sr | 8 | 8 | Broken | <5 | <5 | <5 | <5 | <5 | No | <5 |
| U | -10 | -10 | | <10 | <10 | <10 | <10 | <10 | | <10 |
| Rb | -5 | -5 | Pellet | 5 | <5 | <5 | <5 | <5 | Pellet | <5 |
| Y | -5 | -5 | | 9 | <5 | <5 | <5 | 30 | | <5 |
| Zr | 17 | 16 | | 14 | <5 | <5 | <5 | 10 | | 5 |
| Nb | -3 | -3 | | <3 | <3 | <3 | <3 | <3 | | <3 |
| Mo | 8 | 9 | | 11 | 7 | 10 | 9 | 9 | | 15 |
| Cr | 5 | -5 | -5 | 32 | -5 | 6 | 10 | -5 | 10 | |
| V | -5 | -5 | -5 | 35 | -5 | -5 | -5 | -5 | 5 | |
| Sc | -9 | -9 | -9 | -9 | -9 | -9 | -9 | -9 | -9 | |

Chert

| Reg. No. | 970392 | 970397 | 970097 | 970194 | 970195 | 980022 | 970089 | 970190 | 970191 | 970465 | 970466 |
|--------------------------------|----------------|----------------|--------------------------|--------------------|--------------------|----------------------|--------------------|-------------------|-------------------|------------------------------|-------------------------|
| Field No. | 402190 | 402209 | 107836 | 107889A | 107889B | 108109 | 107829 | 107886A | 107886B | 108039 | 108040 |
| | Chert track | Chert gn pt | Chert Hog. Hill track | um-chert apy pt | um-chert apy pt | um-chert junction | um-chert S bank | um-chert ni pt | um-chert ni pt | Clast-jasper. Fletcher Rd | Conglom. Fletcher Rd |
| SiO ₂ | 90.80 | 96.34 | 98.81 | 96.04 | 95.75 | 93.20 | 86.08 | 85.25 | 87.01 | 88.63 | 85.8 |
| TiO ₂ | 0.28 | 0.03 | 0.01 | 0.01 | 0.01 | 0.25 | 0.4 | 0.57 | 0.41 | 0.01 | 0.01 |
| Al ₂ O ₃ | 2.02 | 0.92 | 0.35 | 0.52 | 0.60 | 2.72 | 7.24 | 7.93 | 6.56 | 0.27 | 0 |
| Fe ₂ O ₃ | 4.58 | 0.78 | 0.02 | 0.29 | 0.48 | 0.97 | 0.77 | 0.6 | 0.73 | 7.38 | 0.02 |
| FeO | 0.26 | 0.58 | 0.26 | 0.45 | 0.51 | 0.19 | 0.96 | 0.64 | 0.7 | 0.52 | 0.26 |
| MnO | 0.01 | 0.01 | 0.00 | 0.01 | 0.02 | 0.01 | 0.02 | 0.02 | 0.01 | 0.01 | 0 |
| MgO | 0.12 | 0.12 | 0.14 | 0.14 | 0.25 | 0.13 | 0.43 | 0.4 | 0.46 | 0.22 | 11.27 |
| CaO | 0.17 | 0.14 | 0.02 | 0.08 | 0.10 | 0.05 | 0.19 | 0.29 | 0.25 | 0.01 | 0 |
| Na ₂ O | 0.00 | 0.03 | 0.03 | 0.00 | 0.00 | 0.07 | 0.05 | 0.01 | 0.01 | 0.01 | 0.01 |
| K ₂ O | 0.44 | 0.08 | 0.00 | 0.01 | 0.01 | 0.02 | 1.78 | 1.82 | 1.46 | 0.01 | 0.02 |
| P ₂ O ₅ | 0.00 | 0.02 | 0.04 | 0.00 | 0.00 | 0.03 | 0.05 | 0.06 | 0.05 | 0.03 | 0 |
| SO ₃ | 0.07 | 0.08 | 0.06 | 0.04 | 0.03 | 0.05 | 0.07 | 0.09 | 0.06 | 0.03 | 0.02 |
| CO ₂ | 0.20 | 0.40 | 0.14 | 0.08 | 0.04 | 0.18 | 0.09 | 0.14 | 0.1 | 0.21 | 0.14 |
| H ₂ O ⁺ | 0.94 | -0.12 | 0.00 | 0.81 | 0.40 | 1.33 | 1.61 | 1.64 | 1.41 | 0.25 | 1.84 |
| Total | 99.87 | 99.41 | 99.88 | 98.47 | 98.20 | 99.19 | 99.75 | 99.45 | 99.22 | 97.57 | 99.37 |
| LOI | 1.11 | 0.22 | 0.11 | 0.84 | 0.38 | 1.49 | 1.6 | 1.71 | 1.43 | 0.40 | 1.95 |
| Ag | 0.2 | 0.8 | <1 | <1 | <1 | <1 | <1 | ~1 | <1 | ~1 | <1 |
| Au | 0.13 | 0.04 | <0.05 | <0.05 | <0.05 | 0.2 | <0.05 | <0.05 | <0.05 | 0.01 | 0.01 |
| Co | | <8 | -8 | 24 | 27 | <8 | 54 | 55 | 66 | <8 | <8 |
| As | | 61 | -20 | 63 | 210 | 135 | 88 | 250 | 470 | <20 | <20 |
| Bi | | <5 | -5 | -5 | -5 | <5 | -5 | -5 | -5 | <5 | <5 |
| Ga | | 9 | -5 | -5 | 5 | <5 | 6 | 6 | -5 | 8 | 8 |
| Zn | | 20 | 26 | 145 | 180 | 115 | 52 | 51 | 48 | 15 | 22 |
| W | | <10 | -10 | -10 | -10 | <10 | -10 | -10 | -10 | <10 | <10 |
| Cu | | 10 | -5 | -5 | 11 | 7 | 11 | 25 | 38 | <5 | <5 |
| Ni | | 15 | 15 | 330 | 440 | 38 | 470 | 610 | 840 | 25 | 9 |
| Sn | | <9 | -9 | -9 | -9 | <9 | -9 | -9 | -9 | <9 | <9 |
| Pb | | 115 | 18 | 20 | 145 | 84 | 24 | 23 | 18 | <10 | <10 |
| Nd | | <20 | -20 | -20 | -20 | <20 | -20 | -20 | -20 | <20 | <20 |
| Ce | | <28 | -28 | -28 | -28 | <28 | -28 | 42 | -28 | <28 | <28 |
| La | | <20 | -20 | -20 | -20 | <20 | -20 | -20 | -20 | <20 | <20 |
| Ba | | 105 | 43 | -23 | -23 | 28 | 105 | 130 | 96 | 69 | 69 |
| Th | | <10 | -10 | <10 | <10 | <10 | -10 | <10 | <10 | <10 | <10 |
| Sr | | <5 | 7 | <5 | <5 | 7 | 17 | 13 | 10 | <5 | <5 |
| U | | <10 | -10 | <10 | <10 | <10 | -10 | <10 | <10 | <10 | <10 |
| Rb | | <5 | -5 | <5 | <5 | <5 | 86 | 83 | 80 | <5 | <5 |
| Y | | <5 | -5 | <5 | <5 | <5 | 9 | 11 | 7 | <5 | <5 |
| Zr | | <5 | 17 | <5 | 13 | 41 | 64 | 62 | 51 | <5 | <5 |
| Nb | | <3 | -3 | <3 | <3 | 5 | 6 | 4 | <3 | <3 | <3 |
| Mo | | 10 | 8 | 8 | 13 | 5 | -5 | <5 | 5 | <5 | <5 |
| Cr | | | 650 | 2500 | 6500 | 1300 | 2900 | 3500 | 3000 | 170 | 35 |
| V | | | -5 | 33 | 20 | 52 | 140 | 130 | 105 | 25 | <5 |
| Sc | | | -9 | 12 | 9 | <9 | -9 | -9 | -9 | <9 | <9 |

Quartz breccia

| Reg No. | 970073 | 970074 | 970075 | 970076 | 970077 | 970078 | 970083W | 970084W | 970085W | 970095 |
|--------------------------------|--------------------|--------------------|--------------------|--------------------|--------------------|--------------------|-------------------------|-------------------------|-------------------------|----------------------------|
| Field No. | 107819A | 107819B | 107819C | 107819D | 107819E | 107819F | 107824A | 107824B | 107824C | 107834 |
| | Qtz breccia BC8 | Qtz breccia BC8 | Qtz breccia BC8 | Qtz breccia BC8 | Qtz breccia BC8 | Qtz breccia BC8 | Qtz breccia near BC7 | Qtz breccia near BC7 | Qtz breccia near BC7 | Breccia Hog. Hill track |
| SiO ₂ | 96.69 | 98.49 | 97.93 | 97.58 | 95.23 | 96.67 | 97.68 | 97.91 | 96.43 | 98.43 |
| TiO ₂ | 0.01 | 0.00 | 0.01 | 0.03 | 0.00 | 0.01 | 0.01 | 0.01 | 0.01 | 0.02 |
| Al ₂ O ₃ | 0.45 | 0.34 | 0.29 | 0.51 | 0.40 | 0.49 | 0.41 | 0.09 | 0.66 | 0.05 |
| Fe ₂ O ₃ | 0.84 | 0.29 | 0.03 | 0.18 | 2.02 | 1.36 | 0.11 | 0.01 | 0.39 | 0.09 |
| FeO | 0.45 | 0.38 | 0.32 | 0.32 | 0.58 | 0.32 | 0.48 | 0.38 | 0.58 | 0.16 |
| MnO | 0.00 | 0.00 | 0.00 | 0.00 | 0.00 | 0.01 | 0.00 | 0.00 | 0.00 | 0.00 |
| MgO | 0.06 | 0.05 | 0.09 | 0.09 | 0.13 | 0.07 | 0.15 | 0.12 | 0.14 | 0.08 |
| CaO | 0.04 | 0.03 | 0.10 | 0.05 | 0.13 | 0.08 | 0.13 | 0.12 | 0.12 | 0.01 |
| Na ₂ O | 0.04 | 0.04 | 0.03 | 0.03 | 0.04 | 0.05 | 0.04 | 0.03 | 0.04 | 0.02 |
| K ₂ O | 0.01 | 0.00 | 0.00 | 0.06 | 0.01 | 0.02 | 0.03 | 0.02 | 0.03 | 0.01 |
| P ₂ O ₅ | 0.03 | 0.02 | 0.02 | 0.02 | 0.03 | 0.02 | 0.03 | 0.02 | 0.02 | 0.02 |
| SO ₃ | 0.03 | 0.03 | 0.03 | 0.04 | 0.05 | 0.03 | 0.03 | 0.03 | 0.03 | 0.07 |
| CO ₂ | 0.18 | 0.11 | 0.14 | 0.11 | 0.25 | 0.21 | 0.12 | 0.11 | 0.15 | 0.23 |
| H ₂ O ⁺ | 0.05 | 0.04 | 0.06 | 0.10 | 0.42 | 0.03 | 0.27 | 0.21 | 0.23 | 0.60 |
| Total | 98.88 | 99.82 | 99.05 | 99.12 | 99.28 | 99.37 | 99.49 | 99.05 | 98.83 | 99.79 |
| LOI | 0.18 | 0.11 | 0.16 | 0.18 | 0.61 | 0.21 | 0.34 | 0.28 | 0.32 | 0.81 |
| Ag | <1 | <1 | <1 | <1 | <1 | <1 | <1 | <1 | <1 | <1 |
| Au | <0.05 | <0.05 | <0.05 | <0.05 | <0.05 | <0.05 | <0.05 | <0.05 | <0.05 | <0.05 |
| Co | -8 | -8 | -8 | -8 | -8 | -8 | 190 | 165 | 175 | -8 |
| As | 53 | 43 | -20 | 26 | 79 | 47 | -20 | -20 | 88 | -20 |
| Bi | -5 | -5 | -5 | -5 | -5 | -5 | -5 | -5 | -5 | -5 |
| Ga | -5 | -5 | -5 | -5 | -5 | -5 | -5 | -5 | -5 | -5 |
| Zn | 15 | 11 | 10 | 15 | 33 | 14 | 8 | 10 | 12 | 53 |
| W | -10 | -10 | -10 | -10 | -10 | -10 | 1200 | 1050 | 1800 | -10 |
| Cu | -5 | -5 | 6 | -5 | -5 | -5 | -5 | -5 | -5 | -5 |
| Ni | 12 | 7 | 5 | 7 | 33 | 6 | -5 | -5 | -5 | -5 |
| Sn | -9 | -9 | -9 | -9 | -9 | -9 | -9 | -9 | -9 | -9 |
| Pb | 22 | 22 | 17 | 45 | 25 | 19 | 23 | 23 | 18 | 48 |
| Nd | -20 | -20 | -20 | -20 | -20 | -20 | | | | -20 |
| Ce | -28 | -28 | -28 | -28 | -28 | -28 | | | | -28 |
| La | -20 | -20 | -20 | -20 | -20 | -20 | | | | -20 |
| Ba | 48 | 39 | 42 | 72 | 40 | 42 | | | | -23 |
| Th | -10 | -10 | -10 | -10 | -10 | -10 | | | | -10 |
| Sr | 10 | 8 | 8 | 13 | 9 | 10 | | | | 7 |
| U | -10 | -10 | -10 | -10 | -10 | -10 | | | | -10 |
| Rb | -5 | -5 | -5 | -5 | -5 | -5 | | | | -5 |
| Y | -5 | -5 | -5 | -5 | -5 | -5 | | | | -5 |
| Zr | 17 | 16 | 16 | 20 | 17 | 17 | | | | 20 |
| Nb | -3 | -3 | -3 | -3 | -3 | -3 | | | | -3 |
| Mo | 9 | 10 | 7 | 9 | 8 | 7 | | | | -5 |
| Cr | 40 | 22 | 10 | 13 | 33 | 40 | 35 | 10 | 14 | 13 |
| V | -5 | -5 | -5 | -5 | 10 | 5 | -5 | -5 | -5 | -5 |
| Sc | -9 | -9 | -9 | -9 | -9 | -9 | -9 | -9 | -9 | -9 |

Quartz breccia/opal

| Reg No. | 970096 | 970110 | 980024 | 970393 | 970069 | 970079 | 970080 | 970086 | 970099 | 970100 |
|--------------------------------|------------------|-------------|----------|-------------|--------|---------|---------|--------|---------|---------|
| Field No. | 107835 | 107805 | 108111 | 402194 | 107814 | 107820A | 107820B | 107826 | 107838 | 107839 |
| | Breccia | Qtz breccia | Silica | Qtz breccia | Opal | Opal | Opal | Opal | Opal | Opal |
| | Hogs. Hill track | roadcut | junction | track | track | nr BC7 | nr BC7 | S bank | Au Adit | Au Adit |
| SiO ₂ | 98.02 | 98.06 | 97.20 | 98.28 | 91.98 | 92.42 | 96.48 | 92.65 | 92.83 | 96.60 |
| TiO ₂ | 0.00 | 0.00 | 0.02 | 0.01 | 0.03 | 0.01 | 0.01 | 0.01 | 0.01 | 0.02 |
| Al ₂ O ₃ | 0.17 | 0.56 | 0.58 | 0.56 | 0.61 | 0.08 | 0.02 | 0.27 | 0.31 | 0.20 |
| Fe ₂ O ₃ | 0.21 | 0.00 | 0.06 | -0.13 | 0.33 | 0.01 | 0.20 | 0.82 | 2.57 | 0.60 |
| FeO | 0.19 | 0.30 | 0.19 | 0.45 | 0.32 | 0.18 | 0.58 | 0.32 | 0.32 | 0.32 |
| MnO | 0.00 | 0.00 | 0.00 | 0.01 | 0.01 | 0.00 | 0.00 | 0.01 | 0.01 | 0.00 |
| MgO | 0.09 | 0.08 | 0.10 | 0.04 | 0.36 | 0.23 | 0.05 | 0.31 | 0.15 | 0.06 |
| CaO | 0.00 | 0.00 | 0.06 | 0.04 | 1.27 | 0.09 | 0.01 | 0.11 | 0.09 | 0.01 |
| Na ₂ O | 0.01 | 0.02 | 0.06 | 0.00 | 0.05 | 0.03 | 0.02 | 0.03 | 0.03 | 0.02 |
| K ₂ O | 0.01 | 0.00 | 0.01 | 0.02 | 0.00 | 0.00 | 0.00 | 0.01 | 0.01 | 0.02 |
| P ₂ O ₅ | 0.02 | 0.02 | 0.03 | 0.00 | 0.03 | 0.03 | 0.02 | 0.03 | 0.03 | 0.02 |
| SO ₃ | 0.05 | 0.06 | 0.04 | 0.07 | 0.07 | 0.04 | 0.03 | 0.04 | 0.11 | 0.05 |
| CO ₂ | 0.23 | 0.14 | 0.09 | 0.04 | 0.16 | 0.17 | 0.12 | 0.36 | 0.47 | 0.28 |
| H ₂ O ⁺ | 0.92 | 0.00 | 0.23 | 0.13 | 3.64 | 5.76 | 1.54 | 3.86 | 2.71 | 1.08 |
| Total | 99.91 | 99.23 | 98.66 | 99.52 | 98.85 | 99.03 | 99.07 | 98.82 | 99.65 | 99.27 |
| LOI | 1.12 | 0.10 | 0.30 | 0.12 | 3.77 | 5.91 | 1.59 | 4.19 | 3.15 | 1.32 |
| Ag | 5 | <1 | <1 | 0.1 | <1 | <1 | <1 | <1 | ~1 | ~1 |
| Au | <0.05 | <0.05 | <0.03 | 0.005 | <0.05 | <0.05 | <0.05 | <0.05 | 0.3 | <0.05 |
| Co | -8 | -8 | <8 | <8 | 17 | -8 | -8 | -8 | -8 | -8 |
| As | -20 | -20 | <20 | <20 | 34 | 25 | -20 | 21 | 110 | -20 |
| Bi | -5 | -5 | <5 | <5 | -5 | -5 | -5 | -5 | -5 | -5 |
| Ga | -5 | -5 | <5 | 8 | -5 | -5 | -5 | -5 | -5 | -5 |
| Zn | 61 | 9 | 8 | 13 | 41 | 15 | 11 | 125 | 180 | 13 |
| W | -10 | -10 | <10 | <10 | -10 | -10 | -10 | -10 | -10 | -10 |
| Cu | -5 | -5 | <5 | 7 | 7 | -5 | 6 | -5 | -5 | 5 |
| Ni | -5 | -5 | 6 | 12 | 145 | 36 | -5 | 5 | 53 | -5 |
| Sn | -9 | -9 | <9 | <9 | -9 | -9 | -9 | -9 | -9 | -9 |
| Pb | 44 | 18 | 17 | <10 | 120 | 28 | 49 | 38 | 105 | 49 |
| Nd | -20 | -20 | <20 | <20 | -20 | -20 | -20 | -20 | -20 | -20 |
| Ce | -28 | -28 | <28 | <28 | 34 | -28 | -28 | -28 | -28 | -28 |
| La | -20 | -20 | <20 | <20 | 24 | -20 | -20 | -20 | -20 | -20 |
| Ba | -23 | 24 | 40 | 79 | -23 | -23 | 31 | 24 | -23 | 63 |
| Th | -10 | -10 | <10 | <10 | -10 | -10 | -10 | -10 | -10 | -10 |
| Sr | 7 | 8 | 8 | <5 | 7 | 6 | 9 | 7 | 8 | 7 |
| U | -10 | -10 | <10 | <10 | -10 | -10 | -10 | -10 | -10 | -10 |
| Rb | -5 | -5 | <5 | <5 | -5 | -5 | -5 | -5 | -5 | -5 |
| Y | -5 | -5 | <5 | <5 | 7 | -5 | -5 | -5 | -5 | -5 |
| Zr | 16 | 17 | 17 | <5 | 21 | 18 | 17 | 21 | 17 | 20 |
| Nb | -3 | -3 | <3 | <3 | -3 | -3 | -3 | -3 | -3 | -3 |
| Mo | -5 | 7 | 5 | 15 | -5 | -5 | 6 | -5 | 8 | -5 |
| Cr | 5 | 10 | 45 | | 63 | 21 | 11 | 14 | 9 | 9 |
| V | -5 | -5 | < | | 52 | 6 | -5 | 13 | 16 | 21 |
| Sc | -9 | -9 | <9 | | 10 | -9 | -9 | -9 | -9 | -9 |

Opal/ophicalcite

| Reg No. | 970104 | 970105 | 970111 | 970196 | 970395 | 970398 | | 970377 | 970382 | 970383 |
|--------------------------------|---------|---------|--------------|--------|--------|--------|---------|-------------|-------------|-------------|
| Field No. | 107843 | 107848 | 107806 | 107890 | 402205 | 402450 | | 402159 | 402170 | 402174 |
| | Sinter | Opal | Opal breccia | Opal | Opal | Opal | | Ophicalcite | Ophicalcite | Ophicalcite |
| | Au adit | Au adit | track | S bank | track | track | average | ddh SW1 | ddh SW2 | ddh SW2 |
| SiO ₂ | 98.11 | 94.75 | 87.77 | 88.70 | 91.27 | 96.21 | 93.31 | 21.93 | 15.14 | 16.09 |
| TiO ₂ | 0.02 | 0.01 | 0.01 | 0.02 | 0.00 | 0.00 | 0.01 | 0.01 | 0.01 | 0.01 |
| Al ₂ O ₃ | 0.21 | 0.08 | 0.26 | 0.22 | 0.34 | 0.42 | 0.25 | 0.36 | 0.67 | 0.15 |
| Fe ₂ O ₃ | 0.07 | 0.64 | 0.04 | 0.97 | 5.63 | 0.11 | 1.00 | 0.15 | 0.07 | 1.69 |
| FeO | 0.32 | 0.70 | 0.19 | 1.79 | 0.71 | 1.10 | 0.57 | 0.32 | 0.13 | 0.45 |
| MnO | 0.00 | 0.03 | 0.00 | 0.05 | 0.02 | 0.05 | 0.01 | 0.01 | 0.01 | 0.02 |
| MgO | 0.11 | 0.96 | 6.00 | 0.94 | 0.04 | 0.15 | 0.78 | 21.09 | 23.65 | 24.40 |
| CaO | 0.06 | 0.56 | 0.03 | 0.22 | 0.03 | 0.19 | 0.22 | 27.88 | 28.77 | 26.19 |
| Na ₂ O | 0.02 | 0.03 | 0.02 | 0.01 | 0.03 | 0.04 | 0.03 | 0.02 | 0.08 | 0.00 |
| K ₂ O | 0.03 | 0.01 | 0.01 | 0.01 | 0.03 | 0.02 | 0.01 | 0.01 | 0.01 | 0.01 |
| P ₂ O ₅ | 0.02 | 0.03 | 0.03 | 0.03 | 0.02 | 0.01 | 0.02 | 0.23 | 0.24 | 0.22 |
| SO ₃ | 0.06 | 0.10 | 0.10 | 0.09 | 0.07 | 0.07 | 0.07 | 0.06 | 0.07 | 0.08 |
| CO ₂ | 0.12 | 0.39 | 0.28 | 1.55 | 0.13 | 0.93 | 0.41 | 22.00 | 24.60 | 20.80 |
| H ₂ O ⁺ | 0.33 | 1.34 | 4.41 | 4.13 | 1.23 | 0.37 | 2.53 | 6.38 | 6.82 | 10.17 |
| Total | 99.48 | 99.63 | 99.13 | 98.71 | 99.55 | 99.66 | 99.24 | 100.45 | 100.27 | 100.30 |
| L.O.I. | 0.42 | 1.65 | 4.67 | 5.48 | 1.28 | 1.17 | 2.88 | 28.35 | 31.40 | 30.92 |
| Ag | ~1 | ~1 | <1 | ~1 | 1 | 0.1 | | 0.2 | 0.2 | 0.8 |
| Au | <0.05 | 0.2 | <0.05 | 0.1 | 0.64 | 0.005 | | 0.03 | 0.005 | 0.1 |
| Co | -8 | -8 | 9 | -8 | 21 | <8 | | | 9 | 8 |
| As | -20 | 65 | -20 | 35 | 230 | <20 | | | 130 | 1550 |
| Bi | -5 | -5 | -5 | -5 | <5 | <5 | | | 5 | <5 |
| Ga | -5 | -5 | -5 | -5 | 8 | 7 | | | 7 | 8 |
| Zn | 12 | 165 | 21 | 195 | 61 | 23 | 71.83 | | 66 | 90 |
| W | -10 | -10 | -10 | -10 | <10 | <10 | | | <10 | <10 |
| Cu | -5 | -5 | -5 | -5 | 26 | <5 | | | <5 | <5 |
| Ni | -5 | 68 | 52 | 47 | 290 | 12 | 57.75 | | 21 | 30 |
| Sn | -9 | -9 | -9 | -9 | <9 | <9 | | | <9 | <9 |
| Pb | 31 | 105 | 79 | 32 | 62 | 14 | 59.33 | | 14 | 25 |
| Nd | -20 | -20 | -20 | -20 | <20 | <20 | | | <20 | <20 |
| Ce | -28 | -28 | -28 | -28 | <28 | <28 | | | <28 | 35 |
| La | -20 | -20 | -20 | -20 | <20 | <20 | | | <20 | <20 |
| Ba | 35 | -23 | -23 | -23 | 74 | 68 | | | 96 | 94 |
| Th | -10 | -10 | -10 | <10 | <10 | <10 | | | 15 | 15 |
| Sr | 10 | 9 | 7 | <5 | <5 | <5 | | | 66 | 67 |
| U | -10 | -10 | -10 | <10 | <10 | <10 | | | <10 | 36 |
| Rb | -5 | -5 | -5 | <5 | <5 | <5 | | | 6 | 7 |
| Y | -5 | 5 | 6 | <5 | <5 | <5 | | | <5 | <5 |
| Zr | 18 | 16 | 19 | 8 | <5 | <5 | | | 6 | 8 |
| Nb | -3 | -3 | -3 | <3 | <3 | <3 | | | 5 | 6 |
| Mo | -5 | 16 | -5 | <5 | 12 | 9 | | | <5 | <5 |
| Cr | -5 | 7 | 27 | 45 | | <5 | | | 10 | 16 |
| V | 5 | 12 | -5 | 18 | | <5 | | | 40 | 80 |
| Sc | -9 | -9 | -9 | -9 | | <9 | | | <9 | <9 |

Ophicalcite/skarn

| Reg No. | 970385 | 970384 | 970386 | 970389 | 970396 | 970378 | 970381 | 970379 | 970387 | 970388 |
|--------------------------------|-------------------------------|-------------------------------|-------------------------------|-------------------------------|------------------------------|---------------------------|---------------------------|----------------------------|----------------------------|----------------------------|
| Field No. | 402174b | 402175 | 402177 | 402179 | 402206 | 402163 | 402169 | 402165 | 402178A | 402178B |
| | <i>Ophicalcite</i> DDH SW2 | <i>Ophicalcite</i> DDH SW2 | <i>Ophicalcite</i> DDH SW2 | <i>Ophicalcite</i> DDH SW2 | <i>Ophicalcite</i> 10900N | <i>Q-skarn</i> DDH SW1 | <i>Q-skarn</i> DDH SW2 | <i>Di-Skarn</i> DDH SW1 | <i>Di-Skarn</i> DDH SW2 | <i>Di-Skarn</i> DDH SW2 |
| SiO ₂ | 17.52 | 9.96 | | | 38.19 | 75.14 | 75.55 | 48.42 | 46.06 | 42.98 |
| TiO ₂ | 0.01 | 0.01 | | | 0.01 | 0.01 | 0.01 | 0.02 | 0.01 | 0.01 |
| Al ₂ O ₃ | 0.81 | 0.19 | | | 0.81 | 0.94 | 1.55 | 0.75 | 0.63 | 1.31 |
| Fe ₂ O ₃ | 2.01 | 0.24 | | | 0.98 | 0.13 | 0.46 | 0.14 | 0.28 | 1.16 |
| FeO | 0.45 | 0.19 | | | 0.52 | 0.58 | 1.10 | 0.58 | 0.32 | 0.58 |
| MnO | 0.02 | 0.01 | | | 0.02 | 0.01 | 0.03 | 0.02 | 0.04 | 0.04 |
| MgO | 24.06 | 23.46 | | | 8.40 | 1.43 | 8.98 | 15.43 | 27.75 | 25.65 |
| CaO | 24.98 | 30.86 | | | 25.28 | 16.86 | 5.21 | 28.39 | 15.82 | 16.76 |
| Na ₂ O | 0.08 | 0.00 | | | 0.01 | 0.09 | 0.16 | 0.03 | 0.04 | 0.17 |
| K ₂ O | 0.01 | 0.01 | | | 0.02 | 0.06 | 0.06 | 0.13 | 0.02 | 0.03 |
| P ₂ O ₅ | 0.20 | 0.25 | | | 0.21 | 0.13 | 0.04 | 0.23 | 0.14 | 0.16 |
| SO ₃ | 0.10 | 0.04 | | | 0.72 | 0.08 | 0.46 | 0.13 | 0.13 | 0.12 |
| CO ₂ | 19.85 | 24.40 | | | 16.19 | 2.11 | 0.00 | 4.67 | 2.92 | 4.79 |
| H ₂ O ⁺ | 9.79 | 10.61 | | | 7.90 | 1.78 | 5.82 | 1.08 | 6.06 | 5.95 |
| Total | 99.89 | 100.23 | | | 99.26 | 99.36 | 99.42 | 100.02 | 100.19 | 99.71 |
| LOI | 29.59 | 34.98 | | | 24.04 | 3.82 | 5.70 | 5.69 | 8.94 | 10.67 |
| Ag | 1 | 0.1 | 0.2 | 0.1 | 0.1 | 0.8 | 1.2 | 0.4 | 0.4 | 0.4 |
| Au | 0.11 | 0.01 | 0.1 | 0.005 | 0.04 | 0.25 | 0.9 | 0.07 | 0.14 | 0.13 |
| Co | <8 | | 12 | 8 | | | | | <8 | 13 |
| As | 1850 | | 22 | <20 | | | | | 54 | 61 |
| Bi | 5 | | 6 | 5 | | | | | <5 | <5 |
| Ga | 8 | | 8 | 7 | | | | | 7 | 8 |
| Zn | 96 | | 400 | 30 | | | | | 190 | 210 |
| W | <10 | | <10 | <10 | | | | | <10 | <10 |
| Cu | <5 | | <5 | <5 | | | | | <5 | <5 |
| Ni | 38 | | 65 | 9 | | | | | 13 | 72 |
| Sn | <9 | | <9 | <9 | | | | | <9 | <9 |
| Pb | 27 | | 29 | 15 | | | | | 36 | 40 |
| Nd | <20 | | <20 | <20 | | | | | <20 | <20 |
| Ce | 57 | | <28 | <28 | | | | | <28 | <28 |
| La | <20 | | <20 | <20 | | | | | <20 | <20 |
| Ba | 94 | | 99 | 115 | | | | | 76 | 80 |
| Th | 14 | | 25 | 24 | | | | | <10 | <10 |
| Sr | 63 | | 105 | 135 | | | | | 10 | 14 |
| U | 36 | | 15 | <10 | | | | | 13 | 13 |
| Rb | 5 | | 6 | 6 | | | | | <5 | <5 |
| Y | <5 | | <5 | <5 | | | | | <5 | <5 |
| Zr | 8 | | 19 | 12 | | | | | <5 | <5 |
| Nb | 5 | | 7 | 7 | | | | | <3 | <3 |
| Mo | <5 | | <5 | <5 | | | | | <5 | <5 |
| Cr | | | | 9 | | | | | 11 | 330 |
| V | | | | 18 | | | | | 28 | 44 |
| Sc | | | | <9 | | | | | <9 | 14 |

Miscellaneous

| Reg No. | 970103W | 970394 | 970400 | 970272 | 970106 | 970197 | 970090 | 970181 | 970112 |
|--------------------------------|----------------------------|-------------------|--------------------|--------------------|-----------------------------|----------------------|--------------------------|----------------------------|----------------------|
| Field No. | 107842 | 402198 | 107643 | 107643 | 107851 | 107891 | 107830 | 107864 | 107852 |
| | Limonite Au adit, clast | Limonite track | Limonite S bank | Limonite S bank | Lim-opal breccia, S bank | Sid-ophic? S bank | Clast? S bank, Clast? | Qtz-prn vein, Jdl, gate | Quartzite? S bank |
| SiO ₂ | 24.02 | 84.48 | 86.79 | | 47.10 | 53.22 | 14.14 | 61.19 | 98.28 |
| TiO ₂ | 0.05 | 0.01 | 0.03 | | 0.01 | 0.01 | 0.01 | 0.07 | 0.02 |
| Al ₂ O ₃ | 3.01 | 0.91 | 1.54 | | 0.08 | 0.33 | 0.84 | 14.70 | 0.28 |
| Fe ₂ O ₃ | 56.49 | 10.69 | 8.60 | | 2.99 | 9.44 | 2.98 | 2.36 | 0.01 |
| FeO | 0.96 | 1.49 | 0.19 | | 24.89 | 13.37 | 43.45 | 0.64 | 0.19 |
| MnO | 0.03 | 0.01 | 0.09 | | 0.71 | 0.64 | 1.38 | 0.04 | 0.00 |
| MgO | 0.84 | 0.07 | 0.19 | | 0.74 | 4.85 | 2.70 | 0.40 | 0.09 |
| CaO | 0.30 | 0.07 | 0.06 | | 1.66 | 1.42 | 2.09 | 17.38 | 0.07 |
| Na ₂ O | 0.10 | 0.01 | 0.00 | | 0.12 | 0.01 | 0.09 | 0.01 | 0.03 |
| K ₂ O | 0.09 | 0.04 | 0.05 | | 0.01 | 0.01 | 0.01 | 0.01 | 0.00 |
| P ₂ O ₅ | 0.17 | 0.01 | 0.04 | | 0.13 | 0.07 | 0.16 | 0.07 | 0.01 |
| SO ₃ | 0.09 | 0.09 | 0.08 | | 0.10 | 0.05 | 0.12 | 0.09 | 0.05 |
| CO ₂ | 3.46 | 0.68 | 0.00 | | 15.92 | 9.98 | 24.34 | 0.14 | 0.24 |
| H ₂ O ⁺ | 9.54 | 0.81 | 1.71 | | 5.15 | 5.52 | 6.52 | 3.54 | -0.03 |
| Total | 99.15 | 99.37 | 99.36 | | 99.61 | 98.90 | 98.83 | 100.63 | 99.23 |
| LOI | 12.89 | 1.33 | 1.69 | | 18.30 | 14.01 | 26.04 | 3.61 | 0.19 |
| Ag | 3 | 6 | 2 | 3 | 3 | 2 | 2 | 1 | <1 |
| Au | 0.4 | 2.87 | 6.72 | 9.1 | <0.05 | <0.05 | <0.05 | <0.05 | <0.05 |
| Co | 620 | | 64 | 67 | 12 | -8 | 22 | -8 | -8 |
| As | 280 | | 105 | 100 | -20 | 52 | 28 | -20 | -20 |
| Bi | 17 | | <5 | -5 | 10 | 7 | 23 | -5 | -5 |
| Ga | 7 | | 11 | 6 | -5 | -5 | -5 | 36 | -5 |
| Zn | 760 | | 74 | 71 | 185 | 145 | 30 | 15 | 9 |
| W | 260 | | <10 | -10 | -10 | -10 | -10 | -10 | -10 |
| Cu | -5 | | 27 | 24 | -5 | -5 | -5 | -5 | -5 |
| Ni | 59 | | 84 | 83 | 31 | 22 | 520 | 13 | -5 |
| Sn | -9 | | <9 | -9 | -9 | -9 | -9 | -9 | -9 |
| Pb | 640 | | 310 | 350 | 36 | 59 | 12 | 17 | 17 |
| Nd | -20 | | <20 | -20 | -20 | -20 | -20 | -20 | -20 |
| Ce | 67 | | 69 | -28 | -28 | -28 | 40 | -28 | -28 |
| La | -20 | | <20 | -20 | -20 | -20 | -20 | -20 | -20 |
| Ba | -23 | | 85 | 580 | 24 | 34 | -23 | -23 | 39 |
| Th | 23 | | <10 | -10 | 22 | 22 | 25 | <10 | -10 |
| Sr | 6 | | <5 | 9 | 8 | <5 | 10 | 25 | 9 |
| U | 16 | | <10 | -10 | -10 | <10 | -10 | <10 | -10 |
| Rb | 29 | | 5 | -5 | 16 | 6 | 25 | <5 | -5 |
| Y | 5 | | <5 | -5 | 15 | 11 | 27 | <5 | -5 |
| Zr | 30 | | 6 | 22 | 18 | <5 | 18 | 11 | 18 |
| Nb | 6 | | <3 | 3 | 4 | <3 | 5 | <3 | -3 |
| Mo | 5 | | <5 | 5 | -5 | <5 | -5 | <5 | 8 |
| Cr | 105 | | 155 | | 21 | 32 | 690 | 28 | 12 |
| V | 79 | | 38 | | 9 | 16 | 18 | 33 | -5 |
| Sc | 22 | | 12 | | -9 | -9 | -9 | -9 | -9 |

Permian

| Reg No. | 970456 | 970457 | 970458 | 970459 | 970460 | 970461 | 970463 | 970464 | 970467 | 970468 | 970469 | |
|--------------------------------|----------|-------------|-------------|-------------|-------------|-------------|-------------|-------------|-------------|-------------|-------------|--------|
| Field No. | 108028 | 108029 | 108030 | 108031 | 108032 | 108033 | 108035 | 108036 | 108041 | 108042 | 108043 | |
| | Mudstone | Mudstone | Mudstone | Mudstone | Mudstone | Mudstone | Mudstone | Mudstone | Mudstone | Mudstone | Mudstone | |
| | S Weld Q | Fletcher Rd | Fletcher Rd | Fletcher Rd | Fletcher Rd | Fletcher Rd | Fletcher Rd | Fletcher Rd | Fletcher Rd | Fletcher Rd | Fletcher Rd | ave. |
| SiO ₂ | 78.5 | 69.42 | 68.18 | 70.6 | 47.19 | 70.58 | 72.08 | 70.48 | 73.92 | 52.76 | 69.98 | 67.61 |
| TiO ₂ | 0.28 | 0.71 | 0.71 | 0.78 | 1.68 | 0.88 | 0.48 | 0.61 | 0.59 | 0.37 | 0.55 | 0.69 |
| Al ₂ O ₃ | 11.48 | 18.9 | 17.63 | 19.48 | 26.26 | 19.71 | 15.23 | 14.95 | 14.09 | 24 | 11.94 | 17.61 |
| Fe ₂ O ₃ | 1.81 | 1.11 | 3.25 | 0.07 | 8.82 | 0.09 | 2.61 | 4.28 | 2.58 | 3.89 | 2.96 | 2.86 |
| FeO | 0.19 | 0.58 | 0.71 | 0.19 | 0.71 | 0.19 | 0.32 | 0.52 | 0.32 | 1.68 | 1.1 | 0.59 |
| MnO | 0.03 | 0.01 | 0.01 | 0 | 0.02 | 0 | 0 | 0 | 0.01 | 0 | 0.04 | 0.01 |
| MgO | 0.83 | 0.81 | 0.76 | 0.02 | 0.42 | 0.07 | 0.99 | 0.98 | 1.08 | 0.6 | 2.57 | 0.83 |
| CaO | 0.44 | 0.06 | 0.01 | 0.01 | 0.02 | 0.02 | 0 | 0 | 0 | 0 | 2.88 | 0.31 |
| Na ₂ O | 3.5 | 0.02 | 0.04 | 0.03 | 0.03 | 0.01 | 0.01 | 0 | 0 | 0.01 | 1.79 | 0.49 |
| K ₂ O | 1.11 | 3.21 | 3.09 | 0.1 | 1.25 | 0.05 | 1.76 | 2.98 | 2.77 | 1.28 | 4.36 | 2.00 |
| P ₂ O ₅ | 0.04 | 0.02 | 0.04 | 0.01 | 0.05 | 0.04 | 0.05 | 0.12 | 0.04 | 0.05 | 0.11 | 0.05 |
| SO ₃ | 0.03 | 0.03 | 0.04 | 0.02 | 0.04 | 0.03 | 0.04 | 0.04 | 0.04 | 0.04 | 0.04 | 0.04 |
| CO ₂ | 0 | 0.15 | 0.13 | 0.2 | 2.43 | 0.12 | 0.18 | 0.36 | 0.22 | 2.9 | 0 | 0.61 |
| H ₂ O ⁺ | 2.09 | 5.16 | 5.06 | 7.71 | 10.01 | 7.64 | 5 | 4.46 | 4.06 | 11.32 | 1.92 | 5.86 |
| Total | 100.32 | 100.19 | 99.62 | 99.2 | 98.91 | 99.41 | 98.74 | 99.79 | 99.73 | 98.9 | 100.28 | 99.55 |
| LOI | 2.07 | 5.24 | 5.12 | 7.89 | 12.37 | 7.73 | 5.14 | 4.76 | 4.25 | 14.04 | 1.8 | 6.40 |
| Ag | <1 | ~1 | ~1 | ~1 | ~1 | ~1 | ~1 | ~1 | ~1 | ~1 | ~1 | |
| Au | 0.02 | 0.02 | 0.02 | 0.01 | 0.01 | <0.005 | 0.01 | <0.005 | 0.01 | 0.01 | 0.01 | |
| Co | <8 | <8 | <8 | <8 | <8 | <8 | <8 | <8 | <8 | <8 | 13 | |
| As | <20 | <20 | <20 | <20 | 74 | <20 | <20 | <20 | <20 | <20 | <20 | |
| Bi | <5 | <5 | <5 | <5 | 5 | <5 | <5 | <5 | <5 | <5 | <5 | |
| Ga | 14 | 21 | 21 | 21 | 23 | 22 | 16 | 18 | 18 | 22 | 16 | 19.27 |
| Zn | 51 | 35 | 42 | 15 | 24 | 25 | 31 | 31 | 27 | 23 | 77 | 34.64 |
| W | <10 | <10 | <10 | <10 | <10 | <10 | <10 | <10 | <10 | <10 | <10 | |
| Cu | <5 | 5 | 8 | <5 | 8 | <5 | 9 | 16 | 8 | <5 | 16 | |
| Ni | 11 | 9 | 9 | <5 | 23 | 12 | 22 | 11 | 10 | 17 | 51 | 17.50 |
| Sn | <9 | <9 | <9 | <9 | <9 | <9 | <9 | <9 | <9 | <9 | <9 | |
| Pb | 16 | 19 | 25 | <10 | 28 | <10 | 17 | 25 | <10 | 33 | 24 | 23.38 |
| Nd | 27 | <20 | <20 | <20 | <20 | <20 | <20 | 22 | <20 | 31 | 34 | |
| Ce | 56 | 46 | 29 | <28 | 31 | <28 | <28 | 73 | <28 | 61 | 53 | |
| La | 28 | 33 | 28 | <20 | <20 | <20 | <20 | 42 | <20 | 30 | 49 | |
| Ba | 250 | 730 | 710 | 65 | 130 | 62 | 290 | 460 | 410 | 250 | 1150 | 409.73 |
| Th | <10 | 17 | 18 | 13 | 38 | 23 | 14 | 15 | 17 | 120 | 13 | |
| Sr | 125 | 14 | 15 | <5 | <5 | <5 | <5 | 11 | <5 | <5 | 220 | |
| U | <10 | <10 | <10 | <10 | 10 | <10 | <10 | <10 | <10 | <10 | <10 | |
| Rb | 45 | 210 | 200 | 8 | 58 | <5 | 94 | 135 | 130 | 73 | 185 | 113.80 |
| Y | 35 | 23 | 24 | 8 | 11 | 6 | 15 | 23 | 17 | 12 | 66 | 21.82 |
| Zr | 220 | 190 | 200 | 330 | 170 | 380 | 230 | 220 | 260 | 280 | 190 | 242.73 |
| Nb | 9 | 15 | 16 | 16 | 27 | 18 | 11 | 14 | 13 | 12 | 12 | 14.82 |
| Mo | <5 | <5 | <5 | <5 | <5 | <5 | <5 | <5 | <5 | <5 | <5 | |
| Cr | 23 | 83 | 84 | 125 | 310 | 220 | 370 | 74 | 79 | 149 | 62 | 143.55 |
| V | 30 | 120 | 125 | 165 | 510 | 150 | 69 | 100 | 85 | 280 | 82 | 156.00 |
| Sc | <9 | 20 | 23 | 14 | 26 | 13 | 10 | 14 | 11 | 17 | 12 | 16.00 |

| Reg No. | 980021 | 980022 | 980025 | 980026 | 970064 | 970065 | 980021 | 980025 | 980026 |
|--------------------------------|---------------------------|------------------------|--------------------|--------------------|---------------------|---------------------|---------------------------|--------------------|--------------------|
| Field No. | 108108 | 108109 | 108112 | 108113 | 107811 | 107812A | 108108 | 108112 | 108113 |
| | Bleached zone junction | Silic cong junction | Bn H/W junction | Bn F/W junction | Chert road junct | Chert road junct | Bleached zone junction | Bn H/W junction | Bn F/W junction |
| SiO ₂ | 62.46 | 93.20 | 64.97 | 91.73 | 82.14 | 70.67 | 62.46 | 64.97 | 91.73 |
| TiO ₂ | 2.50 | 0.25 | 0.71 | 0.24 | 0.01 | 0.01 | 2.50 | 0.71 | 0.24 |
| Al ₂ O ₃ | 21.61 | 2.72 | 8.64 | 4.36 | 7.89 | 20.16 | 21.61 | 8.64 | 4.36 |
| Fe ₂ O ₃ | 1.75 | 0.97 | 13.66 | 0.14 | 2.96 | 0.03 | 1.75 | 13.66 | 0.14 |
| FeO | 0.58 | 0.19 | 0.96 | 0.19 | 0.58 | 0.26 | 0.58 | 0.96 | 0.19 |
| MnO | 0.01 | 0.01 | 0.03 | 0.00 | 0.00 | 0.00 | 0.01 | 0.03 | 0.00 |
| MgO | 0.81 | 0.13 | 1.05 | 0.51 | 0.15 | 0.05 | 0.81 | 1.05 | 0.51 |
| CaO | 0.01 | 0.05 | 0.03 | 0.02 | 0.11 | 0.04 | 0.01 | 0.03 | 0.02 |
| Na ₂ O | 0.08 | 0.07 | 0.07 | 0.06 | 0.04 | 0.02 | 0.08 | 0.07 | 0.06 |
| K ₂ O | 2.48 | 0.02 | 0.07 | 1.30 | 0.00 | 0.01 | 2.48 | 0.07 | 1.30 |
| P ₂ O ₅ | 0.08 | 0.03 | 0.12 | 0.03 | 0.05 | 0.03 | 0.08 | 0.12 | 0.03 |
| SO ₃ | 0.06 | 0.05 | 0.06 | 0.03 | 0.05 | 0.03 | 0.06 | 0.06 | 0.03 |
| CO ₂ | 0.23 | 0.18 | 2.43 | 0.25 | 1.49 | 0.31 | 0.23 | 2.43 | 0.25 |
| H ₂ O ⁺ | 7.08 | 1.33 | 4.69 | 0.99 | 3.49 | 7.82 | 7.08 | 4.69 | 0.99 |
| Total | 99.75 | 99.19 | 97.48 | 99.85 | 98.96 | 99.43 | 99.75 | 97.48 | 99.85 |
| LOI | 7.24 | 1.49 | 7.01 | 1.21 | 4.92 | 8.11 | 7.24 | 7.01 | 1.21 |
| Ag | 1 | <1 | 2 | <1 | ~1 | ~1 | 1 | 2 | <1 |
| Au | <0.03 | 0.2 | 0.2 | 0.1 | 0.2 | 0.2 | <0.03 | 0.2 | 0.1 |
| Co | <8 | <8 | 12 | <8 | -8 | -8 | <8 | 12 | <8 |
| As | 35 | 135 | 740 | <20 | 230 | 22 | 35 | 740 | <20 |
| Bi | <5 | <5 | 6 | <5 | -5 | -5 | <5 | 6 | <5 |
| Ga | 26 | <5 | 12 | 6 | -5 | -5 | 26 | 12 | 6 |
| Zn | 24 | 115 | 97 | 14 | 11 | 8 | 24 | 97 | 14 |
| W | <10 | <10 | <10 | <10 | -10 | -10 | <10 | <10 | <10 |
| Cu | 27 | 7 | 55 | <5 | 18 | 7 | 27 | 55 | <5 |
| Ni | 35 | 38 | 210 | 10 | 67 | 290 | 35 | 210 | 10 |
| Sn | <9 | <9 | <9 | <9 | -9 | -9 | <9 | <9 | <9 |
| Pb | 36 | 84 | 41 | 19 | 43 | 190 | 36 | 41 | 19 |
| Nd | 21 | <20 | <20 | <20 | -20 | 21 | 21 | <20 | <20 |
| Ce | 59 | <28 | 51 | <28 | -28 | 55 | 59 | 51 | <28 |
| La | <20 | <20 | <20 | <20 | -20 | 76 | <20 | <20 | <20 |
| Ba | 145 | 28 | 32 | 90 | 24 | 29 | 145 | 32 | 90 |
| Th | 25 | <10 | 23 | <10 | -10 | -10 | 25 | 23 | <10 |
| Sr | 9 | 7 | 8 | 9 | 9 | 8 | 9 | 8 | 9 |
| U | <10 | <10 | 10 | <10 | -10 | -10 | <10 | 10 | <10 |
| Rb | 110 | <5 | 9 | 39 | -5 | -5 | 110 | 9 | 39 |
| Y | 28 | <5 | 8 | 5 | -5 | -5 | 28 | 8 | 5 |
| Zr | 290 | 41 | 120 | 74 | 21 | 17 | 290 | 120 | 74 |
| Nb | 36 | 5 | 12 | 6 | 3 | -3 | 36 | 12 | 6 |
| Mo | <5 | 5 | 6 | <5 | 16 | 8 | <5 | 6 | <5 |
| Cr | 320 | 1300 | 7000 | 630 | 280 | 450 | 320 | 7000 | 630 |
| V | 290 | 52 | 190 | 39 | 60 | 6 | 290 | 190 | 39 |
| Sc | 57 | <9 | 26 | <9 | -9 | -9 | 57 | 26 | <9 |

| <i>Reg No.</i> | 970082 | 970094 | 980023 | 970067 | 970380 |
|--------------------------------|---------------------------------|---------------------------------|----------------------------|------------------------------|--------------------------------|
| <i>Field No.</i> | 107823 | 107833 | 108110 | 107812C | 402168 |
| | <i>Qtz breccia near BC7</i> | <i>Breccia Fletchers Rd</i> | <i>Silica junction</i> | <i>Chert road junct.</i> | <i>Clay-silica DDH SW2</i> |
| SiO ₂ | 89.41 | 92.05 | 96.23 | 96.82 | 78.51 |
| TiO ₂ | 0.30 | 0.36 | 0.02 | 0.02 | 0.01 |
| Al ₂ O ₃ | 5.83 | 3.46 | 1.04 | 1.07 | 1.07 |
| Fe ₂ O ₃ | 0.04 | 0.76 | 0.23 | 0.05 | 4.74 |
| FeO | 0.32 | 0.32 | 0.32 | 0.22 | 0.30 |
| MnO | 0.00 | 0.00 | 0.00 | 0.00 | 0.02 |
| MgO | 0.62 | 0.17 | 0.19 | 0.09 | 7.90 |
| CaO | 0.05 | 0.09 | 0.02 | 0.12 | 1.03 |
| Na ₂ O | 0.04 | 0.04 | 0.06 | 0.05 | 0.19 |
| K ₂ O | 1.91 | 0.03 | 0.03 | 0.01 | 0.06 |
| P ₂ O ₅ | 0.02 | 0.05 | 0.04 | 0.03 | 0.02 |
| SO ₃ | 0.02 | 0.06 | 0.04 | 0.03 | 0.08 |
| CO ₂ | 0.11 | 0.25 | 0.16 | 0.14 | 0.00 |
| H ₂ O ⁺ | 1.16 | 1.35 | 0.47 | 0.26 | 4.45 |
| Total | 99.81 | 98.99 | 98.85 | 98.90 | 98.38 |
| LOI | 1.23 | 1.56 | 0.59 | 0.37 | 4.42 |
| Ag | <1 | <1 | <1 | <1 | 1.2 |
| Au | <0.05 | <0.05 | 0.04 | <0.05 | 1.07 |
| Co | -8 | -8 | <8 | -8 | |
| As | -20 | 75 | <20 | -20 | |
| Bi | -5 | -5 | <5 | -5 | |
| Ga | 7 | -5 | <5 | -5 | |
| Zn | 28 | 12 | 11 | 9 | |
| W | -10 | -10 | <10 | -10 | |
| Cu | -5 | 14 | <5 | -5 | |
| Ni | 11 | 21 | 16 | 6 | |
| Sn | -9 | -9 | <9 | -9 | |
| Pb | 31 | 18 | 21 | 29 | |
| Nd | -20 | -20 | <20 | -20 | |
| Ce | -28 | -28 | <28 | -28 | |
| La | -20 | -20 | <20 | -20 | |
| Ba | 170 | 47 | 24 | 35 | |
| Th | -10 | -10 | <10 | -10 | |
| Sr | 12 | 10 | 7 | 7 | |
| U | -10 | -10 | <10 | -10 | |
| Rb | 64 | -5 | <5 | -5 | |
| Y | 5 | 6 | <5 | -5 | |
| Zr | 63 | 67 | 20 | 17 | |
| Nb | 5 | 7 | <3 | -3 | |
| Mo | -5 | 6 | 10 | 7 | |
| Cr | 910 | 185 | 135 | 14 | |
| V | 68 | 29 | 8 | -5 | |
| Sc | -9 | -9 | <9 | -9 | |

APPENDIX 8

ICP analyses

| Sample No. | Rock type | Au | Au | Ag | As | Bi | Cd | Ce | Co | Cs | Cu | Ga | In | La | Mo | Nb | Ni | Pb | Rb | Sb |
|------------|----------------|-------|------|------|--------|------|------|------|-------|------|-------|------|------|------|------|------|--------|-------|------|------|
| 402040 | lamprophyre | 0.02 | | 0.1 | 3.5 | -0.1 | -0.1 | 49.5 | 50.0 | 0.5 | 110.0 | 16.5 | 0.1 | 29.0 | 1.2 | 31.0 | 200.0 | 2.5 | 63.0 | -0.5 |
| 107639 | lamprophyre | -0.01 | | -0.1 | 3.0 | 0.1 | -0.1 | 32.5 | 56.0 | 0.1 | 24.0 | 17.0 | 0.1 | 21.0 | 0.6 | 22.5 | 125.0 | 2.0 | 37.5 | -0.5 |
| 402140A | U/B | -0.01 | | 0.2 | 21.0 | -0.1 | -0.1 | 0.5 | 72.0 | 0.1 | 9.5 | 1.9 | -0.1 | 1.2 | -0.1 | -0.5 | 550.0 | 2.0 | 1.4 | -0.5 |
| 402140B | U/B | 0.01 | | 0.2 | 16.0 | -0.1 | -0.1 | 2.0 | 56.0 | -0.1 | 5.5 | 1.9 | -0.1 | 1.4 | 0.1 | -0.5 | 500.0 | 1.5 | 1.1 | -0.5 |
| 402154 | Jdl | 0.55 | | 3.5 | 7.0 | 0.1 | 7.5 | 20.0 | 105.0 | 0.3 | 89.0 | 9.5 | 0.1 | 17.0 | 0.6 | 7.5 | 800.0 | 330.0 | 1.6 | 13.0 |
| 402181 | Jdl | 0.01 | | -0.1 | 3.0 | -0.1 | -0.1 | 20.0 | 51.0 | 1.7 | 97.0 | 16.5 | 0.1 | 12.5 | 0.4 | 7.0 | 76.0 | 4.5 | 39.5 | -0.5 |
| 402163 | quartz-skarn | 0.25 | | 0.8 | 46.0 | -0.1 | 0.9 | -0.5 | 15.5 | 0.9 | 11.0 | 0.6 | -0.1 | 0.7 | 6.5 | -0.5 | 61.0 | 19.5 | 1.8 | 15.0 |
| 402169 | qtz-skarn | 0.90 | | 1.2 | 115.0 | -0.1 | 1.9 | -0.5 | 54.0 | 2.0 | 11.5 | 1.2 | -0.1 | 0.4 | 0.7 | -0.5 | 210.0 | 5.0 | 6.0 | 22.0 |
| 402165 | di-skarn | 0.07 | | 0.4 | 470.0 | 0.2 | 2.7 | 1.5 | 5.5 | 0.3 | 5.0 | 0.3 | -0.1 | 1.4 | 1.1 | -0.5 | 39.0 | 30.5 | 5.0 | 9.0 |
| 402178A | di-skarn | 0.14 | | 0.4 | 48.5 | -0.1 | 1.0 | 1.5 | 3.4 | 0.1 | 4.5 | 1.2 | -0.1 | 1.2 | 1.1 | -0.5 | 14.0 | 37.5 | 0.5 | 9.0 |
| 402178B | di-skarn | 0.13 | | 0.4 | 53.0 | 0.1 | 1.2 | 3.0 | 10.0 | 0.1 | 6.5 | 1.3 | -0.1 | 2.7 | 1.8 | -0.5 | 60.0 | 31.5 | 1.2 | 8.0 |
| 402159 | ophicalcite | 0.03 | | 0.2 | 115.0 | -0.1 | 0.2 | 0.5 | 3.1 | -0.1 | 2.5 | 1.4 | -0.1 | 0.9 | 0.5 | -0.5 | 25.0 | 3.5 | 0.4 | 3.5 |
| 402170 | ophicalcite | -0.01 | | 0.2 | 87.0 | -0.1 | 0.3 | -0.5 | 2.7 | -0.1 | -0.5 | 0.4 | -0.1 | 0.7 | 0.2 | -0.5 | 22.0 | 4.0 | 0.3 | 2.0 |
| 402174 | ophicalcite | 0.10 | | 0.8 | 1100.0 | -0.1 | 0.6 | 1.0 | 2.8 | -0.1 | 6.5 | 0.5 | -0.1 | 1.2 | 0.8 | -0.5 | 26.0 | 10.0 | 0.4 | 6.5 |
| 402175 | ophicalcite | 0.01 | | 0.1 | 68.0 | -0.1 | -0.1 | 1.0 | 2.6 | -0.1 | 0.5 | 0.7 | -0.1 | 1.1 | 0.6 | -0.5 | 16.0 | 10.5 | 0.4 | 1.0 |
| 402174b | ophicalcite | 0.11 | | 1.0 | 1400.0 | -0.1 | 0.7 | 1.0 | 2.7 | -0.1 | 9.0 | 0.6 | -0.1 | 1.0 | 0.8 | -0.5 | 32.0 | 11.0 | 0.3 | 7.5 |
| 402177 | ophicalcite | 0.10 | | 0.2 | 20.5 | -0.1 | 2.3 | 6.5 | 6.5 | -0.1 | 2.0 | 1.4 | -0.1 | 5.0 | 2.9 | 1.5 | 44.0 | 12.0 | 0.3 | 4.0 |
| 402206 | ophicalcite | 0.04 | | -0.1 | 43.5 | -0.1 | 0.4 | 3.5 | 1.6 | 0.1 | 6.0 | 1.1 | -0.1 | 2.7 | 0.5 | -0.5 | 12.0 | 10.0 | 1.4 | 3.0 |
| 402179 | ophicalcite | -0.01 | | 0.1 | 6.0 | -0.1 | 0.1 | 0.5 | 2.1 | -0.1 | 1.0 | 0.2 | -0.1 | 1.1 | 0.5 | -0.5 | 15.0 | -0.5 | 0.3 | 0.5 |
| 402198 | limonite | 2.87 | 2.59 | 6.0 | 1100.0 | 2.1 | 0.6 | 3.0 | 12.5 | 0.1 | 240.0 | 0.9 | -0.1 | 2.5 | 14.5 | -0.5 | 260.0 | 430.0 | 1.6 | 37.0 |
| 107643 | limonite | 6.72 | 7.90 | 2.0 | 135.0 | 1.7 | 0.1 | 40.5 | 71.0 | -0.1 | 43.5 | 3.4 | -0.1 | 2.3 | 1.9 | 0.5 | 97.0 | 450.0 | 1.7 | 42.5 |
| 402168 | opal | 1.07 | 1.30 | 1.2 | 12.0 | 0.6 | 0.6 | 1.5 | 98.0 | 1.9 | 61.0 | 1.0 | -0.1 | 1.4 | 0.2 | -0.5 | 2050.0 | 130.0 | 5.0 | 27.0 |
| 402205 | opal | 0.64 | 0.64 | 1.0 | 290.0 | 0.4 | 0.2 | 3.5 | 30.0 | -0.1 | 43.5 | 0.3 | -0.1 | 2.0 | 3.5 | -0.5 | 350.0 | 77.0 | 1.2 | 14.0 |
| 402450 | opal | -0.01 | | -0.1 | 3.5 | -0.1 | 0.3 | 1.0 | 1.8 | -0.1 | 1.5 | 0.3 | -0.1 | 0.6 | 0.4 | -0.5 | 7.0 | 15.0 | 0.6 | 3.0 |
| 402194 | quartz breccia | -0.01 | | -0.1 | 4.5 | -0.1 | -0.1 | -0.5 | 0.2 | -0.1 | 2.0 | 1.3 | -0.1 | 0.2 | 1.5 | -0.5 | 2.0 | 0.5 | 0.6 | 23.5 |
| 402186 | chert | -0.01 | | 1.0 | 155.0 | -0.1 | 0.2 | 1.5 | 2.4 | 0.1 | 13.0 | 0.7 | -0.1 | 1.0 | 7.0 | 1.0 | 11.0 | 6.0 | 2.9 | 47.0 |
| 402209 | chert | 0.04 | | 0.8 | 115.0 | 0.2 | 0.1 | 2.0 | 1.2 | 0.3 | 18.5 | 1.2 | -0.1 | 1.9 | 1.9 | 1.0 | 15.0 | 250.0 | 3.5 | 58.0 |
| 402190 | chert | 0.13 | | 0.2 | 290.0 | 0.1 | -0.1 | 4.0 | 2.5 | 0.8 | 94.0 | 3.5 | -0.1 | 3.2 | 2.4 | 1.0 | 32.0 | 25.0 | 14.5 | 22.0 |

| Sample No. | Rock type | Se | Sr | Te | Th | Tl | U | W | Y | Zn | Ca | Cr | Fe | K | Mg | Mn | Na | P | Ti | V |
|------------|----------------|------|-------|------|-----|------|------|------|------|--------|--------|------|-------|-------|--------|------|-------|------|------|-----|
| 402040 | lamprophyre | 1.5 | 430.0 | -0.2 | 3.8 | 0.2 | 1.2 | 0.4 | 18.5 | 73.0 | 64200 | 370 | 52800 | 18300 | 59900 | 1000 | 18400 | 1100 | 8350 | 220 |
| 107639 | lamprophyre | 1.5 | 125.0 | -0.2 | 3.2 | 0.2 | 0.8 | 0.4 | 19.0 | 99.0 | 44100 | 185 | 74400 | 12300 | 62100 | 1500 | 23700 | 1300 | 9550 | 240 |
| 402140A | U/B | 0.5 | 8.0 | 0.3 | 0.1 | -0.1 | 0.0 | -0.1 | 1.7 | 44.0 | 38600 | 1600 | 60800 | 190 | 128000 | 650 | 1050 | 40 | 250 | 74 |
| 402140B | U/B | 1.5 | 10.0 | -0.2 | 0.1 | -0.1 | 0.0 | -0.1 | 2.1 | 43.0 | 70500 | 1950 | 57400 | 250 | 116000 | 1000 | 1150 | 40 | 300 | 100 |
| 402154 | Jdl | 1.5 | 25.5 | -0.2 | 3.3 | 0.1 | 1.7 | 1.8 | 23.0 | 3250.0 | 98000 | 96 | 52800 | 350 | 20900 | 370 | 450 | 320 | 4300 | 180 |
| 402181 | Jdl | 1.0 | 140.0 | -0.2 | 3.2 | 0.3 | 0.7 | 0.5 | 18.5 | 80.0 | 68100 | 72 | 59900 | 8000 | 39900 | 1100 | 13700 | 330 | 4350 | 210 |
| 402163 | quartz-skarn | 3.5 | 22.5 | -0.2 | 0.1 | -0.1 | 4.0 | 0.2 | 0.3 | 97.0 | 115000 | 15 | 4550 | 340 | 8200 | 55 | 500 | 15 | 25 | 4 |
| 402169 | quartz-skarn | 2.0 | 20.0 | -0.2 | 0.1 | 0.4 | 1.9 | 0.1 | 0.3 | 2450.0 | 35600 | 2 | 9600 | 350 | 50500 | 165 | 300 | 25 | 35 | 6 |
| 402165 | di-skarn | 1.5 | 30.0 | -0.2 | 0.2 | -0.1 | 3.7 | 0.3 | 1.4 | 420.0 | 197000 | 4 | 4250 | 1250 | 86800 | 95 | 210 | 40 | 90 | 35 |
| 402178A | di-skarn | 1.5 | 13.5 | 0.3 | 0.1 | -0.1 | 9.0 | 1.0 | 1.4 | 195.0 | 113000 | -2 | 3600 | 50 | 154000 | 190 | 55 | 50 | 10 | 26 |
| 402178B | di-skarn | 3.0 | 16.0 | 0.2 | 0.7 | 0.2 | 9.0 | 1.3 | 1.8 | 200.0 | 121000 | 210 | 10600 | 90 | 144000 | 270 | 190 | 65 | 55 | 39 |
| 402159 | ophicalcite | 1.5 | 69.0 | -0.2 | 0.1 | -0.1 | 3.2 | 0.4 | 0.4 | 21.5 | 196000 | 3 | 3350 | 20 | 121000 | 50 | 35 | 60 | 20 | 34 |
| 402170 | ophicalcite | 1.0 | 52.0 | -0.2 | 0.1 | -0.1 | 2.8 | 0.5 | 0.3 | 41.5 | 209000 | -2 | 1050 | 40 | 135000 | 50 | 40 | 55 | 20 | 26 |
| 402174 | ophicalcite | 3.5 | 61.0 | -0.2 | 0.2 | -0.1 | 19.0 | 0.6 | 1.0 | 51.0 | 184000 | 3 | 11800 | 40 | 138000 | 120 | 40 | 95 | 40 | 50 |
| 402175 | ophicalcite | 1.0 | 95.0 | -0.2 | 0.2 | -0.1 | 7.5 | 0.3 | 0.7 | 35.0 | 222000 | -2 | 2300 | 45 | 138000 | 75 | 40 | 50 | 35 | 23 |
| 402174b | ophicalcite | 4.0 | 56.0 | 0.2 | 0.2 | -0.1 | 21.5 | 0.7 | 0.8 | 61.0 | 183000 | 3 | 14900 | 45 | 138000 | 120 | 45 | 50 | 35 | 59 |
| 402177 | ophicalcite | 2.0 | 81.0 | -0.2 | 1.6 | -0.1 | 6.5 | 1.0 | 3.6 | 280.0 | 238000 | 5 | 7600 | 35 | 134000 | 185 | 55 | 195 | 350 | 72 |
| 402206 | ophicalcite | 4.5 | 39.5 | -0.2 | 0.9 | -0.1 | 2.0 | 0.3 | 7.0 | 53.0 | 171000 | 8 | 9150 | 75 | 48100 | 90 | 55 | 50 | 55 | 18 |
| 402179 | ophicalcite | 1.0 | 100.0 | -0.2 | 0.1 | -0.1 | 0.9 | 0.3 | 0.7 | 18.0 | 250000 | -2 | 2600 | 40 | 133000 | 80 | 25 | 65 | 25 | 12 |
| 402198 | limonite | 2.5 | 2.3 | -0.2 | 0.3 | -0.1 | 2.0 | 0.4 | 1.4 | 220.0 | 310 | 33 | 81800 | 190 | 125 | 40 | 130 | 35 | 60 | 40 |
| 107643 | limonite | -0.5 | 2.1 | 0.2 | 0.5 | 0.2 | 2.5 | 2.3 | 1.5 | 88.0 | 420 | 81 | 62000 | 280 | 1150 | 700 | 85 | 190 | 210 | 35 |
| 402168 | opal | -0.5 | 7.0 | -0.2 | 0.1 | 0.1 | 0.6 | 0.2 | 3.7 | 3650.0 | 6400 | 18 | 29000 | 340 | 41600 | 55 | 150 | 20 | 25 | 7 |
| 402205 | opal | -0.5 | 0.3 | -0.2 | 0.3 | 0.8 | 0.8 | 0.6 | 3.9 | 71.0 | 90 | 34 | 47000 | 95 | 50 | 135 | 40 | 90 | -10 | 20 |
| 402450 | opal | -0.5 | 2.8 | -0.2 | 0.2 | -0.1 | 0.5 | -0.1 | 1.0 | 16.0 | 1150 | 4 | 9900 | 45 | 550 | 340 | 25 | 10 | 15 | 3 |
| 402194 | quartz breccia | -0.5 | 1.7 | -0.2 | 0.1 | -0.1 | 1.3 | 0.2 | 0.1 | 6.0 | 170 | 3 | 2650 | 70 | 40 | 30 | 170 | 5 | 35 | -2 |
| 402186 | chert | -0.5 | 14.5 | -0.2 | 0.3 | 0.6 | 0.4 | 1.4 | 0.6 | 32.5 | 3700 | 25 | 7850 | 700 | 700 | 45 | 330 | 25 | 240 | 7 |
| 402209 | chert | -0.5 | 7.5 | -0.2 | 0.6 | 0.2 | 6.0 | 0.8 | 0.6 | 19.5 | 1450 | 21 | 17800 | 700 | 550 | 115 | 290 | 90 | 290 | 16 |
| 402190 | chert | 2.5 | 9.0 | -0.2 | 1.9 | 3.8 | 1.5 | 2.9 | 2.8 | 20.5 | 1000 | 490 | 32200 | 3350 | 750 | 45 | 250 | 25 | 700 | 42 |

APPENDIX 9

Microprobe analyses

| Sample No. | 402139 | 402139 | 402139 | 107640 | 107640 | 107807 | 402165 | 402165 | 402165 | 402177 |
|--------------------------------|-------------------------|----------------------------|------------------------|----------------------|-------------------------------|----------------|-------------|-------------|-------------|---------|
| Description | amphibole actinolite | amphibole Mg-hornblende | amphibole tremolite | amphibole edenite | amphibole ferro-actinolite | amphibole * | apophyllite | apophyllite | apophyllite | brucite |
| SiO ₂ | 56.86 | 53.89 | 57.32 | 45.24 | 50.02 | 42.31 | 54.63 | 57.24 | 53.69 | 1.16 |
| TiO ₂ | 0.20 | 0.11 | 0.05 | 1.69 | 0.07 | 4.18 | 0.01 | 0.00 | 0.00 | 0.03 |
| Al ₂ O ₃ | 3.18 | 6.49 | 2.77 | 10.65 | 2.44 | 11.84 | 0.02 | 0.00 | 0.03 | 0.71 |
| Cr ₂ O ₃ | 0.11 | 1.60 | 0.10 | 0.01 | 0.01 | 0.00 | 0.01 | 0.00 | 0.00 | 0.04 |
| MgO | 18.82 | 20.70 | 21.74 | 12.55 | 9.27 | 12.46 | 0.01 | 0.01 | 0.02 | 72.88 |
| CaO | 11.24 | 12.69 | 12.17 | 10.74 | 11.67 | 11.34 | 26.61 | 26.02 | 26.19 | 0.36 |
| MnO | 0.17 | 0.04 | 0.00 | 0.46 | 1.02 | 0.26 | 0.04 | 0.00 | 0.01 | 0.11 |
| FeO | 8.87 | 3.31 | 3.94 | 15.75 | 21.69 | 13.53 | 0.02 | 0.02 | 0.00 | 2.96 |
| NiO | | | | | 0.38 | | 0.00 | 0.00 | 0.00 | 0.00 |
| Na ₂ O | 0.40 | 0.91 | 0.41 | 2.05 | 0.29 | 2.30 | 0.20 | 0.21 | 0.32 | 0.01 |
| K ₂ O | 0.03 | 0.09 | 0.08 | 0.82 | | 0.94 | 1.91 | 2.32 | 2.31 | 0.00 |
| Cl | 0.12 | 0.15 | 0.09 | | | 0.05 | 0.00 | 0.00 | 0.00 | |
| F | 0.03 | 0.07 | | | | 0.11 | 2.42 | 2.72 | 2.52 | |
| H ₂ O est. | | | | | | | 16.00 | 16.00 | 16.00 | |
| Total | 100.04 | 100.06 | 98.65 | 99.95 | 96.85 | 99.14 | 101.88 | 104.54 | 101.09 | 78.25 |
| -O=F, Cl | -0.04 | -0.06 | -0.02 | 0.00 | 0.00 | -0.04 | 1.02 | -1.15 | -1.06 | |
| Total | 100.00 | 100.00 | 98.63 | 99.95 | 96.85 | 99.10 | 100.86 | 103.39 | 100.03 | |
| Atomic ratios (O,OH,F,Cl) | 23 | 23 | 23 | 23 | 23 | 23 | 29 | 29 | 29 | 1 |
| Si | 7.785 | 7.302 | 7.802 | 6.580 | 7.651 | 6.193 | 8.060 | 8.226 | 7.996 | 0.010 |
| Al(iv) | 0.215 | 0.698 | 0.198 | 1.420 | 0.349 | 1.807 | 0.003 | 0.000 | 0.005 | |
| Total T | 8.000 | 8.000 | 8.000 | 8.000 | 8.000 | 8.000 | | | | |
| Al(vi) | 0.297 | 0.338 | 0.247 | 0.406 | 0.090 | 0.235 | | | | 0.007 |
| Ti | 0.021 | 0.011 | 0.005 | 0.184 | 0.008 | 0.460 | 0.001 | 0.000 | 0.000 | 0.000 |
| Cr | 0.012 | 0.172 | 0.011 | 0.001 | 0.001 | 0.000 | 0.001 | 0.000 | 0.000 | 0.000 |
| Fe | 0.830 | 0.299 | 0.329 | 1.690 | 2.741 | 1.587 | 0.002 | 0.002 | 0.000 | 0.021 |
| Ni | 0.000 | 0.000 | 0.000 | 0.000 | 0.046 | 0.000 | 0.000 | 0.000 | 0.000 | 0.000 |
| Mg | 3.840 | 4.180 | 4.410 | 2.719 | 2.113 | 2.718 | 0.002 | 0.002 | 0.004 | 0.943 |
| Total C | 5.000 | 5.000 | 5.000 | 5.000 | 5.000 | 5.000 | | | | |
| Mn | 0.020 | 0.005 | 0.000 | 0.056 | 0.133 | 0.032 | 0.005 | 0.000 | 0.001 | 0.001 |
| Fe | 0.186 | 0.076 | 0.120 | 0.226 | 0.033 | 0.069 | | | | |
| Ca | 1.649 | 1.843 | 1.775 | 1.675 | 1.912 | 1.779 | 4.207 | 4.007 | 4.180 | 0.003 |
| Na(B) | 0.107 | 0.076 | 0.105 | 0.043 | 0.000 | 0.120 | | | | |
| Total B | 1.962 | 2.000 | 2.000 | 2.000 | 2.078 | 2.000 | | | | |
| Na(A) | 0.000 | 0.162 | 0.003 | 0.536 | 0.085 | 0.533 | 0.057 | 0.059 | 0.092 | 0.000 |
| K | 0.005 | 0.016 | 0.013 | 0.152 | 0.000 | 0.175 | 0.360 | 0.425 | 0.439 | 0.000 |
| Total A | 0.005 | 0.179 | 0.016 | 0.688 | 0.085 | 0.708 | 0.417 | 0.484 | 0.531 | |
| Total cations | 14.967 | 15.179 | 15.016 | 15.688 | 15.163 | 15.708 | 12.699 | 12.721 | 12.718 | 0.986 |
| H | | | | | | | 15.762 | 15.352 | 15.910 | |
| Cl | 0.055 | 0.068 | 0.041 | 0.000 | 0.000 | 0.027 | 0.000 | 0.000 | 0.000 | |
| F | 0.014 | 0.030 | 0.000 | 0.000 | 0.000 | 0.049 | 1.129 | 1.236 | 1.187 | |
| Mg/(Mg+Fe) | 0.791 | 0.918 | 0.908 | 0.587 | 0.432 | 0.621 | | | | |

Amphibole cation distributions and Fe³⁺ calculated using average of minimum and maximum constraints (Holland and Blundy, 1994).

* = Ti=magnesiohastingsite

| <i>Sample No.</i> | <i>402169</i> | <i>402165</i> | <i>403173</i> | <i>403173</i> |
|----------------------|----------------|----------------|----------------|----------------|
| <i>Description</i> | <i>calcite</i> | <i>calcite</i> | <i>calcite</i> | <i>calcite</i> |
| SiO ₂ | 0.08 | 0.00 | 1.86 | 1.28 |
| FeO | 0.06 | 0.05 | 0.06 | 1.08 |
| MnO | 0.02 | 0.00 | 0.03 | 0.00 |
| NiO | | | 0.00 | 0.00 |
| MgO | 0.00 | 0.00 | 1.24 | 0.70 |
| ZnO | 0.00 | 0.07 | 0.04 | 0.26 |
| CaO | 61.81 | 27.16 | 63.96 | 67.76 |
| Na ₂ O | 0.00 | 0.00 | 0.01 | 0.00 |
| K ₂ O | 0.01 | | 0.00 | 0.01 |
| Total | 61.97 | 27.29 | 67.21 | 71.10 |
| <i>Atomic ratios</i> | | | | |
| No. oxygen | 1 | 1 | 1 | 1 |
| Si | 0.001 | 0.000 | 0.013 | 0.008 |
| Fe | 0.001 | 0.001 | 0.001 | 0.012 |
| Mn | 0.000 | 0.000 | 0.000 | 0.000 |
| Ni | 0.000 | 0.000 | 0.000 | 0.000 |
| Mg | 0.000 | 0.000 | 0.026 | 0.014 |
| Zn | 0.000 | 0.002 | 0.000 | 0.003 |
| Ca | 0.998 | 0.996 | 0.947 | 0.955 |
| Na | 0.000 | 0.000 | 0.000 | 0.000 |
| K | 0.000 | 0.000 | 0.000 | 0.000 |
| Total cations | 0.999 | 1.000 | 0.987 | 0.992 |

| <i>Sample No.</i> | <i>400235</i> | <i>400235</i> | <i>400235</i> | <i>400235</i> | <i>403139</i> | <i>403139</i> | <i>403139</i> |
|--------------------------------|-----------------|-----------------|-----------------|-----------------|-----------------|-----------------|-----------------|
| <i>Description</i> | <i>Chromite</i> | <i>Chromite</i> | <i>Chromite</i> | <i>Chromite</i> | <i>Chromite</i> | <i>Chromite</i> | <i>Chromite</i> |
| SiO ₂ | | 0.28 | | | 0.09 | 0.00 | 0.00 |
| TiO ₂ | | | | | 0.03 | 0.02 | 0.01 |
| Al ₂ O ₃ | 5.23 | 5.95 | 4.82 | 4.72 | 3.14 | 10.01 | 19.44 |
| Cr ₂ O ₃ | 70.47 | 66.88 | 72.27 | 70.60 | 61.51 | 57.98 | 46.32 |
| MgO | 8.84 | 10.53 | 9.69 | 10.15 | 4.18 | 9.72 | 11.17 |
| CaO | | | | | | | |
| MnO | | | | | 0.74 | 0.30 | 0.35 |
| FeO | 15.72 | 13.42 | 15.17 | 16.93 | 28.38 | 19.68 | 21.52 |
| NiO | | | | | 0.00 | 0.03 | 0.04 |
| Na ₂ O | | 0.90 (?Zn) | | | | | |
| K ₂ O | | | | | | | |
| Total | 100.26 | 97.96 | 101.95 | 102.40 | 98.06 | 97.73 | 98.85 |
| <i>Atomic ratios</i> | | | | | | | |
| No. oxygen | 4 | 4 | 4 | 4 | 4 | 4 | 4 |
| Si | 0.000 | 0.010 | 0.000 | 0.000 | 0.003 | 0.000 | 0.000 |
| Ti | 0.000 | 0.000 | 0.000 | 0.000 | 0.001 | 0.001 | 0.000 |
| Al | 0.210 | 0.242 | 0.189 | 0.184 | 0.134 | 0.398 | 0.727 |
| Cr | 1.895 | 1.822 | 1.906 | 1.847 | 1.757 | 1.547 | 1.163 |
| Fe | 0.000 | 0.000 | 0.000 | 0.000 | 0.105 | 0.054 | 0.110 |
| <i>Tot tet</i> | 2.105 | 2.073 | 2.095 | 2.031 | 2.000 | 2.000 | 2.000 |
| Mg | 0.448 | 0.541 | 0.482 | 0.501 | 0.225 | 0.489 | 0.528 |
| Fe | 0.447 | 0.387 | 0.423 | 0.468 | 0.752 | 0.502 | 0.461 |
| Ni | 0.000 | 0.000 | 0.000 | 0.000 | 0.000 | 0.001 | 0.001 |
| Mn | 0.000 | 0.000 | 0.000 | 0.000 | 0.023 | 0.009 | 0.009 |
| <i>Tot oct</i> | 0.895 | 0.927 | 0.905 | 0.969 | 1.000 | 1.000 | 1.000 |
| Total | 3.000 | 3.000 | 3.000 | 3.000 | 3.000 | 3.000 | 3.000 |

| Sample No. Description | 402161 <i>hibschite</i> | 402161 <i>hibschite</i> | 402161 <i>hydro-and.</i> | 402161 <i>hydro-and.</i> | 402178 <i>hydro-and.</i> | 402178 <i>hydro-and.</i> |
|--------------------------------|----------------------------|----------------------------|-----------------------------|-----------------------------|-----------------------------|-----------------------------|
| SiO ₂ | 28.27 | 29.51 | 34.97 | 35.89 | 33.27 | 34.50 |
| TiO ₂ | 0.96 | 0.32 | 0.00 | 0.00 | 0.01 | 0.00 |
| Al ₂ O ₃ | 15.73 | 18.12 | 2.38 | 5.07 | 1.01 | 0.15 |
| Cr ₂ O ₃ | 0.00 | 0.00 | 0.00 | 0.03 | 0.00 | 0.01 |
| V ₂ O ₃ | | | | | 0.00 | 0.07 |
| Fe ₂ O ₃ | 6.19 | 4.56 | 24.35 | 20.92 | 24.28 | 25.65 |
| MnO | 0.12 | 0.06 | 0.05 | 0.00 | 0.00 | 0.03 |
| NiO | 0.00 | 0.00 | 0.00 | 0.00 | 0.00 | 0.00 |
| MgO | 1.77 | 1.78 | 0.56 | 0.36 | 0.99 | 1.17 |
| ZnO | | | | | 0.00 | 0.00 |
| CaO | 36.16 | 35.60 | 34.38 | 35.02 | 33.85 | 33.30 |
| Na ₂ O | 0.00 | 0.00 | 0.02 | 0.02 | 0.00 | 0.00 |
| K ₂ O | | 0.02 | 0.00 | 0.00 | 0.00 | 0.00 |
| Total | 89.21 | 89.97 | 96.70 | 97.30 | 93.43 | 94.88 |
| <i>Atomic ratios</i> | | | | | | |
| No. oxygen | 12 | 12 | 12 | 12 | 12 | 12 |
| Si | 2.527 | 2.575 | 3.011 | 3.023 | 2.991 | 3.050 |
| <i>Total T</i> | 2.527 | 2.575 | 3.011 | 3.023 | 2.991 | 3.050 |
| Ti | 0.065 | 0.021 | 0.000 | 0.000 | 0.001 | 0.000 |
| Al | 1.657 | 1.863 | 0.242 | 0.503 | 0.107 | 0.015 |
| Cr | 0.000 | 0.000 | 0.000 | 0.002 | 0.000 | 0.000 |
| V | 0.000 | 0.000 | 0.000 | 0.000 | 0.000 | 0.005 |
| Fe | 0.416 | 0.299 | 1.578 | 1.326 | 1.642 | 1.706 |
| <i>Total B</i> | 2.138 | 2.183 | 1.819 | 1.830 | 1.750 | 1.727 |
| Mn | 0.009 | 0.005 | 0.003 | 0.000 | 0.000 | 0.002 |
| Ni | 0.000 | 0.000 | 0.000 | 0.000 | 0.000 | 0.000 |
| Mg | 0.236 | 0.231 | 0.072 | 0.045 | 0.132 | 0.154 |
| Zn | 0.000 | 0.000 | 0.000 | 0.000 | 0.000 | 0.000 |
| Ca | 3.463 | 3.329 | 3.172 | 3.161 | 3.260 | 3.154 |
| Na | 0.000 | 0.000 | 0.003 | 0.003 | 0.000 | 0.000 |
| K | 0.000 | 0.002 | 0.000 | 0.000 | 0.000 | 0.000 |
| <i>Total A</i> | 3.708 | 3.566 | 3.250 | 3.209 | 3.393 | 3.310 |
| Total cations | 8.372 | 8.324 | 8.081 | 8.063 | 8.134 | 8.087 |

| Sample No. Description | 402169 <i>sap</i> | 402161 <i>chl</i> | 402161 <i>chl</i> | 402161 <i>sep</i> | 402178 <i>srp</i> | 402169 <i>sep?</i> | 402169 <i>tlc</i> | 402169 <i>sep?</i> |
|--------------------------------|----------------------|----------------------|----------------------|----------------------|----------------------|-----------------------|----------------------|-----------------------|
| SiO ₂ | 60.32 | 36.52 | 36.00 | 49.45 | 44.51 | 63.22 | 54.98 | 60.04 |
| TiO ₂ | 0.00 | 0.00 | 0.00 | 0.00 | 0.01 | 0.00 | 0.00 | 0.00 |
| Al ₂ O ₃ | 0.60 | 10.38 | 11.86 | 0.00 | 0.24 | 1.06 | 2.06 | 0.76 |
| Cr ₂ O ₃ | 0.03 | 0.00 | 0.00 | 0.00 | 0.00 | 0.00 | 0.02 | 0.00 |
| V ₂ O ₃ | | | | | 0.00 | 0.00 | 0.07 | 0.00 |
| FeO | 4.63 | 0.76 | 1.11 | 0.48 | 0.19 | 1.92 | 5.20 | 1.93 |
| MnO | 0.04 | 0.06 | 0.16 | 0.00 | 0.08 | 0.13 | 0.00 | 0.07 |
| NiO | 0.03 | 0.04 | 0.00 | 0.81 | 0.01 | 0.00 | 0.95 | 0.00 |
| MgO | 25.54 | 37.67 | 36.66 | 22.59 | 40.83 | 21.87 | 24.53 | 23.97 |
| ZnO | | | | | 0.00 | 0.00 | 0.00 | 0.00 |
| CaO | 2.55 | 0.27 | 0.15 | 0.35 | 0.10 | 0.00 | 0.47 | 1.16 |
| Na ₂ O | 0.12 | 0.02 | 0.01 | 0.07 | 0.06 | 0.00 | 0.03 | 0.08 |
| K ₂ O | 0.07 | 0.00 | 0.00 | 0.09 | 0.00 | 0.00 | 0.06 | 0.06 |
| Total | 93.92 | 85.71 | 85.95 | 73.85 | 86.03 | 88.21 | 88.37 | 88.08 |
| <i>Atomic ratios</i> | | | | | | | | |
| No. oxygen | 11 | 14 | 14 | 16 | 7 | 16 | 11 | 16 |
| Si | 3.805 | 3.412 | 3.344 | 5.863 | 2.063 | 6.100 | 3.673 | 5.879 |
| Al(iv) | 0.045 | 0.588 | 0.656 | 0.000 | 0.000 | 0.000 | 0.162 | 0.087 |
| <i>Total T</i> | 3.850 | 4.000 | 4.000 | 5.863 | 2.063 | 6.100 | 3.836 | 5.966 |
| Al(vi) | 0.000 | 0.556 | 0.643 | 0.000 | 0.013 | 0.120 | 0.000 | 0.000 |
| Cr | 0.001 | 0.000 | 0.000 | 0.000 | 0.000 | 0.000 | 0.001 | 0.000 |
| V | 0.000 | 0.000 | 0.000 | 0.000 | 0.000 | 0.000 | 0.004 | 0.000 |
| Fe | 0.489 | 0.119 | 0.172 | 0.096 | 0.015 | 0.310 | 0.581 | 0.316 |
| Mn | 0.002 | 0.004 | 0.013 | 0.000 | 0.003 | 0.010 | 0.000 | 0.006 |
| Ni | 0.001 | 0.003 | 0.000 | 0.077 | 0.001 | 0.000 | 0.051 | 0.000 |
| Mg | 2.401 | 5.246 | 5.077 | 3.992 | 2.820 | 3.144 | 2.442 | 3.497 |
| Zn | 0.000 | 0.000 | 0.000 | 0.000 | 0.000 | 0.000 | 0.000 | 0.000 |
| <i>Total B</i> | 2.895 | 5.927 | 5.905 | 4.166 | 2.852 | 3.585 | 3.079 | 3.819 |
| Ca | 0.172 | 0.027 | 0.014 | 0.045 | 0.005 | 0.000 | 0.033 | 0.122 |
| Na | 0.015 | 0.004 | 0.002 | 0.017 | 0.005 | 0.000 | 0.004 | 0.016 |
| K | 0.006 | 0.000 | 0.000 | 0.014 | 0.000 | 0.000 | 0.005 | 0.007 |
| <i>Total A</i> | 0.192 | 0.031 | 0.016 | 0.075 | 0.010 | 0.000 | 0.043 | 0.145 |
| Total cations | 6.937 | 9.959 | 9.921 | 10.104 | 4.925 | 9.685 | 6.957 | 9.931 |

| <i>Sample No.</i> | <i>402169</i> | <i>402169</i> | <i>402169</i> | <i>402169</i> | <i>402169</i> |
|--------------------------------|-----------------|-----------------|-----------------|-----------------|-----------------|
| <i>Description</i> | <i>Prehnite</i> | <i>Prehnite</i> | <i>Prehnite</i> | <i>Prehnite</i> | <i>Prehnite</i> |
| SiO ₂ | 42.38 | 42.93 | 42.49 | 42.35 | 42.06 |
| TiO ₂ | 0.01 | 0.00 | 0.00 | 0.00 | 0.00 |
| Al ₂ O ₃ | 19.05 | 20.85 | 19.51 | 20.78 | 20.38 |
| Cr ₂ O ₃ | 0.03 | 0.06 | 0.00 | 0.00 | 0.00 |
| V ₂ O ₃ | | | | 0.00 | 0.00 |
| Fe ₂ O ₃ | 6.68 | 3.66 | 5.85 | 4.74 | 5.34 |
| MnO | 0.00 | 0.03 | 0.00 | 0.00 | 0.00 |
| NiO | 0.00 | 0.00 | 0.00 | 0.00 | 0.00 |
| MgO | 0.00 | 0.00 | 0.07 | 0.03 | 0.00 |
| ZnO | | | | 0.00 | 0.00 |
| CaO | 26.61 | 27.01 | 26.54 | 26.38 | 26.89 |
| Na ₂ O | 0.04 | 0.05 | 0.04 | 0.05 | 0.05 |
| K ₂ O | 0.00 | 0.00 | 0.00 | 0.01 | 0.01 |
| Total | 94.80 | 94.59 | 94.49 | 94.35 | 94.73 |
| <i>Atomic ratios</i> | | | | | |
| No. oxygen | 11 | 11 | 11 | 11 | 11 |
| Si | 3.016 | 3.029 | 3.022 | 3.003 | 2.984 |
| Ti | 0.000 | 0.000 | 0.000 | 0.000 | 0.000 |
| Al | 1.597 | 1.733 | 1.635 | 1.736 | 1.704 |
| Cr | 0.002 | 0.003 | 0.000 | 0.000 | 0.000 |
| V | 0.000 | 0.000 | 0.000 | 0.000 | 0.000 |
| Fe | 0.358 | 0.194 | 0.313 | 0.253 | 0.285 |
| Sum B | 1.957 | 1.930 | 1.948 | 1.989 | 1.989 |
| Mn | 0.000 | 0.002 | 0.000 | 0.000 | 0.000 |
| Ni | 0.000 | 0.000 | 0.000 | 0.000 | 0.000 |
| Mg | 0.000 | 0.000 | 0.007 | 0.003 | 0.000 |
| Zn | 0.000 | 0.000 | 0.000 | 0.000 | 0.000 |
| Ca | 2.029 | 2.041 | 2.023 | 2.004 | 2.045 |
| Na | 0.006 | 0.007 | 0.006 | 0.007 | 0.006 |
| K | 0.000 | 0.000 | 0.000 | 0.001 | 0.001 |
| Sum A | 2.035 | 2.051 | 2.036 | 2.015 | 2.053 |
| Total | 7.008 | 7.010 | 7.006 | 7.007 | 7.025 |

| <i>Anal. No.</i> | 107640 | 107640 | 402141 | 402161 | 402161 | 402163 | 402163 | 402163 | 402163 | 402163 | 402163 | 402163 | 402163 | 402163 | 402164 | 402165 | 402173 | 402178 | 402178 | 402180 | 402180 | 402180 |
|--------------------------------|-----------|-----------|-----------|-----------|-----------|-----------|-----------|-----------|-----------|-----------|-----------|------------|------------|-----------|-----------|-----------|-----------|-----------|-----------|-------------|-------------|-------------|
| <i>Description</i> | <i>di</i> | <i>di</i> | <i>di</i> | <i>di</i> | <i>di</i> | <i>di</i> | <i>di</i> | <i>di</i> | <i>di</i> | <i>di</i> | <i>di</i> | <i>hed</i> | <i>hed</i> | <i>di</i> | <i>di</i> | <i>di</i> | <i>di</i> | <i>di</i> | <i>di</i> | <i>aug?</i> | <i>aug?</i> | <i>aug?</i> |
| SiO ₂ | 51.80 | 49.96 | 55.42 | 52.44 | 54.49 | 52.00 | 50.75 | 51.95 | 51.61 | 54.80 | 53.76 | 49.62 | 49.15 | 54.51 | 54.57 | 55.22 | 54.19 | 55.04 | 49.29 | 53.52 | 49.25 | |
| TiO ₂ | 0.35 | 0.90 | 0.00 | 0.14 | 0.03 | 0.00 | 0.01 | 0.03 | 0.00 | 0.01 | 0.00 | 0.05 | 0.00 | 0.00 | 0.00 | 0.00 | 0.00 | 0.04 | 0.40 | 0.20 | 0.38 | |
| Al ₂ O ₃ | 2.95 | 4.72 | 0.26 | 1.12 | 0.09 | 0.19 | 0.46 | 0.28 | 0.36 | 0.05 | 0.04 | 0.96 | 1.27 | 0.12 | 0.00 | 0.04 | 0.01 | 0.03 | 4.51 | 1.45 | 3.87 | |
| Cr ₂ O ₃ | 0.61 | 0.55 | 0.02 | 0.00 | 0.00 | 0.00 | 0.00 | 0.02 | 0.04 | 0.01 | 0.00 | 0.00 | 0.00 | 0.02 | 0.01 | 0.00 | 0.00 | 0.03 | 0.17 | 0.25 | 0.13 | |
| FeO | 16.83 | 14.93 | 17.80 | 17.10 | 17.41 | 11.03 | 9.48 | 12.49 | 10.40 | 18.01 | 17.97 | 5.06 | 2.92 | 17.08 | 17.66 | 18.26 | 17.58 | 18.11 | 19.50 | 19.36 | 17.98 | |
| MnO | 22.31 | 22.82 | 26.21 | 23.07 | 26.17 | 23.68 | 23.57 | 24.39 | 24.18 | 25.62 | 27.52 | 23.27 | 22.88 | 26.26 | 26.49 | 26.42 | 26.20 | 26.50 | 11.37 | 17.91 | 16.63 | |
| NiO | 0.12 | 0.11 | 0.00 | 0.22 | 0.17 | 0.01 | 0.03 | 0.09 | 0.04 | 0.01 | 0.01 | 0.04 | 0.01 | 0.03 | 0.00 | 0.00 | 0.01 | 0.00 | 0.40 | 0.32 | 0.23 | |
| MgO | 4.06 | 5.66 | 0.75 | 5.11 | 2.07 | 12.37 | 15.06 | 10.02 | 13.02 | 1.68 | 0.69 | 19.42 | 20.71 | 1.79 | 0.15 | 0.41 | 0.79 | 0.93 | 11.52 | 6.84 | 8.85 | |
| CaO | 0.02 | 0.09 | 0.00 | 0.00 | 0.01 | 0.38 | 0.08 | 0.07 | 0.09 | 0.00 | | | | 0.38 | 0.00 | | 0.00 | | 0.02 | 0.00 | 0.03 | |
| Na ₂ O | 0.27 | 0.30 | 0.04 | 0.10 | 0.03 | 0.12 | 0.09 | 0.08 | 0.06 | 0.00 | 0.02 | 0.24 | 0.26 | 0.03 | 0.00 | 0.01 | 0.00 | 0.04 | 0.09 | 0.10 | 0.09 | |
| K ₂ O | 0.01 | 0.03 | 0.01 | 0.00 | 0.01 | 0.00 | 0.00 | 0.00 | 0.01 | 0.00 | 0.00 | 0.01 | 0.02 | 0.00 | 0.02 | 0.00 | 0.00 | 0.00 | 0.02 | 0.00 | 0.02 | |
| Total | 99.33 | 100.07 | 100.50 | 99.30 | 100.47 | 99.77 | 99.55 | 99.44 | 99.84 | 100.20 | 100.01 | 98.67 | 97.22 | 100.23 | 98.89 | 100.36 | 98.79 | 100.72 | 97.31 | 99.96 | 97.49 | |
| <i>Atomic ratios</i> | | | | | | | | | | | | | | | | | | | | | | |
| No. oxygen | 6 | 6 | 6 | 6 | 6 | 6 | 6 | 6 | 6 | 6 | 6 | 6 | 6 | 6 | 6 | 6 | 6 | 6 | 6 | 6 | 6 | |
| Si | 1.909 | 1.848 | 1.944 | 1.980 | 1.986 | 1.988 | 1.971 | 1.975 | 1.980 | 1.987 | 1.990 | 1.996 | 1.996 | 1.984 | 1.961 | 1.985 | 2.006 | 1.991 | 1.864 | 1.954 | 1.865 | |
| Al(iv) | 0.091 | 0.152 | 0.049 | 0.004 | 0.005 | 0.008 | 0.021 | 0.013 | 0.016 | 0.002 | 0.000 | 0.000 | 0.004 | 0.001 | 0.002 | 0.015 | 0.000 | 0.002 | 0.136 | 0.046 | 0.135 | |
| <i>Total T</i> | 2.000 | 2.000 | 1.993 | 1.984 | 1.991 | 1.997 | 1.992 | 1.988 | 1.997 | 1.989 | 1.991 | 1.997 | 2.000 | 1.986 | 1.963 | 2.000 | 2.006 | 1.993 | 2.000 | 2.000 | 2.000 | |
| Al(vi) | 0.037 | 0.054 | 0.000 | 0.000 | 0.000 | 0.000 | 0.000 | 0.000 | 0.000 | 0.000 | 0.000 | 0.000 | 0.007 | 0.000 | 0.000 | 0.030 | 0.061 | 0.000 | 0.065 | 0.017 | 0.038 | |
| Ti | 0.010 | 0.025 | 0.004 | 0.001 | 0.000 | 0.000 | 0.000 | 0.001 | 0.000 | 0.000 | 0.000 | 0.000 | 0.000 | 0.001 | 0.000 | 0.002 | 0.000 | 0.000 | 0.011 | 0.005 | 0.011 | |
| Cr | 0.018 | 0.016 | 0.001 | 0.000 | 0.000 | 0.000 | 0.000 | 0.001 | 0.001 | 0.000 | 0.000 | 0.000 | 0.000 | 0.000 | 0.000 | 0.000 | 0.000 | 0.001 | 0.005 | 0.007 | 0.004 | |
| Fe | 0.125 | 0.175 | 0.023 | 0.159 | 0.063 | 0.396 | 0.489 | 0.319 | 0.418 | 0.051 | 0.021 | 0.650 | 0.707 | 0.055 | 0.004 | 0.012 | 0.024 | 0.028 | 0.364 | 0.209 | 0.280 | |
| Mn | 0.004 | 0.004 | 0.000 | 0.007 | 0.005 | 0.000 | 0.001 | 0.003 | 0.001 | 0.000 | 0.000 | 0.001 | 0.000 | 0.001 | 0.000 | 0.000 | 0.000 | 0.000 | 0.013 | 0.010 | 0.008 | |
| Ni | 0.001 | 0.003 | 0.000 | 0.000 | 0.000 | 0.012 | 0.003 | 0.002 | 0.003 | 0.000 | 0.000 | 0.000 | 0.000 | 0.011 | 0.000 | 0.000 | 0.000 | 0.000 | 0.001 | 0.000 | 0.001 | |
| Mg | 0.924 | 0.823 | 0.955 | 0.945 | 0.943 | 0.629 | 0.549 | 0.708 | 0.595 | 0.974 | 0.977 | 0.302 | 0.178 | 0.927 | 0.963 | 0.981 | 0.962 | 0.973 | 1.099 | 1.054 | 1.015 | |
| <i>Total B</i> | 1.118 | 1.100 | 0.985 | 1.110 | 1.012 | 1.036 | 1.042 | 1.032 | 1.018 | 1.025 | 0.998 | 0.984 | 0.946 | 0.995 | 0.968 | 0.994 | 0.987 | 1.002 | 1.558 | 1.302 | 1.357 | |
| Mn | 0.004 | 0.004 | 0.000 | 0.007 | 0.005 | 0.000 | 0.001 | 0.003 | 0.001 | 0.000 | 0.000 | 0.001 | 0.000 | 0.001 | 0.000 | 0.000 | 0.000 | 0.000 | 0.013 | 0.010 | 0.008 | |
| Ca | 0.881 | 0.904 | 1.011 | 0.916 | 1.019 | 0.970 | 0.981 | 0.994 | 0.994 | 0.996 | 1.076 | 0.997 | 1.001 | 1.025 | 1.039 | 1.021 | 1.031 | 1.024 | 0.461 | 0.700 | 0.675 | |
| Na | 0.019 | 0.022 | 0.003 | 0.007 | 0.002 | 0.009 | 0.007 | 0.006 | 0.005 | 0.000 | 0.001 | 0.019 | 0.021 | 0.002 | 0.000 | 0.001 | 0.000 | 0.003 | 0.007 | 0.007 | 0.007 | |
| K | 0.001 | 0.001 | 0.000 | 0.000 | 0.000 | 0.000 | 0.000 | 0.000 | 0.001 | 0.000 | 0.000 | 0.001 | 0.001 | 0.000 | 0.001 | 0.000 | 0.000 | 0.000 | 0.001 | 0.000 | 0.001 | |
| <i>Total A</i> | 0.904 | 0.931 | 1.015 | 0.930 | 1.027 | 0.979 | 0.989 | 1.003 | 1.001 | 0.997 | 1.077 | 1.018 | 1.023 | 1.028 | 1.039 | 1.022 | 1.032 | 1.026 | 0.481 | 0.718 | 0.690 | |
| Total cations | 4.022 | 4.031 | 4.000 | 4.038 | 4.023 | 4.012 | 4.023 | 4.023 | 4.015 | 4.012 | 4.039 | 4.002 | 3.975 | 4.014 | 4.004 | 4.008 | 4.010 | 4.015 | 4.038 | 4.019 | 4.047 | |
| Mg/(Mg+Fe) | 0.88 | 0.82 | 0.98 | 0.86 | 0.94 | 0.61 | 0.53 | 0.69 | 0.59 | 0.95 | 0.98 | 0.32 | 0.20 | 0.94 | 1.00 | 0.99 | 0.98 | 0.97 | 0.75 | 0.83 | 0.78 | |
| Ca/(Ca+Fe+Mg) | 0.4563 | 0.4753 | 0.5083 | 0.4537 | 0.5032 | 0.4864 | 0.4859 | 0.4918 | 0.4954 | 0.4929 | 0.5187 | 0.5118 | 0.5307 | 0.5106 | 0.5177 | 0.5067 | 0.5110 | 0.5055 | 0.2394 | 0.3568 | 0.3425 | |

| <i>Anal. No.</i> | 402163 | 402163 | 402163 | 402163 | 402163 | 402169 | 402169 | 402169 | 402169 | 402169 | 402169 | 402169 | 402169 | 402169 | 402169 | 402169 | 402177 |
|--------------------------------|---------------|---------------|---------------|---------------|---------------|---------------|---------------|---------------|---------------|---------------|---------------|---------------|---------------|---------------|---------------|---------------|---------------|
| <i>Description</i> | <i>CaFeSi</i> | <i>CaFeSi</i> | <i>CaFeSi</i> | <i>CaFeSi</i> | <i>CaFeSi</i> | <i>CaFeSi</i> | <i>CaFeSi</i> | <i>CaFeSi</i> | <i>CaMgSi</i> | <i>CaMgSi</i> | <i>CaFeSi</i> | <i>CaFeSi</i> | <i>CaFeSi</i> | <i>CaFeSi</i> | <i>CaFeSi</i> | <i>CaFeSi</i> | <i>CaFeSi</i> |
| SiO ₂ | 48.51 | 47.16 | 42.95 | 49.39 | 48.90 | 51.30 | 48.78 | 48.94 | 53.53 | 54.13 | 49.02 | 50.30 | 48.63 | 47.84 | 29.59 | 46.94 | 24.43 |
| TiO ₂ | 0.00 | 0.00 | 0.00 | 0.00 | 0.04 | 0.02 | 0.02 | 0.00 | 0.00 | 0.01 | 0.00 | 0.00 | 0.00 | 0.00 | 0.00 | 0.00 | 0.00 |
| Al ₂ O ₃ | 1.03 | 1.60 | 2.02 | 0.25 | 0.85 | 2.13 | 2.07 | 2.01 | 1.27 | 1.37 | 1.90 | 2.52 | 2.14 | 1.99 | 2.16 | 2.00 | 11.16 |
| Cr ₂ O ₃ | 0.01 | 0.00 | 0.02 | 0.00 | 0.00 | 0.01 | 0.00 | 0.04 | 0.00 | | 0.00 | 0.00 | 0.00 | 0.00 | 0.00 | 0.00 | 0.00 |
| V ₂ O ₃ | | | | | | | | | | | | | 0.00 | 0.08 | 0.00 | 0.00 | 0.00 |
| FeO | 11.98 | 12.90 | 24.54 | 9.61 | 12.95 | 14.01 | 15.86 | 15.47 | 10.37 | 11.45 | 15.73 | 15.38 | 15.22 | 14.68 | 17.05 | 15.36 | 10.61 |
| MnO | 0.05 | 0.02 | 0.00 | 0.04 | 0.00 | 0.13 | 0.02 | 0.00 | 0.07 | 0.06 | 0.12 | 0.17 | 0.06 | 0.04 | 0.01 | 0.07 | 0.07 |
| NiO | 0.00 | 0.09 | 0.07 | | | 0.01 | 0.02 | 0.00 | 0.00 | | 0.00 | 0.00 | 0.00 | 0.02 | 0.00 | 0.00 | 0.00 |
| MgO | 0.21 | 0.36 | 0.61 | 10.48 | 1.31 | 8.35 | 4.89 | 4.28 | 14.46 | 13.97 | 5.55 | 4.68 | 5.80 | 5.30 | 2.50 | 4.46 | 23.22 |
| CaO | 28.73 | 30.77 | 19.98 | 24.96 | 32.54 | 14.42 | 18.03 | 18.90 | 10.45 | 12.00 | 17.06 | 15.89 | 16.91 | 17.80 | 20.50 | 17.65 | 17.33 |
| Na ₂ O | 0.40 | 0.21 | 0.40 | 0.08 | 0.18 | 0.36 | 0.41 | 0.35 | 0.28 | 0.32 | 0.43 | 0.34 | 0.36 | 0.42 | 0.49 | 0.45 | 0.02 |
| K ₂ O | 0.01 | 0.01 | 0.01 | 0.02 | 0.00 | 0.02 | 0.00 | 0.00 | 0.05 | 0.04 | 0.02 | 0.01 | 0.01 | 0.00 | 0.00 | 0.06 | 0.00 |
| Total | 90.94 | 93.12 | 90.60 | 94.83 | 96.77 | 90.75 | 90.10 | 90.00 | 90.46 | 93.35 | 89.83 | 89.29 | 89.10 | 88.17 | 72.31 | 86.99 | 86.84 |
| <i>Atomic ratios</i> | | | | | | | | | | | | | | | | | |
| No. oxygen | 12 | 12 | 12 | 12 | 12 | 12 | 12 | 12 | 12 | 12 | 12 | 12 | 12 | 12 | 12 | 12 | 12 |
| Si | 4.146 | 3.993 | 3.882 | 3.958 | 3.987 | 4.202 | 4.136 | 4.154 | 4.252 | 4.209 | 4.153 | 4.239 | 4.137 | 4.128 | 3.432 | 4.131 | 2.243 |
| Ti | 0.000 | 0.000 | 0.000 | 0.000 | 0.002 | 0.001 | 0.001 | 0.000 | 0.000 | 0.001 | 0.000 | 0.000 | 0.000 | 0.000 | 0.000 | 0.000 | 0.000 |
| Al | 0.103 | 0.160 | 0.215 | 0.024 | 0.082 | 0.206 | 0.207 | 0.201 | 0.119 | 0.125 | 0.190 | 0.250 | 0.214 | 0.202 | 0.296 | 0.207 | 1.207 |
| Cr | 0.001 | 0.000 | 0.002 | 0.000 | 0.000 | 0.000 | 0.000 | 0.003 | 0.000 | 0.000 | 0.000 | 0.000 | 0.000 | 0.000 | 0.000 | 0.000 | 0.000 |
| V | | | | | | | | | | | | | 0.000 | 0.005 | 0.000 | 0.000 | |
| Fe | 0.856 | 0.914 | 1.854 | 0.644 | 0.883 | 0.960 | 1.125 | 1.098 | 0.689 | 0.744 | 1.114 | 1.084 | 1.083 | 1.060 | 1.654 | 1.131 | 0.815 |
| Mn | 0.003 | 0.002 | 0.000 | 0.003 | 0.000 | 0.009 | 0.001 | 0.000 | 0.005 | 0.004 | 0.009 | 0.012 | 0.004 | 0.003 | 0.001 | 0.005 | 0.006 |
| Ni | 0.000 | 0.006 | 0.005 | 0.000 | 0.000 | 0.001 | 0.001 | 0.000 | 0.000 | 0.000 | 0.000 | 0.000 | 0.000 | 0.001 | 0.000 | 0.000 | 0.000 |
| Mg | 0.027 | 0.045 | 0.082 | 1.252 | 0.159 | 1.019 | 0.617 | 0.542 | 1.711 | 1.619 | 0.701 | 0.588 | 0.736 | 0.682 | 0.432 | 0.585 | 3.177 |
| Ca | 2.631 | 2.791 | 1.934 | 2.143 | 2.843 | 1.266 | 1.638 | 1.719 | 0.889 | 0.999 | 1.549 | 1.434 | 1.541 | 1.646 | 2.549 | 1.665 | 1.704 |
| Na | 0.066 | 0.034 | 0.070 | 0.012 | 0.028 | 0.057 | 0.068 | 0.057 | 0.043 | 0.049 | 0.071 | 0.056 | 0.060 | 0.071 | 0.109 | 0.076 | 0.003 |
| K | 0.001 | 0.001 | 0.001 | 0.002 | 0.000 | 0.002 | 0.000 | 0.000 | 0.005 | 0.004 | 0.002 | 0.001 | 0.001 | 0.000 | 0.000 | 0.007 | 0.000 |
| Cl | 0.005 | 0.000 | 0.006 | 0.000 | 0.000 | 0.000 | 0.000 | 0.000 | 0.000 | 0.000 | 0.000 | 0.000 | 0.000 | 0.006 | 0.000 | 0.000 | 0.000 |
| F | 0.000 | 0.000 | 0.000 | 0.000 | 0.000 | 0.000 | 0.000 | 0.000 | 0.000 | 0.000 | 0.000 | 0.000 | 0.020 | 0.006 | 0.002 | 0.001 | 0.000 |
| Total cat. | 7.840 | 7.945 | 8.050 | 8.037 | 7.984 | 7.723 | 7.794 | 7.773 | 7.712 | 7.754 | 7.788 | 7.664 | 7.796 | 7.810 | 8.476 | 7.808 | 9.155 |
| (Ca+Na)/ (Mg+Fe+Al) | 2.7355 | 2.5259 | 0.9317 | 1.1233 | 2.5547 | 0.6055 | 0.8750 | 0.9647 | 0.3701 | 0.4212 | 0.8075 | 0.7750 | 0.7876 | 0.8832 | 1.1158 | 0.9056 | 0.3283 |

| Mineral Sample No. Wt. % | Nickeline 108889 | Nickeline 108889 | Cobaltite 108889 | Gersdorffite 108889 | Co-Gersdorffite 108889 | Gersdorffite 108889 | Gersdorffite 108889 | Ni-marcasite 108889 | Tetrahedrite 108884 | Tetrahedrite 108884 | Cubanite 108884 | Cubanite 108884 | Chalcopyrite 108884 |
|--------------------------------|---------------------|---------------------|---------------------|------------------------|---------------------------|------------------------|------------------------|------------------------|------------------------|------------------------|--------------------|--------------------|------------------------|
| S | 0.39 | 0.34 | 19.53 | 17.17 | 16.02 | 18.02 | 18.84 | 45.65 | 24.18 | 24.21 | 34.28 | 33.90 | 32.74 |
| As | 50.39 | 51.09 | 41.66 | 37.88 | 41.04 | 38.08 | 39.37 | 3.28 | 1.20 | 1.04 | 0.04 | 0.01 | 0.14 |
| Sb | 4.31 | 4.40 | 0.27 | 2.55 | 1.04 | 8.44 | 5.33 | 0.09 | 27.68 | 27.93 | 0.00 | 0.03 | 1.00 |
| Se | 0.23 | 0.22 | 0.20 | 0.16 | 0.27 | 0.22 | 0.20 | 0.01 | 0.08 | 0.02 | 0.04 | 0.00 | 0.07 |
| Bi | 0.00 | 0.00 | 0.00 | 0.00 | 0.00 | 0.00 | 0.00 | 0.00 | 0.32 | 0.00 | 0.48 | 0.00 | 0.00 |
| Mn | 0.00 | 0.03 | 0.01 | 0.00 | 0.00 | 0.06 | 0.03 | 0.02 | 0.00 | 0.00 | 0.03 | 0.01 | 0.04 |
| Fe | 0.15 | 0.11 | 0.91 | 1.18 | 1.63 | 0.16 | 0.31 | 31.34 | 1.84 | 1.92 | 40.05 | 39.37 | 30.14 |
| Co | 1.84 | 1.50 | 31.66 | 4.59 | 13.41 | 0.26 | 3.22 | 0.86 | 0.00 | 0.03 | 0.00 | 0.00 | 0.00 |
| Ni | 42.11 | 43.04 | 3.09 | 28.22 | 19.80 | 34.02 | 31.79 | 10.58 | 0.00 | 0.00 | 0.03 | 0.00 | 0.01 |
| Cu | 0.00 | 0.00 | 0.01 | 0.00 | 0.02 | 0.04 | 0.00 | 0.04 | 37.64 | 37.96 | 22.83 | 22.84 | 32.00 |
| Zn | 0.00 | 0.02 | 0.00 | 0.00 | 0.02 | 0.05 | 0.00 | 0.00 | 6.21 | 6.23 | 0.06 | 0.02 | 0.53 |
| Ag | 0.00 | 0.00 | 0.02 | 0.02 | 0.00 | 0.06 | 0.00 | 0.08 | 1.28 | 1.07 | 0.15 | 0.02 | 0.18 |
| Cd | 0.07 | 0.03 | 0.03 | 0.00 | 0.00 | 0.00 | 0.01 | 0.00 | 0.27 | 0.30 | 0.00 | 0.00 | 0.25 |
| Hg | 0.02 | 0.04 | 0.20 | 0.00 | 0.08 | 0.01 | 0.00 | 0.04 | 0.00 | 0.00 | 0.05 | 0.08 | 0.00 |
| Pb | 0.17 | 0.06 | 0.00 | 0.00 | 0.00 | 0.00 | 0.00 | 0.00 | 0.00 | 0.00 | 0.00 | 0.27 | 0.93 |
| Au | 0.00 | 0.07 | 0.11 | 0.00 | 0.00 | 0.00 | 0.00 | 0.05 | 0.00 | 0.00 | 0.15 | 0.21 | 0.10 |
| Si | 0.02 | 0.02 | 0.07 | 0.16 | 0.55 | 0.05 | 0.03 | 0.65 | 0.00 | 0.01 | 0.25 | 0.15 | 0.01 |
| Total | 99.69 | 100.87 | 97.60 | 91.78 | 93.34 | 99.41 | 99.09 | 91.99 | 100.69 | 100.71 | 98.04 | 96.57 | 98.02 |
| <i>Atomic ratios</i> | | | | | | | | | | | | | |
| No. atoms | 2 | 2 | 3 | 3 | 3 | 3 | 3 | 3 | 29 | 29 | 6 | 6 | 4 |
| S | 0.016 | 0.014 | 1.026 | 0.974 | 0.895 | 0.972 | 1.000 | 1.899 | 12.608 | 12.592 | 2.967 | 2.977 | 1.951 |
| As | 0.911 | 0.912 | 0.937 | 0.920 | 0.982 | 0.879 | 0.894 | 0.058 | 0.267 | 0.231 | 0.001 | 0.000 | 0.004 |
| Sb | 0.048 | 0.048 | 0.004 | 0.038 | 0.015 | 0.120 | 0.075 | 0.001 | 3.801 | 3.825 | 0.000 | 0.001 | 0.016 |
| Se | 0.004 | 0.004 | 0.004 | 0.004 | 0.006 | 0.005 | 0.004 | 0.000 | 0.016 | 0.003 | 0.002 | 0.000 | 0.002 |
| Bi | 0.000 | 0.000 | 0.000 | 0.000 | 0.000 | 0.000 | 0.000 | 0.000 | 0.026 | 0.000 | 0.006 | 0.000 | 0.000 |
| Mn | 0.000 | 0.001 | 0.000 | 0.000 | 0.000 | 0.002 | 0.001 | 0.000 | 0.000 | 0.000 | 0.001 | 0.000 | 0.001 |
| Fe | 0.004 | 0.003 | 0.027 | 0.038 | 0.052 | 0.005 | 0.009 | 0.748 | 0.550 | 0.574 | 1.990 | 1.985 | 1.031 |
| Co | 0.042 | 0.034 | 0.905 | 0.142 | 0.408 | 0.008 | 0.093 | 0.019 | 0.000 | 0.008 | 0.000 | 0.000 | 0.000 |
| Ni | 0.972 | 0.981 | 0.089 | 0.874 | 0.604 | 1.003 | 0.921 | 0.240 | 0.000 | 0.000 | 0.001 | 0.000 | 0.000 |
| Cu | 0.000 | 0.000 | 0.000 | 0.000 | 0.001 | 0.001 | 0.000 | 0.001 | 9.902 | 9.962 | 0.997 | 1.012 | 0.962 |
| Zn | 0.000 | 0.000 | 0.000 | 0.000 | 0.001 | 0.001 | 0.000 | 0.000 | 1.589 | 1.590 | 0.003 | 0.001 | 0.015 |
| Pb | 0.001 | 0.000 | 0.000 | 0.000 | 0.000 | 0.000 | 0.000 | 0.000 | 0.000 | 0.000 | 0.000 | 0.004 | 0.009 |
| Hg | 0.000 | 0.000 | 0.002 | 0.000 | 0.001 | 0.000 | 0.000 | 0.000 | 0.000 | 0.000 | 0.001 | 0.001 | 0.000 |
| Cd | 0.001 | 0.000 | 0.000 | 0.000 | 0.000 | 0.000 | 0.000 | 0.000 | 0.040 | 0.044 | 0.000 | 0.000 | 0.004 |
| Ag | 0.000 | 0.000 | 0.000 | 0.000 | 0.000 | 0.001 | 0.000 | 0.001 | 0.198 | 0.166 | 0.004 | 0.001 | 0.003 |
| Au | 0.000 | 0.000 | 0.001 | 0.000 | 0.000 | 0.000 | 0.000 | 0.000 | 0.000 | 0.000 | 0.002 | 0.003 | 0.001 |
| Si | 0.001 | 0.001 | 0.004 | 0.010 | 0.035 | 0.003 | 0.002 | 0.031 | 0.002 | 0.003 | 0.025 | 0.015 | 0.001 |
| Total cations | 2 | 2 | 3 | 3 | 3 | 3 | 3 | 3 | 29 | 29 | 6 | 6 | 4 |

| Mineral Sample No. Wt. % | Galena 108884 | Galena 108884 | Sphalerite 108884 | Loellingite 402173 1.00 | Galena 402173 4.00 | Sphalerite 402173 5.00 | Loellingite 402174 6.00 | Sphalerite 402166 7.00 | Millerite 402166 8.00 | Sphalerite 107884 11.00 | Millerite 402166 | Millerite 402166 | Fe-rammelsbergite 402164 |
|--------------------------------|------------------|------------------|----------------------|-------------------------------|--------------------------|------------------------------|-------------------------------|------------------------------|-----------------------------|-------------------------------|---------------------|---------------------|-----------------------------|
| S | 12.20 | 11.89 | 31.55 | 0.69 | 12.43 | 31.59 | 0.90 | 32.58 | 35.25 | 31.64 | 35.25 | 35.35 | 2.13 |
| As | 0.03 | 0.00 | 0.00 | 69.60 | 0.04 | 0.00 | 69.46 | 0.03 | 0.01 | 0.01 | 0.01 | | 68.55 |
| Sb | 0.00 | 0.00 | 0.00 | 0.16 | 0.00 | 0.00 | 0.30 | 0.00 | 0.00 | 0.02 | 0.00 | | |
| Se | 0.12 | 0.12 | 0.00 | | | | | | | | | | |
| Bi | 0.00 | 0.00 | 0.07 | | | | | | | | | | |
| Mn | 0.01 | 0.00 | 0.00 | 0.02 | 0.02 | 0.00 | 0.01 | 0.00 | 0.00 | 0.00 | 0.00 | | |
| Fe | 0.00 | 0.03 | 0.42 | 26.87 | 0.66 | 0.07 | 28.09 | 0.71 | 0.17 | 0.27 | 0.17 | 0.16 | 12.39 |
| Co | 0.01 | 0.00 | 0.00 | | | | | | | | 3.54 | 3.54 | 0.05 |
| Ni | 0.04 | 0.00 | 0.00 | | | | | | | | 61.78 | 61.78 | 13.06 |
| Cu | 0.15 | 0.16 | 0.21 | 0.17 | 0.03 | 0.04 | 0.08 | 0.02 | 0.00 | 0.10 | 0.00 | | 0.10 |
| Zn | 0.03 | 0.15 | 65.90 | 0.22 | 1.00 | 62.89 | 0.00 | 64.81 | 1.12 | 65.25 | 1.12 | 1.40 | |
| Ag | 0.11 | 0.23 | 0.10 | 0.00 | 0.00 | 0.00 | 0.00 | 0.00 | 0.02 | 0.06 | 0.02 | | |
| Cd | 0.02 | 0.09 | 0.84 | 0.04 | 0.00 | 2.89 | 0.00 | 0.11 | 0.04 | 0.79 | 0.04 | | |
| Hg | 0.00 | 0.07 | 0.00 | 0.00 | 0.00 | 0.03 | 0.05 | 0.13 | 0.02 | 0.00 | 0.02 | | |
| Pb | 84.48 | 84.39 | 0.00 | 0.03 | 85.65 | 0.00 | 0.06 | 0.00 | 0.00 | 0.06 | 0.00 | | |
| Au | 0.00 | 0.10 | 0.00 | 0.00 | 0.23 | 0.00 | 0.32 | 0.00 | 0.00 | 0.00 | 0.00 | | |
| Si | 0.00 | 0.00 | 0.01 | | | | | | | | | | |
| Total | 97.20 | 97.13 | 99.09 | 97.80 | 100.07 | 97.51 | 99.27 | 98.38 | 36.62 | 98.19 | 101.94 | 102.23 | 96.28 |
| <i>Atomic ratios</i> | | | | | | | | | | | | | |
| No. atoms | 2 | 2 | 2 | 3 | 2 | 2 | 3 | 2 | 1 | 2 | 2 | 2 | 3 |
| S | 0.957 | 0.940 | 0.978 | 0.045 | 0.933 | 0.998 | 0.057 | 1.005 | 0.981 | 0.987 | 0.985 | 0.985 | 0.140 |
| As | 0.001 | 0.000 | 0.000 | 1.935 | 0.001 | 0.000 | 1.900 | 0.000 | 0.000 | 0.000 | 0.000 | 0.000 | 1.922 |
| Sb | 0.000 | 0.000 | 0.000 | 0.003 | 0.000 | 0.000 | 0.005 | 0.000 | 0.000 | 0.000 | 0.000 | 0.000 | 0.000 |
| Se | 0.004 | 0.004 | 0.000 | | | | | | | | | | |
| Bi | 0.000 | 0.000 | 0.000 | | | | | | | | | | |
| Mn | 0.001 | 0.000 | 0.000 | 0.001 | 0.001 | 0.000 | 0.000 | 0.000 | 0.000 | 0.000 | 0.000 | 0.000 | 0.000 |
| Fe | 0.000 | 0.001 | 0.008 | 1.002 | 0.029 | 0.001 | 1.031 | 0.013 | 0.003 | 0.005 | 0.003 | 0.003 | 0.466 |
| Co | 0.001 | 0.000 | 0.000 | | | | | | | | 0.054 | 0.054 | 0.002 |
| Ni | 0.002 | 0.000 | 0.000 | | | | | | | | 0.943 | 0.940 | 0.467 |
| Cu | 0.006 | 0.006 | 0.003 | 0.006 | 0.001 | 0.001 | 0.003 | 0.000 | 0.000 | 0.002 | 0.000 | 0.000 | 0.003 |
| Zn | 0.001 | 0.006 | 1.002 | 0.007 | 0.037 | 0.974 | 0.000 | 0.980 | 0.015 | 0.999 | 0.015 | 0.019 | 0.000 |
| Pb | 1.026 | 1.032 | 0.000 | 0.000 | 0.995 | 0.000 | 0.001 | 0.000 | 0.000 | 0.000 | 0.000 | 0.000 | 0.000 |
| Hg | 0.000 | 0.001 | 0.000 | 0.000 | 0.000 | 0.000 | 0.001 | 0.001 | 0.000 | 0.000 | 0.000 | 0.000 | 0.000 |
| Cd | 0.000 | 0.002 | 0.007 | 0.001 | 0.000 | 0.026 | 0.000 | 0.001 | 0.000 | 0.007 | 0.000 | 0.000 | 0.000 |
| Ag | 0.003 | 0.005 | 0.001 | 0.000 | 0.000 | 0.000 | 0.000 | 0.000 | 0.000 | 0.001 | 0.000 | 0.000 | 0.000 |
| Au | 0.000 | 0.001 | 0.000 | 0.000 | 0.003 | 0.000 | 0.003 | 0.000 | 0.000 | 0.000 | 0.000 | 0.000 | 0.000 |
| Si | 0.000 | 0.000 | 0.000 | | | | | | | | | | |
| Total cations | 2 | 2 | 2 | 3 | 2 | 2 | 3 | 2 | 1 | 2 | 2 | 2 | 3 |

| <i>Mineral</i> | <i>Fe-rammelsbergite</i> | <i>Niccoliite</i> | <i>Ni-Loellingite</i> | <i>Niccoliite</i> | <i>Niccoliite</i> | <i>Niccoliite</i> | <i>Loellingite</i> | <i>Niccoliite</i> |
|----------------------|--------------------------|-------------------|-----------------------|-------------------|-------------------|-------------------|--------------------|-------------------|
| <i>Sample No.</i> | <i>402164</i> | <i>402164</i> | <i>402164</i> | <i>402164</i> | <i>402164</i> | <i>402164</i> | <i>402164</i> | <i>402164</i> |
| <i>Wt. %</i> | | | | | | | | |
| S | 3.50 | 1.67 | 0.46 | 0.75 | 1.39 | 1.79 | 0.50 | 1.09 |
| As | 62.09 | 52.15 | 72.01 | 54.78 | 53.56 | 54.73 | 79.29 | 56.90 |
| Sb | | | | | 1.24 | 4.84 | 0.40 | 4.00 |
| Se | | | | | | | | |
| Bi | | | | | | | | |
| Mn | | | | | | | | |
| Fe | 9.65 | 2.20 | 16.52 | 1.57 | 9.16 | 2.52 | 17.35 | 3.29 |
| Co | 0.07 | 0.11 | 0.00 | 0.06 | | | | |
| Ni | 16.76 | 34.60 | 9.73 | 37.29 | 35.00 | 35.00 | 10.00 | 35.00 |
| Cu | 0.59 | 0.63 | 0.11 | 0.36 | 0.23 | 0.59 | 0.08 | 0.27 |
| Zn | | | | | 0.01 | 0.00 | 0.03 | 0.00 |
| Ag | | | | | 0.00 | 0.07 | 0.02 | 0.06 |
| Cd | | | | | | | | |
| Hg | | | | | | | | |
| Pb | | | | | | | | |
| Au | | | | | | | | |
| Si | | | | | | | | |
| Total | 92.66 | 91.36 | 98.83 | 94.81 | 100.59 | 99.54 | 107.67 | 100.60 |
| <i>Atomic ratios</i> | | | | | | | | |
| No. atoms | 3 | 2 | 3 | 2 | 2 | 2 | 3 | 2 |
| S | 0.233 | 0.075 | 0.030 | 0.033 | 0.056 | 0.076 | 0.030 | 0.046 |
| As | 1.768 | 1.003 | 2.004 | 1.027 | 0.933 | 0.989 | 2.035 | 1.022 |
| Sb | 0.000 | 0.000 | 0.000 | 0.000 | 0.013 | 0.054 | 0.006 | 0.044 |
| Se | | | | | | | | |
| Bi | | | | | | | | |
| Mn | 0.000 | 0.000 | 0.000 | 0.000 | 0.000 | 0.000 | 0.000 | 0.000 |
| Fe | 0.369 | 0.057 | 0.617 | 0.039 | 0.214 | 0.061 | 0.597 | 0.079 |
| Co | 0.003 | 0.003 | 0.000 | 0.001 | 0.000 | 0.000 | 0.000 | 0.000 |
| Ni | 0.609 | 0.849 | 0.346 | 0.892 | 0.778 | 0.807 | 0.328 | 0.802 |
| Cu | 0.020 | 0.014 | 0.004 | 0.008 | 0.005 | 0.013 | 0.002 | 0.006 |
| Zn | 0.000 | 0.000 | 0.000 | 0.000 | 0.000 | 0.000 | 0.001 | 0.000 |
| Pb | 0.000 | 0.000 | 0.000 | 0.000 | 0.000 | 0.000 | 0.000 | 0.000 |
| Hg | 0.000 | 0.000 | 0.000 | 0.000 | 0.000 | 0.000 | 0.000 | 0.000 |
| Cd | 0.000 | 0.000 | 0.000 | 0.000 | 0.000 | 0.000 | 0.000 | 0.000 |
| Ag | 0.000 | 0.000 | 0.000 | 0.000 | 0.000 | 0.001 | 0.000 | 0.001 |
| Au | 0.000 | 0.000 | 0.000 | 0.000 | 0.000 | 0.000 | 0.000 | 0.000 |
| Si | | | | | | | | |
| Total cations | 3 | 2 | 3 | 2 | 2 | 2 | 3 | 2 |

APPENDIX 10

XRD analyses

Skarns

| Reg. No. | Rock type | di | cal | serp | brc | dol | qtz | xon | woll | opal | sid | clay | and | sme | tlc | Other (minor/trace) |
|----------|-------------|-----|-----|------|-----|-----|-----|-----|------|------|-----|------|-----|-----|-----|------------------------|
| G400238 | dolomite | | | | | *** | | | | | | | | | | |
| G400239 | ophicalcite | ** | *** | *** | ** | | | | | | | | | | ? | |
| G400240 | dolomite | | | * | | *** | | | | | | | | | | |
| G400241 | hornfels | *** | | | | | | | | | | | | | | |
| G400263 | hornfels | *** | | | | | *** | ** | | | | | | | | |
| G400299 | dolomite | | | | | *** | | | | | | | | | | |
| G400904 | ophicalcite | | *** | *** | | | | | | ** | | | | | | |
| G402037 | hornfels | *** | ** | *** | ** | | | | | | | | | | | |
| G402141 | skarn | ** | | | | | *** | *** | ** | | | | | | | scawtite, pectolite |
| G402142 | ophicalcite | | *** | ** | * | | | | | *** | | | | | | |
| G402149 | ophicalcite | | *** | *** | | | | | | | | | * | | | |
| G402150 | ophicalcite | | *** | ** | * | | | | | | | | * | | | |
| G402157 | ophicalcite | * | *** | ** | | | | | | | ** | ** | * | | | |
| G402158 | ophicalcite | * | *** | *** | * | | | | | | | | | | | arag |
| G402159 | ophicalcite | | *** | *** | * | | | | | | | | * | | | |
| G402160 | ophicalcite | | *** | ** | | | | | | | | | | | | |
| G402161 | ophicalcite | * | *** | *** | | | ? | | | | | | | | | |
| G402162 | ophicalcite | | *** | ** | ** | | | | | | | | | | | |
| G402163 | skarn | ** | * | | | | *** | *** | | | | | | | | ?, mt, sx |
| G402164 | hornfels | *** | ** | | | | | | | | | | | | | sx |
| G402165 | skarn | *** | *** | | | | * | | | | | | | | | apo, tob, arag |
| G402166 | skarn | ** | * | | | | *** | ** | | | | | | | | sx, tob |
| G402167 | hornfels | *** | | | | | | | | | | | | | | |
| G402169 | skarn | ** | ** | | | | *** | ** | | | | | | | * | ?, prn, sx, laum, arag |
| G402170 | ophicalcite | * | *** | *** | | | | | | | | | | | | |
| G402171 | ophicalcite | * | *** | * | * | | | * | | | | | | | | |
| G402172 | ophicalcite | | *** | *** | * | | | | | | | | | | | |
| G402173 | ophicalcite | *** | *** | *** | | | | | | | | | * | | | sx, arag |
| G402174 | ophicalcite | * | *** | ** | * | | | | | | | ** | | | | sx, mt |
| G402175 | ophicalcite | * | *** | *** | * | | | | | | | * | | | | mt |
| G402177 | ophicalcite | * | *** | ** | | | | | | | | * | | | | sx, mt |
| G402178 | ophicalcite | *** | ** | ** | | | | | | | | | ** | | * | sx, ves |
| G402179 | ophicalcite | * | *** | * | *** | | | | | | | | * | | | |
| G402180 | ophicalcite | ** | ** | *** | * | | | | | | | | | *** | | arag, mica |
| G402206 | ophicalcite | | *** | ** | | | | | | *** | ** | | | | | |
| G402206 | skarn | * | * | | | | *** | | | | | | | | | |

| <i>Reg. No.</i> | <i>Rock type</i> | <i>di</i> | <i>cal</i> | <i>serp</i> | <i>brc</i> | <i>dol</i> | <i>qtz</i> | <i>xon</i> | <i>woll</i> | <i>opal</i> | <i>sid</i> | <i>clay</i> | <i>and</i> | <i>sme</i> | <i>tlc</i> | <i>Other (minor/trace)</i> |
|-----------------|------------------|-----------|------------|-------------|------------|------------|------------|------------|-------------|-------------|------------|-------------|------------|------------|------------|----------------------------|
| G402335 | hornfels | *** | * | * | | | | | | | | | | | | |
| G402336 | ophicalcite | | *** | *** | | | | | | | | | | | | |
| G402440 | hornfels | *** | * | * | | | | | | | | | | | | |
| G402442 | hornfels | *** | *** | *** | | | | | | | | | | | | |
| G402443 | ophicalcite | | *** | *** | | | | | | | ** | | | | | |
| G402444 | hornfels | | | | | | | | | | | | | | | |
| G402480 | hornfels | *** | * | | | | ** | ** | ** | | | | | | | |
| C107644 | dolomite | | | * | * | *** | | | | | | * | | | ? | |
| R007639 | hornfels | *** | | | | | ** | | | ** | | | | | ? | ? |
| R007640 | ophicalcite | | *** | ** | | * | * | | | *** | * | | | | | |
| R007641 | marble | | *** | * | | | ? | | | | | ? | | | *** | trem? |
| R007642 | ophicalcite | * | *** | ** | * | *** | | | | | ? | | | | * | |
| R007646 | marble | | *** | | ** | | | | | | | | | | | |
| R007647 | hornfels | *** | *** | | | | ** | | | | | | | | | |
| R007648 | dolomite | | | * | | *** | * | | | | | | | | | |

Igneous rocks

| <i>Reg. No.</i> | <i>Rock type</i> | <i>qtz</i> | <i>srp</i> | <i>tlc</i> | <i>pl</i> | <i>kf</i> | <i>cpx</i> | <i>chl</i> | <i>am</i> | <i>prn</i> | <i>ze</i> | <i>sid</i> | <i>mt</i> | <i>hem</i> | <i>ha7</i> | <i>ha10</i> | <i>sme</i> | <i>m-layer</i> | <i>gt</i> | <i>Other (mostly trace)</i> |
|-----------------|------------------|------------|------------|------------|-----------|-----------|------------|------------|-----------|------------|-----------|------------|-----------|------------|------------|-------------|------------|----------------|-----------|-----------------------------|
| C107828 | dolerite? | ** | | | ** | * | | ** | * | | | | | | | *** | | | | |
| C107861 | dolerite? | * | | ** | | | | | | | | | | | *** | | | | ** | |
| C107862 | dolerite? | ** | | * | | * | | | | | | | | | *** | | | ** | ** | mica |
| C107863 | dolerite (Jdl) | ** | | | *** | | ** | | | | * | | | | | | ** | | | |
| C107864 | vein in Jdl | ** | | | | | * | | | *** | ** | | | | | | ** | | | |
| G402154 | dolerite (Jdl) | * | | | | | * | | ** | *** | | | | | | | *** | | | |
| G402447 | dolerite (Jdl) | * | | | *** | | *** | | ? | | | | | | | | ** | | | kaolinite |
| R007644 | basalt | * | | | | | ** | | ** | *** | | | | | | | ** | | | kaolinite |
| R007645 | lamprophyre | | | | ** | ** | | | *** | | | | | | | | | ** | | |

Cambrian sediments

| Reg. No. | Rock type | qtz | srp | tlc | pl | kf | cpx | chl | am | prn | ze | sid | mt | hem | ha7 | ha10 | sme | m-layer | gt | Other (mostly trace) |
|----------|------------------|-----|-----|-----|----|----|-----|-----|-----|-----|----|-----|----|-----|-----|------|-----|---------|----|----------------------|
| G402038 | conglomerate | | | *** | | | | ** | | | | | | *** | | | | | | calcite (**) |
| G402039 | conglomerate | | | | ** | | | *** | *** | | | | | | | | | | | mica (**) |
| G402040 | conglomerate | | | | ** | | | *** | *** | | | | | | | | | | | mica (**) |
| G402137 | conglomerate | | | *** | | | | | | | | | | * | | | | | | kaolinite |
| G402138 | conglomerate | | | *** | | | | | *** | | | | | | | | ** | | | kaolinite |
| G402139 | conglomerate | | | ** | | | | | *** | | | | | ** | | | | | | |
| G402140 | conglomerate | | | ** | | | | | *** | | | | | | | | * | | | kaolinite |
| G402437 | conglomerate | | | *** | | | | | | | | | | ** | | | | | | |
| G402438 | conglomerate | | | *** | | | | ** | | | | | | ** | | | | | | |
| G402439 | conglomerate | | | *** | | | | ** | | | | | | ** | | | | | | |
| G402441 | conglomerate | | | ** | ** | | | | *** | | | | | | | | *** | | | |
| G402448 | conglomerate | | | *** | | | | | *** | | | | | | | | ** | | | kaolinite |
| C107830 | clast | ** | | | | | * | | | | | *** | | | | | ** | | | py, srp? |
| C107831 | clast | | | | | | | *** | | | | | | | | | | | | |
| C107858 | clay | | | *** | | | | | * | | | | ** | | | | ** | | | hem |
| C107860 | pyroxenite clast | | | *** | | | | * | * | | | | | | | | | | | |
| G402210 | phyllite | *** | | | ** | ** | | ** | | | | | | | | | ** | | | mica (**) |
| R007643 | conglomerate | | ** | *** | | | * | * | * | | | | | | | | | | | cal |

Permian mudstone

| Reg. No. | Rock type | qtz | opal | tlc | pl | kf | cpx | chl | am | prn | ze | sid | mt | hall | sme | m-layer | mica | gt | Other (trace) |
|----------|----------------|-----|------|-----|-----|----|-----|-----|----|-----|----|-----|----|------|-----|---------|------|----|---------------|
| C107808 | mudstone | *** | | | | | | | | | | | | *** | | | * | | ?sepiolite |
| C107809 | mudstone | ** | | | | | | | | | | | | *** | | | *** | | hem |
| C107810 | mudstone | *** | | | | | ** | | | ** | | | | * | * | | | | |
| C107865 | mudstone | *** | | | ** | ** | | | | | | | | | *** | | | | |
| C108028 | mudstone | *** | | | *** | | | * | | | | | | | *** | | * | | |
| C108029 | mudstone | *** | | | | | | | | | | | | *** | | | *** | | |
| C108030 | mudstone | *** | | | | | | | | | | | | *** | | | *** | | |
| C108031 | mudstone | *** | | | | | | | | | | | | *** | | * | * | | |
| C108032 | mudstone | ** | | | | | | | | | | | | *** | * | | ** | ** | rutile |
| C108033 | mudstone | *** | | | | | | | | | | | | *** | | | | | |
| C108035 | mudstone | *** | | | | | | | | | | | | *** | | ** | ** | | rutile |
| C108036 | mudstone | *** | | | | | | | | | | | | *** | | | *** | * | rutile |
| C108041 | mudstone | *** | | | | | | | | | | | | *** | | | | | |
| C108042 | mudstone | *** | | | | | | | | | | | | *** | | | ** | * | gibbsite (**) |
| C108043 | mudstone | *** | | | ** | ** | | | | | | | | | ** | | * | | |
| C107865 | mudstone | *** | | | ** | ** | | | | | | | | | *** | | | | |
| G402036 | mudstone/chert | *** | | | | | | | | | | | | | | | ** | | |

Silicified rocks

| Reg. No. | Rock type | qtz | opal | tlc | pl | kf | cpx | chl | am | prn | ze | sid | mt | hall | sme | m-layer | mica | gt | Other (trace) |
|----------|-----------------|-----|------|-----|----|----|-----|-----|----|-----|----|-----|----|------|-----|---------|------|----|---------------|
| C108034 | chert | | | ** | | | | | | | | | | *** | | | | | |
| C108037 | quartz | *** | | | | | | | | | | | | * | | | | | |
| C108038 | quartz | *** | | | | | | | | | | | | * | | | | | |
| C108039 | jasperoid clast | *** | | | | | | | | | | | | * | | | | | |
| C108040 | chert | *** | | *** | | | | | | | | | | | | | | | |
| C107820 | chert | *** | | | | | | | | | | | | | | | | | |
| C107829 | chert | *** | | | | | | * | | | | | | | | | * | | hem, py |
| C107832 | chert | *** | *** | | | | | | | | | | | | | | | | |
| C107839 | chert | *** | | | | | | | | | | | | | | | | | ? |
| C107847 | chert | *** | | | | | | | | | | | | | | | | | ? |
| C107849 | chert | *** | *** | | | | | | | | | ** | | | | | | | ? |
| C107851 | opal | *** | * | | | | | | | | | ** | | | | | | | ? |
| G402153 | chert | * | *** | | | | | | | | | | | | ** | | | | |
| G402156 | chert | *** | ? | | | | | | | | | | | | ** | | | | |
| G402182 | opal | ** | *** | | | | | | | | | | | | *** | | | | |
| G402169 | chert | *** | | ** | | | | | | | | | | | | | | | hem, rutile |
| G402183 | clay | | | | | | * | | | | | | | | *** | | | | serpentine |
| G402189 | Chert | *** | | | | | | | | | | | | | | | * | | kaol, rutile |
| G402190 | Chert | *** | | | | | | | | | | | | | | | * | | hem, rutile |
| G402205 | chalcedony | *** | | | | | | | | | | | | | | | | ** | |

See Appendix 2 for abbreviations

*** = >20%, ** = 5-20%, * = <5%

APPENDIX 11

Fluid inclusion data

| Sample No. | Reg. No. | Rock type | FI Type | T_h °C | | T_{mNaCl} | T_{mCO_2} | $T_{m_{clath}}$ | Th_{Final} | Th_{CO_2} |
|------------|----------|----------------|---------|----------|-----|--|-------------|-----------------|--------------|-------------|
| C107830 | | quartz breccia | A2 | 221 | L | | | | | |
| | | | A1 | 369 | V | -4 | | | | |
| | | | A1 | 369 | V | | | | | |
| | | | A1 | 366 | V | | | | | |
| | | | A1 | 395 | V | | | | | |
| | | | A1 | 380 | V | | | | | |
| | | | A2 | 175 | L | | | | | |
| | | | A2 | 285 | L | | | | | |
| | | | A1 | 340 | L | -3.5 | | | | |
| | | | A1 | 377 | V | | | | | |
| C107831 | | quartz | A1 | 335 | V | | | | | |
| | | | A1 | 357 | L | | | | | |
| | | | A1 | 307 | L | | | | | |
| | | | A1 | 364 | L | -3 | | | | |
| | | | A1 | 334 | L | | | | | |
| | | | A1 | 308 | L | -3.2 | | | | |
| | | | A1 | 368 | L | -1.2 | | | | |
| | | | A2 | 249 | L | | | | | |
| | | | A2 | 246 | L | -1.1 | | | | |
| | | | A2 | 248 | L | -1.3 | | | | |
| C107832 | | quartz | A2 | 244 | L | | | | | |
| | | | A2 | 251 | L | -1 | | | | |
| | | | A2 | 248 | L | -0.9 | | | | |
| | | | A2 | 245 | L | | | | | |
| | | | A2 | 243 | L | | | | | |
| | | | A1 | 349 | L | | | | | |
| | | | A1 | 363 | L | | | | | |
| | | | A2 | 246 | L | | | | | |
| | | | A2 | 278 | L | | | | | |
| | | | A2 | 254 | L | | | | | |
| | | | A2 | 256 | L | | | | | |
| | | | A1 | 383 | V | | | | | |
| | | | A1 | 349 | L | | | | | |
| | | | A1 | 369 | L | | | | | |
| | | | A1 | 374 | V | | | | | |
| | | | A1 | 351 | L | | | | | |
| | | | A1 | 369 | L | | | | | |
| | | | A1 | 369 | L | | | | | |
| | | | A1 | 370 | L | | | | | |
| | | | A1 | 372 | L | | | | | |
| | | | A1 | 371 | L | | | | | |
| | | | A1 | 370 | L | | | | | |
| | | | A1 | 374 | L * | Boundary became almost indistinguishable | | | | |
| | | | A1 | 370 | CP? | | | | | |
| | | | A1 | 430 | V | | | | | |
| | | | A1 | 421 | V | | | | | |
| | | | A1 | 343 | L | -3.1 | | | | |
| | | | A1 | 359 | L | -3.2 | | | | |
| | | | A1 | 360 | L | -3.4 | | | | |
| | | | A1 | 362 | L | -3 | | | | |
| | | | A1 | 355 | L | | | | | |
| | | | A1 | 365 | L | | | | | |
| | | | A1 | 340 | V | | | | | |
| | | | A1 | 345 | V | | | | | |
| | | | A1 | 350 | V | | | | | |
| | | | A1 | 349 | V | | | | | |
| | | | A1 | 365 | L | | | | | |
| | | | A1 | 362 | V | | | | | |
| | | | A1 | 380 | L | | | | | |
| | | | A1 | 365 | V | | | | | |

| Sample No. | Reg. No. | Rock type | FI Type | T _h °C | | T _m NaCl | T _m CO ₂ | T _m clath | Th _{Final} | Th _{CO2} |
|------------|----------|----------------|---------|-------------------|---|---------------------|--------------------------------|----------------------|---------------------|-------------------|
| | C107827 | chert | A1 | 336 | | | | | | |
| | C107880 | chert | B1 | | | | | | | 24.9L |
| | | | B1 | | | | | | | 28L |
| | | | B1 | | | | | | | 27L |
| | | | B1 | | | | | | | 26L |
| | | | B1 | | | | | | | 27L |
| | C107829 | chert | A1 | - | | 0.4 | | | | |
| | | | A1 | - | | 0.3 | | | | |
| | | | A1 | - | | -1 | | | | |
| | | | A1 | - | | -1 | | | | |
| | | | A1 | - | | -2.1 | | | | |
| | C107830 | chert | B2 | | | | -60.1 | 8.6 | | |
| | | | | | | | -59.0 | | | |
| | | | B2 | | | | -59.5 | 8 | | |
| SW1-1 | C108165 | quartz breccia | A1 | 316 | L | | | | | |
| | | | A1 | 365 | V | | | | | |
| | | | A1 | 374 | V | | | | | |
| | | | A1 | 379 | V | | | | | |
| | | | A1 | 362 | L | | | | | |
| | | | A1 | 391 | V | | | | | |
| | | | A1 | 373 | V | | | | | |
| | | | A1 | 312 | L | | | | | |
| | | | A1 | 378 | V | | | | | |
| | | | A1 | 346 | L | | | | | |
| | | | A1 | 387 | V | | | | | |
| SW1-2 | C108165 | quartz breccia | A1 | 342 | L | | | | | |
| | | | A1 | 369 | V | | | | | |
| | | | A1 | 369 | V | | | | | |
| | | | A1 | 386 | V | | | | | |
| | | | A1 | 392 | V | | | | | |
| | | | A1 | 371 | V | | | | | |
| | | | A1 | 381 | V | | | | | |
| | | | A1 | 385 | V | | | | | |
| | | | A1 | 389 | V | | | | | |
| | | | A1 | 378 | V | | | | | |
| BCF8 | C108163 | quartz breccia | A2 | 251 | L | 0.5 | | | | |
| | | | A2 | 254 | L | | | | | |
| | | | A2 | 265 | L | 0.4 | | | | |
| | | | A2 | 263 | L | | | | | |
| | | | A2 | 261 | L | 0.3 | | | | |
| | | | A2 | 259 | L | | | | | |
| | | | A2 | 275 | L | 0.5 | | | | |
| | | | A2 | 272 | L | | | | | |
| | | | A2 | 269 | L | | | | | |
| | | | A2 | 265 | L | 0.2 | | | | |
| | | | A2 | 261 | L | | | | | |
| | | | A2 | 260 | L | | | | | |
| | | | A2 | 281 | L | 0.3 | | | | |
| | | | A2 | 282 | L | | | | | |
| | | | A2 | 261 | L | 0.5 | | | | |
| | | | A2 | 258 | L | | | | | |
| | | | A2 | 253 | L | | | | | |
| | | | A2 | 262 | L | | | | | |
| | | | A2 | 270 | L | | | | | |
| | | | A2 | 263 | L | | | | | |
| | | | A2 | 265 | L | | | | | |
| | | | A2 | 259 | L | | | | | |
| | | | A2 | 266 | L | | | | | |
| | | | A2 | 260 | L | | | | | |
| | | | A2 | 256 | L | | | | | |
| | | | A1 | 382 | L | | | | | |
| | | | A1 | 379 | V | | | | | |
| | | | A1 | 372 | V | | | | | |

APPENDIX 12

Corellation coefficients

| | Au | Ag | As | Bi | Cd | Ce | Co | Cs | Cu | Ga | La | Mo | Nb | Ni | Pb | Rb | Sb | Se | Sr | Te | Th | Tl | U | W | Y | Zn | Cr | P | Ti | V |
|----|--------|--------|--------|--------|--------|--------|--------|--------|--------|--------|--------|--------|--------|--------|--------|--------|--------|--------|--------|--------|--------|--------|--------|--------|--------|--------|--------|--------|--------|--------|
| Au | 1.000 | 0.693 | -0.075 | 0.710 | 0.219 | -0.016 | 0.954 | 0.819 | 0.356 | -0.009 | -0.067 | -0.047 | -0.189 | 0.780 | 0.279 | 0.208 | 0.192 | -0.131 | -0.343 | -0.072 | -0.147 | 0.013 | -0.196 | -0.177 | 0.232 | 0.882 | -0.048 | -0.128 | -0.160 | -0.249 |
| Ag | 0.693 | 1.000 | 0.356 | 0.489 | 0.176 | -0.178 | 0.628 | 0.525 | 0.137 | -0.232 | -0.232 | 0.311 | -0.061 | 0.478 | 0.385 | 0.026 | 0.496 | -0.021 | -0.315 | 0.054 | -0.307 | -0.133 | 0.224 | -0.136 | -0.094 | 0.556 | -0.208 | -0.049 | -0.185 | -0.124 |
| As | -0.075 | 0.356 | 1.000 | -0.075 | 0.072 | -0.078 | -0.157 | -0.154 | 0.040 | -0.090 | -0.071 | -0.104 | -0.105 | -0.128 | -0.106 | 0.005 | -0.102 | 0.476 | 0.157 | 0.174 | -0.040 | 0.050 | 0.801 | 0.105 | -0.108 | -0.150 | 0.021 | 0.100 | 0.004 | 0.551 |
| Bi | 0.710 | 0.489 | -0.075 | 1.000 | -0.004 | 0.140 | 0.766 | 0.442 | 0.451 | -0.065 | 0.081 | -0.053 | -0.080 | 0.860 | 0.610 | 0.171 | 0.298 | -0.384 | -0.383 | -0.145 | -0.076 | 0.027 | -0.246 | -0.085 | 0.376 | 0.629 | -0.001 | -0.028 | -0.066 | -0.180 |
| Cd | 0.219 | 0.176 | 0.072 | -0.004 | 1.000 | 0.199 | 0.188 | 0.215 | -0.279 | -0.171 | 0.230 | -0.010 | 0.061 | 0.011 | -0.127 | -0.065 | -0.196 | 0.219 | 0.072 | 0.158 | 0.003 | -0.276 | 0.159 | -0.195 | 0.044 | 0.293 | -0.221 | 0.330 | -0.117 | 0.334 |
| Ce | -0.016 | -0.178 | -0.078 | 0.140 | 0.199 | 1.000 | -0.078 | -0.089 | 0.439 | 0.511 | 0.970 | 0.196 | 0.704 | -0.019 | 0.120 | 0.356 | 0.023 | 0.203 | -0.071 | -0.020 | 0.849 | 0.459 | -0.071 | 0.582 | 0.717 | -0.128 | 0.489 | 0.578 | 0.625 | 0.571 |
| Co | 0.954 | 0.628 | -0.157 | 0.766 | 0.188 | -0.078 | 1.000 | 0.813 | 0.300 | -0.068 | -0.101 | -0.106 | -0.202 | 0.910 | 0.310 | 0.143 | 0.192 | -0.208 | -0.278 | -0.118 | -0.208 | -0.087 | -0.234 | -0.251 | 0.216 | 0.954 | -0.116 | -0.167 | -0.208 | -0.300 |
| Cs | 0.819 | 0.525 | -0.154 | 0.442 | 0.215 | -0.089 | 0.813 | 1.000 | 0.479 | 0.295 | -0.063 | -0.002 | -0.008 | 0.633 | 0.214 | 0.534 | 0.326 | 0.005 | -0.352 | -0.191 | 0.056 | 0.256 | -0.290 | 0.034 | 0.072 | 0.854 | 0.210 | -0.369 | 0.155 | -0.287 |
| Cu | 0.356 | 0.137 | 0.040 | 0.451 | -0.279 | 0.439 | 0.300 | 0.479 | 1.000 | 0.761 | 0.416 | 0.155 | 0.391 | 0.362 | 0.249 | 0.885 | 0.347 | 0.014 | -0.451 | -0.170 | 0.650 | 0.890 | -0.278 | 0.746 | 0.379 | 0.225 | 0.833 | -0.228 | 0.748 | 0.117 |
| Ga | -0.009 | -0.232 | -0.090 | -0.065 | -0.171 | 0.511 | -0.068 | 0.295 | 0.761 | 1.000 | 0.547 | 0.073 | 0.554 | -0.044 | 0.031 | 0.829 | 0.253 | 0.212 | -0.285 | -0.003 | 0.827 | 0.868 | -0.178 | 0.845 | 0.258 | -0.019 | 0.885 | -0.109 | 0.864 | 0.296 |
| La | -0.067 | -0.232 | -0.071 | 0.081 | 0.230 | 0.970 | -0.101 | -0.063 | 0.416 | 0.547 | 1.000 | 0.129 | 0.709 | -0.029 | 0.114 | 0.371 | -0.026 | 0.295 | 0.065 | -0.029 | 0.876 | 0.451 | -0.010 | 0.596 | 0.665 | -0.120 | 0.518 | 0.617 | 0.651 | 0.646 |
| Mo | -0.047 | 0.311 | -0.104 | -0.053 | -0.010 | 0.196 | -0.106 | -0.002 | 0.155 | 0.073 | 0.129 | 1.000 | 0.436 | -0.157 | -0.001 | 0.132 | 0.459 | -0.005 | -0.293 | -0.119 | 0.174 | 0.199 | -0.185 | 0.297 | -0.058 | -0.232 | 0.148 | -0.016 | 0.275 | -0.122 |
| Nb | -0.189 | -0.061 | -0.105 | -0.080 | 0.061 | 0.704 | -0.202 | -0.008 | 0.391 | 0.554 | 0.709 | 0.436 | 1.000 | -0.147 | 0.225 | 0.447 | 0.468 | -0.073 | -0.048 | -0.206 | 0.759 | 0.493 | -0.131 | 0.647 | 0.188 | -0.163 | 0.443 | 0.447 | 0.811 | 0.400 |
| Ni | 0.780 | 0.478 | -0.128 | 0.860 | 0.011 | -0.019 | 0.910 | 0.633 | 0.362 | -0.044 | -0.029 | -0.157 | -0.147 | 1.000 | 0.393 | 0.119 | 0.188 | -0.268 | -0.237 | -0.103 | -0.153 | -0.070 | -0.198 | -0.177 | 0.301 | 0.853 | -0.075 | -0.151 | -0.145 | -0.229 |
| Pb | 0.279 | 0.385 | -0.106 | 0.610 | -0.127 | 0.120 | 0.310 | 0.214 | 0.249 | 0.031 | 0.114 | -0.001 | 0.225 | 0.393 | 1.000 | 0.122 | 0.661 | -0.352 | -0.382 | -0.031 | 0.034 | -0.018 | -0.052 | 0.009 | 0.098 | 0.253 | -0.018 | 0.142 | 0.116 | -0.158 |
| Rb | 0.208 | 0.026 | 0.005 | 0.171 | -0.065 | 0.356 | 0.143 | 0.534 | 0.885 | 0.829 | 0.371 | 0.132 | 0.447 | 0.119 | 0.122 | 1.000 | 0.374 | 0.096 | -0.415 | -0.211 | 0.685 | 0.917 | -0.316 | 0.767 | 0.213 | 0.181 | 0.868 | -0.322 | 0.839 | 0.108 |
| Sb | 0.192 | 0.496 | -0.102 | 0.298 | -0.196 | 0.023 | 0.192 | 0.326 | 0.347 | 0.253 | -0.026 | 0.459 | 0.468 | 0.188 | 0.661 | 0.374 | 1.000 | -0.366 | -0.574 | -0.162 | 0.120 | 0.240 | -0.225 | 0.277 | -0.128 | 0.196 | 0.168 | -0.182 | 0.376 | -0.330 |
| Se | -0.131 | -0.021 | 0.476 | -0.384 | 0.219 | 0.203 | -0.208 | 0.005 | 0.014 | 0.212 | 0.295 | -0.005 | -0.073 | -0.268 | -0.352 | 0.096 | -0.366 | 1.000 | 0.212 | 0.219 | 0.310 | 0.124 | 0.533 | 0.188 | 0.305 | -0.174 | 0.228 | 0.092 | 0.106 | 0.496 |
| Sr | -0.343 | -0.315 | 0.157 | -0.383 | 0.072 | -0.071 | -0.278 | -0.352 | -0.451 | -0.285 | 0.065 | -0.293 | -0.048 | -0.237 | -0.382 | -0.415 | -0.574 | 0.212 | 1.000 | -0.109 | -0.111 | -0.328 | 0.336 | -0.252 | -0.121 | -0.214 | -0.323 | 0.481 | -0.202 | 0.401 |
| Te | -0.072 | 0.054 | 0.174 | -0.145 | 0.158 | -0.020 | -0.118 | -0.191 | -0.170 | -0.003 | -0.029 | -0.119 | -0.206 | -0.103 | -0.031 | -0.211 | -0.162 | 0.219 | -0.109 | 1.000 | -0.114 | -0.145 | 0.485 | 0.114 | -0.078 | -0.088 | -0.029 | 0.011 | -0.194 | 0.232 |
| Th | -0.147 | -0.307 | -0.040 | -0.076 | 0.003 | 0.849 | -0.208 | 0.056 | 0.650 | 0.827 | 0.876 | 0.174 | 0.759 | -0.153 | 0.034 | 0.685 | 0.120 | 0.310 | -0.111 | -0.114 | 1.000 | 0.776 | -0.113 | 0.825 | 0.513 | -0.195 | 0.806 | 0.280 | 0.901 | 0.523 |
| Tl | 0.013 | -0.133 | 0.050 | 0.027 | -0.276 | 0.459 | -0.087 | 0.256 | 0.890 | 0.868 | 0.451 | 0.199 | 0.493 | -0.070 | -0.018 | 0.917 | 0.240 | 0.124 | -0.328 | -0.145 | 0.776 | 1.000 | -0.249 | 0.895 | 0.235 | -0.108 | 0.949 | -0.212 | 0.884 | 0.227 |
| U | -0.196 | 0.224 | 0.801 | -0.246 | 0.159 | -0.071 | -0.234 | -0.290 | -0.278 | -0.178 | -0.010 | -0.185 | -0.131 | -0.198 | -0.052 | -0.316 | -0.225 | 0.533 | 0.336 | 0.485 | -0.113 | -0.249 | 1.000 | -0.031 | -0.191 | -0.196 | -0.165 | 0.327 | -0.180 | 0.611 |
| W | -0.177 | -0.136 | 0.105 | -0.085 | -0.195 | 0.582 | -0.251 | 0.034 | 0.746 | 0.845 | 0.596 | 0.297 | 0.647 | -0.177 | 0.009 | 0.767 | 0.277 | 0.188 | -0.252 | 0.114 | 0.825 | 0.895 | -0.031 | 1.000 | 0.204 | -0.252 | 0.913 | 0.010 | 0.901 | 0.442 |
| Y | 0.232 | -0.094 | -0.108 | 0.376 | 0.044 | 0.717 | 0.216 | 0.072 | 0.379 | 0.258 | 0.665 | -0.058 | 0.188 | 0.301 | 0.098 | 0.213 | -0.128 | 0.305 | -0.121 | -0.078 | 0.513 | 0.235 | -0.191 | 0.204 | 1.000 | 0.142 | 0.237 | 0.248 | 0.229 | 0.204 |
| Zn | 0.882 | 0.556 | -0.150 | 0.629 | 0.293 | -0.128 | 0.954 | 0.854 | 0.225 | -0.019 | -0.120 | -0.232 | -0.163 | 0.853 | 0.253 | 0.181 | 0.196 | -0.174 | -0.214 | -0.088 | -0.195 | -0.108 | -0.196 | -0.252 | 0.142 | 1.000 | -0.128 | -0.197 | -0.168 | -0.266 |
| Cr | -0.048 | -0.208 | 0.021 | -0.001 | -0.221 | 0.489 | -0.116 | 0.210 | 0.833 | 0.885 | 0.518 | 0.148 | 0.443 | -0.075 | -0.018 | 0.868 | 0.168 | 0.228 | -0.323 | -0.029 | 0.806 | 0.949 | -0.165 | 0.913 | 0.237 | -0.128 | 1.000 | -0.192 | 0.851 | 0.295 |
| P | -0.128 | -0.049 | 0.100 | -0.028 | 0.330 | 0.578 | -0.167 | -0.369 | -0.228 | -0.109 | 0.617 | -0.016 | 0.447 | -0.151 | 0.142 | -0.322 | -0.182 | 0.092 | 0.481 | 0.011 | 0.280 | -0.212 | 0.327 | 0.010 | 0.248 | -0.197 | -0.192 | 1.000 | 0.064 | 0.648 |
| Ti | -0.160 | -0.185 | 0.004 | -0.066 | -0.117 | 0.625 | -0.208 | 0.155 | 0.748 | 0.864 | 0.651 | 0.275 | 0.811 | -0.145 | 0.116 | 0.839 | 0.376 | 0.106 | -0.202 | -0.194 | 0.901 | 0.884 | -0.180 | 0.901 | 0.229 | -0.168 | 0.851 | 0.064 | 1.000 | 0.378 |
| V | -0.249 | -0.124 | 0.551 | -0.180 | 0.334 | 0.571 | -0.300 | -0.287 | 0.117 | 0.296 | 0.646 | -0.122 | 0.400 | -0.229 | -0.158 | 0.108 | -0.330 | 0.496 | 0.401 | 0.232 | 0.523 | 0.227 | 0.611 | 0.442 | 0.204 | -0.266 | 0.295 | 0.648 | 0.378 | 1.000 |